

**Evaluating the natural attenuation of synthetic organic  
chemicals in a chalk aquifer**

**Karen A. Hampson**

Submitted for the Degree of Doctor of Philosophy

University of East Anglia

School of Environmental Sciences

July 2013

© This copy of the thesis has been supplied on condition that anyone who consults it is understood to recognise that its copyright rests with the author and that use of any information derived there from must be in accordance with current UK Copyright Law. In addition, any quotation or extract must include full attribution.

## ABSTRACT

Hydrocarbon contaminants regularly leach into groundwater because of human activities and accidental chemical spills. Here, the contaminants pose a threat to the environment and valuable drinking water resources. Many subsurface environments are able to purify the groundwater of such contaminants, thus lowering the cost of remediation. This has sparked an interest in the use of naturally occurring processes to degrade contaminants in the subsurface and has opened up an area of research focusing on '*natural attenuation*'.

For the successful application of natural attenuation and in order to obtain regulatory approval a reliable assessment of the mechanisms responsible for the removal of contaminants in an aquifer is essential. This thesis presents evidence to support the natural attenuation of isoproturon (IPU) and sulphanilamide (SULPH) in a chalk aquifer and assesses *in-situ* biodegradation by: (a) analysing historical monitoring data to identify and support biodegradation processes at the contaminated field site; (b) the development of *in-situ* microcosm approaches, (c) determining the catabolic activity present across the site using *ex-situ* microcosm studies that replicate *in-situ* aquifer conditions and, (d) identifying and quantifying biodegradation in the aquifer (of SULPH) using compound specific isotope analysis.

Based on the historical data and *ex-situ* microcosms IPU biodegradation was found to be occurring at the site; albeit at very low levels (2 %). It is suggested that the high concentrations of other contaminants at the site (up to 650 mg L<sup>-1</sup>), compared to the low IPU concentrations (9 µg L<sup>-1</sup>) may have impeded IPU biodegradation.

However, even these low levels of IPU biodegradation may be important in aquifers exhibiting long residence times. The historical data and *ex-situ* microcosms further indicated the biodegradation of around 50% of the SULPH present at the site.

The development of novel compound specific isotope analysis indicates 56 % of the SULPH has undergone biodegradation at the site. These three approaches; historical data, *ex-situ* microcosms and compound specific isotope analysis, provide strong evidence to support the occurrence of natural attenuation at the site. Of particular originality, is the identification of natural attenuation of SULPH in a chalk aquifer and the quantification of its biodegradation using compound specific isotope analysis.

# LIST OF CONTENTS

<b>Chapter 1: Introduction and Thesis Overview</b>	<b>16</b>
1.1 Introduction	16
1.1.1 <i>Groundwater in Society</i>	16
1.1.2 <i>Natural Attenuation – A key service provided by groundwater</i>	18
1.1.3 <i>The field study site</i>	19
1.2 Thesis overview	20
1.2.1 <i>Aims</i>	20
1.2.2 <i>Structure of the Thesis and chapter objectives</i>	20
<b>Chapter 2: Natural attenuation of hydrocarbons in groundwater environments – a review</b>	<b>23</b>
2.1 Natural attenuation	23
2.2 Evidence of natural attenuation in groundwater environments	29
2.2.1 <i>Identification of metabolites as evidence to support natural attenuation</i>	32
2.2.2 <i>Carbon Isotope Analysis as evidence to support natural attenuation</i>	33
2.2.3 <i>Microcosms as evidence to support natural attenuation</i>	35
2.3 Contaminant natural attenuation in groundwater environments	36
2.3.1 <i>BTEX compounds</i>	38
2.3.2 <i>Methyl-tert-butyl ether</i>	40
2.3.3 <i>Chlorinated compounds</i>	41
2.3.4 <i>Agrochemicals</i>	41
2.4 Enhanced natural attenuation	42
2.5 Conclusion	44
<b>Chapter 3: Overview and site characterisation of the chemical production plant</b>	<b>46</b>
3.1 Introduction	46
3.1.1 <i>Defining natural attenuation</i>	46
3.1.2 <i>History of study area</i>	47
3.2 Methods	50
3.2.1 <i>Site-wide monitoring report</i>	50
3.2.2 <i>Collation and preparation of data</i>	50
3.2.3 <i>Aquifer characteristics methodology</i>	51
3.2.4 <i>Contaminant properties</i>	51
3.2.5 <i>Receptor/compliance point</i>	52
3.3 Results and discussion	53
3.3.1 Aquifer Characteristics	53
3.3.1.1 <i>Groundwater protection zones</i>	54
3.3.1.2 <i>Groundwater velocity</i>	56
3.3.2 Contaminant properties	58
3.3.2.1 <i>Contaminant source and history of release</i>	58
3.3.2.2 <i>Contaminant plume characteristics</i>	60
3.3.2.3 <i>Background groundwater chemistry</i>	65
3.3.2.4 <i>Nature of contamination</i>	70
3.3.2.5 <i>Evidence to support biodegradation at the site</i>	71
3.3.3 Receptors/compliance points	73
3.4 Conclusion	76

<b>Chapter 4: Support materials suitable for <i>in-situ</i> microcosms examining hydrophilic hydrocarbons</b>	<b>78</b>
4.1 Introduction	79
4.1.1 <i>Surface Area and Porosity</i>	83
4.1.2 <i>Sorption Capacity</i>	84
4.1.3 <i>Biofilm Development</i>	86
4.1.4 <i>Readily Available Materials</i>	89
4.2 Materials and methods	91
4.2.1 <i>Compound Selection</i>	91
4.2.2 <i>Chemicals</i>	91
4.2.3 <i>Support Material Selection</i>	92
4.2.4 <i>Support Materials</i>	93
4.2.5 <i>Instrumentation</i>	95
4.2.6 <i>Adsorption</i>	95
4.2.6.1 <i>Adsorption Mass Balance Calculations</i>	97
4.2.7 <i>Loading Support Materials</i>	98
4.2.8 <i>Desorption</i>	101
4.2.8.1 <i>Desorption Mass Balance Calculations</i>	101
4.2.9 <i>Kinetic Modelling</i>	102
4.2.10 <i>Statistical Analysis</i>	104
4.3 Results/discussion	106
4.3.1 <i>Adsorption</i>	106
4.3.2 <i>Loading Support Materials</i>	109
4.3.3 <i>Desorption</i>	113
4.3.4 <i>Kinetic Models</i>	122
4.3.4.1 <i>First-order Model</i>	126
4.3.4.2 <i>Elovich Model</i>	127
4.3.4.3 <i>Modified Freundlich Model</i>	128
4.4 Conclusion	133
<b>Chapter 5: Ex-situ Microcosm Studies of Sulphanilamide and Isoproturon Natural and Enhanced degradation in the presence of chalk aquifer material</b>	<b>134</b>
5.1 Introduction	143
5.2 Methods	141
5.2.1 <i>Collection of core samples and groundwater</i>	141
5.2.2 <i>Chemicals</i>	144
5.2.3 <i>Ex-situ Microcosms</i>	145
5.2.4 <i>Statistical Analysis</i>	148
5.3 Results/discussion	149
5.3.1 <i>IPU Microcosm Study</i>	149
5.3.2 <i>Sulphanilamide Microcosm Studies</i>	156
5.3.2.1 <i>Relating SULPH biodegradation to the field study site conditions</i>	161
5.4 Conclusion	174
<b>Chapter 6: Compound Specific Isotope Analysis – a tool to substantiate sulphanilamide biodegradation in a chalk aquifer</b>	<b>177</b>
6.1 Introduction	177
6.1.1 <i>Stable Isotopes</i>	177
6.1.2 <i>Compound specific isotope analysis</i>	180
6.1.3 <i>Biodegradation and compound specific isotope analysis</i>	181
6.2 Method	184
6.2.1 <i>Chemicals</i>	185
6.2.2 <i>Sample selection</i>	185

6.2.3 <i>Pre-concentration of SULPH groundwater samples using freeze drying techniques</i>	<b>185</b>
6.2.4 <i>Collection of SULPH fractions using HPLC fractionation techniques (quantification).</i>	<b>186</b>
6.2.5 <i>Isotope analysis of SULPH</i>	<b>187</b>
6.3 Results/discussion	<b>189</b>
6.3.1 <i>Linearity, uncertainty and detection limit of isotope mass spectrometer</i>	<b>189</b>
6.3.2 <i>Compound specific isotope analysis</i>	<b>191</b>
6.3.3 <i>Quantifying biodegradation at the field site</i>	<b>193</b>
6.3.4 <i>Disadvantages of compound specific isotope analysis</i>	<b>194</b>
6.4 Conclusion	<b>197</b>
<b>Chapter 7: Summary and Conclusion</b>	<b>199</b>
7.1 Summary of research and how it was achieved	<b>199</b>
7.2 The main findings	<b>200</b>
7.3 Future research/further work	<b>203</b>
7.4 Contribution and significance of research to field of natural attenuation	<b>203</b>
<b>References</b>	<b>206</b>
<b>Appendices</b>	
Appendix 1 Mass calculations	<b>224</b>
Appendix 2 Calculation of sulphate and nitrate concentrations for enhanced biodegradation study	<b>227</b>
Appendix 3 Liquid scintillation Analyser's detection limit calculation	<b>229</b>
Appendix 4 Quench curve	<b>231</b>
Appendix 5 LC/IRMS method development for compound specific isotope analysis of non-volatile organic compounds	<b>233</b>

## LIST OF FIGURES

### Chapter 2: Natural attenuation of hydrocarbons in groundwater environments – a review

- Figure 2.1* - Conceptual illustration of the important natural attenuation processes that affect the fate of hydrocarbon contaminants in aquifers. 26

### Chapter 3: Overview and site characterisation of the chemical production plant

- Figure 3.1* – Aerial photograph of chemical production plant. 48
- Figure 3.2* - Simplified geological maps of Norfolk. 53
- Figure 3.3* - Classification of the geological formations found in the U.K. with highlighted formations representing those typical of Norfolk. 54
- Figure 3.4* - Groundwater protection zones near to the field study site. 55
- Figure 3.5* – Map showing the zones of groundwater vulnerability in and around the Norwich area. 56
- Figure 3.6* - Aerial view of field study site showing where and when contaminant spills occurred at the site. 59
- Figure 3.7* – The average proportion of Asulam to Sulphanilamide, in key boreholes, at the field study site between 2005 and 2006. 60
- Figure 3.8* – Diagram of SULPH plume created from concentration data. 61
- Figure 3.9* – Diagram of toluene plume created from concentration data. 62
- Figure 3.10* – Types of naturally attenuating plumes. 63
- Figure 3.11* - The extent of sulphanilamide plume at time, t1 (2006) compared to the extent of the plume at t2 (2007). 64
- Figure 3.12* – Schematic of chemical works showing location of monitoring areas at the site. 66
- Figure 3.13* - The effect of organic contaminants on redox chemistry in groundwater. 68
- Figure 3.14* – Redox ladder showing conditions dominant at field study site. 69
- Figure 3.15* – Areal view of field study site and the surrounding area. 75

### Chapter 4: Support materials suitable for *in-situ* microcosms examining hydrophilic hydrocarbons

- Figure 4.1* – Schematic showing the characteristics required by a support material to succeed as a surrogate support for *in-situ* microcosms. 82
- Figure 4.2* – Scanning Electron Micrographs (SEM) showing the surface and porous structures of graphite felt, Bio-sep® Bead, perlite and pumice. 83
- Figure 4.3* – Three stages of biofilm development; attachment, colonisation and growth. 87
- Figure 4.4* – Scanning electron micrograph images of biofilm development on perlite and pumice. 88
- Figure 4.5* – Schematic showing manufacturing process of granulated

activated carbon.	89
<i>Figure 4.6</i> – Images of studied support materials.	93
<i>Figure 4.7</i> – Batch Adsorption Experiment Design.	96
<i>Figure 4.8</i> – Diagram of Batch Adsorption Flask.	97
<i>Figure 4.9</i> – Mass balance calculations for the transfer of <sup>14</sup> C-activity during adsorption study.	98
<i>Figure 4.10</i> – Experiment design for loading the support materials	99
<i>Figure 4.11</i> – Mass balance calculations for detected <sup>14</sup> C-activity at the different stages of the desorption study.	101
<i>Figure 4.12</i> – Flow diagram of statistical analysis used in SPSSv.18.	105
<i>Figure 4.13</i> – Effectiveness of Graphite Felt, Pumice Pellets and Expanded Perlite to remove <sup>12</sup> C/ <sup>14</sup> C Isoproturon and <sup>12</sup> C/ <sup>14</sup> C Sulphanilamide from the aqueous phase.	107
<i>Figure 4.14</i> – The bar groupings represent the same concentrations, shown as the percentage of <sup>14</sup> C-activity adsorbed of <sup>12</sup> C/ <sup>14</sup> C isoproturon and <sup>12</sup> C/ <sup>14</sup> C sulphanilamide loaded onto different support materials.	110
<i>Figure 4.15</i> – The bar groupings represent the same support materials loaded with different concentrations of <sup>12</sup> C/ <sup>14</sup> C isoproturon and <sup>12</sup> C/ <sup>14</sup> C sulphanilamide.	111
<i>Figure 4.16</i> – A comparison of 100 mg g <sup>-1</sup> of <sup>12</sup> C/ <sup>14</sup> C isoproturon and <sup>12</sup> C/ <sup>14</sup> C sulphanilamide loaded onto graphite felt, pumice pellets and expanded perlite.	112
<i>Figure 4.17</i> – Desorption of <sup>12</sup> C/ <sup>14</sup> C Isoproturon and <sup>12</sup> C/ <sup>14</sup> C Sulphanilamide from Graphite Felt, Pumice Pellets, and Expanded Perlite.	116
<i>Figure 4.18</i> –mass balance graphs represent the percentage of Isoproturon and Sulphanilamide; desorption, adsorption and run-off during loading from/to Graphite Felt Pumice Pellets and Expanded Perlite and during the loading and off-loading desorption experiments.	119
<i>Figure 4.19</i> – Four main types of adsorption isotherms (S, L, H and C) which explain sorption processes.	123
<i>Figure 4.20</i> – First Order desorption model showing IPU and SULPH desorbed from different support materials, at set time intervals, after an initial loading of 100 mg g <sup>-1</sup> of support material.	126
<i>Figure 4.21</i> - Elovich desorption model showing IPU and SULPH desorbed from different support materials, at set time intervals, after an initial loading of 100 mg g <sup>-1</sup> of support material.	127
<i>Figure 4.22</i> – Modified Freundlich desorption model showing IPU and SULPH desorbed from different support materials, at set time intervals, after an initial loading of 100 mg g <sup>-1</sup> of support material.	128
<i>Figure 4.23</i> – Schematic picture showing diffusion process involved during adsorption.	129

## **Chapter 5: Ex-situ Microcosm Studies of Sulphanilamide and Isoproturon Natural and Enhanced degradation in the presence of chalk aquifer material**

<i>Figure 5.1.1</i> – Biodegradation pathways for Asulam and Isoproturon.	137
<i>Figure 5.1.2</i> - Simplified illustration of the metabolic pathways used by microbes in aquifer environments.	138
<i>Figure 5.2.1</i> - Schematic showing the habitats of microbial	

communities found in a fractured, karstic aquifer.	141
<i>Figure 5.2.2</i> – Map of field study site showing position of 11 new monitoring wells.	142
<i>Figure 5.2.3</i> - Drilling rig COMACHIO MC305 used to collect core samples and a schematic of a Hollow-Stem Augur apparatus.	143
<i>Figure 5.2.4</i> - Collection of core sample.	144
<i>Figure 5.2.5</i> - Flask-based <sup>14</sup> C-respirometer system.	146
<i>Figure 5.2.6</i> – Ex-situ microcosm experimental approach.	147
<i>Figure 5.3.1</i> - Percentage of <sup>14</sup> C-IPU biodegradation vs. time, shown as no. of days.	150
<i>Figure 5.3.2</i> - Bacterial growth curve.	155
<i>Figure 5.3.3</i> – Percentage of <sup>14</sup> C-SULPH biodegradation vs. time, shown as no. of days.	157
<i>Figure 5.3.4</i> - Map of field study site showing the positions of the new boreholes and the transects used to explore biodegradation processes occurring across the site.	163
<i>Figure 5.3.5</i> - Transect 1: Extent of SULPH biodegradation after 84 days.	164
<i>Figure 5.3.6</i> - Transect 2: Extent of SULPH biodegradation after 84 days.	169
<i>Figure 5.3.7</i> - Transect 3: Extent of SULPH biodegradation after 84 days.	172

## **Chapter 6: Compound Specific Isotope Analysis – a tool to substantiate sulphanilamide biodegradation in a chalk aquifer**

<i>Figure 6.1</i> – Stable carbon isotopes.	178
<i>Figure 6.2</i> - The energy a bond possesses in its ground state is referred to as the zero- point energy. This represents the starting point for the reactivity differences between isotopologues.	179
<i>Figure 6.3</i> – Schematic of method development: 1) HPLC fractionation, to isolate SULPH; 2) Separation and preparation of SULPH for stable isotope analysis and, 3) Measurement of carbon isotope ratio.	184
<i>Figure 6.4</i> – Linearity test: mass of SULPH (mg) vs. peak amplitude of mass 44 (V).	189
<i>Figure 6.5</i> – Plot of peak amplitude of mass 44(V) vs. $\delta^{13}\text{C}_{\text{SULPH}}$ (‰).	190
<i>Figure 6.6</i> – Concentrations and carbon isotope ratios of SULPH downgradient of source zone.	192
<i>Figure 6.7</i> – Suggested drivers in biodegradation of SULPH at the field site.	195

## LIST OF TABLES

### Chapter 1: Introduction and Thesis Overview

Table 1.1 – Major stocks of water found on Earth, with the water available for human consumption highlighted in red.	16
Table 1.2 – Human population increases and useable water, available for human consumption, predictions for 2025.	17
Table 1.3 Goods and Services Associated with Healthy Groundwater Environments	18

### Chapter 2: Natural attenuation of hydrocarbons in groundwater environments – a review

Table 2.1 - Advantages and disadvantages of using natural attenuation to remediate contaminated groundwater	24
Table 2.2 – Overview of existing natural attenuation regulatory approaches/frameworks in various countries	28
Table 2.3 - Ideal characteristics for indicators of metabolism	32
Table 2.4 Evidence of natural attenuation of contaminants in groundwater	37
Table 2.5 – Limitations to the concentration of electron acceptors that can be added to contaminated groundwater	44

### Chapter 3: Overview and site characterisation of the chemical production plant

Table 3.1 – Physical and chemical properties of contaminants	49
Table 3.2 – Data required for initial screening of natural attenuation at a field site	51
Table 3.3 – Classification of geological formations found in the UK	54
Table 3.4 – Chalk aquifer characteristics and how they implicate groundwater monitoring	58
Table 3.5 – Summary of background groundwater composition at the field study site compared to that found in Norfolk chalk groundwater	67
Table 3.6 - Biological and chemical oxygen demands for the contaminated groundwater at the field study site	71

### Chapter 4: Support materials suitable for *in-situ* microcosms examining hydrophilic hydrocarbons

Table 4.1 – Disadvantages of using ex-situ biodegradation methods to determine NA in groundwater environments	81
Table 4.2 – Physical and Chemical Properties of Support Materials	94
Table 4.3 – Actual Loadings of Compound onto Support Material	100
Table 4.4 – Empirical Kinetic Models	103
Table 4.5 – Mass Balance of <sup>14</sup> C- IPU Adsorption	108
Table 4.6 – Mass Balance of <sup>14</sup> C- SULPH Adsorption	108
Table 4.7 – Potential Support Materials for In-situ Microcosms	121
Table 4.8 – Mass Balance of <sup>14</sup> C-IPU Desorption	121
Table 4.9 – Mass Balance of <sup>14</sup> C-SULPH Desorption	122
Table 4.10 – Kinetic Model Parameters	131
Table 4.11 – Summary of desorption rates for each kinetic model	132

**Chapter 5: Ex-situ Microcosm Studies of Sulphanilamide and Isoproturon  
Natural and Enhanced degradation in the presence of chalk aquifer  
material**

Table 5.3.1 - Extent of <sup>14</sup> C-IPU biodegradation in sampled boreholes after 84 days of respirometry assays	<b>151</b>
Table 5.3.2 - Extent of <sup>14</sup> C-SULPH biodegradation in sampled boreholes after 84 days of respirometry assays	<b>158</b>
Table 5.3.3 – Student T test results for Transect 1: significant difference between the extent of biodegradation for the same treatments and different wells	<b>165</b>
Table 5.3.4 – Student T test results for Transect 2: significant difference between the extent of biodegradation for the same treatments and different wells	<b>168</b>
Table 5.3.5 – Student T test results for Transect 3: significant difference between the extent of biodegradation for the same treatments and different wells	<b>173</b>

**Chapter 6: Compound Specific Isotope Analysis – a tool to substantiate  
sulphanilamide biodegradation in a chalk aquifer**

Table 6.1 Natural Abundance of Stable Isotopes H C N O S	<b>178</b>
Table 6.2 - HPLC Fraction Collector Settings	<b>187</b>
Table 6.3 – results of isotope analysis for each well sampled at the site	<b>191</b>

## LIST OF BOXES

### **Chapter 2: Natural attenuation of hydrocarbons in groundwater environments – a review**

- Box 2.1 - Considerations affecting *in-situ* biodegradation of contaminants in groundwater **30**

### **Chapter 3: Overview and site characterisation of the chemical production plant**

- Box 3.1 – ‘Porosity of Norfolk chal’ as ‘Effective porosity of Norfolk chalk’. **57**  
Box 3.2 - An estimation of the mass of SULPH removed via natural attenuation **73**

### **Chapter 5: Ex-situ Microcosm Studies of Sulphanilamide and Isoproturon Natural and Enhanced degradation in the presence of chalk aquifer material**

- Box 5.3.1 - Half-life calculations for IPU **152**  
Box 5.3.2 - Half-life calculations for SULPH **159**

### **Chapter 6: Compound Specific Isotope Analysis – a tool to substantiate sulphanilamide biodegradation in a chalk aquifer**

- Box 6.1 - Stable Isotope Nomenclature **187**  
Box 6.1 – Quantifying the extent of biodegradation at the field site **194**

## ABBREVIATIONS

<b>BTEX</b>	Acronym for benzene, toluene, ethylbenzene, and xylene
<b>GC/IRMS</b>	Gas chromatography/isotope ratio mass spectrometry
<b>LC/IRMS</b>	Liquid chromatography/isotope ratio mass spectrometry
<b>MTBE</b>	Methyl <i>tert</i> -butyl ether
<b>PCE</b>	Perchloroethene
<b>TCE</b>	Trichloroethene
<b>TCA</b>	1,2 – dichloroethane
<b>mbs</b>	Metres below surface
<b>IPU</b>	Isoproturon
<b>AFCEE</b>	Air Force Centre for Environmental Excellence
<b>SULPH</b>	Sulphanilamide
<b>BOD</b>	Biological oxygen demand
<b>COD</b>	Chemical oxygen demand
<b>SSSI</b>	Sites of Special Scientific Interest
<b>SAC</b>	Special Area of Conservation
<b>ETP</b>	Effluent treatment plant
<b>CEH</b>	Centre for Ecology and Hydrology
<b>EA</b>	Environment Agency
<b>GF</b>	Graphite felt
<b>EP</b>	Expanded perlite
<b>PP</b>	Pumice pellets
<b>PAH</b>	Poly aromatic hydrocarbon
<b>NA</b>	Natural Attenuation
<b>MNA</b>	Monitored Natural Attenuation

**CERTIFICATE OF ORIGINALITY**

I certify that the work contained in the thesis submitted by me for the degree of Doctor of Philosophy is my original work (1), except where due reference is made to other authors, and has not previously been submitted by me for a degree at this or any other University (2).

Signed (candidate) .....Date: 31 July 2013

- (1) Give details and extent of Joint Work
- (2) If the thesis is in furtherance of a previous dissertation, state where and when the previous submission was made

Word count: 51486

“The important thing is to not stop questioning. Curiosity has its own reason for existing.”

*Albert Einstein*

## **ACKNOWLEDGEMENTS**

Thank you to the Natural Environment Research Council who provided the funding to support this research. This dissertation would not have been possible without the guidance and help of several individuals who in one way or another contributed and extended their valuable assistance in the preparation and completion of this study.

First and foremost, my utmost gratitude to my advisor Dr. Brian Reid, whom I am truly fortunate to have had the opportunity to work with, as he has been my inspiration as I hurdle all the obstacles to reach the finishing point of this research.

A big thank you to the environmental science laboratory technicians: Paul Disdle, Kimberly Goodey, Liz Rix, John Brindle, Judith Mayne and Emma Hooper, whose unfailing support and expertise played an invaluable role in my being able to complete this study. An additional thank you to Paul and Kim, whose efforts afforded me the makings of my final chapter.

Dr Simon Kelly, my second advisor, who facilitated the working relationship with Bayer Cropscience and whose kind concern for my academic development shared valuable insights into the world of isotopes.

Paul Griffiths and Paul Brett, of Bayer Cropscience Ltd, for their enthusiasm and willingness to entertain site visits and provide valuable field samples for me to work with and not forgetting their generous support with research expenses.

My family and friends, especially the Norwich ladies, who carried me through the rough times – you know who you are. My Mum and Dad, who never stopped believing and my two beautiful children Aurora and George, who insisted I stay up late to get the job done.

Finally, I would be remiss if I did not make a special acknowledgment of the innumerable sacrifices made by my dear friend Dr Lauren Roffey, who shouldering far more than her fair share of “woe is me’s” when I refused to face the music.

# Chapter 1:

## Introduction and thesis overview

---

### 1.1 Introduction

#### 1.1.1 Groundwater in Society.

Groundwater is the major source of fresh drinking water, used for human consumption. 68.5% of the freshwater on Earth is locked up in glaciers; this leaves 31.5 % available for human consumption (Table 1.1). The vast majority of this fresh drinking water is stored in groundwater reservoirs. In England groundwater provides one third of the drinking water and is worth £8 billion to the British economy (Environment Agency, 2012).

<i>Major stocks of water</i>	<i>Volume (10<sup>3</sup> km<sup>3</sup>)</i>	<i>% Total water</i>	<i>% Fresh water</i>
<i>Salt water</i>			
Oceans	1 338 000	96.54	
Saline/brackish water	12 870	0.93	
Salt water lakes	85	0.006	
<i>Inland waters</i>			
Glaciers	24 064	1.74	68.5
Permafrost ice	300	0.022	0.86
<b>Fresh groundwater</b>	<b>10 530</b>	<b>0.76</b>	<b>30.06</b>
Freshwater lakes	91	0.007	0.26
Marshes, wetlands	11.5	0.001	0.03
Rivers	2.12	0.002	0.006
Soil moisture	16.5	0.001	0.05
Atmospheric water	12.9	0.001	0.04
Living organisms	1.12	0.0010	0.003
<i>Total water</i>	1 386 000	100	
<i>Total fresh water</i>	35 029		100

**Table 1.1** – Major stocks of water found on Earth, with the water available for human consumption highlighted in red. Source: (Danielopol et al., 2003).

Pollution is a serious threat to groundwater resources and acknowledgement of this has led to the introduction of legislation on a global scale to ensure its future sustainability (European Community, 2000).

Three main sources of pollution threaten groundwater resources (Burke and Moench, 2000):

- 1) *Agricultural* – the application of fertilisers, pesticides and herbicides to farmland, along with excess nutrient contamination via high levels of animal waste leaching from feeding lots.
- 2) *Urban* – leaking sewers, run off and storm drain flood events.
- 3) *Industrial* – fuel transport and storage systems, heavy metals from textile and paper industries, abandoned oil and gas production sites and accidental chemical spills.

In addition to pollution stressor, the rapid increase in global human populations creates an ever-increasing demand for drinking water resources. While the global population has doubled in the last 50 years volumes of usable water, remain unchanged and will not rise to meet the growing demand from human consumption (Table 1.2).

<i>Area</i>	<i>Population (millions)</i>		<i>Usable water supply (km<sup>3</sup> yr<sup>-1</sup>)</i>	
	<i>1985</i>	<i>2025</i>	<i>1985</i>	<i>2025</i>
World	4830	8010	39 300	37 100
Africa	543	1440	4520	4100
Asia	2930	4800	13 700	13 300
Australia + Oceania	22	33	714	692
Europe	667	682	2770	2790
North America	395	601	5890	5870
South America	267	454	11 700	10 400

**Table 1.2** – Human population increases and usable water, available for human consumption, predictions for 2025. Source: (Danielopol et al., 2003).

Historically, groundwater was thought to be a replenishable resource with reserves so great that the impact from one generation would not significantly affect the next (Burke and Moench, 2000). However, in light of the ever growing global population, the pollution stressors that prevail and the recognition of the key services provided by groundwater, concerns regarding its future sustainability have come to the fore (Salzman et al., 2001). Table 1.3 lists the main goods and services associated with healthy groundwater environments.

**Table 1.3 Goods and Services Associated with Healthy Groundwater Environments**

Goods	Services
<ul style="list-style-type: none"> <li>• Safe drinking water for human consumption</li> <li>• Stable supply of water for human needs (agriculture, industry and domestic needs)</li> <li>• Water for sustainable life of microorganisms, plants and animals</li> </ul>	<ul style="list-style-type: none"> <li>• Purification of water (microbiological and physiochemical processes)</li> <li>• Attenuation and/or elimination of chemical contaminants</li> <li>• Contribution to the sustainability of surface ecosystems (e.g. wetlands)</li> </ul>

Source: (Danielopol et al., 2003).

Of particular interest to this thesis is the service provided by groundwater, by virtue of the microorganisms contained within it, to attenuate or remove contaminants and thereby improving water quality. This intrinsic ability to eradicate pollution has been termed ‘natural attenuation’.

*1.1.2 Natural Attenuation – A key service provided by groundwater.*

Over the past decade there has been considerable interest in an aquifer’s ability to naturally attenuate contaminants. The processes, inherent to natural attenuation (NA), include dispersion, dilution, sorption, volatilisation and biodegradation (Environment Agency, 2000b, Rügner et al., 2006, United States Environment Protection Agency, 1999, Wiedemeirer et al., 1995). NA is a non-intrusive physical, chemical or biological process, which does not require human intervention (Wiedemeirer et al., 1999). Its non-intrusive nature makes NA an attractive *in-situ* approach when treating hard to access, sub-surface environments, such as contaminated groundwater (Wiedemeirer et al., 1995). NA has been applied to a wide range of organic contaminants present in a range of environmental settings. There is evidence in the literature to suggest NA is a serious remediation choice for synthetic organic contaminants. This is hardly surprising, as microorganisms have been using natural organic compounds as food sources for millions of years. In order to exploit NA to remediate contaminated soil and/or groundwater it is paramount that the processes involved are closely monitored. Regulating authorities

refer to this as Monitored Natural Attenuation (MNA) and its application is meant to ensure that any contamination remains contained, i.e. does not spread into surrounding environments, and is removed/remediated within a reasonable time-frame (Environment Agency, 2000a).

### *1.1.3 The field study site*

This thesis is directed specifically towards the evaluation of natural attenuation opportunities at an industrial site located in Norwich. The field study site has been operating as a chemical works since the 1950s. Known contacts existed at the site, which facilitated collaboration, beneficial to this research. In that, a recent site-wide report, conducted by the site owners, provided a valuable insight of the contaminated groundwater beneath the site, which spanned a decade and, prompted the drilling and construction of a series of groundwater monitoring wells. Having access to both, the site-wide report and substrate materials, provided during the drilling of the new wells, offered a unique opportunity to study the subsurface environment at the site. Furthermore, groundwater monitoring of the site had drawn attention to unacceptable levels of groundwater contamination. The contaminants of particular concern to the site owner and of potential interest to this study included: the solvents, toluene and 1,2-dichloroethane; the herbicides bromoxynil, ioxynil, isoproturon and Asulam (unstable), and; sulphanilamide a breakdown product of Asulam. The contaminants selected to form the focus of this research and presented herein were determined following the literature review, presented in Chapter 2, which highlighted a limited understanding of the natural attenuation potential for the mobile organic compounds, isoproturon and sulphanilamide.

In addition to the novel contaminants mentioned above, the literature review (Chapter 2) also drew attention to the lack of understanding of natural attenuation processes in chalk groundwater environments, with the majority of studies focusing on shallow sandy aquifers. Therefore having access to this field study site has afforded a unique opportunity to study the natural attenuation potential of novel synthetic organic compounds situated below a chemical production plant within a fractured chalk aquifer.

## *1.2 Thesis overview*

### *1.2.1 Aims*

The main aim of this research was to investigate the natural attenuation potential of isoproturon and sulphanilamide in a chalk groundwater environment. Primarily, this body of work aims to consider *in-situ* and *ex-situ* assessments of these mobile organic compounds to evaluate natural attenuation. The evaluation was made from a number of perspectives with the following objectives: (i) to make use of different lines of evidence to appraise the existence (and vigour) of natural attenuation processes within the aquifer; (ii) to establish if these processes might be enhanced and; (iii) to advance the practical techniques with which to monitor natural attenuation.

The utilisation of natural attenuation processes in contaminated sandy groundwater environments has become widely accepted as a viable tool to remediate immobile organic compounds. This research aims to examine the *in-situ* assessment of mobile organic compounds in a chalk aquifer and, in particular, investigate the natural attenuation potential of sulphanilamide in a chalk groundwater environment.

### *1.2.2 Structure of the Thesis and chapter objectives*

Beyond this introductory section, Chapter 2 provides a review of the literature relating to natural attenuation of synthetic organic compounds in groundwater systems. This chapter has the objective of setting the scene for the subsequent chapters by providing an account of the conceptual underpinning of natural attenuation, and, thereafter, the framing of these concepts from a Regulatory perspective. Given the originality of the research very little literature exists regarding natural attenuation of herbicide compounds (and their metabolites) particularly where they are present at greatly elevated concentrations in association with point source contamination. Consequently, in order to outline the natural attenuation approach and to evidence its applicability, the review makes use of literature relating to more conventional hydrocarbon contaminants.

In Chapter 3, a fuller account of the site is provided. It is the objective of this chapter to give the reader an overview of the spatial distribution of contaminants at the field study site. This chapter synthesises historically collected data to tease out spatial distinct zones of contamination on site. The chapter also reviews the spatial

distribution of electron acceptors across the site and how the distributions of such, evince degradation processes within the aquifer.

Thereafter, three lines of evidence were sought through which to substantiate the applicability of natural attenuation to the field study site. These approaches were *in-situ* assessments of substrate utilisation loaded onto surrogate support materials (Chapter 4), *ex-situ* microcosms studies (Chapter 5) and the use of compound specific stable isotope fractionation techniques (Chapter 6).

Chapter 4 accounts the development of surrogate support media to be used to sample *in-situ* microbial biomass with a view to establishing the specific utilisation of the compounds of interest. Three surrogate support media (pumice, perlite and graphite felt) were appraised with respect to compound loading and compound off-loading. The motivation of the chapter was to develop approaches with which to load surrogate support media with the  $^{13}\text{C}$ -variants of the contaminants of interest and then deploy these loaded-supports within boreholes at the site.

Chapter 5 presents the results of an intrusive collection of aquifer material and groundwater and their use in *ex-situ* microcosm studies to assess the levels of microbial activity, with respects to the two compounds of interest, across the site. These *ex-situ* microcosm studies were undertaken under a range of redox conditions with a view to establishing how redox conditions might be manipulated to enhance catabolic competence within the microbial community. This chapter couples with Chapter 3 and thereby provides an account of synergies and antagonisms that can be used to explain the levels of microbial catabolic competence along three site transects.

While not without their usefulness the *ex-situ* techniques accounted in Chapter 5 have limitations. Most significantly, because material is removed from the site and then screened under laboratory conditions, *ex-situ* methods are subject to criticism regarding their representativeness of onsite conditions. To counter these shortcomings *in-situ* techniques provide the opportunity to make assessments under prevalent environmental conditions. However, efforts to develop *in-situ* microcosms (Chapter 4) had to be abandoned due to the levels of compound off-load from the support materials. This coupled with a change in guidance from the Environment Agency meant these supports could not be deployed at the site. Subsequently, compound specific isotope approaches were used to evidence *in-situ* biodegradation

of the compounds of interest instead (Chapter 6)<sup>1</sup>. Chapter 6 accounts the development of compound specific isotope fractionation approaches with which to unequivocally evidence *in-situ* biodegradation. It was the objective of this chapter to develop novel analytical approaches with which to make this assessment for the specific compounds of interest. The data obtained is presented in the main chapter while the method development is contained within its appendix.

Chapter 7, in keeping with the aims of the research, provides an overarching summary of the preceding chapters. Overall conclusions and recommendations for further work follow thereafter.

---

<sup>1</sup> Had the <sup>13</sup>C-loaded supports been deployed this work would have been precluded (as the off-loaded <sup>13</sup>C-compounds would have altered the <sup>13</sup>C/<sup>12</sup>C ratio in the groundwater).

# Chapter 2: Natural attenuation of hydrocarbons in groundwater environments – a review

---

Hydrocarbon contaminants, present in subsurface environments, threaten drinking water resources and so must be removed. Indigenous microbes, found in groundwater environments, can biodegrade many of these contaminants that threaten drinking water resources (Holliger et al., 1997). Over the past decade, natural attenuation has emerged as a remediation technique that relies on the assimilative capacity of groundwater, and in particular biodegradation processes, to clean up contaminated groundwater (Wiedemeirer et al., 1995).

This review will present the concept of natural attenuation and discuss the processes involved in naturally attenuating contaminants in groundwater environments. In addition, the view adopted by regulating authorities and the evidence required to authorise the implementation of natural attenuation at a contaminated site will be considered. Attention will also be given to emerging techniques, (*in situ* microcosm studies, isotope fractionation and identifying metabolic intermediates) which are able to provide the evidence sought by regulators. Finally, examples of the contaminants, reported in the literature, successfully attenuated will also be discussed.

## *2.1 Natural attenuation*

Over the past decade, research has shown that naturally occurring processes can work to clean up contaminated groundwater, which has, in turn, led to the use of natural attenuation, as a viable remediation tool for treating contaminated groundwater (Sinke and Le Hecho, 1999). Other terms, associated with natural attenuation, found in the literature include intrinsic remediation/bioremediation, *in-situ* bioremediation, passive remediation, and remediation by natural attenuation (RNA). Although often used synonymously with natural attenuation, many of these terms have their own specific meanings (Environment Agency, 1999).

Natural attenuation is a non-intrusive physical, chemical or biological process, which does not require human intervention (Wiedemeirer et al., 1999). Its non-intrusive nature makes natural attenuation an attractive *in-situ* approach when treating hard to access, sub-surface environments, such as contaminated groundwater (Wiedemeirer et al., 1995). Moreover, natural attenuation is often acknowledged as being more cost-effective and less complicated than alternative engineered approaches (e.g. pump and treat). So much so, that in the United States of America, natural attenuation has gained favour with regulators, who demand that engineered techniques be avoided unless evidence can be shown that natural attenuation approaches are less effective (Rice et al., 1995a). Table 2.1 highlights some of the main advantages and disadvantages of using natural attenuation compared to engineered techniques to remediate groundwater.

**Table 2.1 - Advantages and disadvantages of using natural attenuation to remediate contaminated groundwater.**

Advantages	Disadvantages
<ul style="list-style-type: none"> <li>• Contaminant transformation into less or non-toxic species (ideally complete mineralization).</li> <li>• Minimal disturbance to site.</li> <li>• No exposure of contaminants to new environments.</li> <li>• Less expensive than engineered options.</li> <li>• No downtime of works at contaminated site.</li> <li>• Mobile contaminants are usually biodegraded <i>in situ</i>.</li> </ul>	<ul style="list-style-type: none"> <li>• Changes to chemistry and geochemistry can influence natural attenuation.</li> <li>• Non-homogeneous sites can be problematic.</li> <li>• Long time-frame.</li> </ul>

(source: Wiedemeirer et al.(1995))

One advantage of natural attenuation, which involves biodegradation processes, is that contaminants, which are harmful to the environment, can be transformed into safer products (e.g. carbon dioxide and water). Additionally, the non-intrusive nature of natural attenuation means there is no disruption to a contaminated site so the site can remain operative during the remediation process. Furthermore, natural attenuation is not restricted by downtime, unlike engineered techniques, which often need to be manned. Moreover, engineered techniques may be more detrimental to the environment than natural attenuation, in allowing the contaminant to spread (e.g. exposure of groundwater during pump and treat remediation may cause the movement of volatile contaminants to move into the atmosphere).

A disadvantage of natural attenuation can be changes in geochemistry, groundwater velocity, pH, electron acceptor availability, and/or point source contamination, which can alter its effectiveness. Additionally, site characterization can be complicated in non-homogeneous aquifers. However, this can also be problematic for engineered techniques. Furthermore, the period for natural attenuation to remediate a site may be too long. Although, Wilson and Brown (1989) found natural attenuation of petroleum hydrocarbon, via biodegradation processes, was 50 % cheaper and 30 % faster when compared to simple pump and treat techniques.

The processes, inherent to natural attenuation, include dispersion, dilution, sorption, volatilisation and biodegradation (Environment Agency, 2000b, Rügner et al., 2006, United States Environment Protection Agency, 1999, Wiedemeier et al., 1995).

Figure 2.1 shows the natural attenuation processes at work in a contaminated aquifer.

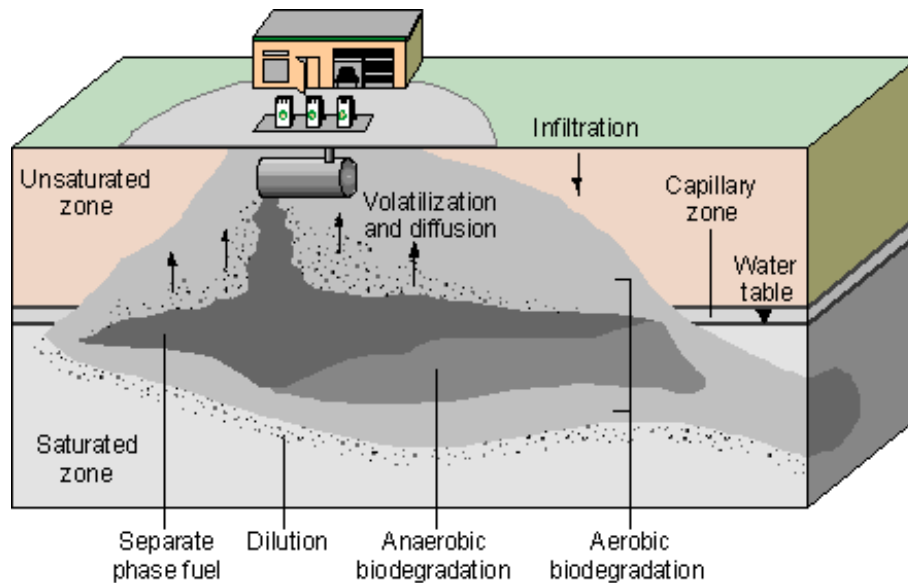


**Figure 2.1** - Conceptual illustration of the important natural attenuation processes that affect the fate of hydrocarbon contaminants in aquifer. Sourced from Bekins et al. (2001).

Natural attenuation is considered most effective when it does not involve the transfer of contamination from one medium or phase to another (Wiedemeirer et al., 1999). Therefore, of these processes, biodegradation is favoured most by regulators as it serves to remove a contaminant from the environment (Environment Agency, 1999). Biodegradation, being a destructive process, removes contaminant mass from the environment. In contrast, the remaining processes (dispersion, dilution, sorption and volatilisation), are non-destructive and so the contaminant mass remains unchanged but the concentration is reduced through contaminant relocation to a different phase or location within the groundwater environment (Wiedemeirer et al., 1999). Hence, the success of natural attenuation, measured by the removal of contaminants from groundwater, relies on the notion that *in-situ* microbial processes can transform contaminants into non-toxic products so they do not pose a risk to the environment. Therefore, to use natural attenuation to manage contaminated sites, it is necessary to demonstrate the occurrence of such microbial processes (Smets and Pritchard, 2003). Conversely, the reliance on microbial processes to remediate contaminated groundwater is not a new phenomenon and was first reported in 1971 when a gasoline pipeline broke, releasing approximately 400,000 L of petroleum into the environment, contaminating the nearby aquifer and subsequently, the local municipal water supply of the Whitmarsh Township in Pennsylvania (Chapelle, 1999).

Interestingly, prior to this, it was widely believed that populations of microbes decreased with depth (in soil) and that groundwater environments were predominantly sterile (Chapelle, 1999).

In the past ten years, regulators have acknowledged natural attenuation as a viable remediation option, in removing hydrocarbon contaminants from groundwater environments (Environment Agency, 1999, United States Environment Protection Agency, 1999, Rügner et al., 2006, Sinke and Le Hecho, 1999). In particular, studies of 271 petroleum plumes in America, have either; reached a steady state equilibrium (59 %) within a short distance from the source or have started to recede (33 %) as a result of natural attenuation processes (Rice et al., 1995a).

The United States Environmental Protection Agency was the first to initiate the regulatory requirements for natural attenuation, following extensive research of leaking underground fuel storage tanks (Rice et al., 1995a, Rice et al., 1995b, United States Environment Protection Agency, 1999, Wiedemeier et al., 1995). The main considerations when comparing remediation options are:

- a) does the contaminated site become clean within a realistic length of time?
- b) is the contaminant prevented from reaching a receptor (e.g. local water supply) (United States Environment Protection Agency, 1999)?

Subsequently, these regulations have been adopted and developed by regulators in the United Kingdom and Europe (Environment Agency, 1999, Rügner et al., 2006, Sinke and Le Hecho, 1999). Rügner et al. (2006) provides a review of the current natural attenuation concepts adopted by each country, which is summarised in Table 2.2.

**Table 2.2 – Overview of existing natural attenuation regulatory approaches/frameworks in various countries**

	United States of America	United Kingdom	Netherlands	Germany	Denmark
<b>Publishing regulating agency</b>	U.S. EPA	England & Wales EA	NOBIS	LABO	DK-EPA
<b>Contaminated land and groundwater management concepts</b>	Human health oriented/risk-based	Human health oriented/risk-based	Human health oriented/risk-based	Groundwater oriented/limit-based (e.g. groundwater is principle receptor)	Groundwater oriented/limit-based (e.g. groundwater is principle receptor)
<b>Demonstration of the efficiency of natural attenuation processes</b>	Three lines of evidence	Three lines of evidence	Three lines of evidence	Decreasing contaminant mass with distance from source	Three lines of evidence
<b>Max. acceptable plume length</b>	-	-	-	-	1 y/100 m
<b>Acceptable time frame</b>	Comparable to other more active measures	30 y	Comparable to other more active measures	-	-

*Source: Rügner et al. (2006)*

A major challenge facing researchers is the development of monitoring tools, capable of substantiating the presence of natural attenuation at a contaminated site. To allow natural attenuation as a remediation option, regulators insist on three lines of evidence (listed below). For natural attenuation to be accepted as a suitable remediation technique for a specific site, the first line of evidence must be met in all cases along with either two or three (Environment Agency, 1999, United States Environment Protection Agency, 1999):

1. An observed reduction in contaminant concentrations along the flowpath downgradient from the contaminant source.
2. A documented loss of contaminant mass at the field scale using chemical and geochemical analytical data (e.g. decreasing parent

contaminant concentrations, increasing concentrations of biodegradation by-products, changes in concentration of electron acceptors and donors, increasing concentration of metabolic by-products). A conservative tracer and a rigorous estimate of the residence time along the flow path to document contaminant mass reduction and to calculate biological decay rates at the field scale.

3. Microbiological laboratory data (e.g. microcosm studies) that supports the occurrence of biodegradation and ascertains biodegradation rates.

The three lines of evidence often centre on the probability of biodegradation. For example, measuring contaminant loss does not provide direct evidence of biodegradation because the loss could be the result of a non-destructive process (i.e. dispersion, dilution, sorption and volatilisation). Furthermore, the Environment Agency (1999) do not accept dilution as a favourable natural attenuation process because its effect is too small to be considered as a suitable remediation option. Therefore, the second and third lines of evidence are required to demonstrate the occurrence of biodegradation processes.

Biodegradation is considered the dominant process involved in natural attenuation because it is the only process that results in significant mass reduction (Wilson et al., 2004). Thus, the evidence sought during the assessment of natural attenuation generally relies on whether biodegradation is occurring at a contaminated site (Wiedemeirer et al., 1995). Therefore, the use of the term, natural attenuation, in the remainder of this chapter will relate to biodegradation processes only.

## *2.2 Evidence of natural attenuation in groundwater environments*

Obtaining evidence to support natural attenuation can be problematic because many factors can influence the *in-situ* biodegradation of contaminants in groundwater (Farhadian et al., 2008). Box 2.1 summarises some of the factors that may affect the success of natural attenuation in the field:

**Box 2.1 Considerations affecting *in-situ* biodegradation of contaminants in groundwater**

- Source and concentration of contaminant
- Chemistry and toxicity of contamination
- Solubility, transport, adsorption, dispersion and volatility of contaminant
- Chemistry, physics and microbiology of groundwater
- Chemistry and mechanics of soil at contaminated site
- Hydrogeology and hydrology of contaminated site
- Environmental conditions, nutrient sources and presence of electron acceptors
- Biodegradability of contaminant, and the presence of a competent biodegrading population of microorganisms

*Source: Farhadian et al. (2008)*

If a source of groundwater contamination is not removed, resulting in a continued influx of fresh contaminant to the groundwater, then natural attenuation processes may be unsuccessful in stabilising the spread of the contaminant plume. Studies by Rice et al. (1995a) found it was possible to predict a distance from a contaminant source, where natural attenuation can prevent a contaminant plume from increasing further, in mass or length. The predicted distance was related to the contaminant source input and the rate of biodegradation by indigenous microbes. Therefore, Rice et al. (1995a) suggested that if the contaminant source was removed a decrease in the plume mass and length would be expected, by as much as 50-60 % a year, until such time as the contamination was completely removed/cleaned up by biodegradation processes.

Natural attenuation can also be influenced by the environmental conditions of the contaminated groundwater. Wiedemeier et al. (1999) explains how in a closed system biodegradation would continue until either; all the contaminant was degraded, the electron acceptors were exhausted, or the environment became toxic to

the indigenous microorganisms. However, aquifers are not closed systems and so they can become replenished by additional contaminant and/or electron acceptors. Therefore, a comparison between biodegradation and contaminant concentration can only be qualitative (i.e. the presence of biodegradation maybe linked to contaminant removal). If quantitative analysis were required (e.g. how much of the contaminant reduction results from biodegradation) it would be necessary to include other factors (e.g. dispersion, advection, sorption and volatilization) that affect the fate and transport of the contaminant. Therefore, it is important to acknowledge which factors are involved when monitoring natural attenuation.

Biodegradation is generally better suited to aqueous phase contaminants because the toxicity of non-aqueous phase contaminants usually prevents microbes, nutrients and oxygen from becoming resident and so biodegradation cannot occur (Wiedemeirer et al., 1999). With regard to natural attenuation, indigenous microorganisms usually have an advantage over non-indigenous species because they are already adapted to the contaminant in their subsurface environment. Although more time consuming, anaerobic degradation is believed to support ongoing natural attenuation more effectively than aerobic degradation in groundwater environments (Farhadian et al., 2007). This is because the oxygen found in groundwater is quickly utilised by aerobic microorganisms as an electron acceptor and its recharge is usually slow, which means it is unable to sustain prolonged aerobic degradation. In comparison, anaerobic processes are more persistent during natural attenuation because there is usually a more generous supply of electron acceptors (e.g.  $\text{NO}_3^-$ ,  $\text{Fe}^{3+}$ ,  $\text{SO}_4^{2-}$ ) associated with the process (Farhadian et al., 2007).

Biodegradation has been shown to be a selective process, with some contaminants being more favourable to biodegradation. The laws of thermodynamics usually govern this with the contaminants requiring less energy to degrade, taking precedence over those needing more. For example, Acton and Barker (1992) have discovered BTEX compounds degrade in a specific order; toluene, m-xylene, ethyl benzene, o-xylene and benzene. Therefore, complex mixtures can often create situations where the biodegradation, of individual contaminants within the mixture, becomes either inhibited or accelerated (Schirmer and Butler, 2004). In some cases the contaminant may even remain recalcitrant (e.g. benzene) when in the presence of a more favourable carbon source (Acton and Barker, 1992).

### 2.2.1 Identification of metabolites as evidence to support natural attenuation

Metabolites, which are unique bi-products of biodegradation processes involving parent compounds, can provide evidence to support the occurrence of natural attenuation. In particular, during anaerobic biodegradation of ethylbenzene, identification of metabolites have been used to support natural attenuation in groundwater (Beller, 2000). Table 2.3 lists the characteristics required for a metabolite:

**Table 2.3 - Ideal characteristics for indicators of metabolism.**

<b>Characteristic of metabolite</b>	<b>Significance</b>
An unequivocal and unique biochemical relationship to the parent hydrocarbon	When found in groundwater, the compound can be definitively related to the metabolism of a specific contaminant
No commercial or industrial uses	When found in groundwater, the compound can be definitively related to metabolism and not to anthropogenic releases of the compound itself
Biological and chemical stability	Stability increases the probability of detecting the compound in groundwater
Generation as an intermediate of mineralization rather than as a product of co-metabolism	The goal of bioremediation is mineralization to innocuous products, not transformation to potentially toxic metabolites

---

*Sourced: Beller (2000)*

There are examples, in the literature, of degradation products being analysed in contaminated groundwater in order to identify biodegradation processes and ultimately support natural attenuation. Martus and Püttmann (2003), identified

metabolites from the anaerobic degradation of alkylbenzenes at a site contaminated with jet-fuel, containing BTEX compounds, which could be used to document *in-situ* biodegradation of alkylated benzenes. The trichloroethylene degradation product, dichloroethylene, was identified at a former fire training area at an air force base and was used to support the occurrence of natural attenuation at the site (Kao and Prosser, 1999). The detection of the metabolite, benzylsuccinic acid identified the presence of anaerobic toluene degradation at a BTEX contaminated site in Germany (Kästner et al., 2006). The biodegradation of methyl-*tert*-butyl ether to *tert*-butyl alcohol was identified at a gasoline spill site and subsequently acknowledged as evidence to support natural attenuation at the site (Wilson et al., 2005). Detection of potential biological processes responsible for the removal of herbicides in a sandstone aquifer were identified by analysing isoproturon metabolites (Johnson et al., 2003b).

### *2.2.2 Carbon Isotope Analysis as evidence to support natural attenuation*

In the past, carbon isotope analysis considered changes in carbon dioxide levels within an aquifer (Landmeyer et al., 1996). It was thought that an increase in carbon dioxide levels brought about by microbial respiration would indicate biodegradation processes. However, the results were often non representative because the carbon dioxide increases would also include the respiration of microbes not involved in the degradation process, and natural sinks of carbon dioxide within the aquifer (Sherwood Lollar et al., 2001).

It has since been established that carbon isotope fractionation occurs during biodegradation processes. When a contaminant is biodegraded the bonds, which hold the compound together, are actively broken. This destruction requires energy and so those bonds that are easiest to break (e.g.  $^{12}\text{C}$ - $^{12}\text{C}$ ) are usually broken first. This means that during the biodegradation process there is a natural enrichment of all the bonds which contain  $^{13}\text{C}$  (McKelvie et al., 2007a, Sherwood Lollar et al., 2001). Compound specific isotope analysis can be used to measure this enrichment and use it as direct evidence of biodegradation. Although, fractionation may also occur during other natural attenuation processes, the levels are usually too small to determine with analytical certainty (Sherwood Lollar et al., 2001). Therefore, when considering the isotope fractionation associated with biodegradation as evidence of

natural attenuation, it would be reasonable to assume that the majority of the fractionation observed results from biodegradation rather than other natural attenuation processes (e.g. dispersion, dilution, sorption and volatilisation).

Research by Sherwood Lollar et al. (2001) demonstrated that gas chromatography/isotope ratio mass spectrometry (GC/IRMS) techniques can be used to obtain evidence of  $^{13}\text{C}$  enrichment of trichloroethene. Their study identified a 40 % reduction in trichloroethene mass compared to the trichloroethene found in the source area. This reduction was attributed to biodegradation due to the enrichment of  $^{13}\text{C}$  observed in the residual trichloroethene located downgradient of the source area. This study was the first to provide definitive proof of biodegradation of both tetrachloroethene and trichloroethene using isotope fractionation techniques. GC/IRMS is very sensitive at identifying the isotopic fractions of contaminants at low concentrations in groundwater. Therefore, it is promising as a new tool for analysing hydrocarbon contamination.

Fischer et al. (2007) determined the presence of anaerobic biodegradation of benzene, using isotope fractionation techniques, in the groundwater beneath a former chemical plant in Germany. Moreover, by analysing both carbon and hydrogen isotope fractionations, Fisher et al. (2007) were also able to determine whether the biodegradation process was aerobic or anaerobic. Natural attenuation of BTEX compounds, in an aquifer; situated beneath a former gasworks site (Griebler et al., 2003) and, contaminated by a leaking fuel storage tank (Richnow et al., 2003), was evaluated using isotope fractionation and the results provided conclusive evidence to support *in-situ* biodegradation of benzene, toluene and xylene. Isotope fractionation has also successfully identified monochlorobenzene biodegradation, with carbon isotope enrichment observed at the outer fringes of a contaminant plume, located in an aquifer contaminated with chlorinated organic compounds (Kaschl et al., 2005). An observed carbon isotope enrichment was able to establish that anaerobic biodegradation of methyl-*tert*-butyl ether was the dominant natural attenuation process occurring in the groundwater beneath a gasoline spill site (Kolhatkar et al., 2002).

Isotope fractionation has the potential to become a key analytical technique in determining natural attenuation because observed isotopic shifts in groundwater can be taken as a direct indicator of biodegradation (Meckenstock et al., 2004).

### *2.2.3 Microcosms as evidence to support natural attenuation*

Microcosm studies are used to understand biodegradation processes. *In-situ* assessments are favoured over ex-situ approaches (that rely upon removing samples from their natural environment) because they are more representative of the field environment (Environment Agency, 1999). This said, laboratory based microcosm studies are habitually used to decide whether biodegradation of a contaminant is likely to occur in the sampled aquifer. A criticism of samples collected from aquifers is that the groundwater removed often targets planktonic microbes, which are suspended in the water column, and overlooks sessile microbes, which become attached to aquifer material (Sturman et al., 1995a). Furthermore, attached microorganisms, which form biofilms, are considered the main proliferators of biodegradation processes (Albrechtsen et al., 1996a). Therefore, both groundwater and aquifer material should be sampled to obtain a true representation of the biodegradation processes, which may be present in a contaminated aquifer. However, it is often difficult to obtain solid aquifer material, especially from deep wells.

Wiedemeirer et al. (1999) lists some factors which can influence the efficacy of laboratory-based studies:

- a) Biodegradation of a contaminant can be the result of a group of microorganisms. Obtaining a field sample can alter the relationship between these groups.
- b) It is very difficult, when studying anaerobic degradation, to remove and transport a sample to the laboratory without it becoming contaminated by oxygen.
- c) Laboratory studies can be costly, imposing limitations on the length of time a study can run. Therefore, it may be possible to underestimate biodegradation processes if the study does not allow sufficient time for biodegradation to become established (i.e. there is often a lag phase).

In addition, it is very difficult to replicate aquifer conditions in the laboratory because of the multifaceted nature associated with sub-surface environments. Therefore, *in-situ* microcosms, designed to imitate aquifer conditions, by their very nature should provide more realistic results than those obtained via laboratory-based studies. The development of *in-situ* samplers, which use (for example) bio-sep® beads to replicate the natural support matrices found inside aquifers, have been successful in determining BTEX biodegradation processes in groundwater contaminated by a gasoline spill (Sublette et al., 2006). Further development of the *in-situ* samplers has led to their use in understanding the roles played by individual microorganisms, within the biofilm community. This is achieved by loading the bio-sep beads with an isotopic tracer, which can later be tracked to an individual species of microorganism (Geyer et al., 2005a). In terms of remediation by natural attenuation, evidence of biodegradation occurring in contaminated groundwater and the microorganisms involved has been established for methyl-*tert*-butyl ether, monochlorobenzene and BTEX (Biggerstaff et al., 2007, Braeckevelt et al., 2007a, Geyer et al., 2005a, Stelzer et al., 2006a, Sublette et al., 2006).

### *2.3 Contaminant natural attenuation in groundwater environments*

Most of the reported cases documenting the occurrence of natural attenuation in groundwater relates to petroleum hydrocarbon contaminants in shallow, unconfined aquifers (of dissimilar textural attributes - sand, silt and clay). In this section (2.3) evidence documented in the literature is reviewed with respect to the most commonly studied contaminants; these being BTEX compounds, Methyl-*tert*-butyl ether, chlorinated compounds and agrochemicals. This review is not intended to be exhaustive but rather to provide a broad canvas upon which to set the specifics of the Thesis. Table 2.4 provides a summary of the current literature.

**Table 2.4 Evidence of natural attenuation of contaminants in groundwater**

Contaminant	Biodegradation processes	Aquifer	Depth (mbs)	Reference
<b>BTEX compounds:</b>				
BTEX	Aerobic (plume edge) and methanogenic (within plume)	Sandy	1.3	(Kampbell et al., 1996)
BTEX	Aerobic (plume edge) and methanogenic (within plume)	Sand to sandy loam	1.2	(Kao and Prosser, 2001)
BTEX	Mainly iron reduction	Clay and fine to medium sands	0.8-1.2	(Kao and Wang, 2000)
BTEX	Anaerobic	Sand and gravel	shallow	(Griebler et al., 2003)
BTEX	Anaerobic	Sand and gravel	shallow	(Richnow et al., 2003)
BTEX	Sulphate reduction	Sandstone and silt	2.3 - 5	(Sublette et al., 2006)
BTEX and MTBE	Aerobic	Sand	-	(Schirmer et al., 1999)
Benzene	-	Sand and gravel	shallow	(Rice et al., 1995b)
Benzene	Anaerobic	Sand and gravel	shallow	(Fischer et al., 2007)
Benzene and toluene	-	Sand and gravel	shallow	(Geyer et al., 2005a)
Benzene and toluene	Iron and sulphate reduction	Sand and gravel	shallow	(Stelzer et al., 2006a)
Ethylbenzene	Anaerobic	Sand	shallow	(Beller, 2000)
Toluene	Anaerobic	Sand and gravel	shallow	(Kästner et al., 2006)
Alkyl benzenes	Mainly sulphate reduction	-	4-5	(Martus and Püttmann, 2003)
<b>Methyl tert-butyl ether (MTBE):</b>				
Methyl tert-butyl ether (MTBE)	Aerobic	Clayey sand	0.6-3.9	(Landmeyer et al., 2001)
Methyl tert-butyl ether (MTBE)	Anaerobic	Layers of coarse sand and silty clay	1.2	(Wilson et al., 2005)
Methyl tert-butyl ether (MTBE)	Anaerobic	Sand and clay layers	0.3-1	(Kolhatkar et al., 2002)
Methyl tert-butyl ether (MTBE)	Aerobic	-	-	(Stocking et

				al., 2000)
Methyl <i>tert</i> -butyl ether (MTBE)	Aerobic	Chalk	20	(Shah et al., 2009)
<b>Chlorinated compounds:</b>				
Tetrachloroethene and trichloroethene	Anaerobic reductive dechlorination	Sand and gravel	12-17	(Sherwood Lollar et al., 2001)
Vinyl chloride	Fe(III) reduction	Sand and gravel	shallow	(Bradley et al., 1998)
Chlorinated solvents (perchloroethene (PCE), trichloroethene (TCE), 1,1,1-trichloroethene (TCA and 1,2 – dichloroethane)	Anaerobic	Sand and gravel	shallow	(McGuire et al., 2004)
Vinyl chloride	Fe(III) reduction	Sand and gravel	shallow	(Bradley et al., 1998)
Monochlorobenzene	Anaerobic	Glaciofluvial sands and gravel	-	(Kaschl et al., 2005)
<b>Agrochemicals:</b>				
Isoproturon	-	Sandstone	7	(Johnson et al., 2003b)
Isoproturon, mecoprop and acetochlor	-	Sand and limestone	40	(Janniche et al., 2010)
Phenoxy acid herbicides (4-chlor-2-methylphenoxypropionic acid (MCP))	Aerobic	Silt and sand	15-16	(Tuxen et al., 2003)

### 2.3.1 BTEX compounds

In the Californian region of the United States of America, the groundwater, situated 6 metres below surface (mbs), in a shallow, sandy aquifer was contaminated, mainly with benzene, from leaking underground fuel tanks, at 271 different sites. A study focused on the plume characteristics at each site and found that 90 % of the plumes had become stable within a very short distance from the source (76 m) and some were even beginning to shrink. On further investigation, this phenomenon was linked to natural attenuation processes occurring at the sites (Rice et al., 1995b).

Petroleum hydrocarbons are usually soluble, mobile and toxic to the environment. Of these compounds, the BTEX suite of compounds is given prominence by regulators because it poses the biggest threat to groundwater environments (Wiedemeirer et al., 1999, Holliger et al., 1997). Therefore, BTEX compounds have

received the most attention, in terms of evaluating its potential for natural attenuation. Although microbes, capable of degrading petroleum hydrocarbons, are widespread the low solubility of oxygen in water ( $10 \text{ mg L}^{-1}$  at  $15^\circ\text{C}$ ) can limit aerobic processes in groundwater environments. Therefore, anaerobic processes which utilise electron acceptors that are more readily available in groundwater environments (i.e. Fe(III) oxides are usually abundant in aquifers) are more likely to dominate (Holliger et al., 1997).

The assimilative capacity of a shallow sandy aquifer to naturally attenuate BTEX was evaluated by Kampbell et al. (1996) by measuring the hydrochemistry, metabolites and reduction in concentration of contaminants in the groundwater. The assimilative capacity of the aquifer was calculated to be  $18\,690 \text{ } \mu\text{g L}^{-1}$ . The BTEX contamination was  $7300 \text{ } \mu\text{g L}^{-1}$ , which was much lower than the assimilative capacity of the aquifer. Therefore, the evidence supported the complete remediation of BTEX through natural attenuation. Moreover, Kampbell et al. (1996) found a direct relationship between the reduction in BTEX concentration and an increase in methane concentration (from a background level of  $1 \text{ mg l}^{-1}$  to  $14.6 \text{ mg l}^{-1}$ ), which indicated methanogenic processes were occurring at the site.

Kao and Prosser (2001) also found methanogenic processes were responsible for the removal of up to 89 % of the mass of BTEX from a gasoline spill, which contaminated a shallow sand/sandy loam aquifer. Kao and Prosser (2001) utilised mass flux calculations and tracer tests to establish that the BTEX plume had become stabilised by natural attenuation and so no longer posed a threat to offsite receptors. The natural attenuation of BTEX, following a gasoline spill, has also been reported under iron reducing conditions, which resulted in the biodegradation of 93 % of the original BTEX mass (Kao and Wang, 2000).

Although there is evidence to support BTEX natural attenuation in groundwater, there have been incidences where the rate of BTEX biodegradation reduces in the presence of other contaminants. Studies by Schrimmer and Butler (2004) show that BTEX biodegradation becomes significantly inhibited when methanol is present in the contaminant plume. BTEX biodegradation reduced from 93 % to 69 % when methanol was present. Of the BTEX compounds, benzene degradation was the most affected decreasing from 84 % to 37 %. This study highlights the difficulty in

establishing natural attenuation processes at sites that contain a mixture of contaminants.

### 2.3.2 Methyl-*tert*-butyl ether

The chemical and physical properties of MTBE make it an unlikely candidate for natural attenuation (NA) process because it is not: retarded by aquifer material, open to microbial attack, easily volatilized from groundwater and it exists in the aqueous phase. Therefore, MTBE can move quite quickly towards a receptor if left to NA processes. Owing to its high aqueous solubility methyl-*tert*-butyl ether will move at the same rate as groundwater (Deeb et al., 2000, Wiedemeirer et al., 1999), which suggests natural attenuation may not be suitable in groundwater having short residence times, where methyl-*tert*-butyl ether is more likely to reach a receptor.

Usually methyl-*tert*-butyl ether biodegradation is limited to aerobic process and because contaminated groundwater is often quickly depleted of oxygen, it is unusual to observe the natural attenuation of methyl-*tert*-butyl ether in the environment.

Nevertheless, high rates of natural attenuation of methyl-*tert*-butyl ether were observed in Florida. The unique characteristics of the site facilitated a high groundwater recharge rate, which in turn continually replenished the groundwater with oxygen. This study suggests, with enough oxygen, that methyl-*tert*-butyl ether could be effectively attenuated (Stocking et al., 2000). In addition, studies have propose that if the groundwater movement is slow then, once the MTBE has migrated beyond the anaerobic zone within an aquifer, biodegradation can become established at a rate considered acceptable for remediation by NA (National Water Research Institute, 2004). More recently, studies have shown that methyl *tert*-butyl ether can degrade under anaerobic conditions where its migration is impeded.

Wilson et al. (2005) carried out studies on a 10 year old, small methyl *tert*-butyl ether plume (40m) in New Jersey. They found that the plume had been attenuated by biodegradation of the methyl *tert*-butyl ether to *tert*-butyl alcohol and that the plume had not migrated far from the source area, as was expected compared to other studies of methyl *tert*-butyl ether. Evidence of biodegradation was presented by the increased concentration of *tert*-butyl alcohol, measured downgradient of the source.

Studies by Landmeyer et al (2001) demonstrate how significant levels of NA of extensive and persistent MTBE plumes can occur if the oxygen limitations are

removed. In their study, however, the addition of oxygen to the groundwater system, moves their approach into the realms of enhanced NA (see section 2.4).

Collectively these reports demonstrate that natural attenuation of methyl-*tert*-butyl ether may be practicable in certain situations.

### 2.3.3 Chlorinated compounds

Chlorinated ethenes (e.g., tetrachloroethene (PCE), trichloroethene (TCE) and vinyl chloride) are the most dominant chlorinated contaminants found in groundwater environments. Chlorinated ethenes are only degraded, via reductive dechlorination, under anaerobic conditions (Holliger et al., 1997). Bradley et al. (1998) found that the extent of vinyl chloride degradation under Fe(III) reducing conditions made it a suitable candidate for natural attenuation in anaerobic groundwater environments. Natural attenuation also plays an important role at a former fire-training site in Florida, where the surficial aquifer (typically < 30 mbs - comprising of shallow beds of sea shells and sand) had been exposed to organic solvents. In particular, methanogenesis is the dominant process, which is successfully attenuating a trichloroethylene plume beneath the site (Kao and Prosser, 1999).

A survey of 191 chlorinated solvent sites and 45 contaminant plumes, in the United States and Europe, was conducted to evaluate the role of natural attenuation. Natural attenuation was considered a viable remediation option at 75 % of the sites. Factors preventing natural attenuation at the remaining sites included: plume not stable, remediation time frame too long, hydrogeology prohibitive, non-destructive processes dominate, geochemical footprint of biodegradation not present (McGuire et al., 2004).

### 2.3.4 Agrochemicals

While a plethora of agrochemicals have been developed and used in the environment studies in to the natural attenuation of them has been limited. This lack of attention is likely due to the diffuse nature of the problem rather than the point-source instances (see above) where natural attenuation has been studied more specifically.

Janniche et al.(2010) analyse an *ex-situ* microcosm, compiled of groundwater and solid material, obtained from a deep sandy aquifer, overlaid with 40 m of unsaturated

limestone. The field site was situated in an agricultural catchment area, resulting in the groundwater becoming contaminated with the pesticides IPU, mecoprop and acetochlor. The microcosm studies established minimal amounts of biodegradation ( $\leq 28\%$  for mecoprop,  $< 5\%$  for IPU and  $6\%$  for acetochlor).

Thrasher et al. (2004) describes mecoprop as a widely used herbicide, which commonly enters groundwater via landfill leachate because it is soluble in water and has a low sorption coefficient. Little research has focused on the biodegradation of mecoprop once it reaches groundwater. Although aerobic biodegradation has been widely observed in the topsoil at depths of  $< 1\text{m}$  the Environment Agency suggest that natural attenuation of Mecoprop should not be considered in groundwater risk assessment until there is sufficient evidence to support attenuation by biodegradation processes (Thrasher et al., 2004).

Evidence of the biodegradation of isoproturon was observed by the detection of the metabolite monodesmethyl–isoproturon in the groundwater which accounted for about  $30\%$  of the lost parent compound (Johnson et al., 2000b). It should be noted that due to the complexities associated with fractured rock aquifers that isoproturon biodegradation can vary both spatially and temporally even in boreholes situated within  $10\text{ m}$  of one another (Johnson et al., 2000b).

#### *2.4 Enhanced natural attenuation*

In some cases of groundwater contamination, it may be possible to enhance natural attenuation so remediation process can be speeded up. Hydrocarbon contaminants can act as a carbon source for microorganisms. In addition, microorganisms also require nutrients (N, P,  $\text{Ca}^{2+}$ ,  $\text{Mg}^{2+}$ ,  $\text{Na}^+$ ,  $\text{K}^+$  and  $\text{S}^{2-}$ ), electron acceptors (oxygen is the electron acceptor for aerobic metabolism and nitrate, sulphate, ferric, manganese and carbon dioxide in anaerobic processes) and optimal environmental conditions (pH and temperature) in order to utilise the hydrocarbon contaminant in a biodegradation process. Therefore, it may be possible to accelerate the natural biodegradation process by providing the degrading microorganisms with increased concentrations of nutrients and electron acceptors (Farhadian et al., 2008).

Studies have reported that benzene biodegradation under anaerobic conditions (aquifer depth of  $3\text{ -}4\text{ mbs}$  with coarse grained sediment) was stimulated under

sulphate reducing conditions and so by injecting additional sulphate into the aquifer the biodegradation rate was enhanced because the availability of the electron acceptor, sulphate, was no longer a limiting factor (Anderson and Lovley, 2000). An advantage on adding sulphate is that it does not react with reduced metabolites like oxygen would which would take the added electron acceptor away from the benzene degraders (Anderson and Lovley, 2000).

Injection of electron acceptors (nitrate and sulphate) was found to be preferential to only injecting one electron acceptor in the enhanced natural attenuation of BTEX, in particular xylene and benzene. This is because it enhanced two redox zones within the contaminated plume at the same time. In addition, by adding two acceptors at the same time problems of regulatory limits (particularly with respect to nitrate addition) were overcome i.e. constraints relating to total nitrate concentrations were abated by 'splitting' the electron acceptor addition across two species (sulphate and nitrate). By increasing xylene degradation through these manipulations benzene degradation was subsequently stimulated; as the xylene carbon source was depleted less preferred compounds (namely, benzene) were then removed (Cunningham et al., 2001).

Of course manipulating the subsurface redox situation is not without its challenges; these include the practical constraints of making the addition and the regulatory limits associated with certain electron acceptors. Table 2.5 lists some of the problems associated with adding additional electron acceptors to groundwater.

**Table 2.5 – Limitations to the concentration of electron acceptors that can be added to contaminated groundwater**

electron acceptor	max. concentration (mg L <sup>-1</sup> )	reason for limitation
O <sub>2</sub>	9 - 10	aqueous solubility; clogging from formation or from oxidation of Fe(II) to Fe(III)
NO <sub>3</sub> <sup>-</sup>	80 - 100	regulatory concern - drinking water limit 50 mg L <sup>-1</sup>
SO <sub>4</sub> <sup>2-</sup>	100 - 250	formation of inhibitory sulphide; regulatory concern - drinking water limit 250 mg L <sup>-1</sup>
Fe <sup>3+</sup>	0 - 1	Fe(III) salts have very low aqueous solubilities; aquifer clogging from precipitation of FeS

Source: Cunningham et al. (2001)

### 2.5 Conclusion

The aim of this review was to consider the present utilisation of natural attenuation as a viable option to remediate contaminated groundwater. From this study it is clear that much of the research has focused on the fuel contamination of groundwater in shallow, sandy aquifers. Furthermore, the majority of research which supports the use of natural attenuation relates to ideal aquifer conditions (e.g. shallow sandy aquifers with uniform flow) (Rice et al., 1995a, Rice et al., 1995b, Wiedemeirer et al., 1999, Wiedemeirer et al., 1995). This is because they are easily contaminated as they have no confining layer and only a thin unsaturated zone to protect them. In complicated aquifers (e.g. fractured chalk and limestone) the groundwater flow can

be hard to predict and so natural attenuation, as a remediation option, is often thought of as being too expensive because of the high costs associated with complex site characterisation (Environment Agency, 1999). This said, studies in the UK and Europe have demonstrated that biodegradation can occur at levels that may prove suitable for natural attenuation consideration in fractured chalk and limestone aquifers, (Janniche et al., 2010, Johnson et al., 2000b).

Through the review of the literature it has become apparent that limited research exists regarding agrochemicals. Likely factors are that agrochemicals are usually found at low concentrations in groundwater, because they are generally utilised at the point of application (soil); this in turn reducing amounts of compound able to leach into groundwater. In addition, agrochemical inputs to the land are diffuse and as a consequence high concentration point-source contamination is unusual.

This thesis has positioned itself to explore novel aspects of natural attenuation (as indicated by the knowledge gaps in the literature review presented above).

Originality in the research reported in this thesis is evident with regards to: i) chemical class (namely, agrochemicals), ii) their occurrence in high concentrations owing to their point-source origin, and iii) aquifer type (a fractured chalk aquifer).

# Chapter 3: Overview and site characterisation of the chemical production plant

---

## *3.1 Introduction*

The focus of this chapter is to assess the site-wide groundwater monitoring data for a contaminated chemical production plant and to establish any evidence to support the use of natural attenuation as a risk-based remediation strategy. Therefore, the aims and objectives are to synthesise and evaluate the groundwater data in order to:-

- Characterise the present state of the contaminant plume at the site,
- Calculate and estimate the percentage of biodegradation occurring using biological and chemical oxygen demands recorded for the site,
- Identify the redox zones present in the contaminated plume in order to understand which biodegradation processes may dominate.

### *3.1.1 Defining natural attenuation*

Natural attenuation may be applied as a risk-based remediation strategy if it can be established that contaminants are or will be reduced to an acceptable level before reaching a receptor/compliance point (Wilson et al., 2004). Natural attenuation processes generally comprise of sorption, dilution, dispersion, volatilisation and biodegradation processes. However, only biodegradation processes are proficient in reducing a contaminant mass. Therefore, gathering evidence to support natural attenuation often focuses primarily on whether biodegradation is occurring at a rate that will protect surrounding receptors from risk of contamination (Air Force Centre for Environmental Excellence (AFCEE), 1995, Wiedemeier et al., 2007d, Environment Agency, 2000a).

The Environment Agency (2000) define natural attenuation in groundwater as follows:

*“The effect of naturally occurring physical, chemical and biological processes, or any combination of those processes, to reduce the load, concentration, flux or toxicity of polluting substances in groundwater. For natural attenuation to be effective as a remedial action, the rate at which those processes occur must be sufficient to prevent polluting substances entering identified receptors and to minimise expansion of pollutant plumes into currently unpolluted groundwater. Dilution within a receptor, such as in a river or borehole, is not natural attenuation.”*

Three lines of evidence are required to demonstrate natural attenuation at field sites: (1) documented loss of contaminant mass over time, (2) geochemical and biochemical indicators resulting from the reduction in contaminant concentrations and, (3) microbiological data supporting the occurrence of biodegradation (Environment Agency (EA), 2000, Wiedemeier et al., 2007d, United States Environmental Protection Agency (EPA), 1999).

In this chapter, attention will be given to the first two lines of evidence. The third, involving exploration of microbiological data, will be considered using *ex-situ* microcosm studies (presented in Chapter 5) and compound specific isotope analysis (presented in Chapter 6).

### *3.1.2 History of study area*

The field study site has been operating as a chemical works since the 1950s with the present owners taking over management of the site in 2000 (Norwich City Council, 2010). Figure 3.1 shows an aerial view of the field study site.



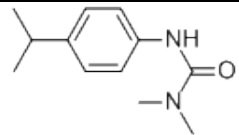
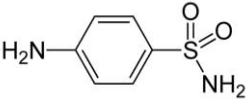
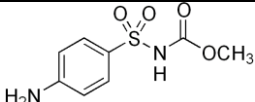
*Figure 3.1 – Aerial photograph of chemical production plant (Google Maps, 2012).*

The site is divided into 10 working vicinities (grouped according to the industrial processes and type of chemical production taking place), which combined, contain 92 monitoring wells. Groundwater monitoring of the site, since ownership in 2000, has drawn attention to unacceptable levels of groundwater contamination, in 4 of the 10 working vicinities, which now require remediation. The contaminants of particular concern to the site owner include, toluene, 1,2-dichloroethane, sulphanilamide (SULPH), Asulam, bromoxynil, ioxynil and isoproturon (IPU). Currently the site houses its own effluent treatment plant, situated south of the site (bottom, centre of the aerial photograph in Fig. 3.1), which utilises pump and treat methods to remediate the groundwater before it is discharged from the site.

The findings of this review suggest, for the contaminants of interest i.e. SULPH and IPU that concentrations are reducing at the site. The physical and chemical properties of which are shown in Table 3.1, along with those for the parent compound of SULPH, Asulam. This evidence coupled with the results of the

remedial indicators, which highlight favourable conditions for the removal of approximately 40 % of the contaminants via biodegradation processes suggests natural attenuation may be occurring at the site.

**Table 3.1** – Physical and chemical properties of contaminants.

	<b>Isoproturon</b>	<b>Sulphanilamide</b>	<b>Asulam</b>
Compound Type	Herbicide	1. Metabolite of Asulam 2. Veterinary treatment	Herbicide
Chemical Group	Urea	Sulphonamide	Carbamate
Mode of Action	Inhibits photosynthesis	Inhibits enzymatic reactions	Inhibits enzyme synthesis
Formula	C <sub>12</sub> H <sub>18</sub> N <sub>2</sub> O	C <sub>6</sub> H <sub>8</sub> N <sub>2</sub> O <sub>2</sub> S	C <sub>8</sub> H <sub>10</sub> N <sub>2</sub> O <sub>4</sub> S
Chemical Structure			
CAS Name	N,N-dimethyl-N'-[4-(1-methylethyl)phenyl]urea	4-aminobenzenesulfonamide	methyl [(4-aminophenyl)sulfonyl]carbamate
Molecular Weight (g mol <sup>-1</sup> )	206.3	172.2	230.2
Solubility 20°C (g L <sup>-1</sup> )			
Water	0.07	7.5	5 (sodium salt > 600)
Methanol	0.075	-	0.3
Acetone	0.04	≥ 100	0.3
K <sub>ow</sub> pH7, 20°C	Log P = 2.5	Log P = -0.62	Log P = 0.15
K <sub>oc</sub> (ml g <sup>-1</sup> )	36 - 241	124 - 179	40
Degradation			
DT50(days)			
water-phase	40	-	-
water-sediment	149	-	71.9

## *3.2 Methods*

### *3.2.1 Site-wide monitoring report*

The site-wide monitoring report, comprising of 192 pages, contained 122 tables that listed the individual components measured in groundwater samples collected between 2000 and 2007 (Arcadis Geraghty & Miller International Ltd, 2008). The groundwater analysis considered 72 volatile organic carbons, 60 semi-volatile organic carbons, 20 metals, 11 remedial indicators and 9 pesticides. In addition, hydrochemistry measurements were recorded, for each monitoring well, and included the pH, redox potential, conductivity, temperature and dissolved oxygen of the groundwater. There was no indication in the report of variations in sampling to account for temporal or spatial trends. Moreover, it was unclear on the reasoning behind repeat samples with some wells being monitored every 6 months, annually and bi-annually. In its initial form, the information contained in the report was unworkable, in terms of identifying evidence to support natural attenuation, and so, as a first step, the required numbers were transferred to an Excel spreadsheet to facilitate data analysis.

### *3.2.2 Collation and preparation of data*

Data obtained from the monitoring report, alongside supporting literary evidence was collated to complete an initial screening stage, which was subsequently broken down into three main categories; aquifer characteristics, contaminant properties and receptor/compliance points, the details of which are listed in Table 3.2 (Environment Agency, 2000a). The data, in the monitoring report, was presented as discrete values, obtained from non-repeat samples, taken either annually or at six monthly intervals. Whilst collating data for this study, efforts were made to use data that represented the same sampling depth, the area of the site downgradient of the contaminant source and monitoring wells which were sampled consecutively (i.e. over at the very least a two year period). This information was then analysed for trends and used to create a representation of the pathway taken by the groundwater contaminants beneath the site, evaluate the risk of contaminants impacting off-site receptors, determine the plume dimensions and estimate contaminant mass removal via biodegradation processes.

**Table 3.2** – Data required for initial screening of natural attenuation at a field site.

Data	Information
<b>Aquifer characteristics</b>	<ul style="list-style-type: none"> <li>• aquifer status groundwater source protection zone</li> <li>• flow mechanism e.g. fissure/intergranular</li> <li>• direction of groundwater</li> <li>• groundwater velocity</li> </ul>
<b>Contaminant properties</b>	<ul style="list-style-type: none"> <li>• contaminant source and history of release</li> <li>• contaminant plume characteristics</li> <li>• background groundwater chemistry at site and surrounding areas</li> <li>• nature of contamination</li> <li>• evidence to support biodegradation at the site</li> </ul>
<b>Receptor/compliance points</b>	<ul style="list-style-type: none"> <li>• location of receptors e.g. springs, rivers, estuaries, abstraction sites, and their proximity to the site</li> </ul>

*(Modified from Environment Agency (2000))*

### 3.2.3 Aquifer characteristics methodology

A review of government and scientific literature was conducted to obtain the aquifer characteristics. Groundwater protection zones and vulnerability maps were consulted and representative examples created to show zones impacted by the field study site. The groundwater velocity was calculated by retrieving the necessary data from the site-wide report to determine the hydraulic gradient, which was then applied to Darcy’s law to calculate the groundwater velocity at the site. The values required for porosity and hydraulic conductivity were unavailable from the site-wide report and so were sourced from the literature.

### 3.2.4 Contaminant properties

An Excel spreadsheet was compiled, using data from the site-wide report, of contaminant concentration, monitoring well distance from the source of contamination and depth of well to the groundwater. Complete data sets were established, which would facilitate the construction of two-dimensional diagrams to illustrate the location and extent of the contaminant plume beneath the site.

Diagrams were created for both SULPH and toluene to establish whether the plumes did or were likely to create a zone of mixing. Monitoring wells, where repeated concentration measurements were available, spanning a two year period, were used to produce a graph to ascertain the state of the plume, in terms of its type with relation to natural attenuation prospects.

Redox measurements, recorded for each well, were grouped and then presented as a redox ladder to establish which redox conditions were dominant at the site. Redox measurements for both the source area and main vicinities, contaminated with SULPH and toluene, were identified in order to understand and discuss any influence they may have on biodegradation processes. By-products from redox reactions, listed as remedial indicators in the report, were analysed and compared with redox potentials for the same monitoring wells to identify any favourable biodegradation zones.

The hydrochemistry, concentrations of contaminants, metals, remedial indicators and redox potentials were identified from the report, for the monitoring wells up gradient of the source zone, to establish what the background concentrations were for the groundwater at the site. This was necessary so a fair comparison could be made of the groundwater before and after contamination at the site. The values obtained were then compared with background groundwater chemistry for the surrounding area to check their comparability. The reasoning behind this was to clarify whether the up gradient groundwater was representative of uncontaminated groundwater in the surrounding area or whether it was contaminated by an unknown source at the site.

### *3.2.5 Receptor/compliance point*

The location of the site, with respect to nearby residential areas, sites of scientific interest, conservation areas and abstraction sites were located using aerial maps and by consulting published literature. A map was compiled to identify the proximity of such areas (receptors) to the contaminated site, as they would be considered at risk by contaminated groundwater should it not be contained at the site.

### 3.3 Results and discussion

#### 3.3.1 Aquifer Characteristics

The maps in Figure 3.2 represent a simplified view of the geology found in and around central Norfolk, U.K.

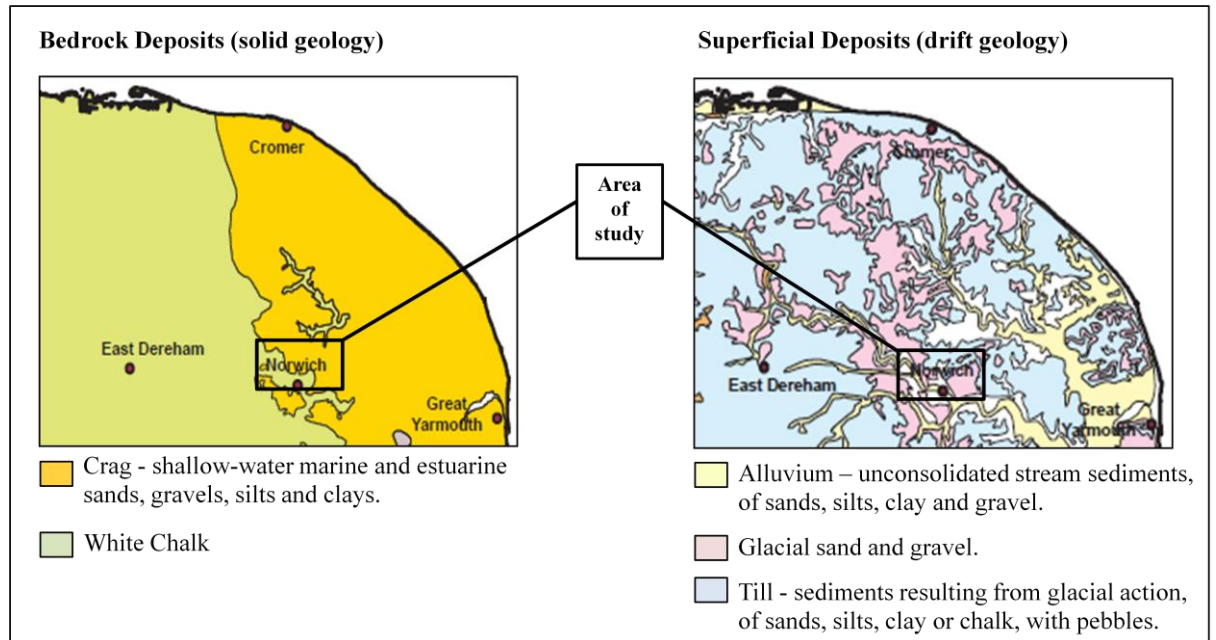


**Figure 3.2** - Simplified geological maps of Norfolk, modified from Holt-Wilson (2010). The area of study highlighted, indicates the region where sampling occurred.

In summary there are two main layers: the bedrock deposits, forming the solid geology and the superficial deposits, also known as the ‘drift’, which overlay the bedrock (Holt-Wilson, 2010). The drift deposits are the result of a succession of sea level rises, stretching as far west as Norwich, followed by periods of glaciations during the Pleistocene period, covering a time scale of approx. 2 million years (Rose, 2009). The bedrock deposit beneath the site is white chalk. The upper surface of which has become softened and weathered to a ‘putty chalk’ by cryoturbation during the Pleistocene (Moorlock et al., 2000 cited in Ander et al., 2006). The drift deposits mainly consist of till, glacial sand and gravel, and alluvium. The type of geology present at the site will affect the chemistry of the local groundwater. For example, higher concentrations of sulphate are recorded in groundwater percolating through glacial drift (till), found at the field study site, compared to those which have permeated Crag (Price, 1987 cited in Ander et al., 2006).

The chalk bedrock beneath the site forms part of a Principal Aquifer – previously classified as Major Aquifers, in that it supports a high level of water storage (Environment Agency (EA), 2012a). Table 3.3 shows the dominant groundwater flow associated with the Principle Aquifers is fracture flow (Environment Agency (EA), 2000).

<b>Dominant flow mechanism</b>	Intergranular flow	Oxford Clay; Blue Lias; Peat; Lacustrine deposits	Alluvium; Fluvio-Glacial Sands & Gravels	Thames Greensands Gravels;
	Intergranular and fracture flow	Jurassic Lower Lias; Mercia Mudstone	Coal Measures; Devonian (Old Red) Sandstone	Permo-Triassic Sherwood Sandstone; Pleistocene Norwich Crag; Triassic Penarth Group
	Fracture flow	Silurian Shales	Millstone Grit	Magnesian Limestone; Carboniferous Limestone; Chalk; Lower Permian Basal Breccias, Conglomerates and Sandstones; Middle Jurassic Limestones.
		Non-aquifer	Minor Aquifer	Major Aquifer
<b>Strategic groundwater resource value</b>				

**Table 3.3** - Classification of the geological formations found in the U.K. with highlighted formations representing those typical of Norfolk (Environment Agency (EA), 2000).

### 3.3.1.1 Groundwater protection zones

Protection zones mark areas where groundwater is abstracted for use as potable water. The zones are ranked from 1 to 3, depending on the risk of pollution from activities occurring on the surface and the distance of such activities from the point of water abstraction (Environment Agency (EA), 2012c). Thus, surface activities, which may cause pollution, occurring closest to abstraction points are considered of greater risk than those located further away. The field site is located within a groundwater catchment area, where the water is abstracted for human consumption and is categorised as zone 3 (Fig 3.4).

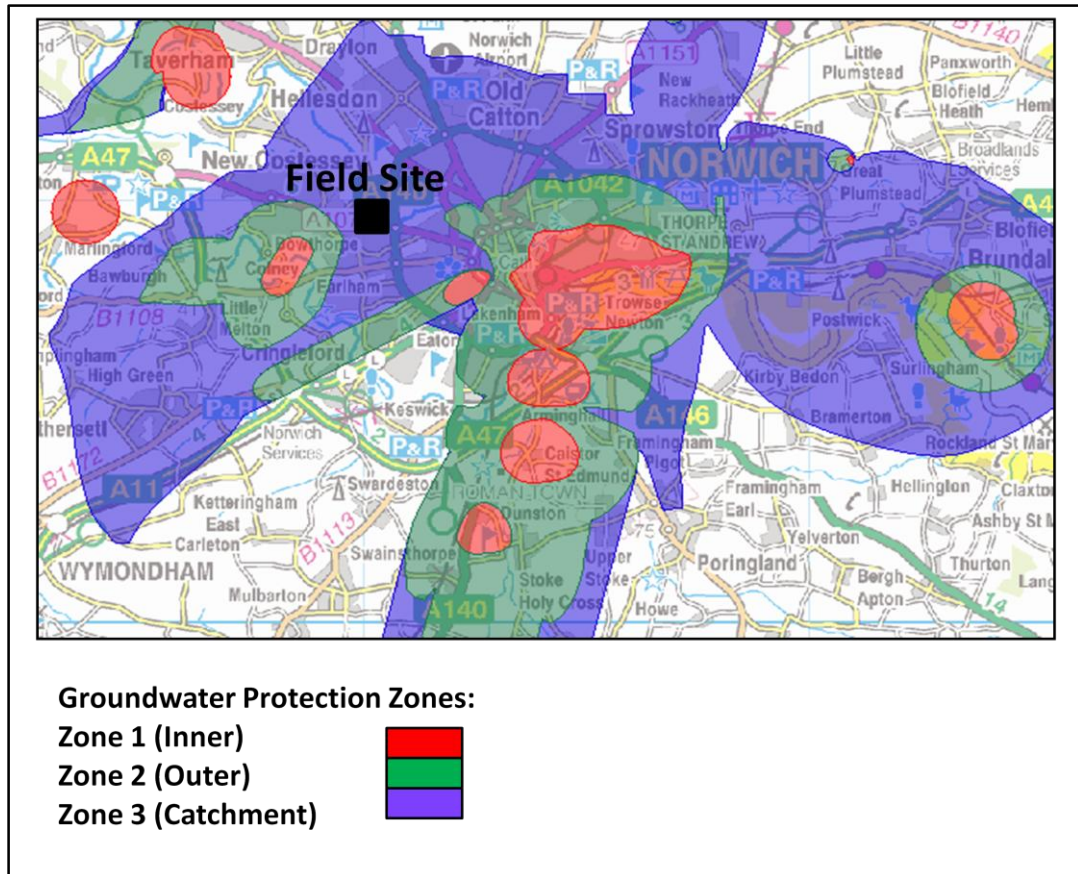


*Figure 3.4 - Groundwater protection zones near to the field study site (Environment Agency (EA), 2012b).*

Furthermore, the type of geology associated with this region offers limited/no attenuating properties (which could work to slow the pathway of contaminants from the surface to the water table (Scottish Environment Protection Agency (SEPA), 2004)). Therefore, in addition to the abstraction protection zone, the groundwater is classed as having a “high vulnerability” (Fig. 3.5).

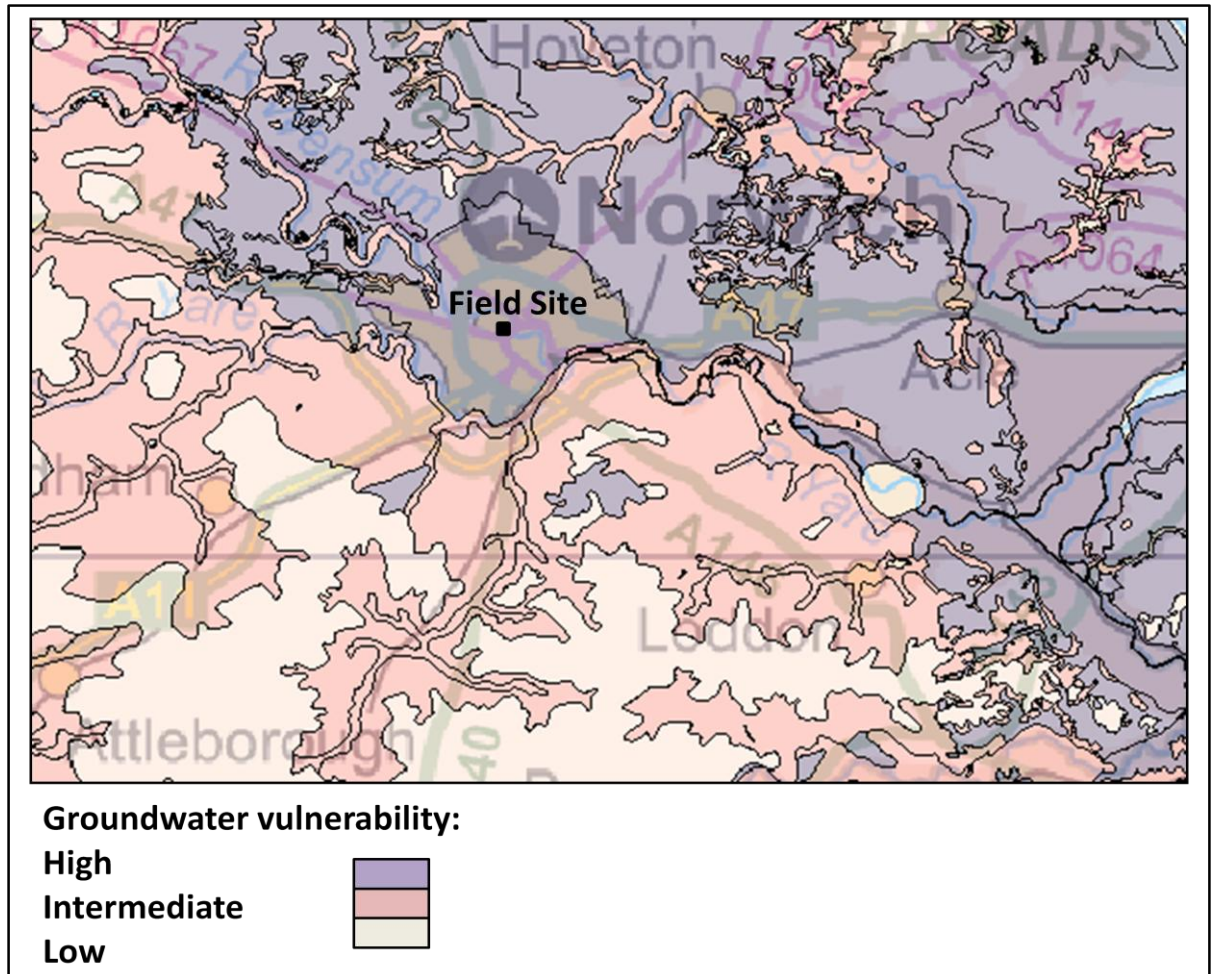


**Figure 3.5** – Map showing the zones of groundwater vulnerability in and around the Norwich area (Environment Agency (EA), 2012b).

### 3.3.1.2 Groundwater velocity

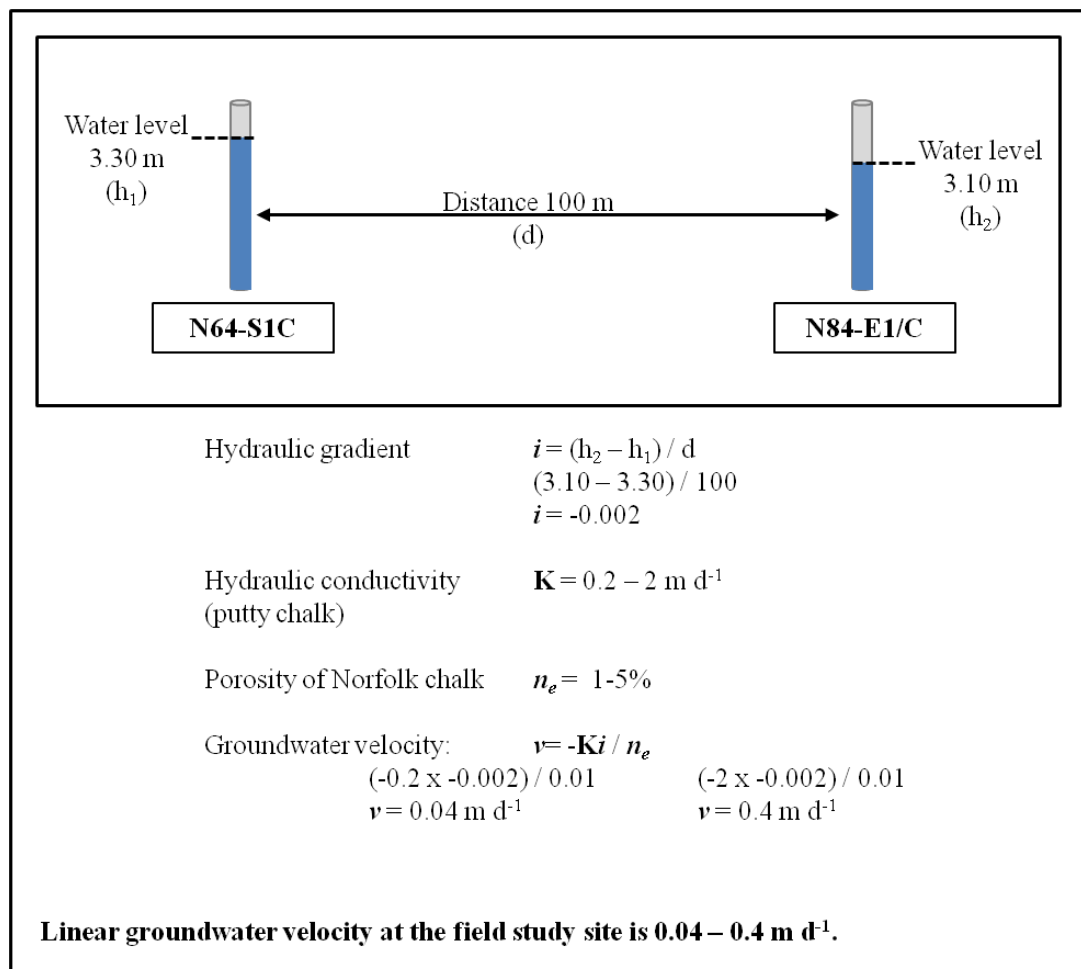
Groundwater velocity or the speed at which it moves through the bedrock is of importance when considering soluble contaminants because they may travel, with the groundwater, from an area of contamination to a point down-gradient whereby they could put environmental receptors at risk. It is possible to estimate the linear groundwater velocity at the site using Darcy’s Law, with an effective porosity term. The equation is

$$v = \mathbf{K}i / n_e$$

where  $v$  is the average linear groundwater velocity;  $\mathbf{K}$  the hydraulic conductivity;  $i$  is the horizontal hydraulic gradient; and  $n_e$  the effective porosity (Hall et al., 1991).

The average linear groundwater velocity at the field study site is 0.04 – 0.4 m d<sup>-1</sup> (Box 3.1). The groundwater movement at the site is slow; this estimation uses the effective porosity value for chalk, which considers clay-bound water and water trapped inside pores.

**Box 3.1** – ‘Porosity of Norfolk chalk’ as ‘Effective porosity of Norfolk chalk’.



*Porosity sourced from Ander et al. (2006) and hydraulic conductivity for putty chalk from Allen (1995).*

Although it is possible to manipulate mathematical equations to predict groundwater flow for a chalk aquifer, the results obtained only offer a guide. This is because Darcy’s Law is based on empirical data obtained from models of aquifers that assume uniform, intergranular flow, such as is seen in sandstones and gravels (represent previously in Table 3.3, whereas the flow through chalk is usually non-uniform, due to its fractured nature. Table 3.4, below, lists the characteristics found

in a chalk aquifer and how these features implicate monitoring of the groundwater. This is evident in the range of ground water velocity calculated for chalk being between 0.04 and 0.4 m d<sup>-1</sup> (Box 3.1). Therefore using such values to interpret contaminant movement through a chalk aquifer, could be problematic in terms of remediation calculations, with time frames for a contaminant to reach a receptor ranging from 10s to 100s of years.

**Table 3.4** – Chalk aquifer characteristics and how they implicate groundwater monitoring.

Chalk Aquifer Characteristics	Implications to monitoring
<ul style="list-style-type: none"> <li>• Fracture/fissure flow</li> <li>• Preferential pathways</li> <li>• Rapid flow</li> <li>• Low fissure porosity/high matrix porosity</li> <li>• Variation in vertical and horizontal permeability</li> <li>• Large seasonal water table variation</li> <li>• Large dispersion</li> <li>• Regional variations in aquifer (e.g. solution features are typical in south-east England)</li> </ul>	<ul style="list-style-type: none"> <li>• borehole location in relation to preferential pathways</li> <li>• variable and rapid travel times influence attenuation and monitoring regime</li> <li>• short-circuiting of normal flow system at times of high water table</li> <li>• thick aquifers and deep unsaturated zones may cause high investigation costs</li> </ul>

(Source: modified from Environment Agency (2000)).

### 3.3.2 Contaminant properties

#### 3.3.2.1 Contaminant source and history of release

Between 1970 and 2005 there have been several reported accidental spills at the site (Arcadis Geraghty & Miller International Ltd, 2008). The details of which are presented in Fig. 3.6. Of particular interest to this study is the interceptor collapse (at building N61), which occurred in 1970, causing a large spill of the chemical Asulam. The actual quantity of the Asulam contamination is unknown. An interceptor works by trapping chemical/waste spills before it can enter a drainage system. In this instance, the collapse of the interceptor enabled a large quantity of

Asulam to enter the drainage system and subsequently contaminate the groundwater beneath the site.

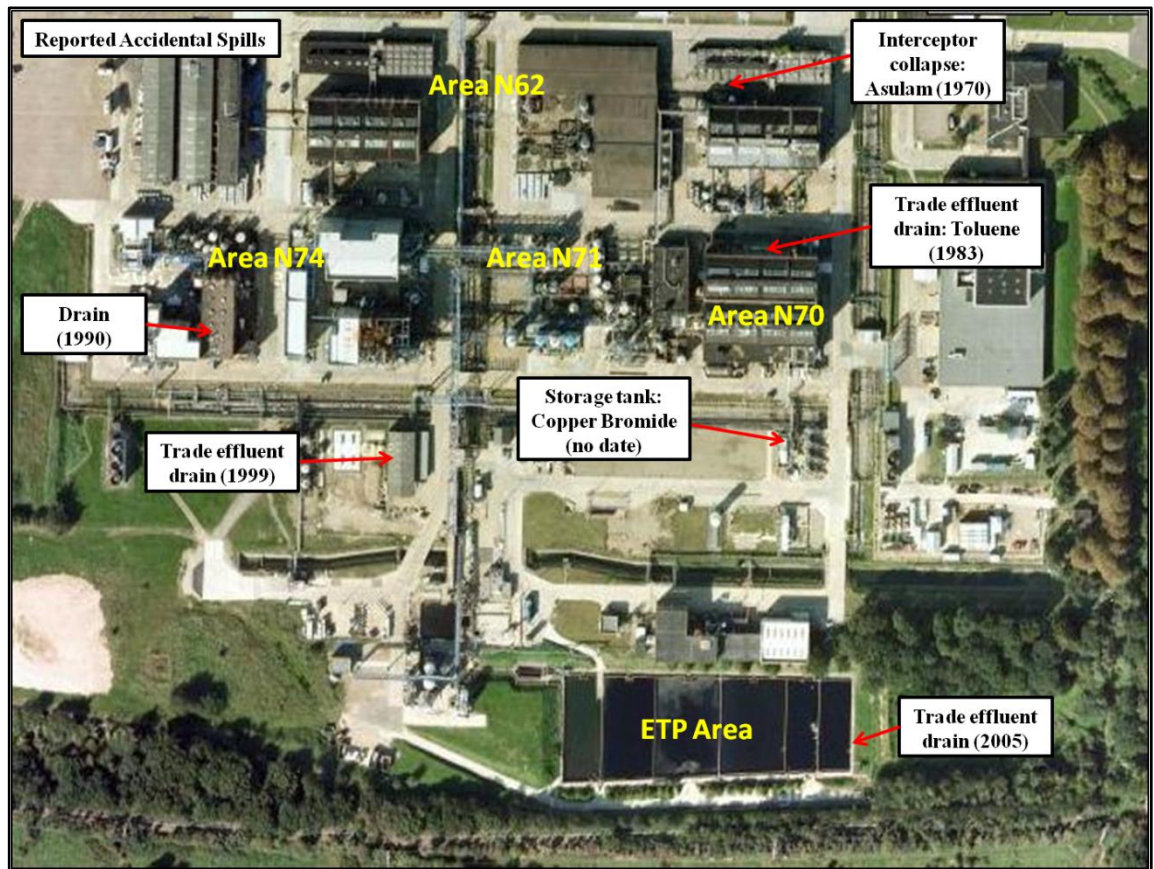


*Figure 3.6 - Aerial view of field study site showing where and when contaminant spills occurred at the site.*

Sulphanilamide (SULPH) is a metabolic bi-product, resulting from the biodegradation of Asulam (Franci et al., 1981). As no SULPH was stored at the site, the large quantities present in the groundwater are believed to result from the biodegradation of the Asulam, spill from 1970. Data documented in the site report, which monitored a consecutive period of two years, was used to calculate the proportion of Asulam to SULPH present in the groundwater and the resulting percentages are plotted in Fig. 3.7, below.

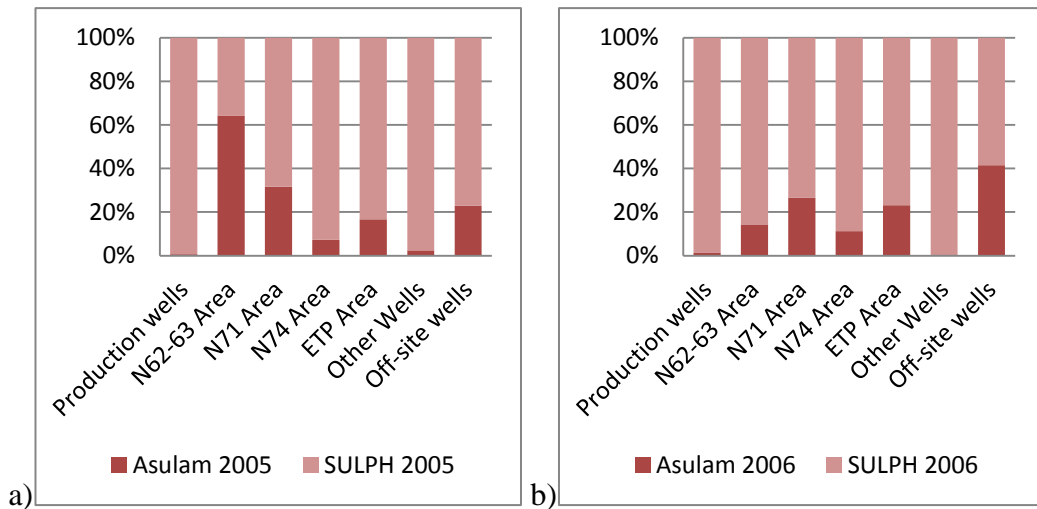


**Figure 3.7** – The average proportion of Asulam to Sulphanilamide, in key boreholes, at the field study site between 2005 and 2006.

The greatest change in the proportion of Asulam to SULPH was observed in the area (N62-63), which is located closest to the source zone (N61). Here, the proportion of Asulam decreased from approximately 65 to 15 %, between 2005 and 2006 and the proportion of SULPH increased from 35 to 85 %. The most likely explanation is that the 50 % reduction in Asulam is the result of its biodegradation to SULPH, which has subsequently increased by 50%. Moving downgradient from the source area, the proportional differences varied less between 2005 and 2006. Why this should be the case is unclear. One factor may be that once the SULPH plume reaches the toluene plume (N71 area), the presence of a more favourable carbon causes a switch in the biodegradation process (Drillia et al., 2005).

### 3.3.2.2 Contaminant plume characteristics

After identifying and analysing the contaminant concentrations for the monitoring wells, situated at a depth of 10 mbs, it was possible to construct a two dimensional diagram of the SULPH plume beneath the field study site. Figure 3.8 represents the results for the SULPH plume, which extends in a south south-westerly direction, approximately 300 m downgradient from the source area, the position of the monitoring wells, relative to the source area are shown, along with the recorded concentrations of SULPH for each well. Note: the diagram is spatially

representative of the site and was constructed by overlaying the concentration data onto the site map.

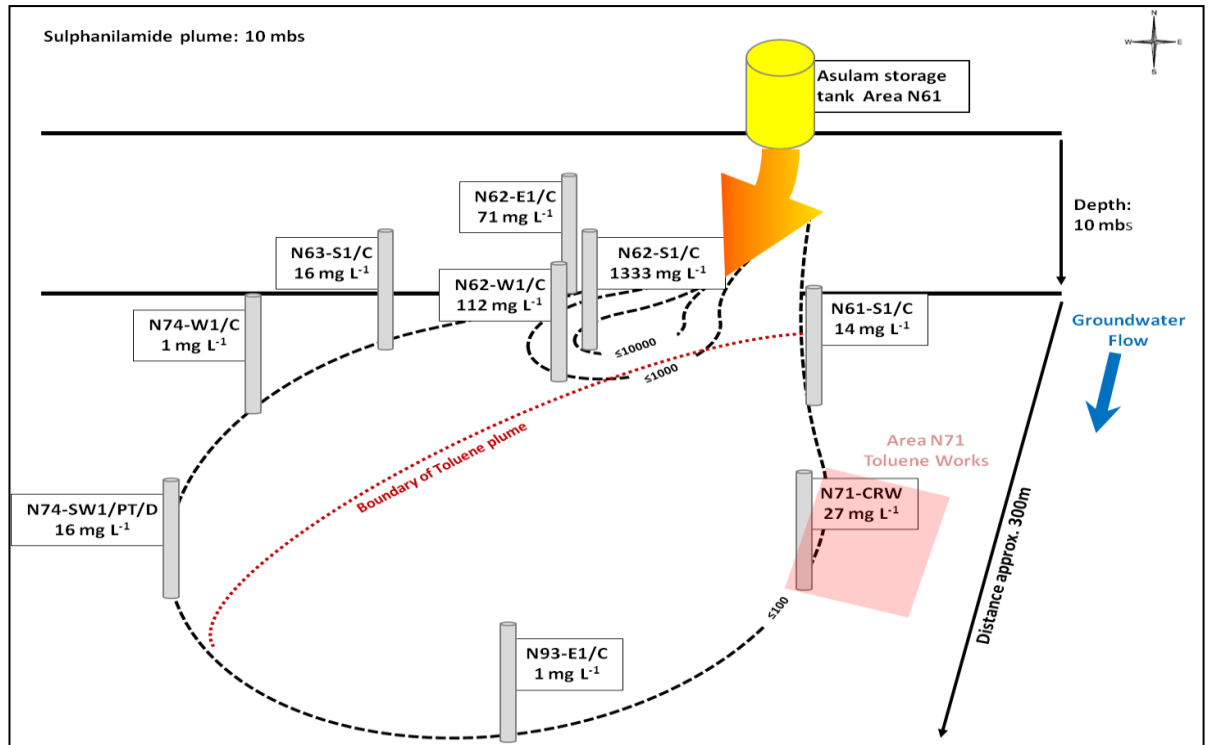


*Figure 3.8 – Diagram of SULPH plume created from concentration data.*

In terms of identifying evidence to support biodegradation processes at the site, the plume, presented in Fig. 3.8, infers a loss in SULPH mass, when comparing concentration verses distance from the source area (Wilson et al., 2004).

Concentrations of SULPH decrease from  $1333 \text{ mg L}^{-1}$  (in the source zone area) to between  $1\text{-}27 \text{ mg L}^{-1}$ , downgradient and at the outer fringes of the plume. However, as discussed previously (Section 3.1.1) a reduction in contaminant concentration, on its own, is insufficient when establishing evidence to support biodegradation process as it may just indicate dispersion or dilution processes (Environment Agency, 2000a, Wiedemeier et al., 2007b). Therefore, further investigation of the reason for the reduction in SULPH is investigated during microcosm and compound specific isotope studies presented in the following Chapters (5 and 6).

Of additional interest, is the location of the toluene works (Area N71) and its proximity to the SULPH plume. The direction of groundwater flow implies the

SULPH plume will spread towards the area containing the toluene works. The concentrations of SULPH, recorded in the monitoring well, in this area support this. Furthermore, as discussed earlier, an accidental toluene spill occurred in the area of the toluene works in 1983, 13 years following the said Asulam spill. Therefore, a zone of mixing is likely to occur when the SULPH plume, which follows the direction of groundwater flow, reaches the toluene works area containing the toluene contamination. Figure 3.9 shows the extent of the toluene plume, which has been constructed using data obtained from the site report. Both Figures 3.8 and 3.9 show the boundaries of the SULPH and toluene plumes so that the zone of mixing can be visualised.

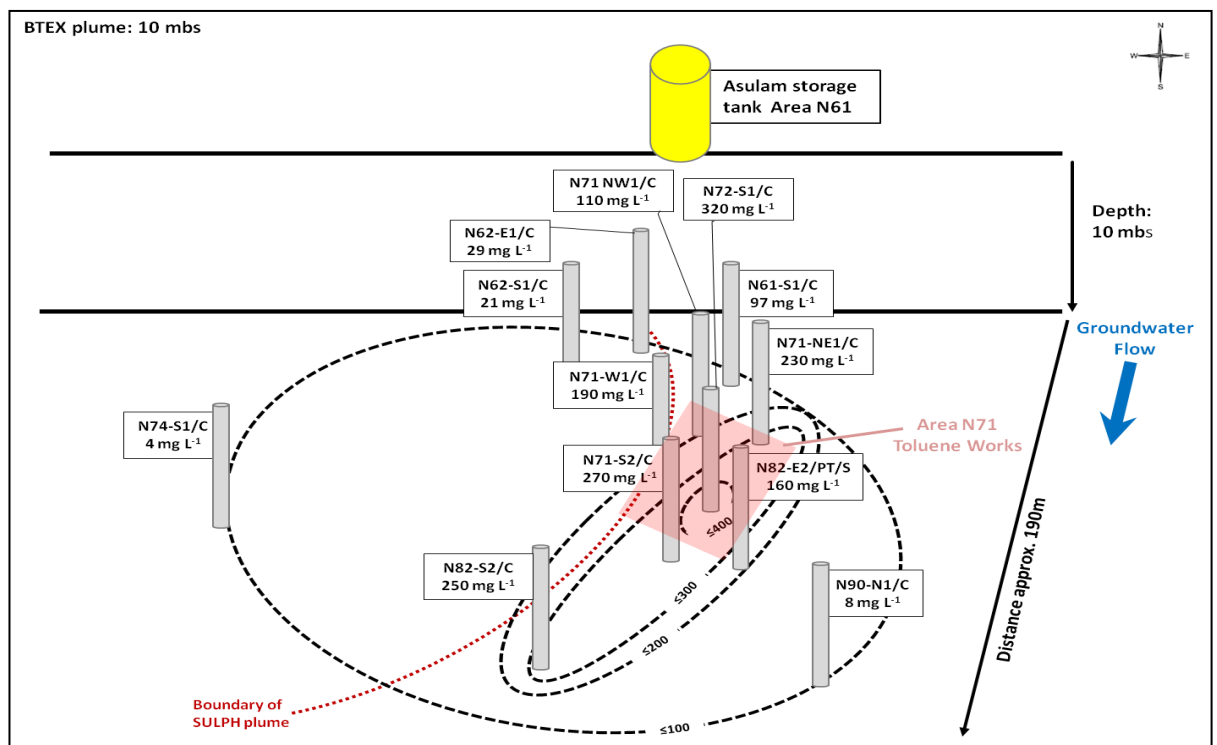
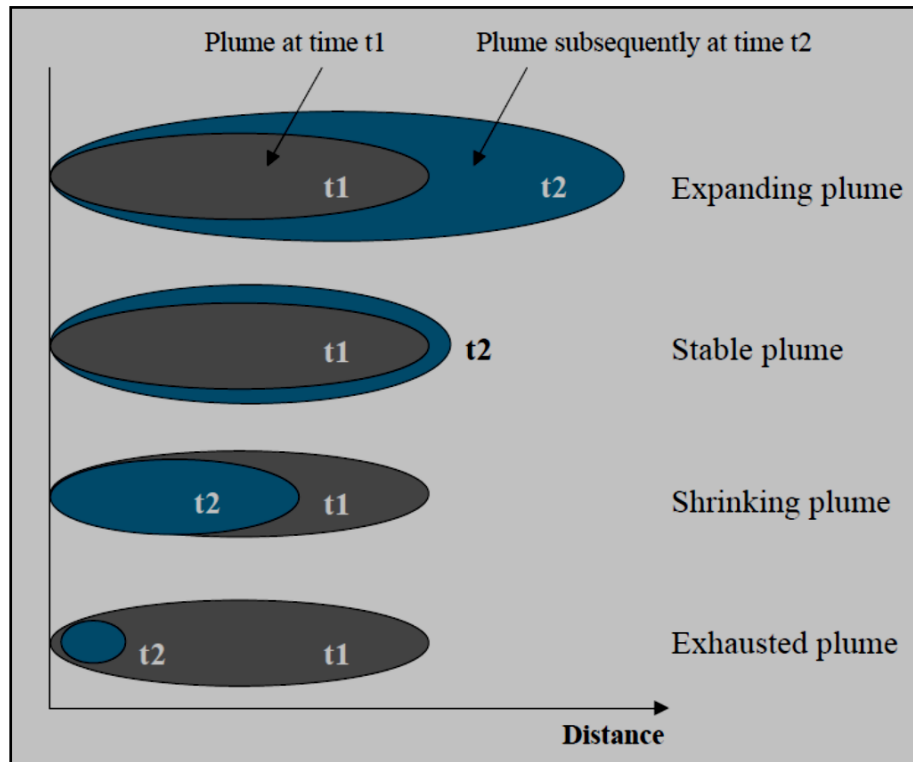


Figure 3.9 – Diagram of toluene plume created from concentration data.

It is likely that, should natural attenuation be present at the site, then the biodegradation processes within this zone of mixing would be impacted by the preferences of the indigenous microbial population towards a carbon source i.e. SULPH and/or toluene. Studies show that variability in plume environmental conditions can significantly influence the adaptations of the microbial population present in the sub-surface environment (Haack and Bekins, 2000). Moreover, in the presence of more than one carbon substrate, microbial populations usually utilize

them consecutively, depending on the energy level required by the microbes to breakdown the contaminant (Schmidt and Alexander, 1985).

Naturally attenuating contaminant plumes can take on several forms; they may be exhausted, shrinking, stable or expanding, depending on the processes responsible for the reduction in contaminant concentration, dissolved in the groundwater (Fig. 3.10).



*Figure 3.10 – Types of naturally attenuating plumes(Wiedemeier et al., 2007d) .*

An expanding plume represents a contaminant that is spreading. This type of plume would pose a threat to any receptors, which lay within its path. Expanding plumes usually indicate that either the source of the contamination is still present and/or the mass input of contaminant is greater than the restorative capacity of the aquifer. Identification of a stable or shrinking plume generally leads to direct evidence of natural attenuation. Stable plumes suggest there are no significant changes occurring and the restorative capacity of the aquifer is capable of maintaining the length of the plume. By comparison, shrinking plumes are those whereby the restorative capacity of the aquifer is capable of reducing the mass of the plume. Exhausted plumes are

usually associated with plumes of very low concentrations, where no change in mass is observed (Wiedemeier et al., 2007d, TNO Institute of Environmental Sciences Energy Research and Process Innovation (NICOLE Report), 1999).

Figure 3.11, below, shows the extent of the SULPH plume, measured at 10 mbs at the study site.

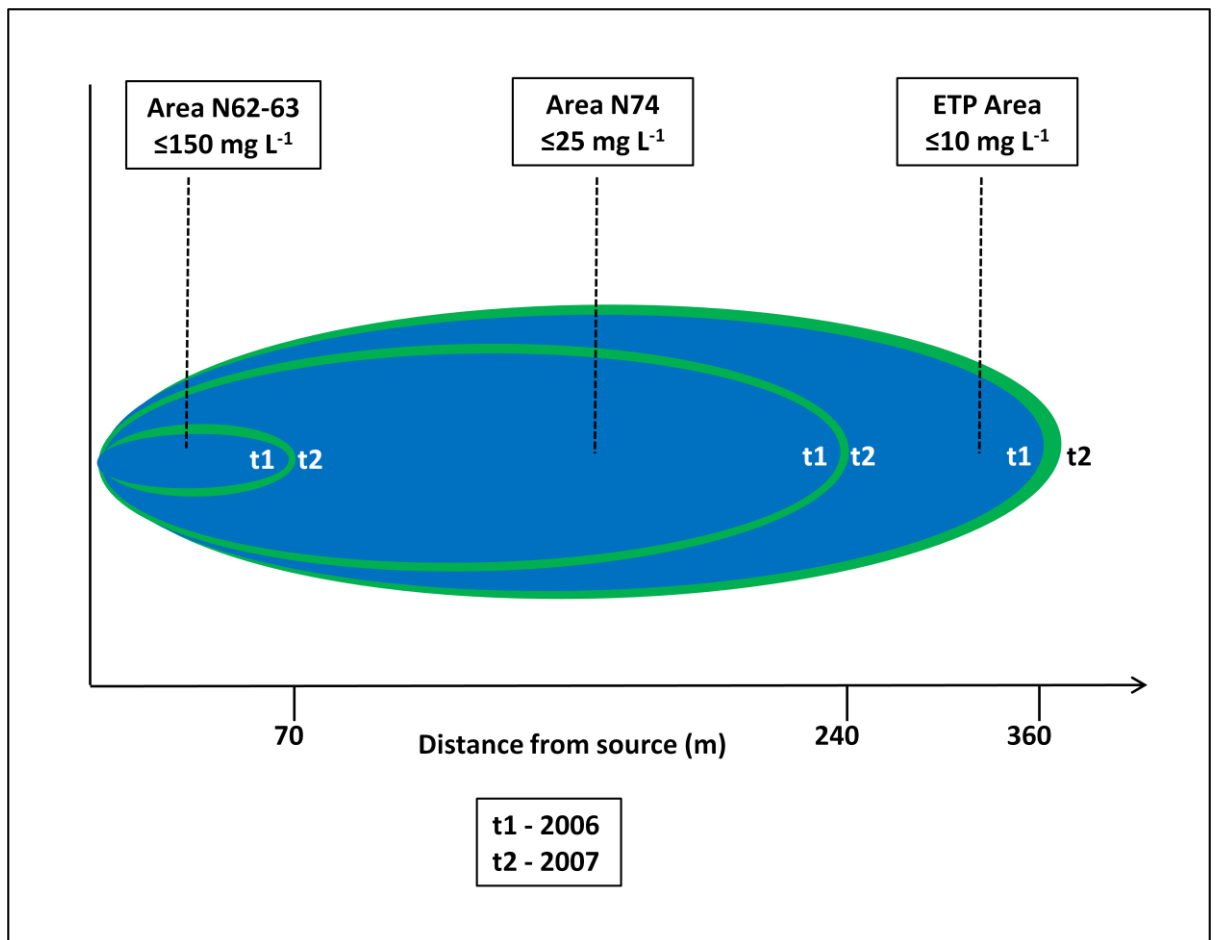


**Figure 3.11** - The extent of sulphanylplume at time, t1 (2006) compared to the extent of the plume at t2 (2007).

The plume is approx. 360 m in length and the concentration of SULPH, dissolved in the groundwater, reduces by one order of magnitude as it moves downgradient of the source. Data recorded for 2006 and 2007. This evidence shows the plume to be stable, which, as discussed above, suggests the restorative capacity of the aquifer may be capable of maintaining the length of the SULPH plume at the study site (TNO Institute of Environmental Sciences Energy Research and Process Innovation (NICOLE Report), 1999).

Alternatively, what appears to be the identification of a stable SULPH plume may just be an indication of a different scenario altogether. In that the plume is not spreading horizontally, downgradient of the source zone but instead is spreading vertically, downwards. This scenario is equally likely because, as discussed earlier (Box 3.1), the groundwater velocity at the site is slow, and so what was observed as a stable plume could simply mean there was no noticeable groundwater movement within the time period studied. Unfortunately, there was insufficient data in the report to consider the extent of the plume for isoproturon.

#### *3.3.2.3 Background groundwater chemistry*

To identify and understand changes in the groundwater chemistry, at the site, it is important to know the composition of the groundwater prior to any contamination episode. The groundwater flow at the site follows a south to south-west direction. Therefore, data (Arcadis Geraghty & Miller International Ltd, 2008) from the monitoring wells situated north of the main chemical works areas (N62-63, N71, N74 and ETP) were used to obtain information on the groundwater chemistry prior to its flow downgradient to the contaminated areas of the site (Fig. 3.12).

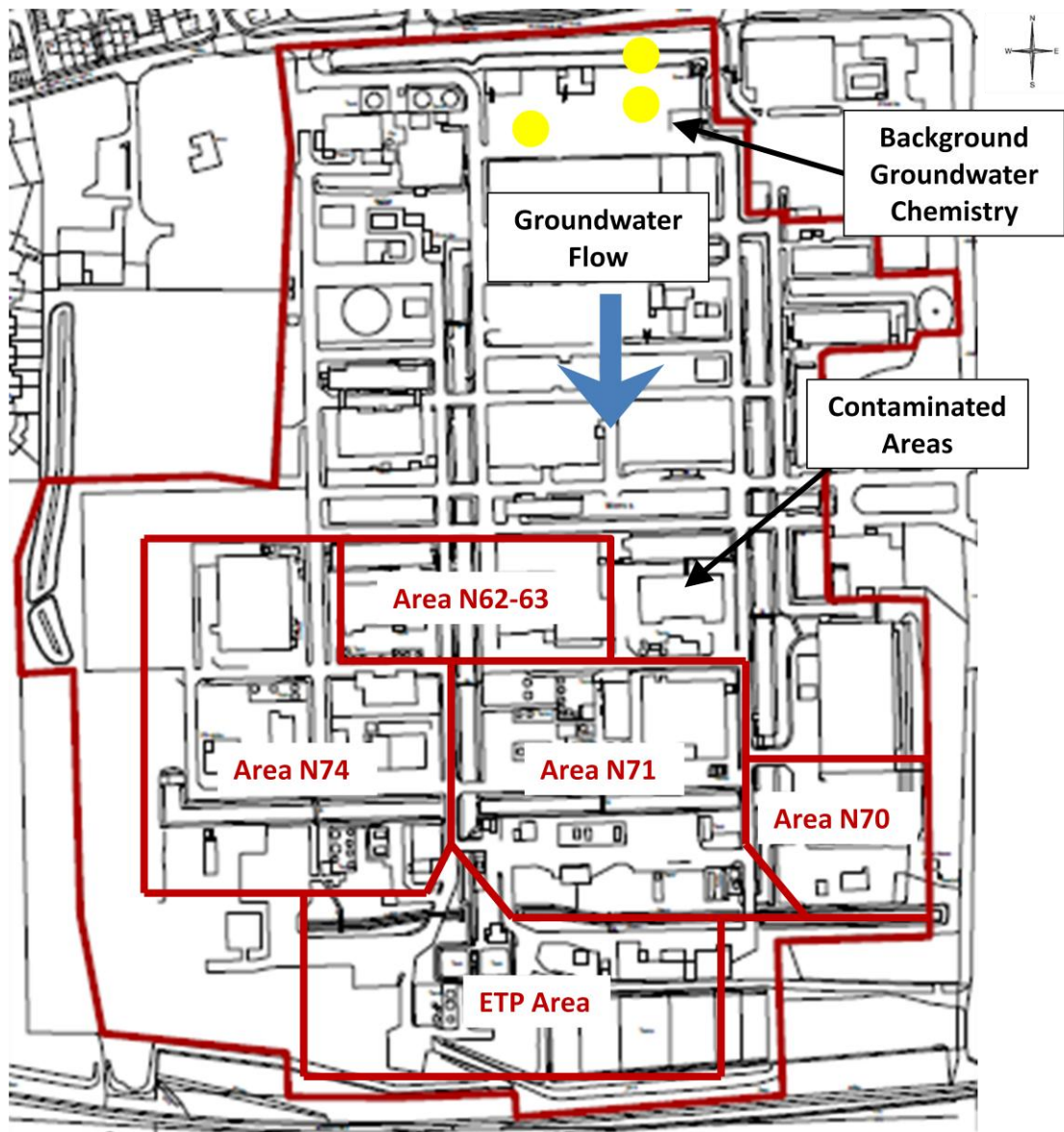


*Figure 3.12 – Schematic of chemical works showing the location of different monitoring areas at the site. Yellow circles represent wells used to obtain data for background groundwater chemistry at the site.*

To establish whether the groundwater chemistry values, obtained from the north (up gradient of the contaminated zone) were a true representation of uncontaminated water the values were compared with literature values for chalk groundwater found in the surrounding area of the chemical plant. Table 3.5 shows the values of the background groundwater chemistry at the site and surrounding areas.

**Table 3.5** – Summary of background groundwater composition at the field study site compared to that found in Norfolk chalk groundwater.

<b>Groundwater Chemistry:</b>	<b>Field study site</b>	<b>Norfolk chalk groundwater (mean)*</b>
pH	7.8	7.1
Redox potential (Eh)	0.2 V	0.03 V
Temp	11.4 °C	11.6 °C
Dissolved Oxygen	3.2 mg L <sup>-1</sup>	≤0.05 mg L <sup>-1</sup>
Nitrate	≤60 mg L <sup>-1</sup>	≤0.09 mg L <sup>-1</sup>
Nitrite	-	≤0.09 mg L <sup>-1</sup>
Ammoniacal Nitrogen	≤1.1 mg L <sup>-1</sup>	≤0.0005 mg L <sup>-1</sup>
Ferric Iron Fe(III)	≤0.4 mg L <sup>-1</sup>	**
Ferrous Iron (Fe(II))	-	**
Sulphate	≤69 mg L <sup>-1</sup>	71 mg L <sup>-1</sup>
Sulphide	-	-
Methane	≤5 µg L <sup>-1</sup>	-
Dissolved Arsenic	2 µg L <sup>-1</sup>	0.85 µg L <sup>-1</sup>
Contaminants:		
Chlorinated hydrocarbons	-	-
BTEX compounds	-	-
Site specific pesticides	-	-

\*Chalk groundwater data sourced from Ander et al. (2006) and the Environment Agency (2009).

\*\*Dissolved iron concentrations vary from 5 – 16600 mg L<sup>-1</sup>, with an average concentration of 402 mg L<sup>-1</sup>, due to its ubiquitous occurrence throughout the Norfolk chalk aquifer, which enables high concentrations to be reached when reducing conditions dominate (Ander et al., 2006).

The data obtained for uncontaminated groundwater chemistry was comparable to other studies. For example, the Table (3.5) shows that pH, temperature, redox conditions (Fe(III) reduction) and sulphate concentrations are the same at the site as those found in the surrounding area (Ander et al., 2006, Environment Agency, 2009). However, dissolved oxygen levels do differ at the site compared to average levels found elsewhere. This discrepancy is likely to be the result of analytical error in the

value reported for the site. Seeing that, the presence of oxygen is unlikely in the presence of methane (Wiedemeier et al., 2007b), which is also reported at the site and, measuring dissolved oxygen levels in the field is extremely problematic due to contamination by the atmosphere once the well water reaches the surface (Rose and Long, 1988).

### Redox Conditions

As mentioned earlier, the groundwater situated beneath the main working areas N62-63, N71, N74 and ETP (Fig. 3.12) has become contaminated, predominantly with SULPH and toluene. When such contaminants enter a pristine aquifer, they alter the groundwater chemistry. Typically the addition of a carbon substrate drives a reduction in dissolved oxygen and as a consequence strongly reducing redox conditions, in and around the source area of the contamination develop (Christensen et al., 2000). The order of change in redox conditions generally follows aerobic > denitrification > Fe (III) reduction > sulphate reduction > methanogenesis, with increasing distance from the source of contamination (Fig.3.13).

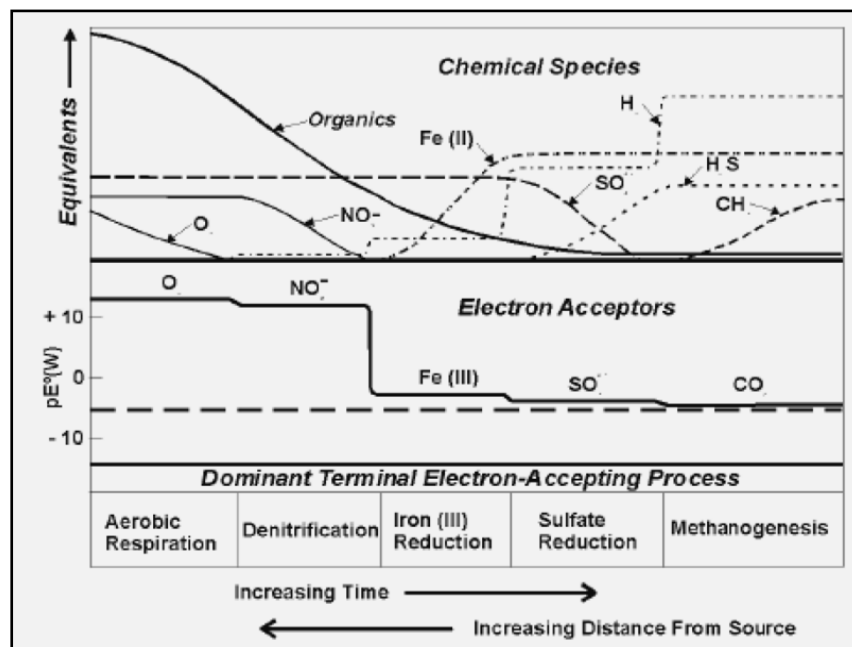


**Figure 3.13** - The effect of organic contaminants on the redox chemistry in groundwater modified from Bower and McCarty (1984).

Measuring redox potentials (Eh) in groundwater can offer valuable insights of an aquifer's hydrochemistry. Redox measurements in the uncontaminated groundwater, recorded up gradient of the contaminant source zone, indicated that the groundwater was predominantly Fe(III) reducing. The graph shown in Figure 3.14 represents the redox potentials measured for all of the monitoring wells across the field study site.

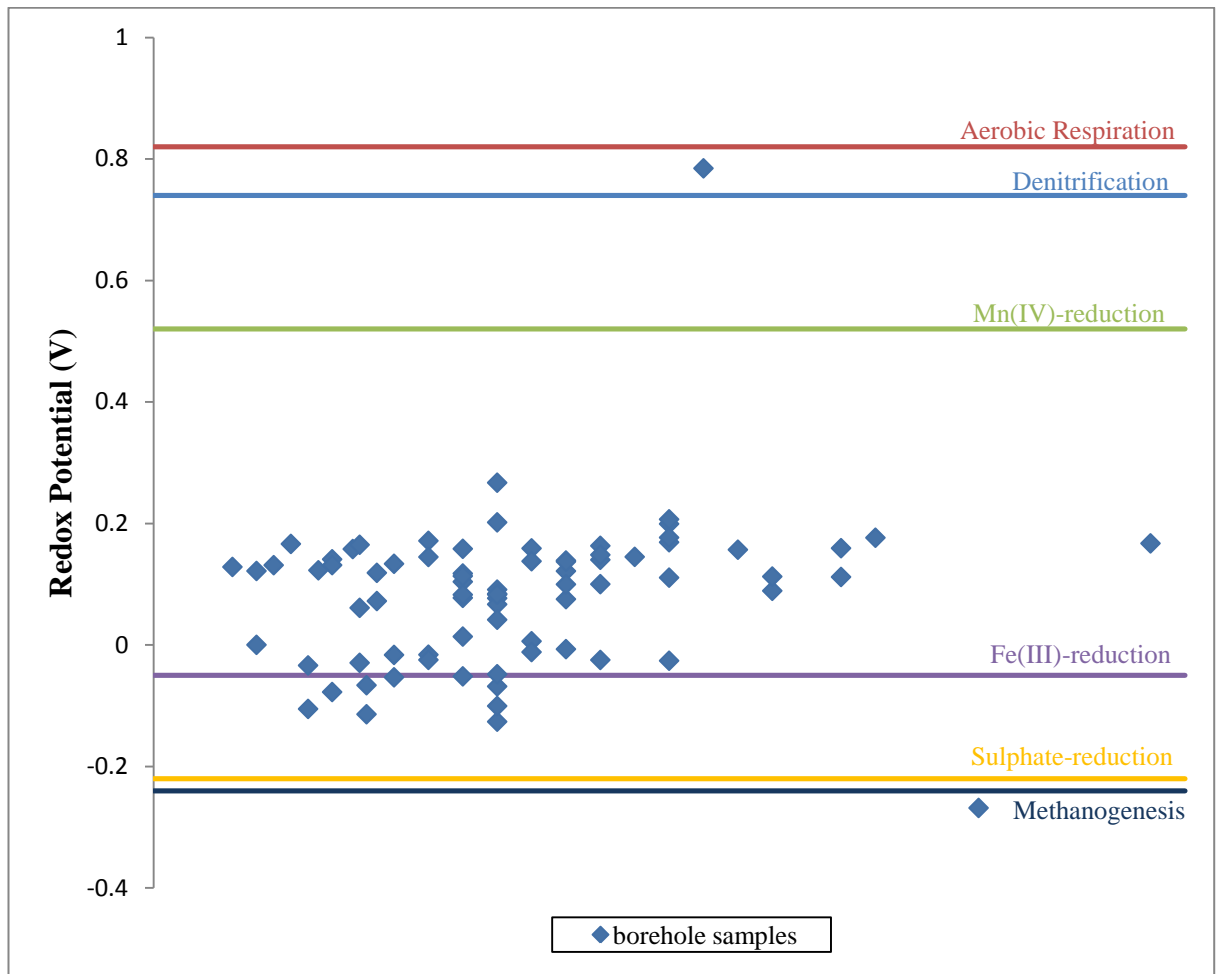


**Figure 3.14** – Redox ladder showing conditions dominant at field study site. Prevailing redox conditions are those samples situated above the data line for each redox potential.

The results in Figure 3.14 show the vast majority of monitoring wells at the site have a redox potential within the Fe(III) reduction zone. This suggests, that overall, the contamination episodes have not changed the redox conditions of the groundwater beneath the site, from those observed in the background groundwater measurements (0.2 V). However, there has been a shift in redox potential from 0.2 V (background

levels) to -0.5 to 0.1 V, which suggesting the environment has become more strongly reduced (Christensen et al., 2000). Furthermore, several monitoring wells are now within the sulphate reduction zone, which may indicate a shift in the catabolic activity of the indigenous microbes. The blue squares on the graph represent individual monitoring wells. The depth of the wells was not of interest as the purpose of this investigation was to identify any shift in redox potential at the site.

#### *3.3.2.4 Nature of contamination*

The nature of the contamination at the field study site results from a complex mixture of various chemical compounds, typically associated with an industrial chemical production plant. The site-wide groundwater monitoring programme, administered by Arcadis Geraghty & Miller International Ltd (2008), groups key hydrocarbon contaminants into volatile organic contaminants (VOCs), semi volatile organics (sVCOs) and site-specific pesticides. Of those listed, the sVCOs are outside the scope of this study and are not considered further. The report indicates that the majority of VOCs present consisted of the chlorinated hydrocarbons: 1-2 dichloroethane and chloroform and, the BTEX compound: toluene. The bulk of the site-specific pesticides were listed as Asulam, sulphanilamide and isoproturon. Of the 141 contaminants listed, the most prevalent contaminants measured at the site were toluene (320 mg L<sup>-1</sup> in Area N71); 1-2 dichloroethane (27 mg L<sup>-1</sup> in Area N71), Asulam (17 mg L<sup>-1</sup> in Area N62-63), SULPH (133 mg L<sup>-1</sup> in Area N62-63), isoproturon ( $\leq 9 \mu\text{g L}^{-1}$  in Areas N62-63 and N70-74) and Bromoxynil (2 mg L<sup>-1</sup> in Areas N71-74). (Fig. 3.11 shows where the contaminated areas are situated).

The solubility of SULPH and toluene at 20 °C is 500 and 470 mg L<sup>-1</sup> respectively. As the levels of SULPH and toluene contamination recorded at the site are less than this, it is fair to assume that both these contaminants will be in the dissolved phase and located in the groundwater. This means that both SULPH and toluene will be mobile and capable of moving with the direction of groundwater flow. This is also true of Asulam and isoproturon, whose solubilities are >5,000 and 70 mg L<sup>-1</sup> respectively, and so are likely to be in the dissolved phase also.

As discussed earlier, groundwater flow at the site is slow,  $\leq 0.4 \text{ m d}^{-1}$  (Box 3.1). The distance from the source of SULPH and toluene contamination to the environmental receptors, situated south of the site is approximately 400 m. Thus if the dissolved contaminants followed the linear velocity path proposed for the groundwater (Box 3.1) it would take between 2.7 and 27.4 years for the contaminants to migrate to the environmental receptors. However, as noted earlier, predicting groundwater flow at the site is challenging because of groundwater flow along fissures rather than through the bulk chalk matrix. To complicate matters further, groundwater flow is also distorted because groundwater abstraction takes places at the southern edge of the site (to facilitate current pump and treat methods of groundwater remediation).

### 3.3.2.5 Evidence to support biodegradation at the site

The values obtained for the biological and chemical oxygen demands of the groundwater were isolated from the report for the areas where the highest levels of contamination were observed, so as to calculate the likelihood of biodegradation occurring at the site. Table 3.6 below, lists the data obtained and the results for the BOD/COD ratios.

**Table 3.6** - Biological and chemical oxygen demands for the contaminated groundwater at the field study site.

Vicinity at Site	BOD	COD	BOD/COD Ratio
<b>N61</b>	873	1900	0.5
	21	53	0.4
<b>N62</b>	No data	No data	-
<b>N71</b>	83	250	0.3
	193	738	0.3
	139	405	0.3
	71	300	0.2
	120	290	0.4
	277	899	0.3
<b>N74</b>	22	107	0.2
	26	143	0.2

Biological and chemical oxygen demands may be used to establish the percentage of contaminants that are likely to be biodegradable within a groundwater environment. Once the ratios for BOD/COD are obtained, different methods may be employed to interpret them. For example, a value between 0.1 and 1 has been assigned to the ratios calculated in Table 3.6. Here, zero would indicate the contaminants were not biodegradable and 1 that they were highly degradable (Robinson and Thorn, 2005). Biodegradability indexes are often used to assist in the decision making process when regarding bioremediation (Srinivas, 2008):

***Biodegradability index:***

BOD/COD	>0.6	fairly degradable and can be effectively treated biologically
BOD/COD	0.3 - 0.6	seeding required to treat biologically
BOD/COD	<0.3	cannot be treated biologically

Regulators often consider 60 % (BOD/COD x 100 = % biodegradable) as the cut off point for remediation via biodegradation processes because ratios greater than 0.6 indicate easily degradable contaminants and those below 0.3 are hardly degradable (Robinson and Thorn, 2005, United States Environmental Protection Agency, 2002).

Relating the biodegradability index to the calculations made for the field study site it would appear the greatest percentage of biodegradation is likely to occur in the N61 area (with a BOD/COD ratio of 0.5 (Table 3.6). Although, it is worth noting that the ratios calculated for the site will represent the fraction of all the contaminants in the groundwater that are biodegradable (United States Environmental Protection Agency, 2002). Furthermore, the ratios are only an indicator of potential and not a direct measure of actual biodegradation.

Other remedial indicators may be useful to identify whether biodegradation is occurring at the site, for example, when SULPH is biodegraded, an observed increase in sulphate concentration may be detectable in the groundwater (van Haperen et al., 2001). Evidence of this was observed in the data presented for borehole N61-S1/C, where sulphate concentrations had increased from a background level of 68 to 980 mg L<sup>-1</sup>. Stoichiometric calculations, shown in Appendix 1 show



an electron acceptor rather than for its carbon source, which would render its utilization as an electron donor. This possibility is expanded on further in Chapter 5.

### *3.3.3 Receptors/compliance points*

Figure 3.15 shows an aerial view of the chemical plant and the location of receptors and compliance points in the surrounding area. In 1986 and 1993 the areas to the south and south-west of the site were designated as Sites of Special Scientific Interest (SSSI) by English Nature “*in recognition of it being one of the best examples of a naturally enriched calcareous lowland river*” (Sear et al., 2006, Norwich City Council, 2010). In addition, in 2000, the area to the south-east was acknowledged as a Special Area of Conservation (SAC) under the European Habitats Directive as an excellent example of a wetland habitat (Sear et al., 2006).

The hydrology of the nearby river, which travels the southern corners of the site, west to east, is dominated by upwelling groundwater (Sear et al., 2006). Therefore, these protected areas, also known as environmental receptors, could be at risk should the groundwater beneath the site become contaminated via leaking subsurface structures such as sumps or drains, failure of surface areas in storage or processing areas and/or leakage from above ground storage tanks (Norwich City Council, 2010). Further environmental receptors of concern, from contaminated groundwater, are also the residential areas located to the south and south-west of the site.

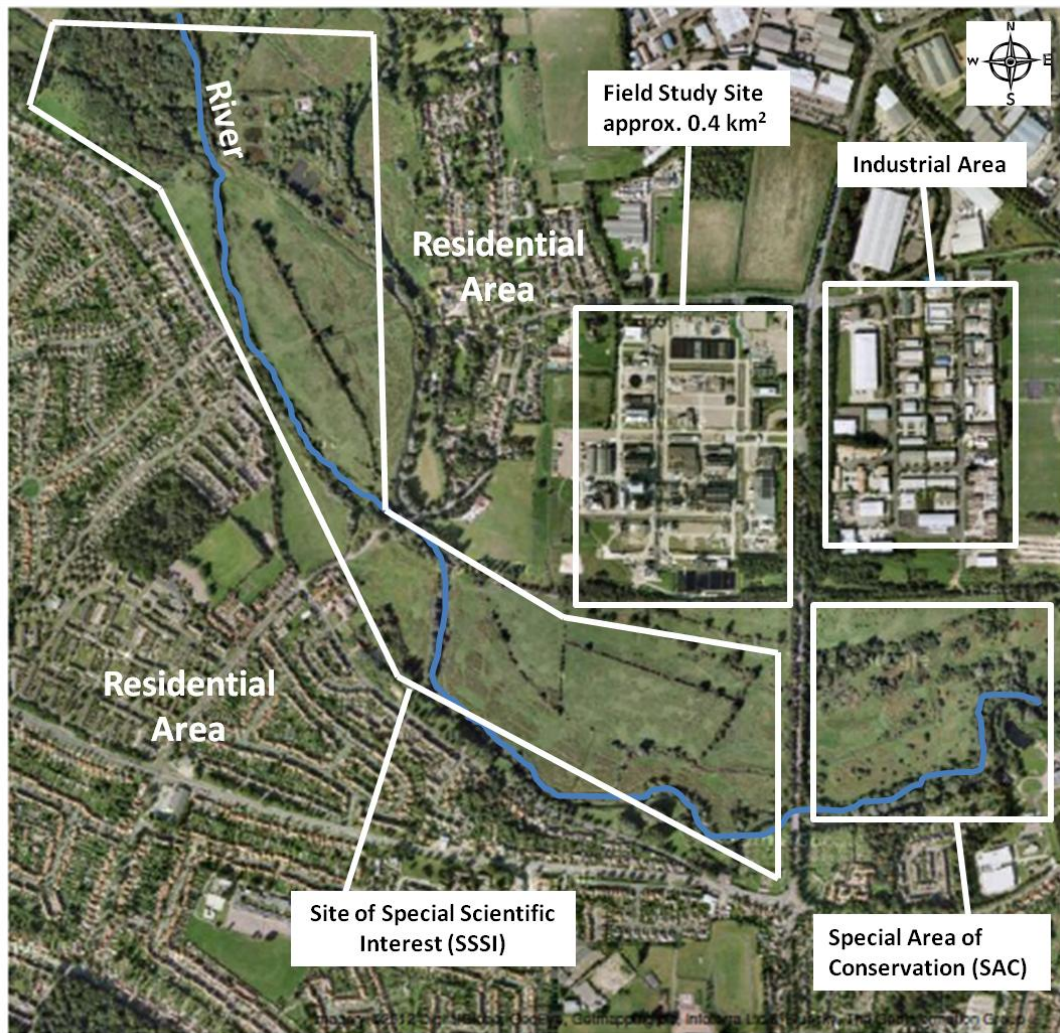


*Figure 3.15 – Areal view of field study site and the surrounding area (Google Maps, 2012).*

### *3.4 Conclusion*

Returning to the objectives raised in the introduction, the first objective was “characterise the present state of the contaminant plume at the site”. The results of the assessment of the site-wide monitoring report focused primarily on SULPH, as it is a novel contaminant in terms of evaluation for natural attenuation. Furthermore, the data available for IPU (also of interest in this research) was not only limited but also concentrations were extremely low compared to those reported for other principal contaminants at the site, for example, SULPH and toluene were typically two orders of magnitude higher than IPU. The analysis conducted in this chapter suggests the SULPH plume, starting in the source area (N61), extends downgradient for a distance of approximately 300 m. The concentration of SULPH reduces by two orders of magnitude along the plume pathway from approximately 130 to 1 mg L<sup>-1</sup>. Further investigative work of the pathway, taken by the SULPH plume, indicated that after approximately 140 m, it encounters a toluene plume. Evidence suggests the SULPH plume may be stable; however, the groundwater velocity, calculated for the site, makes this assumption unreliable. Moreover, abstraction wells, situated along the southern regions of the site (ETP area), which are used to facilitate pump and treat techniques to remove and treat contaminated groundwater; also make it unclear as to whether the SULPH plume would extend beyond this area.

Objective two was, “calculate and estimate the percentage of biodegradation occurring using biological and chemical oxygen demands recorded at the site”. The results of the BOD/COD ratios suggest that the composition of the groundwater environment has the capacity to enable up to 50 % of the remaining contaminants, present in the groundwater, to be removed via biodegradation processes. However, this percentage relates to the total fraction of contaminants present and so is not useful in terms of identifying the biodegradation of individual contaminants. Conversely, mass balance calculations, which took account of the increased levels of sulphate present in the groundwater – thought to be the result of SULPH biodegradation implies as much as 90 % of the SULPH, originally present in the groundwater, has undergone some form of biodegradation. Both these findings provide evidence to support the presence of biodegradation processes at the site.

The third objective was, “identify the redox zones present in the contaminated plume in order to understand which biodegradation processes may dominate”. Information gleaned from the historical data indicated the redox conditions of the groundwater beneath the site were mainly Fe(III) reducing. Although the background hydrochemistry for the groundwater in the local area of the site was primarily Fe(III) reducing, the redox potentials recorded at the site showed there was a shift to a more strongly reducing environment. In particular, the areas where high levels of SULPH and toluene contamination dominated (N62 and 71), there was a shift from Fe(III) to sulphate reduction.

A study of the site-wide historical data was undertaken to establish whether there was any evidence to support the use of natural attenuation as a remediation strategy at the site. The data were consulted with two lines of evidence in mind, which are recommended by the Environment Agency (2000a): (1) to document the loss of contaminant mass over time and, (2) to identify geochemical and biological indicators resulting from the reduction in contaminant concentration.

The first line of evidence was difficult to obtain from the concentration data available. Although, SULPH concentrations were identifiable as reducing with distance from the source zone, it was not obvious from the report whether the decrease in concentration could be distinguished between dilution, dispersion or biodegradation. However, the high levels of sulphate, observed near the source zone, do support biodegradation of SULPH (van Haperen et al., 2001). There is no other likely explanation, evident in the report, as to why sulphate concentrations should be extremely high in this area of the site (areas N61/71), for example, no reported storage of sulphate on site. From this a fair assumption was made that biodegradation of SULPH may account for a reduction in SULPH mass of approximately 90 %.

A second line of evidence may be considered in evaluating SULPH as a metabolic by-product of Asulam. A documented chemical spill was recorded at the site for Asulam but no evidence to support the storage or subsequent spillage of SULPH at the site. Furthermore, there was a correlation between the calculations that matched the proportion of Asulam, which decreased over time, with the proportion of SULPH, which increased within the same time frame. These findings suggest that

an increase in SULPH (as a biological indicator) resulted in a reduction in concentration of the contaminant, Asulam.

To summarise, the results from this chapter tentatively suggest two lines of evidence to support the occurrence of natural attenuation at the field study site. However, as stated at the beginning of this chapter, these lines of evidence only act as an *indicator* in supporting the collection of more robust data, in the form of microbiological analysis. The next two chapters aim to substantiate these two lines of evidence with microcosm studies and compound specific isotope analysis to identify evidence of specific contaminant biodegradation.

# Chapter 4: Support materials suitable for *in-situ* microcosms examining hydrophilic hydrocarbons

---

## 4.1 Introduction

This chapter explores the use of alternative support materials; graphite felt, pumice pellets and expanded perlite, and focuses on adsorption and desorption processes. This is a first step approach using support materials that have already proved successful for biofilm development (Ginsburg and Karamanev, 2007, Lyew et al., 2007, Şen and Demirer, 2003, Teas et al., 2001) and so assumptions were made that the only limiting factor to development of an *in-situ* microcosm, matching that already established using bio-sep and subsequent bactrap methods (Braeckevelt et al., 2007b, Chang et al., 2005, Chauhan and Ogram, 2005, Geyer et al., 2005b, Kästner et al., 2006, Peacock et al., 2004, Stelzer et al., 2006b, Sublette et al., 2006) would be the capacity of the supports to retain a tracer. The purpose of this investigation was to establish if these alternative support materials were suitable, specifically with the two compounds, IPU and SULPH, already acknowledged as being biodegradable in the environment (Johnson et al., 2000a, Johnson et al., 2003a, Johnson et al., 2004, Kristensen et al., 2001, Walker, 1978) could be contenders for NA.

Of particular interest was:

1. Would the background concentrations of IPU and SULPH, already present at the study site, contaminate the supports and in so doing compromise the loaded tracer?
2. Could a tracer be loaded onto the support materials and if so how would each support compare?
3. Could a viable concentration of tracer be retained, by the support material, for an adequate timeframe and allow biofilm development, in the presence of the carbon substrate of interest?

4. The application of kinetic models in order to: i) develop an understanding of the sorption processes taking place and, ii) to establish desorption rate coefficients to assist in the evaluation of which support material was best disposed to retain an isotopic tracer.

*In-situ* microcosms, used to provide evidence of NA, are widely accepted as a suitable tool for hydrophobic, petrochemical based compounds (Air Force Centre for Environmental Excellence (AFCEE), 1995, Environment Agency (EA), 1999, TNO Institute of Environmental Sciences Energy Research and Process Innovation (NICOLE Report), 1999, United States Environmental Protection Agency (EPA), 1999). Although NA exists for some herbicides (Centre for Ecology and Hydrology (CEH), 2000) there has been little in the way of research using *in-situ* microcosm techniques to establish its significance in contaminated groundwater. This may be due to herbicides being very mobile in the natural environment due to their hydrophilic character. This can cause their initial application concentrations to become quickly diluted should they come into contact with groundwater. This along with their limited adsorption capacity, which would retain them long enough to afford biodegradation by indigenous microbes, questions their suitability for remediation using NA. However, in circumstances of large point source contamination, along with slow flowing groundwater, such as an accidental spill at a chemical production plant, NA may become feasible (Tuxen, 2002).

In contrast to *in-situ* methods, *ex-situ* biodegradation assessments are often criticised because they do not truly represent natural groundwater environments. A summary of the main disadvantages of *ex-situ* approaches are included in Table 4.1. Using unrepresentative samples can lead to a misinterpretation of the actual situation and subsequently undermine the effective application of a NA strategy. This is acknowledged by the regulating authorities, responsible for approving NA as a viable remediation option, who regard *in-situ* methods as a necessity. In light of this, this chapter investigates potential surrogate materials that may be suitable for deployment as *in-situ* microcosms. As a comparison, Chapter 5 explores *ex-situ* microcosms with a view to compare the two approaches.

**Table 4.1** – Disadvantages of using *ex-situ* biodegradation methods to determine NA in groundwater environments.

<i>Ex-situ</i> Methods	Disadvantages	Reference
<b><i>Ex-situ</i> Microcosms</b>	<p>Collecting sediment samples from saturated zone is problematic:</p> <ul style="list-style-type: none"> <li>• drilling techniques can contaminate samples</li> <li>• microbial community sensitive to disturbances</li> <li>• heterogeneity of the environment</li> </ul>	(Goldscheider et al., 2006, Hirsch and Rades-Rohkohl, 1988)
<b>Groundwater Analysis</b>	<ul style="list-style-type: none"> <li>• Groundwater yields unattached (planktonic) microbes (but &gt; 95 % of the community active in biodegradation, are attached (sessile) microbes).</li> </ul>	(Harvey et al., 1984, Lehman et al., 2001)
<b>Lab-based Cultivation Techniques</b>	<ul style="list-style-type: none"> <li>• Frequently based on single-species cultures so give an incomplete picture of biodegradation.</li> <li>• Many groundwater microbes are viable but non-culturable.</li> <li>• Biodegradation rates often 4-10 times slower in the field compared to lab-based studies.</li> </ul>	(Costerton et al., 1995, Goldscheider et al., 2006, Sturman et al., 1995b)

Designing a tool to indicate biodegradation in the subsurface is challenged by the imposition of a mixed-media approach because the groundwater-contaminant-degrader system is dynamic and highly dependent on mechanisms which govern sorption-desorption, microbial growth and substrate utilisation (Bedient and Rifai, 1992, Pignatello and Xing, 1995). In addition, these complex interactions require integration of phenomena operating at scales ranging from a microbial cell ( $10^{-6}$  m) to that of a geological scale (10-1000 m) (Sturman et al., 1995b). Furthermore,

sampling aquifer material requires expensive drilling techniques which do not allow for repeat sampling of a single site and so the opportunity to study attached microbial communities *in-situ* over time is not possible. To overcome this, *in-situ* microcosms are usually composed of a support material, which acts as a surrogate aquifer material, which is then deployed in existing boreholes and exposed to contaminated groundwater (Griebler et al., 2002). Although surrogate support materials are not identical to those found in a contaminated aquifer, sampling biomass in this way has the advantage of higher cell density to that found in the groundwater and so is more representative of surface attached communities (Kuder and Philp, 2008).

The characteristics required of a support material are derived from the necessity to imitate the subsurface environment. Thus, an ideal support material should provide an environment conducive to microbial colonisation in that it: has a structure which enables cell attachment and biofilm development; permits groundwater flow to replenish nutrients, and; has a sorptive capacity to retain and subsequently release contaminants utilised as a “food source”. In addition, the material needs to be inexpensive and readily available to ensure the future sustainability of NA Figure 4.1, below, highlights the key characteristics required.

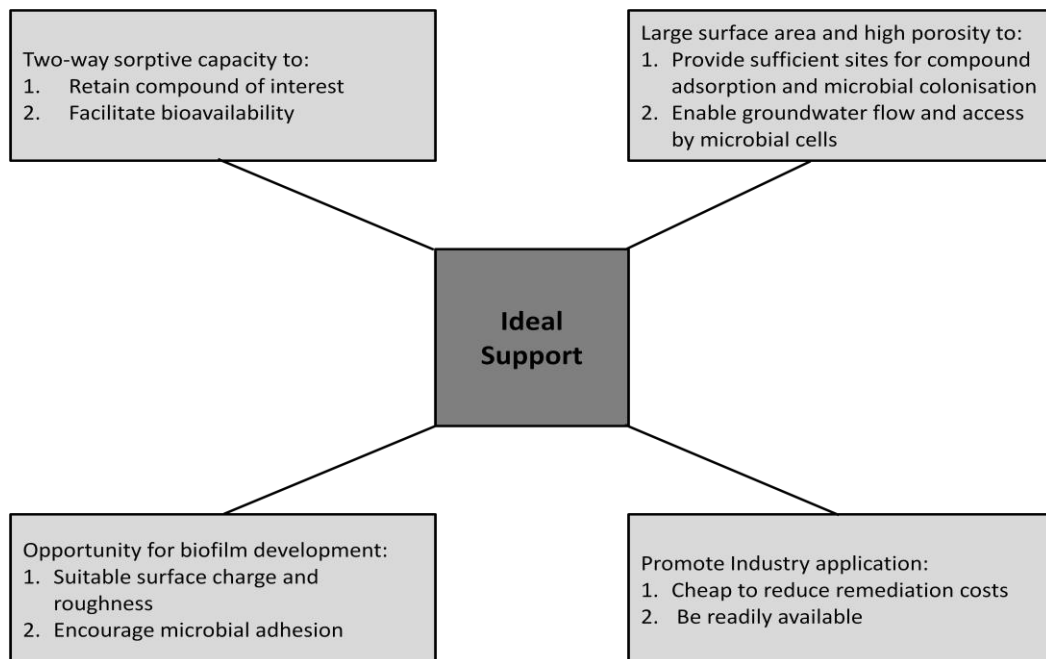


**Figure 4.1** – Schematic showing the characteristics required by a support material to succeed as a surrogate support for *in-situ* microcosms.

#### 4.1.1 Surface Area and Porosity

Surface area and porosity are central features of a support material. The extent of the surface area determines the number of available attachment sites for microbes and adsorption sites for the contaminant of interest. Likewise, the degree of porosity can place limitations on the; available surface area for microbial attachment should the porous structure be too small to permit cell access, the flow of groundwater which in turn would limit the flow of necessary nutrients and sorption processes which would subject the contaminant of interest to diffusive constraints and so restrict its bioavailability (Alfreider et al., 1997, Griebler et al., 2002, Lyew et al., 2007, Pignatello and Xing, 1995). In general, a microbial cell is about 0.5-5  $\mu\text{m}$  and so a support with pores larger than this would allow microbes to make use of the entire surface area for attachment. Figure 4.2, below, shows scanning electron micrographs of four support materials which have suitable pore sizes.

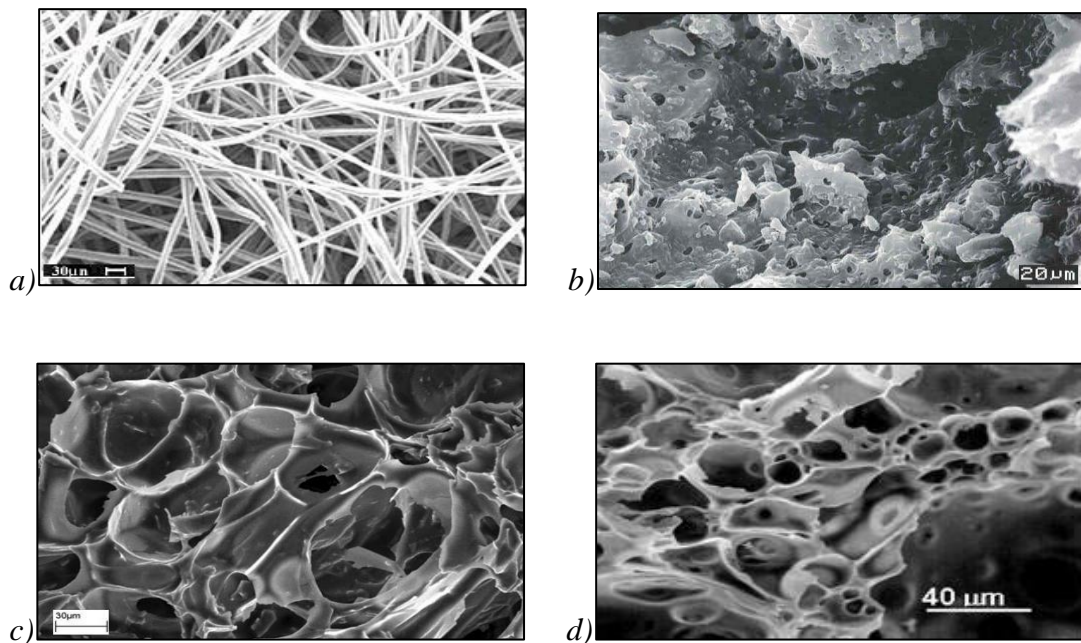


**Figure 4.2** – Scanning Electron Micrographs (SEM) showing the surface and porous structures of a) graphite felt (Vilar et al., 2003), b) Bio-sep® Bead (Bush-Harris et al., 2006), c) perlite (Gamarra et al., 2010) and d) pumice (Di Lorenzo et al., 2005).

Studies comparing the surface areas and porosities of support materials found that biomass recovery rates increased with increasing surface area and porosity.

Alfreider et al. (1997) found increasing the surface area, of the sandy deposits enclosed in a wire mesh, resulted in greater biomass recovery and concluded that; this was due to a rise in attachment sites for the microbes and the subsequent increase in porosity which enabled the flow of necessary nutrients for biomass development. Peacock et al. (2004) compared glass wool and Bio-sep® beads, which consist of powdered activated carbon, coated in a porous membrane made from an aramid polymer (Nomex). They recovered seven times more biomass from the beads than the glass wool and attributed this to the beads having a larger surface area and a greater propensity to adsorb nutrients from the groundwater environment, making them a more favourable environment for the microbes. Lyew et al. (2007) compared granulated activated carbon (GAC) and perlite. They established, even though GAC had a greater adsorptive capacity for the contaminant of interest (Methyl tert-butyl ether (MTBE)), that perlite, with its larger surface area, was able to sustain the attachment of a larger microbial community.

High porosity assists groundwater flow through the support material, which is needed to sustain the ecosystem of the *in-situ* microcosm. Griebler et al. (2002) used sand enclosed in a wire mesh and compared deployment in stagnant well water to one receiving freshly pumped contaminated groundwater. They found biofilm development in the one pumped with groundwater to be 8.6 times higher than that recovered from the well and argue that if groundwater flow is too slow, causing the well water to become stagnant, then the introduction of fresh planktonic species to the biofilm, through groundwater flow, is limited. Although these findings relate to groundwater flow they underline the importance of porosity in that without the continued introduction of fresh nutrients and opportunistic planktonic microbes then biomass is unlikely to accumulate on the support material.

#### 4.1.2 Sorption Capacity

Although an increased surface area and porosity can influence the number of adsorption sites on a support material, these characteristics are only relevant if the material has a sorption capacity for the contaminant of interest. Permeable Reactive Barriers (PRBs), used to treat contaminated groundwater, rely on the sorption capacity of support materials to adsorb a contaminant, during groundwater flow, so it can be utilised by microbes colonizing the support material. This adsorption step is

essential in accumulating sufficient levels of contaminant to warrant exploitation by the microbes (Bouwer and McCarty, 1982). *In-situ* microcosms, used to obtain NA evidence of specific contaminants, rely on the sorption capacity to both; load a support material with an isotopic tracer and facilitate the tracers release, once deployed, rendering it bioavailable (Braeckevelt et al., 2007b, Geyer et al., 2005b, Kästner et al., 2006).

Previously, contaminants sorbed onto solid matrices were assumed to reduce bioavailability because microbes metabolise contaminants more readily from liquid than the sorbed states (Pignatello and Xing, 1995). However, recent studies indicate that this may not be the case. Leglize et al. (2006) found that polycyclic aromatic hydrocarbon (PAH) sorption on activated carbon and pouzzolana – a volcanic ash, did not reduce bioavailability but instead significantly increased the biodegradation rate. This phenomenon may be explained by attached microbes, which form biofilms, being responsible for > 95% of biodegradation (Harvey et al., 1984, Lehman et al., 2001), along with a biofilms ability to excrete biosurfactants to make a contaminant bioavailable (Emitiazi et al., 2005). Although the intricacies of microbial ecology are beyond the scope of this work, this does suggest that once a tracer, of the contaminant of interest, is loaded onto a support material, any microbe, already degrading the contaminant *in-situ*, should have the necessary tools to utilise it as a food source.

Activated carbon is an established liquid-phase adsorbent and has been used extensively to remove hydrocarbon contaminants during both wastewater treatment and groundwater remediation. The US Environmental Protection Agency (2002) consider granulated activated carbon (GAC) as the best available adsorbent for removing organic contaminants from water and advise that the use of alternative adsorbents must, at the very least, be as equally effective. Powdered activated carbon (PAC) is the main constituent of Bio-sep® beads which have gained much prominence as a support material for *in-situ* microcosms (Braeckevelt et al., 2007b, Chang et al., 2005, Chauhan and Ogram, 2005, Geyer et al., 2005b, Kästner et al., 2006, Peacock et al., 2004, Stelzer et al., 2006b, Sublette et al., 2006).

A number of studies have focused attention on alternative support materials, which have comparable sorption potentials to activated carbon, in removing petrochemicals, PAHs and MTBE contaminants. Naturally occurring materials such as pouzzolana, perlite and pumice, all of which are produced during volcanic

eruptions, have received particular attention because they are readily available in the environment (Joseph and Rodier, 1994, Leglize et al., 2006, Lyew et al., 2007, Teas et al., 2001). Of these materials, perlite was shown to have comparable petrochemical adsorptive capacities to activated carbon (Teas et al., 2001). In addition, when perlite was considered as a surrogate support material, in that it had characteristics pertaining to both adsorption and biofilm development, it was found to be better suited as an *in-situ* microcosm material, for studying MTBE degradation, than activated carbon because the favourable surface of perlite to adhesion, retention, growth, and activity, outweighed the advantages of the increased adsorptive capacity of GAC (Lyew et al., 2007).

#### 4.1.3 Biofilm Development

The use of support materials to aid biofilm development is not a new concept and has been employed, by the U.K. wastewater industry for over 20 years, during secondary treatment of wastewater. As mentioned earlier, the vast majority of biodegradation is accomplished by attached rather than planktonic microbes. Therefore, the success of an *in-situ* microcosm will depend on how conducive the support material is to microbial attachment. Ginsburg and Karamanev (2007) found that microbial attachment favours rougher surfaces as it allows for greater adhesion. In particular, they found that carbon felt supported more biofilm growth than carbon cloth because it had a rougher surface. The surface chemistry of support materials is also believed to affect biofilm growth. Studies show that support materials, which have a surface charge are more favourable than materials without a charge and hydrophobic materials, support more biofilm growth than hydrophilic materials (Shrove et al., 1991).

Figure 4.3, below, provides a simplified view of biofilm development. When planktonic microbes, in the groundwater (represented by bulk fluid), pass close to a favourable support material, they will excrete extracellular polysaccharides to assist in adhesion (Ginsburg and Karamanev, 2007). Once attached the microbes multiply and colonise the surface, with attachment taking seconds to minutes, colonisation hours to days and growth days to years.

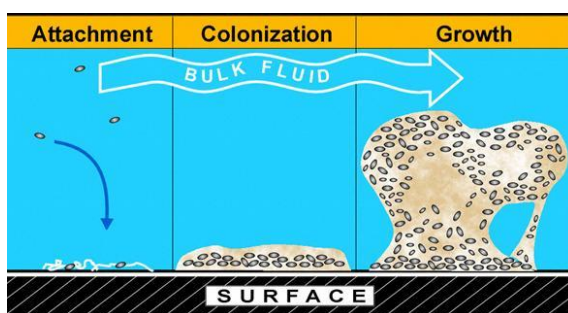


**Figure 4.3** – Three stages of biofilm development; attachment, colonisation and growth (Noble, 2004).

Other factors such as nutrient supply can also trigger a move from a planktonic to a sessile mode of living. It is believed that unfavourable surface characteristics can be overcome through genetic modifications by the microbes, to improve adhesion, should the environmental conditions be worthwhile (O’Toole et al., 2000).

Therefore, *in-situ* microcosms that include both a support material favourable to microbial attachment and a food source that is bioavailable are more likely to be colonised than *in-situ* microcosms containing a support alone. This highlights the importance of a mixed media approach in determining biodegradation potentials in contaminated groundwater because the type of microcosm used can greatly influence the percentage of biomass accumulated.

Biofilm development has been exploited for many years in the treatment of municipal wastewater for the *in-situ* regeneration of activated carbon in fixed-bed reactors (Walter, 1974). This mixed media approach is well established in the water industry for removing organic wastes. More recently, as mentioned in Section 4.1.1, activated carbon in powdered form has gained recognition as a support material for *in-situ* microcosms using Bio-sep® beads. The success of the beads can be accredited to the long-established capability of activated carbon to concentrate nutrients required for biofilm development, and offer a large surface area to accommodate multiple attachment sites for microbes (Bush-Harris et al., 2006).

In a drive to find sustainable materials, which match the qualities of activated carbon, research has focused on using cheaper alternatives as support materials. Figure 4.4, below shows scanning electron micrographs of biofilm development on two such alternatives, namely, perlite and pumice.

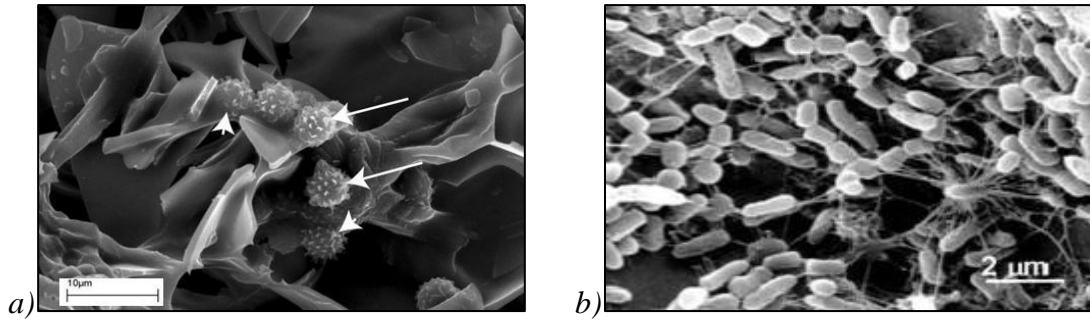


**Figure 4.4** – Scanning electron micrograph images of biofilm development on a) perlite (Gamarra et al., 2010) and b) pumice (Di Lorenzo et al., 2005) (b).

Liu et al. (2006) found the surface area and porosity of expanded perlite was favourable to biofilm development during lab-based column trials. They noted that MTBE degraders readily colonised the perlite after 3 days and the subsequent biofilm was able to remove 50% of the contaminant. Emitiazi et al. (2005) ascertained that biodegradation of petroleum oil in contaminated soil was unstable. However, when they provided the soil microbes with perlite as a support material, the subsequent biofilm development made biodegradation more successful. The findings were linked to the production of a biosurfactant, by the biofilm, which assisted in the degradation process by mobilising the petroleum oil. This innate ability to mobilise contaminants highlights the important role that attached microbes, which form biofilms, play in removing contaminants from the environment and why providing suitable support materials for indigenous microbes may improve their ability to do so. Another material of volcanic origin, pumice, was effectively used as an *in-situ* biobarrier to treat groundwater contaminated with toluene. Di Lorenzo et al. (2005) found the pumice favourable to biofilm development by the indigenous microbial population, with the biofilm degrading 99% of the toluene present in the groundwater. Pumice has also been used as a microbial support to treat wastewater in the textile industry and when this biological method was compared to adsorption methods using activated carbon it was found to be more efficient (Şen and Demirer, 2003).

#### 4.1.4 Readily Available Materials

Although activated carbon is considered to be the preeminent material for environmentally driven applications involving sorption processes, there is a continued emphasis from regulating authorities and industry towards the sustainability and cost-effectiveness of using activated carbon. Therefore, there is an interest in using readily available, natural materials, which require less manufacturing for purpose, rather than focusing attention on “end-of-pipe” solutions (Marsh and Rodriguez-Reinoso, 2006). The production of activated carbon is very expensive, both financially and environmentally. Figure 4.5 below, summarises the manufacturing process.

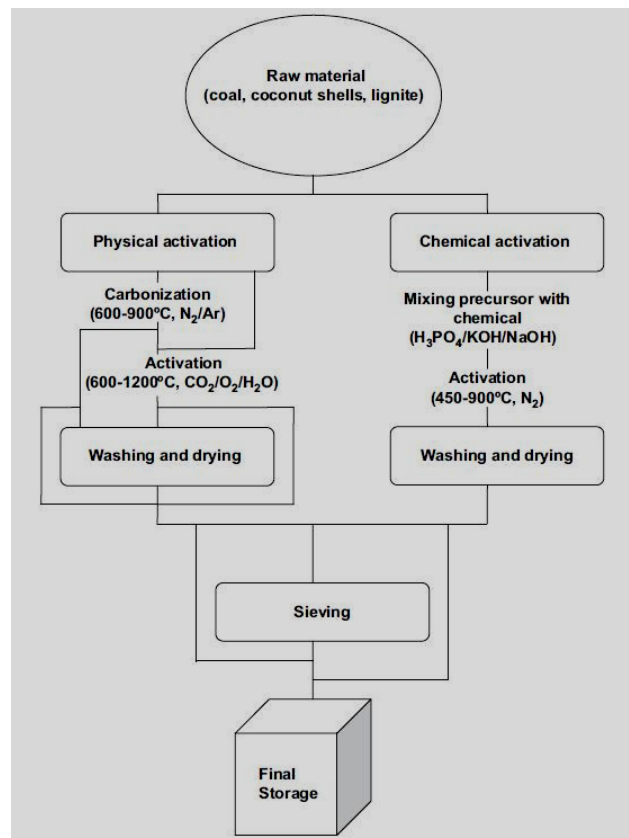


**Figure 4.5** – Schematic showing the manufacturing process of granulated activated carbon (Gupta and Suhas, 2009).

During production 1600 kWh of energy, 12 tonnes of water vapour and 330 m<sup>3</sup> of natural gas is required to convert 3 tonnes of coal into 1 tonne of activated carbon. In addition, once the activated carbon is spent i.e. all the adsorption sites are occupied, reactivation of the material involves similar conditions to those described for production. Furthermore, transporting the materials, an average of 400 km, between coal-mining regions, the manufacturer and end user generates further financial and environmental costs (Bayer et al., 2005).

However, there is a caveat to using alternative materials in that they must equal the effectiveness of activated carbon (United States Environmental Protection Agency (EPA), 2002). Consequently, a number of studies have focused on comparative work between activated carbon and naturally occurring volcanic materials, such as; pouzzolana, perlite and pumice, to remove hydrocarbon contaminants from the environment (Joseph and Rodier, 1994, Leglize et al., 2006, Lyew et al., 2007, Teas et al., 2001). The details of which were discussed earlier (Section 4.1.2). Of these materials, perlite and pumice were found to be equally as effective to activated carbon in their ability to remove petrochemicals via adsorption treatments (Teas et al., 2001), and act as a surrogate support material during the biological treatment of wastewater (Şen and Demirer, 2003), respectively. In addition, perlite and pumice did not require activation before use in these two mentioned studies and so the environmental and financial production costs, described for activated carbon products above, are eliminated, making them a more economically attractive alternative.

## 4.2 Materials and methods

In the following experiments the adsorption characteristics, loading quotient and subsequent desorption kinetics of isoproturon and sulphanilamide onto/from graphite felt, pumice pellets and expanded perlite were studied to examine whether the compounds and support materials would be suitable for *in-situ* microcosm studies of a contaminated groundwater environment.

### 4.2.1 Compound Selection

Primarily, selections of compounds were confined to those present at the contaminated field study site. Of particular interest were the hydrocarbon compounds, isoproturon and sulphanilamide.

Little is known about the fate of sulphanilamide in the environment. However, early studies of its parent compound, Asulam, have shown it to be biodegradable in soils (Babiker and Duncan, 1977, Franci et al., 1981, Walker, 1978). In addition, Ingerslev and Halling-Sørensen (2000) have shown, despite it belonging to the sulphonamide group of compounds, which have antimicrobial properties, sulphanilamide was biodegradable during activated sludge treatments.

Isoproturon was selected because it demonstrated a potential for use in *in-situ* microcosm studies. *Ex-situ* microcosms have been widely investigated for chalk, sandstone and limestone aquifers and all document the presence of indigenous microbes capable of degrading isoproturon (Besien et al., 2000, Centre for Ecology and Hydrology (CEH), 2000, Johnson et al., 2001, Kristensen et al., 2001).

Although there is evidence to support that indigenous microbes are capable of degrading both sulphanilamide and isoproturon, their hydrophilic nature would present a challenge as to their suitability for *in-situ* microcosms, in so far as: could they be retained by a support material to encourage biofilm development?

### 4.2.2 Chemicals

Sulphanilamide was obtained from Bayer Cropscience, UK, isoproturon from Aventis Cropscience, UK, and their radiolabelled analogues, sulphanilamide [ring- $^{14}\text{C}$ (U)] from American Radiolabeled Chemicals Inc., USA, and [benzene ring-UL- $^{14}\text{C}$ ] isoproturon from Amersham Co. Ltd., UK. The physical and chemical

properties of which were presented previously in Chapter 3, Table 3.1. Analytical grade (99%), acetone and methanol were obtained from Fisher Scientific, UK. The scintillation cocktails; Carbosorb-E, Permafluor-E and Ultima Gold™ XR were obtained from Perkin Elmer Life & Analytical Sciences, UK.

#### *4.2.3 Support Material Selection*

Albrechtsen et al. (1996b) underlines the importance of support materials in accurately predicting biodegradation of hydrocarbon contaminants in groundwater. The main characteristics required by support materials have been described in the literature (Albrechtsen et al., 1996b, Lyew et al., 2007) and are represented in Section 4.1 (Fig.4.1). The selection of the studied support materials; graphite felt, pumice pellets and expanded perlite were based on their likeness to these characteristics.

- Graphite felt, with its large surface area, has been shown to outperform other activated carbon materials, in acid mine drainage treatment trials, in facilitating the adhesion of ferrous oxidising microbes (Ginsburg and Karamanev, 2007). It is also widely accepted that activated carbon materials have a high adsorptive capacity for hydrocarbon based contaminants (Lyew et al., 2007).
- Pumice, which is cheap and readily available, has been used successfully as a support material in: bioreactors to treat wastewater (Kocadagistan et al., 2005); in treating contaminated groundwater with toluene degrading microbes (Di Lorenzo et al., 2005); and in biological phenol treatment systems (Pazarlioğlu and Telefoncu, 2005).
- Perlite, which is also cheap and readily available, has been shown to outperform activated carbon materials and pumice as a support material in groundwater remediation by MTBE degraders (Lyew et al., 2007). Microbial preference for adhesion to Perlite ( $2 \times 10^8$  cell g<sup>-1</sup> perlite) has also been recognized when investigated as a seeding medium for hydrocarbon utilising microbes (Emitiazi et al., 2005).

#### 4.2.4 Support Materials

Pumice pellets were obtained from Techfil Europe Ltd., UK, expanded perlite from William Sinclair Holdings PLC., UK and graphite felt from Alfa Aesar GmbH & Co., Germany. The physical and chemical properties of which, are presented in Table 4.2 and images in Figure 4.6.



Graphite Felt

Pumice Pellets

Expanded Perlite

**Figure 4.6** – Images of studied support materials.

**Table 4.2 – Physical and Chemical Properties of Support Materials.**

	<b>Graphite Felt</b>	<b>Pumice Pellets</b>	<b>Expanded Perlite</b>
Chemical Properties (%)			
Carbon	100	-	-
Silicon Dioxide	-	74.55	71– 75
Aluminium Oxide	-	12.45	12.5 – 18
Potassium Oxide	-	4.50	4.0 – 5.0
Sodium Oxide	-	4.00	2.9 – 4.0
Ferric Oxide	-	<2.00	-
Ferric Trioxide	-	-	0.1 – 1.5
Calcium Oxide	-	<2.00	0.5 – 2.0
Magnesium Oxide	-	<2.00	0.03 – 0.05
Titanium Dioxide	-	<2.00	0.03 – 2.0
Sulphur Trioxide	-	<0.20	<0.1
Manganese Oxide	-	<0.10	-
Manganese Dioxide	-	-	<0.1
Carbon Dioxide	-	<0.10	-
Ferrous Oxide	-	0.06	<0.1
Phosphorus Pentoxide	-	0.005	-
Barium	-	-	<0.1
Lead(II) Oxide	-	-	<0.5
Chromium	-	-	<0.1
Combined Water	-	4.35	-
Physical Properties			
Bulk Density (g/cm <sup>3</sup> )	2.25	2.31	2.24
Porosity (%)	>90	95-90	70-85
Size	1.12 cm thick	3 - 8 mm	3 - 6 mm

#### 4.2.5 Instrumentation

A Canberra Packard Tri-Carb® 2900TR Liquid Scintillation Analyser (LSA) was used to monitor  $^{14}\text{C}$ -activity, for both sulphanilamide and isoproturon, during adsorption and desorption processes associated with the support materials. The assay parameters were set to count  $^{14}\text{C}$  disintegrations per minute (DPM) for a period of 10 minutes and the  $^{14}\text{C}$  half-life was set to 5728.49 years. The counting efficiency, established before the samples were counted was 96% and the detection limit for  $^{14}\text{C}$ -sulphanilamide and  $^{14}\text{C}$ -isoproturon was 0.4 and 0.5  $\mu\text{g L}^{-1}$  respectively (calculations in Appendix 3). Quench corrections were also established for the preparation of 10 ml of Ultima Gold™ XR scintillation cocktail mixed with 9 ml acetone, as an alternative solvent to water, and can be found in Appendix 4.

A Packard Sample Oxidiser Model 307 was used to ascertain the quantity of  $^{14}\text{C}$ -sulphanilamide and  $^{14}\text{C}$ -isoproturon adsorbed to the support materials. Spent support materials were loaded into cellulose combusto-cone™ (*Perkin Elmer life & Analytical Sciences, UK*) and combusted. The burn time was set to 2 min. The  $^{14}\text{CO}_2$  was trapped in 10 ml of Carbosorb-E and washed into a 20 ml HDLP plastic vial (*Meridian biotechnologies Ltd. UK*) with 10 ml of Permafluor-E. The trapping efficiency calculated prior to sample oxidation was 85%.

#### 4.2.6 Adsorption

Ultimately, the support materials would be used as *in-situ* microcosms and deployed in existing boreholes at the field study site. Therefore, the decision on batch adsorption concentrations considered background contaminant levels of sulphanilamide and isoproturon in the environment using values reported for groundwater contamination by Johnson et al. (2001) and Pérez et al. (2005), the field study site and the detection limit of the LSA.

Batch adsorption experiments were set up as per Figure 4.7, using an adaptation of the methods described by OECD (2000), Adhoum and Monser (2004), Doğan et al. (2000) and Feryal (2005).

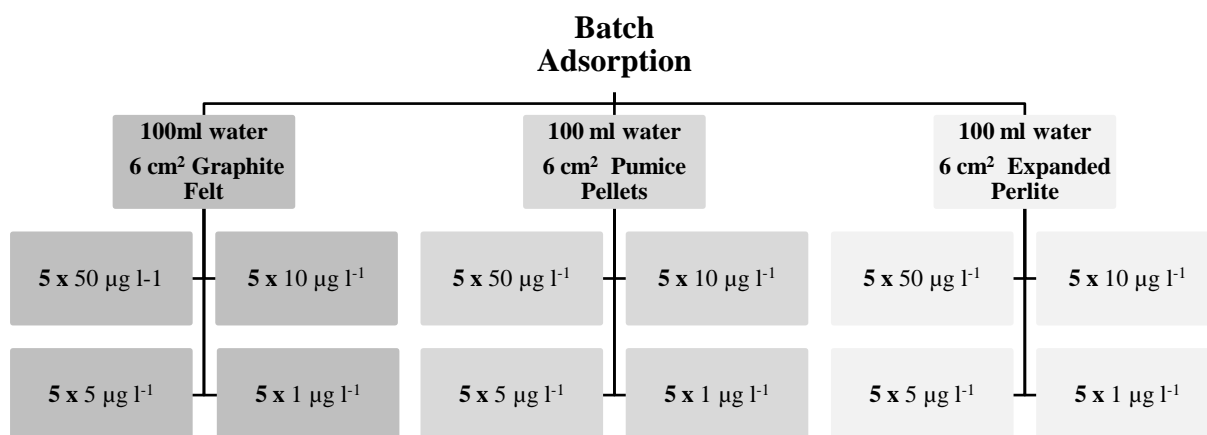


**Figure 4.7** – Batch Adsorption Experiment Design. The values represent (replicates in bold) the concentration of isoproturon and sulphanilamide in the aqueous phase.

100 ml of Milli-Q water: resistivity 18.2 MΩ.cm, was placed in 250 ml clear DURAN® flasks and autoclaved (*Touchclave®*, *LTE Scientific Ltd., UK*). The flasks were spiked with a standard of <sup>12</sup>C/<sup>14</sup>C-Sulphanilamide or <sup>12</sup>C/<sup>14</sup>C-Isoproturon and left to equilibrate. Sulphanilamide standards were prepared in acetone and Isoproturon in methanol to deliver concentrations of 1, 5, 10 and 50 µg L<sup>-1</sup> and a <sup>14</sup>C-activity of 3800 Bq 100 ml<sup>-1</sup> of aqueous solution. The starting <sup>14</sup>C-activity was established by placing 100 µl aliquots (n=3), of the standard addition stocks, into 7 ml Packard's Pico glass vials (*Perkin Elmer Life & Analytical Sciences, UK*) containing 6 ml of Ultima Gold™ XR. The DPM were counted using the LSA.

2 x Blanks (n=3) were produced: one set containing only Milli-Q water and the other set Milli-Q water and support material. This was to account for background radiation and any <sup>14</sup>C contamination resulting from experimental error.

The support materials were prepared to give an external surface area of ~ 6 cm<sup>2</sup> (graphite felt 1 x 1.12 cm cubes, pumice 2 x 5-8 mm pellets and expanded perlite 5 x 4 mm pellets) and their weights (mg) measured. They were autoclaved and added to the flasks as represented in Figure 4.8.

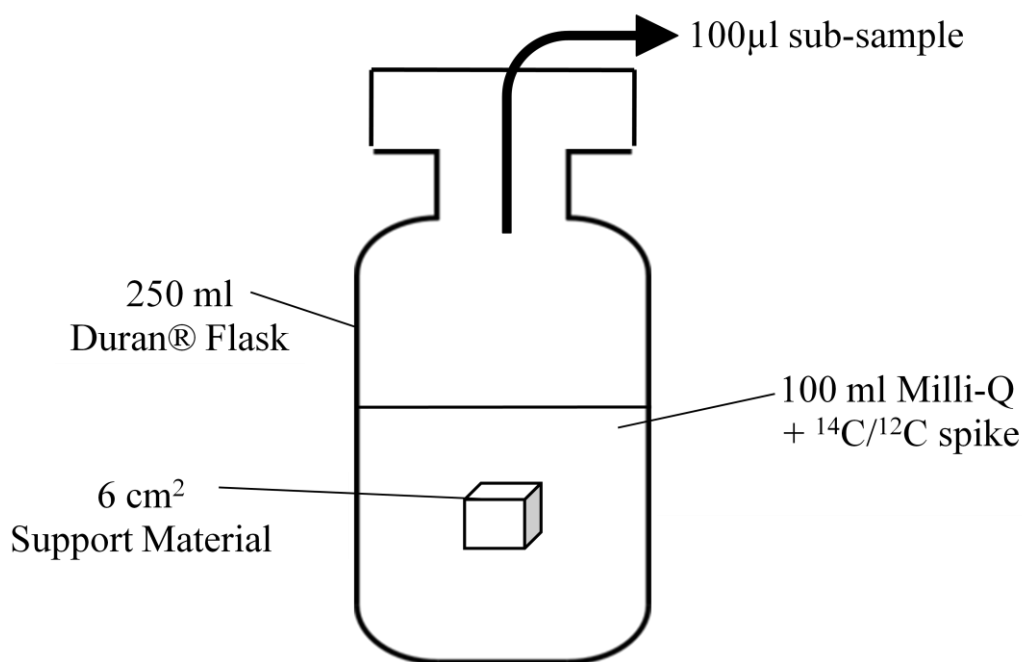


**Figure 4.8** – Diagram of Batch Adsorption Flask.

The flasks were stood on a laboratory work bench at room temperature ( $\sim 21^\circ\text{C}$ ). At set time intervals over a period of 24 days (0, 0.5, 1, 2 and then every 2 days) a 100 µL sub-sample was removed from each flask, placed in a 7 ml Packard's Pico glass vial containing 6 ml Ultima Gold<sup>TM</sup> XR and the DPM counted as described previously. Prior to the removal of each sub-sample the flasks were swirled.

After 24 days the support materials were removed from the flasks and allowed to drip dry. Once dry, they were packed into an individual cellulose combusto-cone<sup>TM</sup> and combusted by the sample oxidiser and the DPM recorded as already described.

#### 4.2.6.1 Adsorption Mass Balance Calculations

The amount of  $^{14}\text{C}$ -activity was monitored during the adsorption experiment; aqueous phase at the start, during and at the end of experiment, and the support material once removed and dried at the end of the experiment. Mass balance calculations were then carried out to ensure the transfer of carbon could be fully accounted for. Figure 4.9, below represents the different stages of mass transfer:

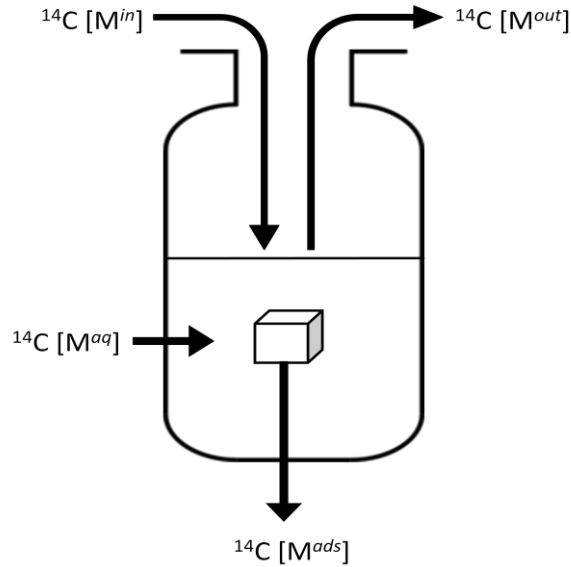


**Figure 4.9** – Mass balance calculations for the transfer of  $^{14}\text{C}$ -activity during adsorption study.

The mass transfer of  $^{14}\text{C}$ -IPU and  $^{14}\text{C}$ -SULPH were checked using scintillation counting methods to track the sum of Carbon-14 entering and leaving the batch adsorption system as follows:

$$^{14}\text{C} [M^{out}] + ^{14}\text{C} [M^{ads}] + ^{14}\text{C} [M^{aq}] = ^{14}\text{C} [M^{in}]$$

Where:

M	mass of $^{14}\text{C}$ shown as a percentage
<i>in</i>	$^{14}\text{C}$ loaded at the start of experiment
<i>out</i>	$^{14}\text{C}$ removed from the aqueous phase during the experiment
<i>ads</i>	$^{14}\text{C}$ adsorbed to support material at the end of experiment
<i>aq</i>	$^{14}\text{C}$ remaining in the aqueous phase at end of experiment

#### 4.2.7 Loading Support Materials

When deployed as microcosms the support material simulates the natural environment with the loaded compound being utilised by the indigenous microbes. Therefore, the amount of sulphanilamide or isoproturon loaded was a reflection of published values for loadings of  $^{13}\text{C}$  labelled hydrophobic compounds onto Bio-Sep® beads, by Braeckevelt et al., (2007b) and Stelzer et al., (2006b), and

concentration levels required for catabolic activity of sulphanimide by Perez et al. (2005) and isoproturon by Johnson et al. (2004).

The experiment to load labelled compounds onto support material was set up as per Figure 4.10.

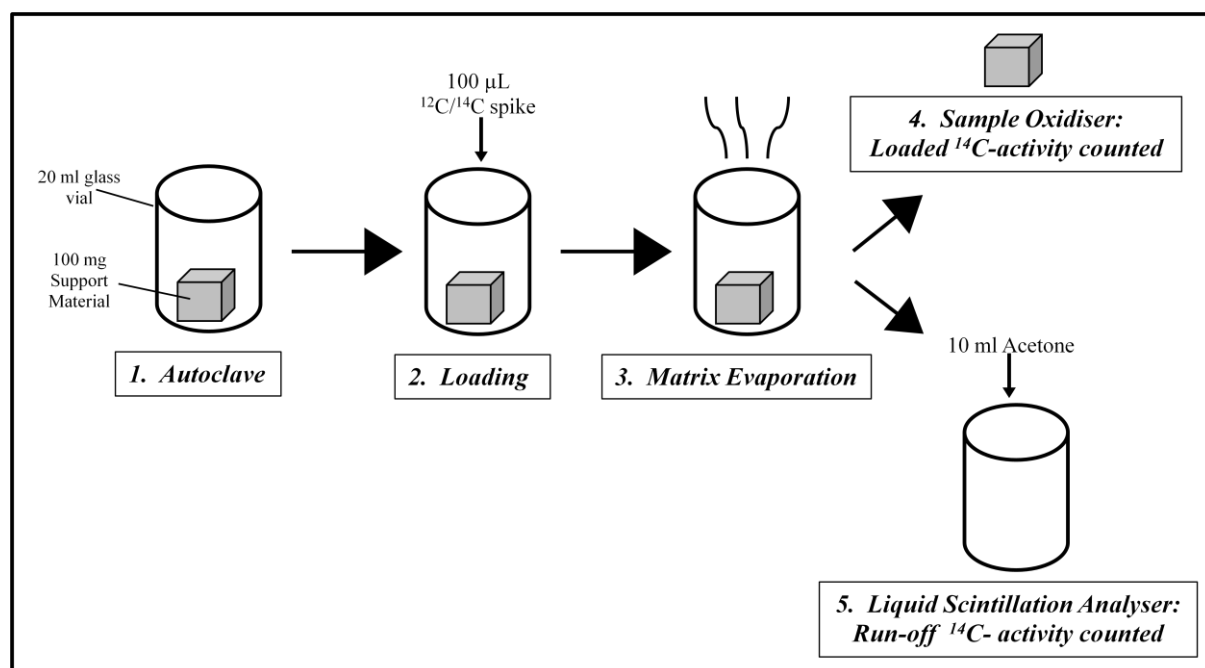


**Figure 4.10** – Experiment design for loading the support materials.

The support materials were prepared as described in the adsorption experiment and placed in individual 20 ml glass scintillation vials (*Cole-Palmer Industrial Co. Ltd., UK*) and autoclaved. Each support material was spiked with a 100 µl standard of  $^{12}\text{C}/^{14}\text{C}$ -sulphanilamide or  $^{12}\text{C}/^{14}\text{C}$ -isoproturon as four aliquots of 50 µl, pipetted directly onto the surface of the material. The vials were placed inside a fume cupboard and left overnight to allow the solvent matrix to evaporate.

Sulphanilamide standards were prepared in acetone and isoproturon in methanol to deliver 10, 50 and 100 mg g<sup>-1</sup> of support material and a  $^{14}\text{C}$ -activity of 2000 Bq per loading. The starting  $^{14}\text{C}$ -activity was established by removing 100 µl aliquots (n=3) of the standard addition stocks as described in the batch adsorption experiment.

Because of the variations in weight compared to area of the support materials, efforts

were made to use comparable weights: 6 cm<sup>2</sup> graphite felt weighed 108 +/- 7 mg, one pumice pellet 150 +/- 11 mg and ten expanded perlite pellets 105 +/- 5 mg. For no particular reason, other than it weighed the most, an average weight for pumice pellets was used to calculate the loadings. The actual loadings and weights of the support materials are shown in Table 4.3 and were replicated for both sulphanilamide and isoproturon.

**Table 4.3 – Actual Loadings of Compound onto Support Material.**

<b>Support Material</b>	<b>Loading (mg g<sup>-1</sup>)</b>	<b>Weight of Support Material (mg)</b>	<b>Actual Loading (mg)</b>
<b>Graphite Felt</b>	100	108	10.8
	50	108	5.4
	10	108	1.08
<b>Pumice Pellets</b>	100	150	15
	50	150	7.5
	10	150	1.5
<b>Expanded Perlite</b>	100	105	10.5
	50	105	5.25
	10	105	1.05

The support materials were removed from the fume cupboard and placed in a cellulose combusto-cone<sup>TM</sup> and combusted as described previously. The DPM counted represented the amount of compound adsorbed to the support material.

10 ml of acetone was added to the glass vials, which contained the support material, shaken and 10 ml of Ultima Gold<sup>TM</sup>XR added. The <sup>14</sup>C-activity remaining in the vials, due to run-off during loading, was counted and used in mass balance calculations.

This method was repeated to produce a second set of loaded support materials for use in the desorption experiment (section 4.2.8).

#### 4.2.8 Desorption

Using the loaded support materials prepared in Section 4.2.7, desorption of  $^{12}\text{C}/^{14}\text{C}$ -sulphanilamide and  $^{12}\text{C}/^{14}\text{C}$ -isoproturon was studied using modifications of the OECD (2000) parallel method and the kinetic desorption studies by Elkhatib et al., (2007). Whereby, the loaded support materials were placed individually, in sterile 20 ml glass scintillation vials and 10 ml of Milli-Q water added. At set time intervals, over a period of 35 days (0.5, 2.5, 6.5, 9.5, 13.5, 27.5 and 34.5 days), 9 ml of the aqueous phase was removed and placed in a 20 ml HDLP plastic vial containing 10 ml of Ultima Gold™XR. The  $^{14}\text{C}$ -activity was then counted as described previously. A further 10 ml of Milli-Q water was added to the support material. The procedure was repeated until desorption equilibrium was reached. After 35 days, the support materials were removed from the vials and allowed to drip dry. Once dry, they were placed in a cellulose combusto-cone™ and oxidised as described previously.

##### 4.2.8.1 Desorption Mass Balance Calculations

The amount of  $^{14}\text{C}$ -activity was monitored at the different stages in the desorption experiment: loading, run-off during loading, desorption, and; amount retained by the support material at the end of the experiment. Mass balance calculations were then carried out to ensure the transfer of carbon could be fully explained by sorption processes. Figure 4.11 below represents the different stages of mass transfer:

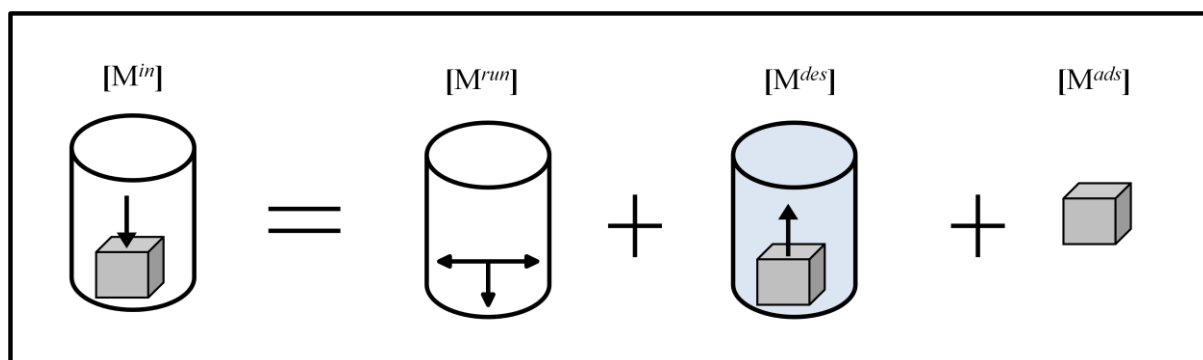


**Figure 4.11** – Mass balance calculations for detected  $^{14}\text{C}$ -activity at the different stages of the desorption study.

The mass transfer of  $^{14}\text{C}$ -IPU and  $^{14}\text{C}$ -SULPH were checked using scintillation counting methods to track the sum of Carbon-14 entering and leaving the batch desorption system as follows:

$$^{14}\text{C} [M^{in}] = ^{14}\text{C} [M^{run}] + ^{14}\text{C} [M^{des}] + ^{14}\text{C} [M^{ads}]$$

Where:

*M* mass of  $^{14}\text{C}$  shown as a percentage

*in* represents 100%, being the mass loaded at the start of the experiment

*run* run-off during loading

*des* amount desorbed subsequent to loading at the end of 35 days

*ads* amount still adsorbed after 35 days

#### 4.2.9 Kinetic Modelling

Desorption data were fitted to three empirical kinetic models; First-order, Elovich and Modified Freundlich, described in Table 4.4. The models were used to investigate the effects of time, concentration of analyte and type of support material on the sorption rate of sulphanilamide and isoproturon. A fit to the First-order model suggests the rate of sorption increases in keeping with increased concentration. A fit to the Elovich model proposes multilayer sorption which is driven by diffusion. A fit to the Modified Freundlich model suggests sorption processes occur at the surface of an adsorbent and so will reach a point of saturation at higher concentrations.

**Table 4.4 – Empirical Kinetic Models.**

Kinetic Model	Equation
<p>First-order</p>	<p><b><math>\ln[C_t] = -kt + \ln[C_0]</math></b></p> <p>Where: C = concentration</p> <p>t = time</p> <p><math>C_0</math> = concentration at t = 0</p> <p>A plot of <math>\ln[C_t]/[C_0]</math> vs. t gives a linear plot and slope <math>-k</math></p>
<p>Elovich (Elkhatib et al., 2007)</p>	<p><b><math>q = (1/\alpha)\ln(a\alpha) + (1/\alpha)\ln t</math></b></p> <p>Where, q = the amount of contaminant released in time t</p> <p>a = constant</p> <p><math>\alpha</math> = a constant, related to the initial rate of the reaction</p> <p>A plot of q vs. <math>\ln t</math> gives a linear plot, slope <math>(1/\alpha)</math> and intercept <math>(1/\alpha)\ln(a\alpha)</math></p>
<p>Modified Freundlich (Elkhatib et al., 2007)</p>	<p><b><math>q = k_d C_0 t^{1/m}</math></b></p> <p>Where: q = desorbed contaminant</p> <p><math>C_0</math> = initial concentration</p> <p>t = reaction time</p> <p><math>k_d</math> = desorption rate</p> <p>1/m = constant</p> <p>A plot of <math>\log q</math> vs. <math>\log t</math> gives a linear plot, slope 1/m and the intercept <math>K_d C_0</math></p>

#### *4.2.10 Statistical Analysis*

An analysis of variance (ANOVA) test was performed using SPSS v.18 to establish whether there were any significant differences ( $p \leq 0.05$ ) among the three support materials and the two compounds studied. Any significant differences highlighted in the group were then analysed using appropriate post-hoc tests, depending on whether equal variance was established, to identify which, if any, of the three supports materials and two compounds were significantly different ( $p \leq 0.05$ ).

In the first instance a Levene Test, for homogeneity of variances, was run to check the appropriate use of the ANOVA statistic, which assumes equal variance. If the resulting  $p > 0.05$ , the assumptions of ANOVA were considered as met, and the subsequent identification of any support materials having a significant difference ( $p \leq 0.05$ ) were tested using Tukey's Test. In the cases where the Levene Test result was  $p < 0.05$  then the variances were not equal and ANOVA was not used. Instead a further homogeneity of variance test (Welch and/or Brown-Forsythe) was performed to test the robustness of the means within the groups. Consequently, if  $p > 0.05$  then the results of ANOVA could be utilized and a subsequent Tukey's Test calculated or, if  $p < 0.05$  then Dunnetts' T3 Test was used in place of Tukey's to account for the unequal variances. The flow chart below (Figure 4.12), describes the analysis approach used.

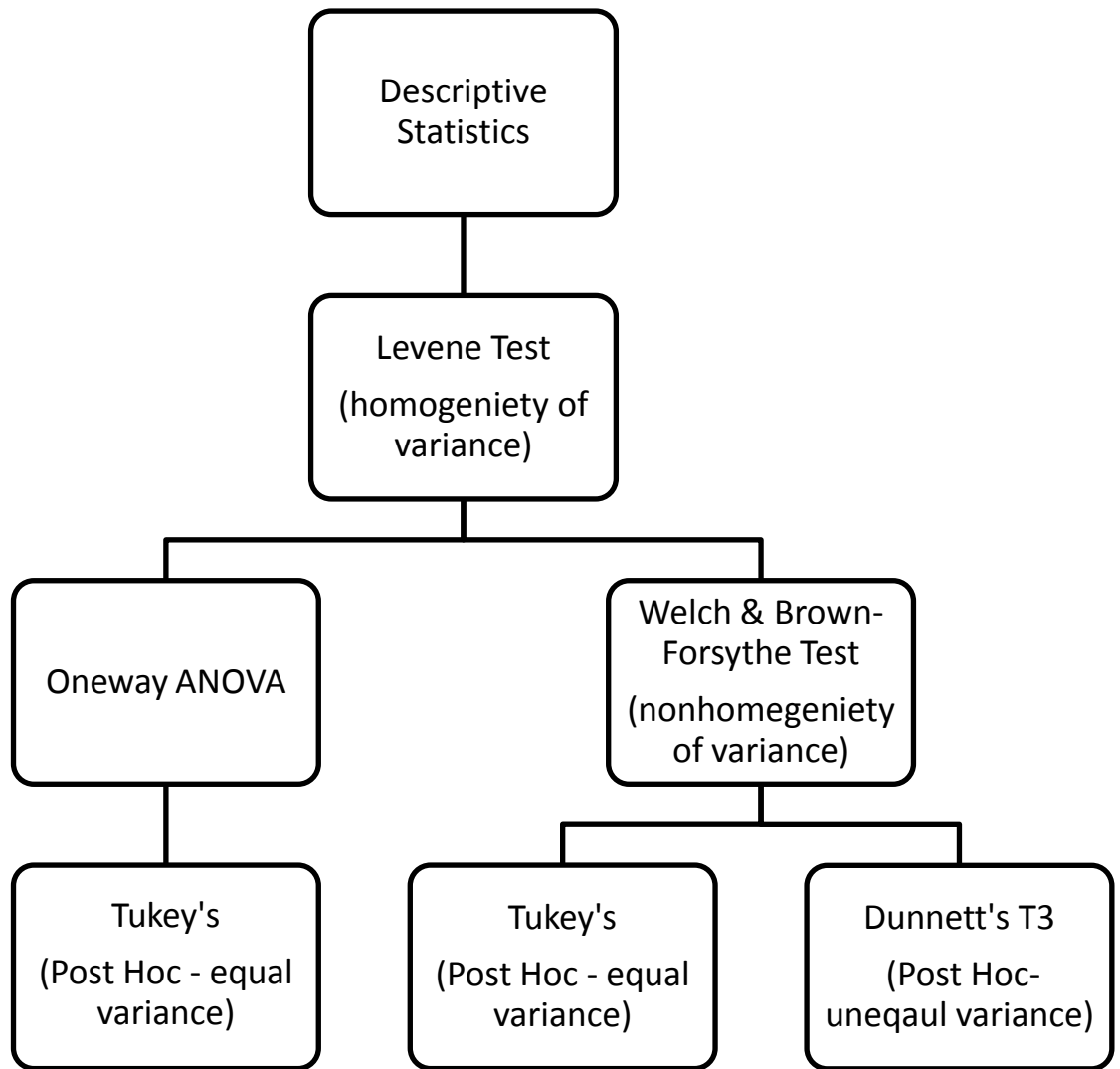


*Figure 4.12 – Flow diagram of statistical analysis steps used in SPSS v.18.*

The statistical analysis was approached in view of the following key research questions:

1. Does the loading concentration affect the quantity of compound adsorption?
2. Do the support materials have comparable sorptive abilities?
3. Do the support materials show sorptive preference to either compound?

### 4.3 Results/discussion

#### 4.3.1 Adsorption

Figure 4.13 below, shows the concentrations of  $^{14}\text{C}$ - IPU and  $^{14}\text{C}$ - SULPH, in the aqueous phase, *vs.* time. The curve remains unchanged throughout the duration of the batch adsorption experiment (a period of 35 days). This implies no adsorption; from the aqueous phase that simulated background concentrations, which ranged from 0.1 to 50 mg L<sup>-1</sup> occurred. Both IPU and SULPH are extremely soluble in water, 0.07 and 7.5 g L<sup>-1</sup> respectively, and so the results are not surprising. However, being organic compounds, there were expectations that they may be more attracted to the support material that contained the highest carbon content i.e. graphite felt, because it is widely known that organic compounds are retained more by matrices (e.g. soil/sediments) containing higher levels of organic carbon than those with lower levels (Babiker and Duncan, 1977). Therefore, although graphite felt contains 99.9% carbon and both pumice pellets and expanded perlite contain none (Table 4.3), no adsorption, from the background concentrations, was observed for the graphite felt. These findings concur with the low adsorption coefficients ( $K_{oc}$ ) reported earlier (Chapter 3, Table 3.1) for IPU and SULPH, which were <241 and <179 ml g<sup>-1</sup> respectively. Adsorption coefficients are a measure of a compounds tendency to adsorb to organic material, with values of <500 being indicative of little or no adsorption (Kumar, 2008).

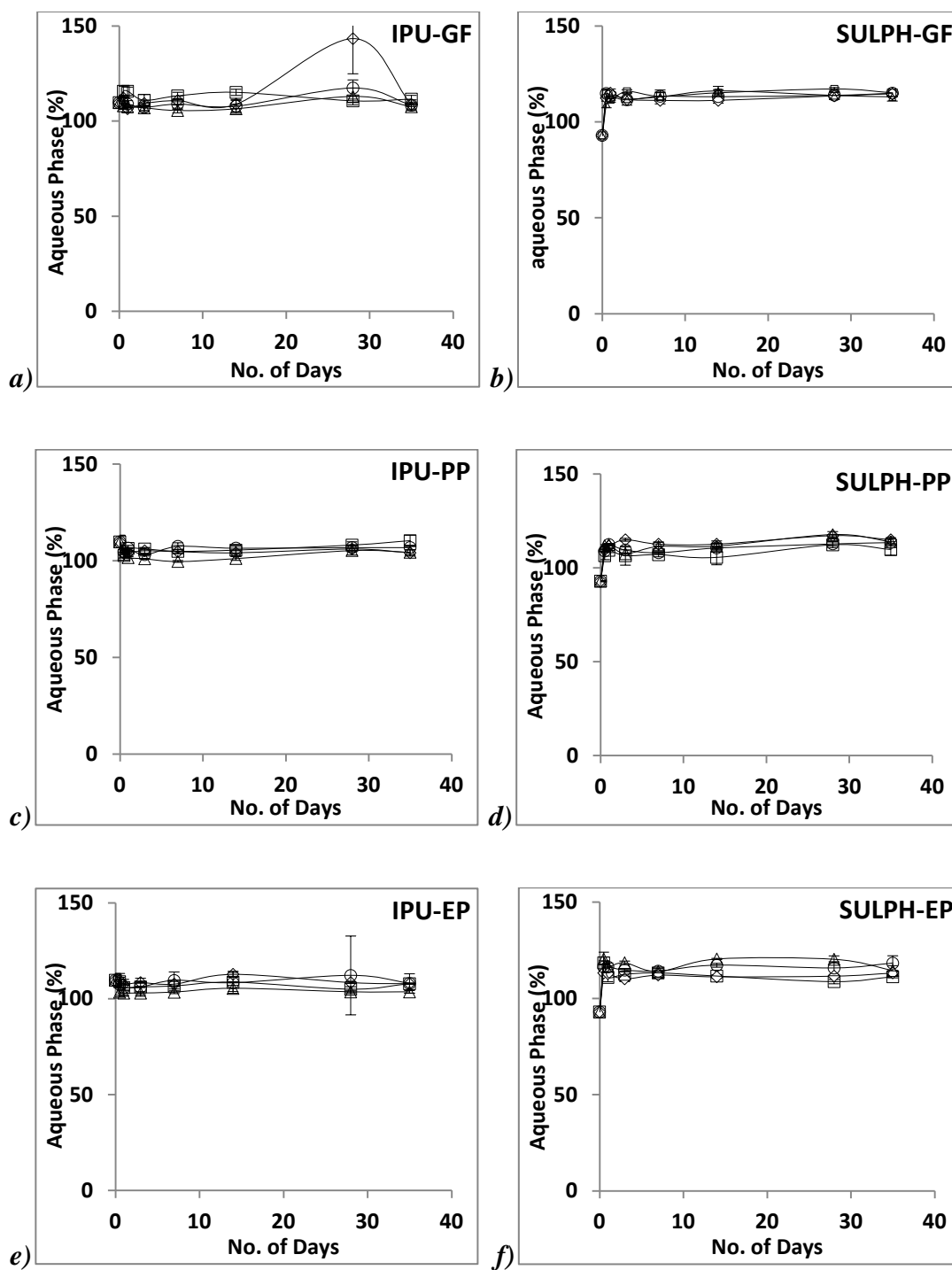


**Figure 4.13** – Effectiveness of Graphite Felt (GF) (a, b), Pumice Pellets (PP) (c, d), and Expanded Perlite (EP) (e, f), to remove  $^{12}\text{C}/^{14}\text{C}$  Isoproturon (IPU) and  $^{12}\text{C}/^{14}\text{C}$  Sulphanilamide (SULPH) from the aqueous phase, shown as the percentage of  $^{14}\text{C}$ -activity remaining in solution at:  $\diamond$  50,  $\square$  10,  $\circ$  1 and  $\triangle$  0.1  $\text{mg L}^{-1}$ . The error bars represent 95% confidence intervals.

The mass balance results for IPU (Table 4.5) and SULPH (Table 4.6) are represented below. The inputs of  $^{14}\text{C}$ -activity at the start of the adsorption experiments were calculated to be 100 %. The confidence intervals represent  $p \leq 0.05$ .

**Table 4.5 – Mass Balance of  $^{14}\text{C}$ - IPU Adsorption**

Adsorbent	IPU ( $\text{mg L}^{-1}$ )	$[\text{M}^{\text{out}}]$ %	$[\text{M}^{\text{ads}}]$ %	Total %
Graphite Felt	0.1	$107.6 \pm 2.1$	$0.7 \pm 0.7$	$108.3 \pm 2.8$
	1	$108.4 \pm 0.5$	$1.5 \pm 0.0$	$109.9 \pm 0.6$
	10	$111.6 \pm 1.5$	$1.4 \pm 0.1$	$113.0 \pm 1.6$
	50	$108.7 \pm 2.1$	$1.7 \pm 0.1$	$110.4 \pm 2.8$
Pumice Pellets	0.1	$104.4 \pm 2.0$	$0.5 \pm 0.1$	$104.9 \pm 2.0$
	1	$106.9 \pm 2.2$	$0.5 \pm 0.0$	$107.4 \pm 2.2$
	10	$110.4 \pm 0.7$	$0.4 \pm 0.0$	$110.7 \pm 0.7$
	50	$104.1 \pm 1.5$	$0.5 \pm 0.0$	$104.6 \pm 1.6$
Expanded Perlite	0.1	$103.7 \pm 2.5$	$0.9 \pm 0.0$	$104.5 \pm 2.5$
	1	$108.0 \pm 1.7$	$0.7 \pm 0.0$	$108.7 \pm 1.7$
	10	$103.5 \pm 2.8$	$0.8 \pm 0.0$	$104.4 \pm 2.9$
	50	$108.0 \pm 3.2$	$0.8 \pm 0.0$	$108.7 \pm 3.2$

**Table 4.6 – Mass Balance of  $^{14}\text{C}$ - SULPH Adsorption**

Adsorbent	SULPH ( $\text{mg L}^{-1}$ )	$[\text{M}^{\text{out}}]$ %	$[\text{M}^{\text{ads}}]$ %	Total %
Graphite Felt	0.1	$115.0 \pm 0.3$	$1.4 \pm 0.2$	$116.4 \pm 0.5$
	1	$113.0 \pm 1.9$	$2.1 \pm 0.5$	$115.1 \pm 2.4$
	10	$115.2 \pm 1.6$	$1.4 \pm 0.2$	$116.6 \pm 1.8$
	50	$114.6 \pm 1.2$	$1.3 \pm 0.1$	$115.9 \pm 1.3$
Pumice Pellets	0.1	$113.9 \pm 1.2$	$0.2 \pm 0.0$	$114.1 \pm 1.3$
	1	$113.5 \pm 1.6$	$0.3 \pm 0.1$	$113.8 \pm 1.6$
	10	$109.7 \pm 2.7$	$0.3 \pm 0.0$	$110.0 \pm 2.8$
	50	$115.0 \pm 0.8$	$0.3 \pm 0.0$	$115.3 \pm 0.8$
Expanded Perlite	0.1	$114.5 \pm 2.2$	$0.8 \pm 0.1$	$115.3 \pm 2.3$
	1	$118.3 \pm 3.6$	$0.8 \pm 0.0$	$119.1 \pm 3.6$
	10	$111.2 \pm 0.3$	$0.9 \pm 0.0$	$112.1 \pm 0.3$
	50	$113.2 \pm 0.5$	$0.6 \pm 0.1$	$113.8 \pm 0.6$

To satisfy the mass balance of  $^{14}\text{C}$  during the experiment the total values shown in Tables 4.5 & 4.6 should be  $100 \pm 10 \%$ , which takes into account the detection limitations of the liquid scintillation analyser and sampler oxidiser described in Section 4.2.5. The calculations for IPU (Table 4.5) fall within the expected value. However, the totals calculated for SULPH (Table 4.6) are slightly high, but not so as to detract from the findings of the adsorption study.

In summary, the results of the adsorption studies suggest there is no risk of contamination to graphite felt, pumice pellets and expanded perlite from background concentrations of IPU and SULPH found at the field site. The experimental concentrations ranged from  $0.1 - 50 \text{ mg L}^{-1}$  for both IPU and SULPH to reflect those recorded at the field study site, which range from;  $3.9 - 18.4 \text{ mg L}^{-1}$  for SULPH and  $0.03 - 0.5 \text{ mg L}^{-1}$  for IPU (Arcadis Geraghty & Miller International Ltd, 2008).

#### 4.3.2 Loading Support Materials

To utilise graphite felt (GF), pumice pellets (PP) or expanded perlite (EP) as support materials for *in-situ* microcosms, a  $^{13}\text{C}$ -labelled compound would need to be successfully loaded prior to deployment in the field. Other NA studies, involving  $^{13}\text{C}$ -labelled *in-situ* microcosms, have loaded volatile petrochemical contaminants at concentrations ranging from  $38 - 112 \text{ mg g}^{-1}$  onto support materials, in particular Bio-Sep® beads containing powdered activated carbon, using vapour exposure under partial vacuum techniques (Braeckevelt et al., 2007b, Geyer et al., 2005b, Kästner et al., 2006). However, the non-volatile nature of IPU and SULPH made this approach unsuitable. In addition, the results from the adsorption study indicated loading the support materials in the aqueous phase would not facilitate adsorption. Therefore, IPU and SULPH were loaded using solvent evaporation methods. However, using this method may have restricted adsorption to the external surface of the support materials because in the absence of a vacuum the adsorbates entry into the porous structure of the support material as a vapour would have been hindered (He et al., 2009).

Initial observations revealed GF and EP to have considerable potential as supports for both compounds (Fig. 4.14) while PP performed much less favourably.

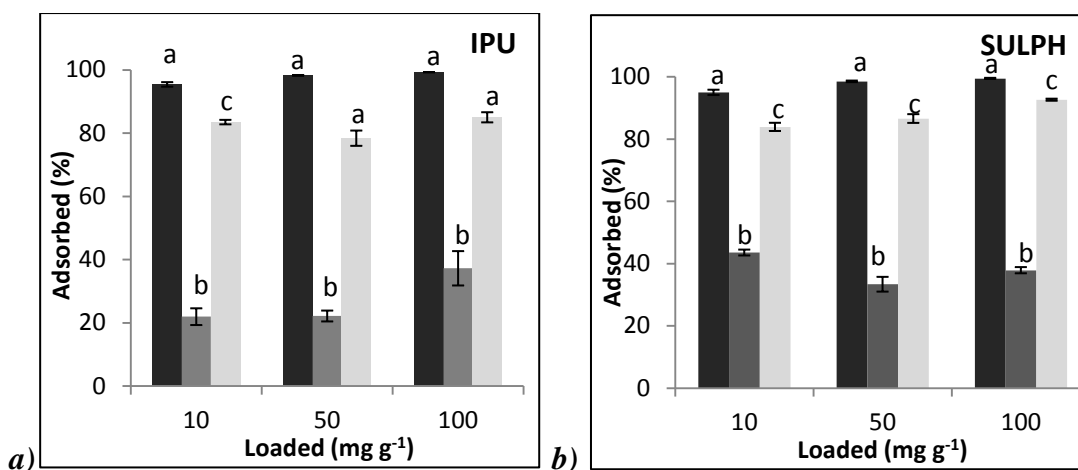


**Figure 4.14** – The bar groupings represent the same concentrations, shown as the percentage of  $^{14}\text{C}$ -activity adsorbed of  $^{12}\text{C}/^{14}\text{C}$  isoproturon (IPU), (a) and  $^{12}\text{C}/^{14}\text{C}$  sulphanilamide (SULPH), (b) loaded onto different support materials; graphite felt ■, pumice pellets ■, and expanded perlite ■. The error bars represent 95% confidence intervals. The lower case letters show the significant difference ( $p \leq 0.05$ ) observed between the three support materials.

Statistical analysis was conducted to compare whether there was a difference between the three support materials when loaded with the same concentration of IPU and SULPH. Overall, the results represented in Fig. 4.14 show a significant difference ( $p \leq 0.05$ ) between the types of support used when loaded with the same concentration of IPU (a) and SULPH (b). The statistical analysis highlights no significant difference ( $p \leq 0.05$ ) between GF and EP when loaded with 50 and 100  $\text{mg g}^{-1}$  of IPU. However, the error bars (Fig. 4.14), which signify 95% confidence intervals, do not overlap and so suggest there may be a difference, as observed in the 10  $\text{mg g}^{-1}$  loading for all three support materials.

Having established a significant difference between the types of support used, further analysis looked at whether loading different concentrations of IPU and SULPH onto the same support material would affect the percentage of analyte loaded. Therefore, concentrations of 10, 50 and 100  $\text{mg g}^{-1}$  were loaded onto support materials of the same weight to establish limitations to surface adsorption. The expectation was that once the surface bonding sites became saturated further adsorption would be restricted. Overall, the results represented in Fig. 4.15 show that, despite different starting concentrations, there was no significant difference ( $p \leq 0.05$ ) in the percentage of IPU (a) and SULPH (b) loaded onto each support material. However, the statistical analysis does suggest a significant difference ( $p \leq 0.05$ ) between

loading  $10 \text{ mg g}^{-1}$  and the other concentrations of both IPU and SULPH onto GF. But, on further investigation, the error bars (Fig. 4.15), which signify 95% confidence intervals, show the actual difference ( $p \leq 0.05$ ) to be very small.

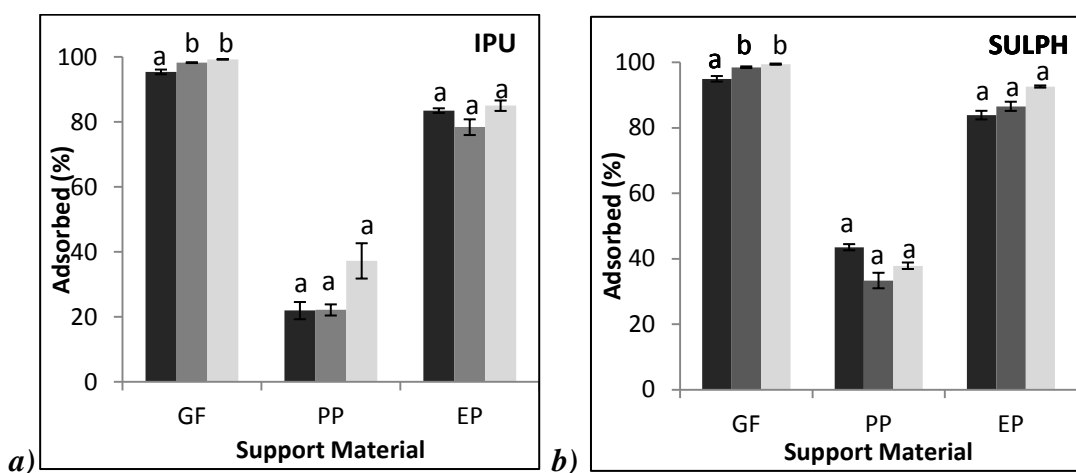


**Figure 4.15** – The bar groupings represent the same support materials loaded with different concentrations; 10  $\blacksquare$ , 50  $\blacksquare$  and 100  $\blacksquare$   $\text{mg g}^{-1}$  of  $^{12}\text{C}/^{14}\text{C}$  isoproturon (IPU), (a) and  $^{12}\text{C}/^{14}\text{C}$  sulphanilamide (SULPH), (b), shown as the percentage of  $^{14}\text{C}$ -activity adsorbed. The error bars represent 95% confidence intervals. The lower case letters show the significant difference ( $p \leq 0.05$ ) observed between the three support materials.

The felt structure of GF made loading the herbicides relatively easy because it acted like a sponge. Additionally, there was no noticeable run off. By comparison the hard, stony like structure of PP and EP allowed the herbicides to run off the surface of the material. This was more noticeable for PP than EP. After loading, the carrier solvent evaporated and crystals of the herbicides were visible on the surface of the support materials. In the case of PP, there were also visible crystals on the base of the vial holding the support material consequential of the run off. Run off also occurred during the loading of EP, however, there was less crystal formation on the base of the vial than seen with PP. This was most likely attributable to the number of EP pellets used, which covered the base of the vial, and so left less room for run off compared to the PP vials, which only contained one pellet. Mass balance distributions of the actual loadings and run-off are given in Section 4.2.8.1.

Furthermore, mention should be made to the surface area of each support. The

concentrations loaded were calculated using equal weights of support material. Therefore, the external surface areas for each support were different; GF ~ 6 cm<sup>2</sup>, PP ~ 2 cm<sup>2</sup> and EP ~ 9 cm<sup>2</sup>. The results shown in Fig. 4.15 indicate the following order; GF > EP > PP, in which each support material performs, with respect to their adsorptive capacity for IPU and SULPH. However, these results may be biased towards either ease of loading or surface area rather than being truly indicative of the capacity of the support materials to adsorb IPU and SULPH.

A final comparison was made between the same concentration (100 mg g<sup>-1</sup>) of IPU and SULPH to establish whether either was more favourable to each of the three support materials. The results are represented in Fig. 4.16 and show there was no significant difference ( $p \leq 0.05$ ) between the two compounds.

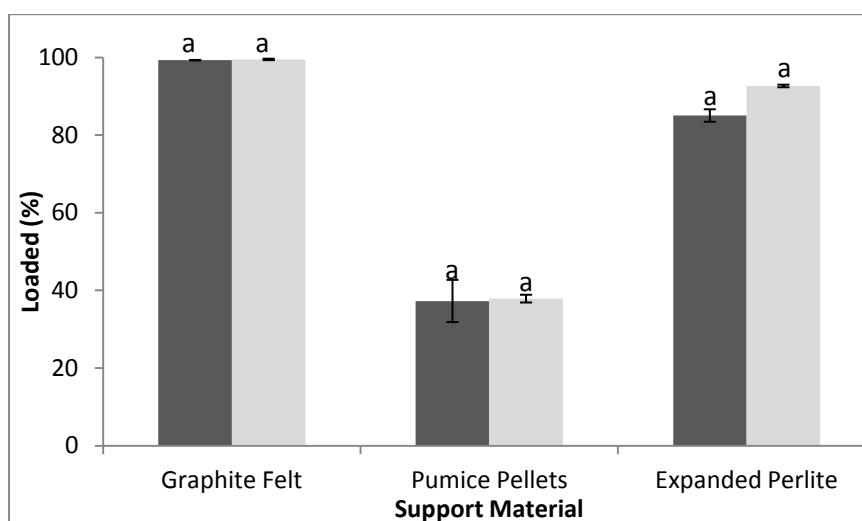


**Figure 4.16** – A comparison of 100 mg g<sup>-1</sup> of <sup>12</sup>C/<sup>14</sup>C isoproturon ■ and <sup>12</sup>C/<sup>14</sup>C sulphanilamide ■ loaded onto graphite felt, pumice pellets and expanded perlite after a correction for the amount lost due to run off. The error bars represent 95% confidence intervals. The lower case letters show the significant difference ( $p \leq 0.05$ ) observed between the different herbicides.

Therefore, in summary, the initial concentration of IPU and SULPH loaded did not influence the final percentage of compound loaded/adsorbed. This was true for each support (Fig. 4.15) and for each compound (when compared at 100 mg g<sup>-1</sup>, Fig. 4.16). The type of support material used did influence the percentage of compound loaded with GF performing best, followed closely by EP. PP was notably lower with regard to its capacity to accept both SULPH and IPU. It is reiterated that it is not

clear if the observed differences are the result of different surface areas or the adsorptive capacity of the material used. Furthermore, although there was an expectation for the compounds to interact with the solid surfaces of the support materials during loading there is also a possibility that diffusion of the compounds, into the material pore space, could account for a fraction of the total sorbed mass.

#### 4.3.3 Desorption

The concept behind using isotopically labelled *in-situ* microcosms, to support NA, hinges on the ability of indigenous microbes to metabolise an isotopic tracer so as to facilitate its subsequent detection in the microbial phospholipid fatty acids (Bush-Harris et al., 2006, Geyer et al., 2005b). Therefore, the amount of tracer, loaded onto the support material, should be high enough to determine the presence of microbes involved in the biodegradation of the target compound. Factors influencing this can be; the relative abundance of the biodegrading microbes and the final concentration of the tracer in their phospholipid fatty acids (Boschker and Middelburg, 2002). This is further hindered by the fact that initial site investigations, of NA processes, are often blind in that the abundance, if any, of indigenous microbes, naturally attenuating the target compound, is generally unknown. To overcome this, high levels of tracer have traditionally been used to ensure analytical detection of its incorporation into the phospholipid fatty acids (Braeckevelt et al., 2007b, Geyer et al., 2005b, Kästner et al., 2006, Stelzer et al., 2006b, Tomohito, 1999, United States Environmental Protection Agency (EPA), 2008).

Boschker and Middleburg (2002) found that 0.1 % of a stable isotope tracer was detected in the phospholipid fatty acids of microbes and it accounted for a 10 ‰ increase in the  $^{13}\text{C}$   $\delta$  value. Earlier studies, involving a tenfold increase in label concentration resulted in a 90 ‰ increase (Boschker et al., 1998). Likewise, Geyer et al. (2005b) found that 17% of a 88 mg g<sup>-1</sup> loading of  $^{13}\text{C}_6$ -benzene was detectable in phospholipid fatty acids and resulted in a 13,410 ‰ increase in  $^{13}\text{C}$   $\delta$  value.

Similarly, high  $^{13}\text{C}$   $\delta$  values have been reported for a 38 mg g<sup>-1</sup> loading of  $^{13}\text{C}_6$ -chlorobenzene, 13,410 ‰ (Kästner et al., 2006) and 88 mg g<sup>-1</sup> of  $^{13}\text{C}_6$ -toluene, 13,360 ‰ (Geyer et al., 2005b), which are not entirely necessary to ascertain biodegradation, when analytical detection limits, of shifts in isotopic signatures, are

as little as 0.05 ‰ (McKelvie et al., 2007b). Therefore, the elevated values reported above suggest the initial concentrations of tracer are somewhat generous.

In addition to consideration of tracer concentration, a support material should retain the tracer long enough to sustain biofilm development, which can take from as little as hours to days. Morgenroth and Milferstedt (2009) explain how initial attachment can take minutes to hours, biofilm development – days, followed by weeks, months and years for growth and detachment. In addition, lab based trials, which study biofilm development, are usually limited to 2 weeks. Therefore, the length of deployment, of loaded microcosms, needs to reflect these time frames in order to facilitate the recovery of viable biomass for detection of the  $^{13}\text{C}$  incorporation into the lipids. *In-situ* microcosms are typically deployed for a period of 1-2 months (Alfreider et al., 1997, Peacock et al., 2004, Stelzer et al., 2006b). However, biofilm development can occur very rapidly in natural and industrial environments (Costerton et al., 1995) with maximum growth, on surrogate support materials, reported between 5 days (Claret, 1998) and 6 weeks (Griebler et al., 2002) in groundwater environments. Also, an assumption can be made that once a biofilm develops, on the support material, that this will further impede the desorption of a loaded tracer to the groundwater as it will impose additional diffusion constraints, typically two orders of magnitude greater (Holden et al., 1997) on the tracer's release.

The aim of the desorption study was to ascertain whether, having considered a time frame for biofilm development, there would be an adequate amount of tracer remaining on the support material to facilitate its utilization by indigenous microbes and its subsequent detection using PFLA techniques. Therefore, an estimate was made allowing for a two week period for biofilm development and a final tracer concentration of the same order of magnitude as that reported in the literature for other tracers used, in particular the minimum amount of  $38 \text{ mg g}^{-1} [^{13}\text{C}_6\text{-chlorobenzene}]$  (Kästner et al., 2006). However, attention should be given to the concentration of carbon based compounds used as this will also depend on the number of labelled carbon atoms in the molecule. In this instance both the  $^{13}\text{C}_6\text{-chlorobenzene}$ , used by Kästner et al., (2006), and the IPU and SULPH, of interest in this study, contain a  $^{13}\text{C}$ - labelled benzene ring so a comparison should be fair.

Desorption studies were set up using three different concentrations: 10, 50 and 100 mg g<sup>-1</sup> of radio-labelled IPU and SULPH loaded onto three different support materials; GF, PP and EP. Comparisons were drawn between different loading concentration, to establish whether this would influence the rate of desorption, and different support materials, to ascertain their suitability in retaining the tracer. In terms of suitability, it is expected that the support materials would be able to retain ~ 30 % of the tracer after a period of two weeks, which would equate to a final concentration of 3, 15 and 30 mg g<sup>-1</sup>, respectively. Considering the high <sup>13</sup>C δ values already discussed above, the proportion of tracer remaining after two weeks is regarded as generous for the initial 100 mg g<sup>-1</sup> loading and reasonable for the 50 and 10 mg g<sup>-1</sup>. Figure 4.17 below, shows the percentage of IPU and SULPH remaining on GF, PP and EP during an experimental period of 35 days.

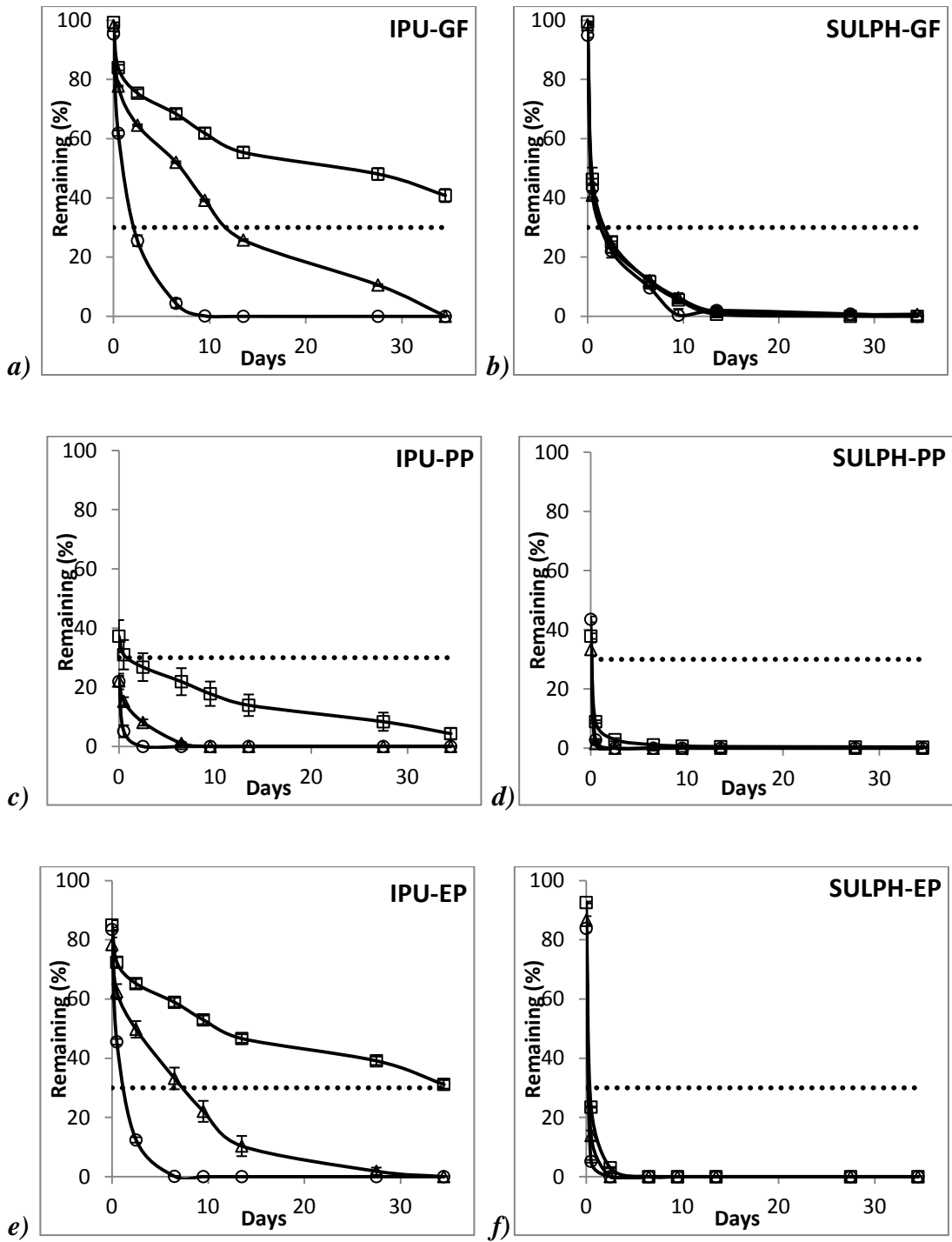


**Figure 4.17** – Desorption of  $^{12}\text{C}/^{14}\text{C}$  Isoproturon (IPU) and  $^{12}\text{C}/^{14}\text{C}$  Sulphanilamide (SULPH) from Graphite Felt (GF) (a, b), Pumice Pellets (PP) (c, d), and Expanded Perlite (EP) (e, f), shown as the percentage of  $^{14}\text{C}$ -activity remaining on the support material at different concentrations:  $\square$  100,  $\triangle$  50,  $\circ$  10  $\text{mg g}^{-1}$  of support material. The error bars represent 95% confidence intervals ( $n=3$ ). The dotted line represents the proportion of IPU and SULPH loading required after a period of 14 days.

The desorption results for SULPH (Fig. 4.17b, d and f) show that after 2 weeks none of the isotopic tracer remained on any of the support materials. 100 % of the tracer was desorbed from GF after 2 weeks and from PP and EP, after 2 days, of starting the experiment. Therefore, SULPH would not be suitable for *in-situ* microcosm studies because it is unlikely that the indigenous microbes would have had suitable time to utilise and incorporate the tracer. Figure 4.17a, c, and e represent the results for IPU desorption. After 2 weeks there was >30 % of the 100 mg g<sup>-1</sup> tracer remaining, which had been loaded onto GF and EP. There was ~60 % IPU remaining on GF and ~50 % on EP. After the same period of time a sufficient quantity of IPU was not observed for the 10 and 50 mg g<sup>-1</sup> loadings on GF and EP. With regard to PP none of the three concentrations of tracer loaded were remaining after 2 weeks. This suggests GF and EP may be more suitable for use as support materials when loaded with 100 mg g<sup>-1</sup> of IPU.

The desorption studies were conducted using fresh Milli-Q water and so the results represent a “worst case scenario” because when deployed in the field there will be other factors influencing the rate of desorption: a) the deployment site already has high levels of IPU and SULPH (0.5 and 18.4 mg L<sup>-1</sup>, respectively) (Arcadis Geraghty & Miller International Ltd, 2008) and so desorption due to equilibrium processes will be slower in the field; b) as already mentioned, biofilm development on the support will subsequently slow desorption by imposing further diffusion constraints on the tracer (Holden et al., 1997); and c) should NA already be present at the field site for IPU and SULPH, then the loaded tracer need not be at levels required to initiate catabolic activity and so biofilm development should be rapid because no adaption period would be necessary (Ingerslev et al., 2000).

The mass balance calculations are presented in Figure 4.18 as area graphs to highlight the movement of carbon mass during the loading and off loading stages of the desorption investigation. The actual values for IPU (Table 4.8) and SULPH (Table 4.9) are represented below. The inputs of <sup>14</sup>C-activity at the start of the desorption experiment were calculated to be 100 %. The confidence intervals represent  $p \leq 0.05$ .

The blue areas of the graph (Figure 4.18) represent the percentage of carbon lost during loading of IPU and SULPH onto the three support materials and are meant as

an indication of ease of loading using solvent evaporation methods. The red areas correspond to the percentage of IPU and SULPH retained by the support materials and, should the support materials be suitable as *in-situ* microcosms, would signify the percentage of carbon available to indigenous microbes as food source after a 35 day desorption period. The green areas show the percentage of IPU and SULPH desorbed from the support materials after a 35 day desorption period and would represent the loss of tracer to the environment should the support materials be deployed as *in-situ* microcosms in groundwater.

The results in Figure 4.18 highlight that it was easier to load both IPU and SULPH onto GF (a, b) and EP (e, f) than PP (c, d). During loading only 1-5 % of both IPU and SULPH was lost from GF (a, b), due to run-off. The relative ease of loading GF is most likely attributable to its “sponge-like” characteristics. Whereas, in the case of PP (c, d) > 50 % and EP (e, f) >20 % of the adsorbates were lost due to run off. Neither EP, despite having a larger external surface area than GF, nor PP was able to soak up the adsorbate as readily as the GF. This was probably due to their rigid, consolidated surface characteristics. Furthermore, as discussed previously, the IPU and SULPH would have been restricted to surface adsorption only, as the lack of any vacuum during loading would have hindered entry to the porous structure within the support material. However, this said, during loading it was noted that the IPU and SULPH were able to saturate the GF material. By comparison, the adsorbates quickly ran off the surface of both PP and EP and so there was less contact time for adsorption.

Run-off was less in the case of the 100 mg g<sup>-1</sup> loading than in the case of the 10 and 50 mg g<sup>-1</sup> loadings of IPU onto PP (Fig. 4.18.c). However, the mass balance calculations in Table 4.8 highlight a broad confidence margin ( $p \leq 0.05$ ) for 100 mg g<sup>-1</sup> of IPU loaded onto PP. Furthermore, the statistical analysis conducted in section 4.2.7 (*Loading Support Materials*) suggested there was no significant difference ( $p \leq 0.05$ ) between the different IPU concentrations loaded onto PP. Therefore, this difference may be a trait associated with the difficulties in loading PP rather than differences in sorption processes linked to loading concentration.

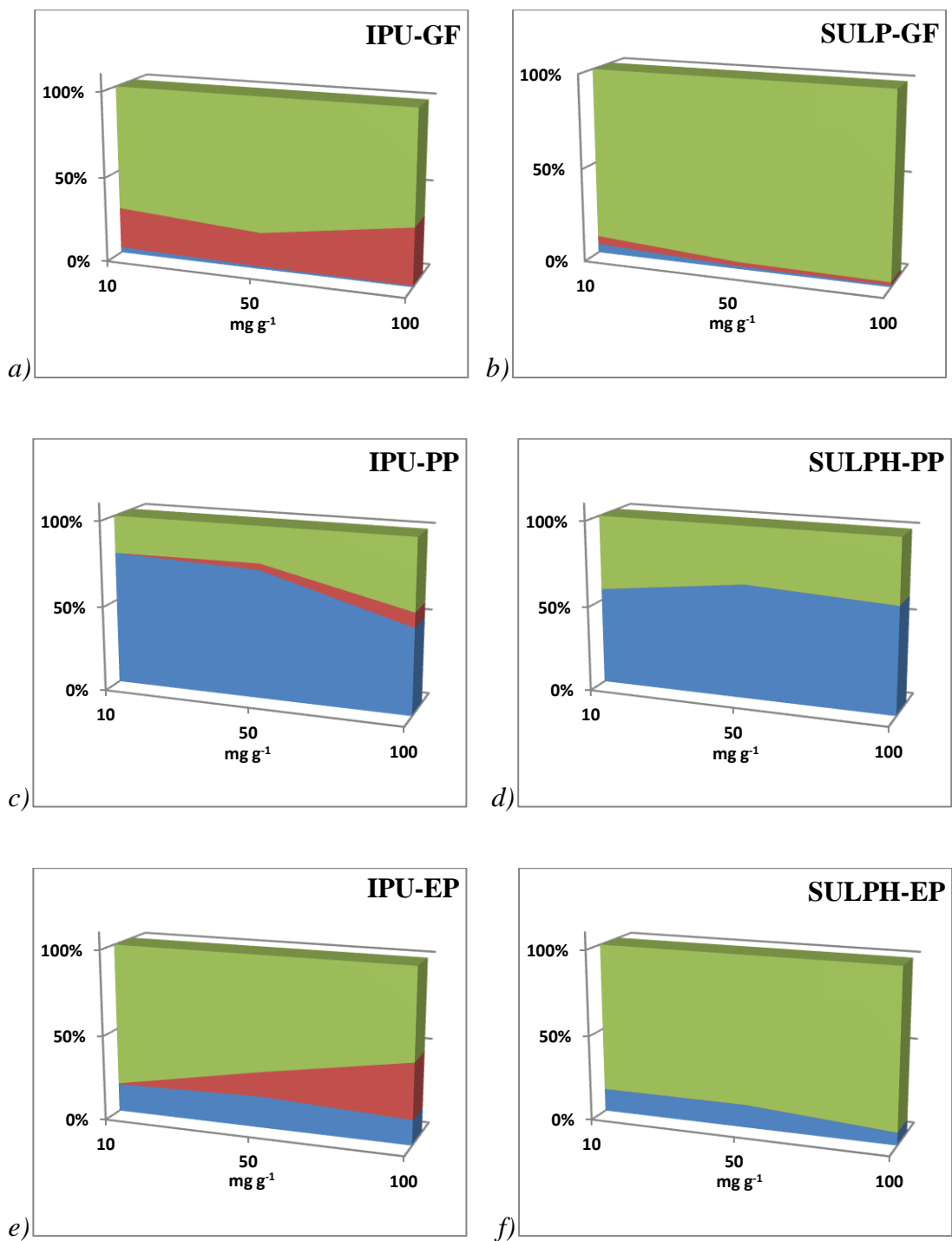


**Figure 4.18** – The above mass balance graphs represent the percentage of Isoproturon (IPU) and Sulphanilamide (SULPH); desorption (green), adsorption (red) and run-off during loading (blue) from/to Graphite Felt (GF) (a, b), Pumice Pellets (PP) (c, d) and Expanded Perlite (EP) (e, f) during the loading and off-loading desorption experiments.

The frames of Figure 4.18, suggest the following order for ease of loading; GF > EP > PP. However, the surface area of the PP ( $\sim 2 \text{ cm}^2$ ) to weight ratio ( $\sim 100 \text{ mg}$ , for all three support materials) was much smaller than that for GF ( $\sim 6 \text{ cm}^2$ ) and EP ( $\sim 9 \text{ cm}^2$ ) and so it is difficult to ascertain with certainty how much of this is attributable to differences in surface area. Therefore, further work would be prudent to focus on surface area as opposed to the mass of support material, to gain further insights into the mechanisms at work.

The red areas of the frames of Figure 4.18, illustrate the percentage of IPU and SULPH retained by the three support materials at the end of the 35 day desorption period. They show adsorption of IPU (a, c and e) was greater than SULPH (b, d and f) on all three support materials. With only negligible amounts of  $\sim 2\text{-}5\%$  observed for SULPH onto GF (b) and  $<1\%$  for PP (d) and EP (f), whereas,  $>30\%$  of IPU was retained by both GF (a) and EP (e) and up to  $7\%$  for PP (c). Adsorption of IPU onto GF (a) was more uniform across the range of concentrations loaded, whereas, higher concentrations of IPU loaded onto both PP (c) and EP (e) appear to be more favourable with respect to their sorption. However, as mentioned above, these differences may simply reflect difficulties in loading, which is further supported by the statistical analysis that established no significant differences between loading concentrations. Interestingly, the  $100 \text{ mg g}^{-1}$  of IPU loaded onto GF (a) and EP (e) show similar adsorption percentages, with both having the capacity to retain  $\sim 30\%$  of IPU after a 35 day desorption period. Therefore, these two support materials would be of particular interest for use as *in-situ* microcosms for the compound IPU. However, the difficulty in loading IPU onto PP, mentioned above, along with PP limited capacity to retain IPU (c) renders this support unfit for purpose.

The green areas of the frames of Figure 4.18 show the total percentage of IPU and SULPH desorbed after a 35 day period. Under the conditions of the experiment, the graphs (b, d and f) draw attention to the complete SULPH desorption from all three support materials. Most of which occurred within the first two days of the period of desorption (Figure 4.17b, d and f). By comparison, after 35 days, only  $\sim 70\%$  of the IPU had desorped for both the GF (a) and EP (e) loaded with  $100 \text{ mg g}^{-1}$ . The rapid desorption of SULPH may be attributed to SULPH having a high solubility ( $7.5 \text{ g L}^{-1}$ ), in water, two orders of magnitude greater than that of IPU ( $0.07 \text{ g L}^{-1}$ ). As discussed earlier, the suitability of a support material would be determined by its

ability to retain ~30 % of a tracer after a deployment time in the field of 2 weeks. In reality, this percentage matters from an aqueous contamination perspective but the carbon mass available as a “food source” is key to the success of an *in-situ* microcosm. The desorption data represented in Figure 4.18 suggests that only GF (a) and EP (b), for the compound IPU fits this criteria, with PP (c, d) being unsuitable for both tested adsorbates and GF (b) and EP (f) being unsuitable for SULPH. Table 4.7, below, summarises the findings and highlights the materials which may be suitable for use as surrogate supports for *in-situ* microcosms.

**Table 4.7 – Potential Support Materials for *In-situ* Microcosms.**

Support Material	Isoproturon	Sulphanilamide
Graphite Felt	YES	NO
Pumice Pellets	NO	NO
Expanded Perlite	YES	NO

**Table 4.8 – Mass Balance of <sup>14</sup>C-IPU Desorption.**

Adsorbent	IPU (mg g <sup>-1</sup> )	[M <sup>run-off</sup> ] %	[M <sup>ads</sup> ] %	[M <sup>desorbed</sup> ] %	Total %
Graphite Felt	10	4.6 ± 0.4	33.9 ± 23.4	102.4 ± 0.8	140.9 ± 24.6
	50	1.7 ± 0.0	25.2 ± 1.6	98.7 ± 6.6	125.6 ± 8.2
	100	0.7 ± 0.0	30.2 ± 4.6	58.9 ± 6.2	89.8 ± 10.8
Pumice Pellets	10	78.2 ± 2.7	0.03 ± 0.0	21.9 ± 1.2	100.1 ± 3.9
	50	78.1 ± 3.6	4.0 ± 1.8	22.2 ± 0.2	104.3 ± 5.6
	100	39.8 ± 21.7	6.8 ± 1.0	32.8 ± 1.3	79.4 ± 24.0
Expanded Perlite	10	16.5 ± 0.4	0.5 ± 0.0	83.8 ± 5.0	100.8 ± 5.4
	50	21.5 ± 0.9	16.7 ± 0.4	78.6 ± 3.0	116.8 ± 4.3
	100	15.0 ± 0.6	33.3 ± 1.4	54.1 ± 3.6	102.4 ± 5.6

**Table 4.9 – Mass Balance of <sup>14</sup>C-SULPH Desorption.**

Adsorbent	SULPH (mg g <sup>-1</sup> )	[M <sup>run-off</sup> ] %	[M <sup>ads</sup> ] %	[M <sup>desorbed</sup> ] %	Total %
Graphite Felt	10	5.0 ± 0.5	4.6 ± 0.2	95.3 ± 5.1	104.9 ± 5.8
	50	1.5 ± 0.2	2.4 ± 0.1	98.3 ± 6.3	102.2 ± 6.6
	100	1.0 ± 0.3	1.7 ± 0.0	99.8 ± 6.1	102.5 ± 6.4
Pumice Pellets	10	56.6 ± 2.6	0.1 ± 0.0	43.6 ± 1.7	100.3 ± 4.3
	50	66.8 ± 1.8	0.1 ± 0.0	33.3 ± 0.3	100.2 ± 2.1
	100	62.3 ± 3.0	0.1 ± 0.0	37.6 ± 1.6	100.0 ± 4.6
Expanded Perlite	10	16.1 ± 0.3	0.1 ± 0.0	84.1 ± 4.0	100.3 ± 4.3
	50	13.4 ± 0.6	0.1 ± 0.0	86.8 ± 4.0	100.3 ± 4.6
	100	7.4 ± 0.1	0.1 ± 0.0	93.0 ± 5.5	100.5 ± 5.6

To satisfy the mass balance of <sup>14</sup>C during the experiment the total values shown in Tables 4.8 & 4.9 should be 100 ± 10 %, which takes into account the detection limitations of the liquid scintillation analyser and sampler oxidiser described in the instrumentation section (4.2.5). The calculations for SULPH (Table 4.9) fall within the expected value ( $p \leq 0.05$ ). In the case of IPU (Table 4.8), the totals calculated for PP and EP fall within the expected values ( $p \leq 0.05$ ). However, those calculated for the 10 mg g<sup>-1</sup> of IPU desorbed from GF are unreasonably high, which suggests the samples may have become compromised during the desorption experiment. In terms of this investigation, this should not detract from further discussion of the results, which will focus on kinetic model comparisons between the 100 mg g<sup>-1</sup> sorption processes of IPU and SULPH onto the three different support materials.

#### 4.3.4 Kinetic Models

Sparks (2003) proposes that sorption processes can be explained by four types of isotherms (S, L, H and C). Figure 4.19, below, depicts the curves of these isotherms. They are representative of adsorption isotherms and so, should adsorption be reversible, then desorption isotherms would be characterised by the same.

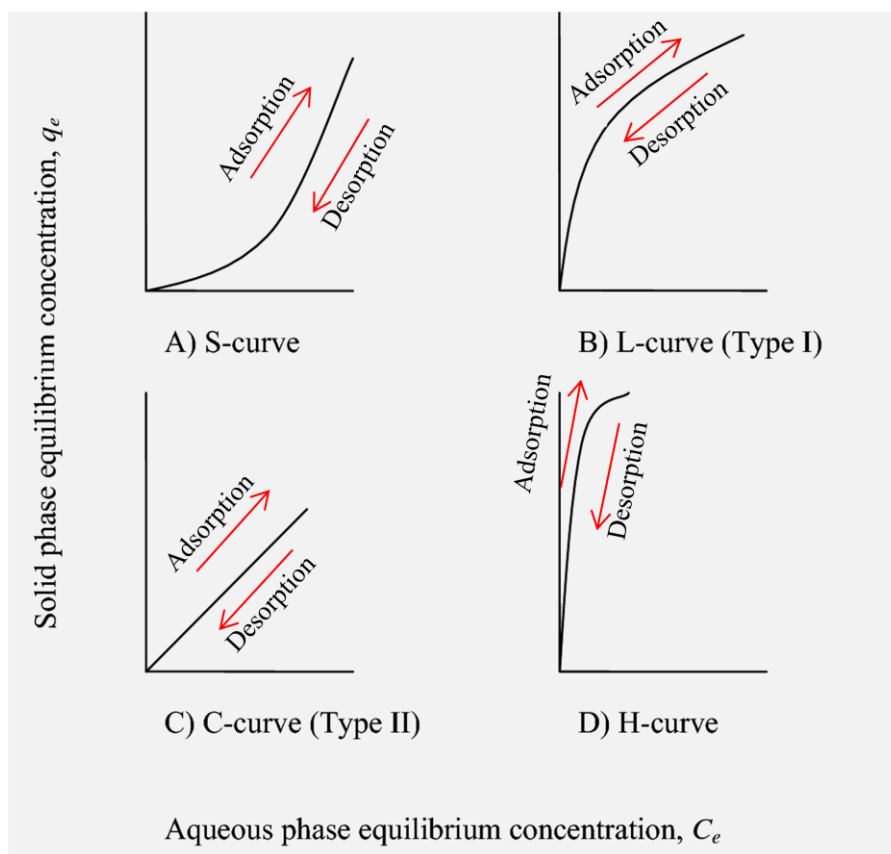


**Figure 4.19** – Four main types of adsorption isotherms (S, L, C and H) which explain sorption processes, adapted from Palomo (2008).

Figure 4.19a represents an S-type isotherm, which is typical of adsorbents having a lower affinity for adsorbates at low concentrations than those at high concentrations. At first, the slope is seen to increase with adsorbate concentration but in time, as adsorbent sites become filled the slope would begin to plateau (not shown in Fig. 4.19a). The L-shaped, or Langmuir, isotherm (Fig. 4.19b) describes the opposite characteristics of the S-type isotherm, in that it has a higher affinity for adsorbates at low concentrations than those at high concentrations. This is characterised by a decreasing slope because as the adsorbate concentration increases the number of vacant adsorption sites decrease, which causes a reduction in the rate at which adsorption can occur. Figure 4.19c represents the C-type isotherm, usually depicted by a linear relationship. This type of isotherm is indicative of sorption processes governed by partitioning mechanisms such as diffusion. C-type isotherms are also suggestive of reversible adsorption/desorption and temperature dependent processes.

Finally, the H-type isotherm (Fig. 4.19d), known as the high-affinity isotherm, is representative of a strong adsorbate-adsorptive interaction (Sparks, 2003).

The results obtained during the desorption studies (Section 4.3.3), for both IPU and SULPH desorption from GF, PP and EP and represented in Figure 4.17 (a-f), suggest a fit to the L-shaped isotherm, indicative of the Langmuir model. This model would suggest that at the start of the experiment many of the adsorption sites are filled and so the concentration of adsorbate was high causing desorption to occur rapidly. But, as desorption continued, the concentration of adsorbate decreases as more and more adsorption sites become vacant, causing the rate of desorption to slow down. However, in using this model to interpret sorption processes there must be an awareness of the assumptions made by Langmuir in that the process is believed to be monolayer coverage with each adsorption site being identical and holding only one molecule, the surface of the adsorbent is homogeneous and there is no attraction between adsorbate molecules (Sparks, 2003). The surface of the three support materials used in this study are heterogeneous and so do not meet all the assumptions made by Langmuir. However, the L-shape isotherms produced may be used for purely descriptive purposes in suggesting that sorption process may be concentration dependent. This is particularly noticeable in the graphs for IPU desorption (Fig. 4.17 a, c and e). Here the desorption rates were visibly slower at higher concentrations with the slopes decreasing in the following order  $10 > 50 > 100 \text{ mg g}^{-1}$  for all three support materials. This pattern was also observed in the graphs for SULPH (Fig. 4.17 b, d and f) for all three supports.

Though observations from the batch desorption studies can offer some insights of the adsorbate-adsorptive interactions in reaching equilibria, these insights are limited to the final state of the desorption reaction. Whereas, looking at the kinetics, which regards the time-dependent nature of sorption, provides information relating to the rate at which the reaction occurs (Saeid, 2004). Once known, the kinetic rates can be used to better evaluate potential adsorbent materials. Therefore, the data obtained during the studies of desorption of IPU and SULPH from the three support materials was further investigated using kinetic models to gain further insights into the mechanisms driving the reactions and the reaction rates for each support material.

A First-order model was selected to establish the half-life of the desorption reactions so that the data could be used to ascertain a hierarchy of which support material would be best able to retain IPU and/or SULPH. As discussed previously, the success of an *in-situ* microcosm is dependent on its ability to hold on to a loaded isotopic tracer. As already mentioned, the heterogeneous surface of the support materials invalidates the assumptions made by the Langmuir model. Therefore, a modified Freundlich model was used, which has been adapted for use with heterogeneous materials and in particular, porous structures, which is in keeping with the characteristics of GF, PP and EP, used in this study (Elkhatib et al., 2007, Skopp, 2009). The Freundlich model also predicts monolayer adsorption but in addition suggests the mechanisms are governed by diffusion. Finally, to test the assumption of monolayer coverage by the adsorbates an Elovich model was employed. A fit to this model proposes multilayer sorption, which would suggest an affinity between adsorbate molecules, and like the Freundlich model, it also predicts sorption is driven by diffusion processes (Šćiban and Klačnjica, 2002, Sparks, 2003).

The following models focus on the results which represent initial loadings of 100 mg g<sup>-1</sup> of IPU onto the three different support materials. For comparative purposes 100 mg g<sup>-1</sup> SULPH loaded onto GF and PP were also modelled, even though they had been found to be unsuitable for use as *in-situ* microcosms (Table 4.7). The data obtained for desorption of SULPH from EP was incomplete, in that it occurred too rapidly, to include in the modelling step. Furthermore, in applying the models an assumption was made that adsorption of IPU and SULPH on GF, PP and EP was reversible. The experimental values of  $q$  and  $C$  were used to determine the model parameters (Table 4.10) using the linear form of the equations (shown in Table 4.4 of methods section). The isotherm curves were then recalculated using the data points obtained from the line of best fit to obtain theoretical values. The linear correlation coefficients ( $R^2$ ), shown in Table 4.10, represent the goodness of fit of the experimental data to the linear forms of the model equations. Average percentage errors (APE) were subsequently calculated to show the fit between the experimental and theoretical values of desorption used to plot the model curves and are also listed in Table 4.10 (Hamdaoui and Naffrechoux, 2007). The APE values give a clearer indication of which models best describe the experimental results when comparing the behaviour of IPU and SULPH desorption from the three tested support materials

because the calculation takes into account the distance of each experimental data point along the curve, whereas the linear correlation coefficient considers the data set as a whole.

#### 4.3.4.1 First-order Model

Figure 4.20 (a & b) show the First-order plots of  $\ln C_t/C_0$  vs. reaction time (days) for IPU and SULPH desorption from GF, PP and EP. A linear fit suggests the reaction rate is influenced by the adsorbate concentration and the number of free sites for adsorption (Šćiban and Klačnja, 2002, Sparks, 2003).

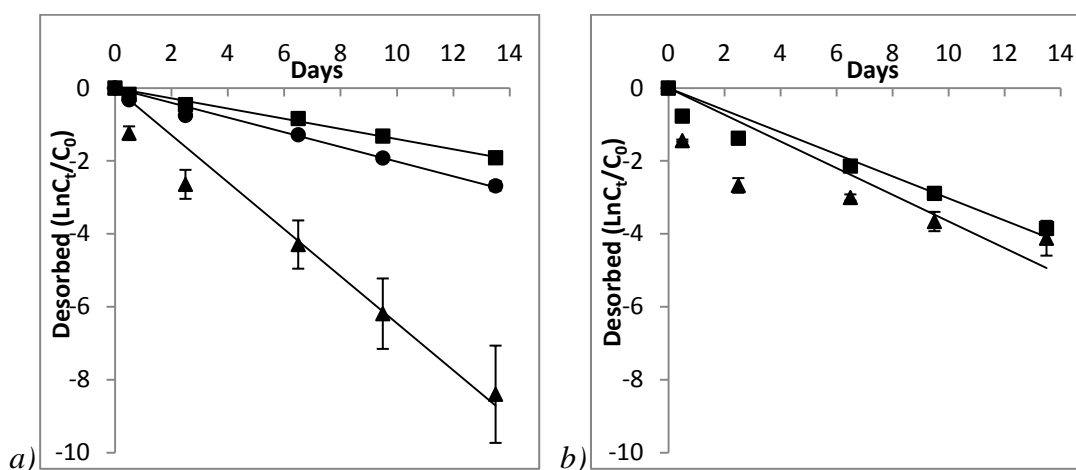


**Figure 4.20** – First Order desorption model showing IPU (a) and SULPH (b) desorbed from different support materials; Graphite Felt (■), Pumice Pellets (▲) and Expanded Perlite (●), at set time intervals, after an initial loading of  $100 \text{ mg g}^{-1}$  of support material. The error bars represent 95 % confidence intervals.

This model was used to find the half-life of the desorption reaction to establish which support material could retain the isotope tracer, IPU and SULPH, most effectively. First-order equation parameters were determined from the slope of the linear plots and are presented in Table 4.10. Despite good correlation coefficients for IPU ( $R^2 = 0.96-0.99$ ), the high average percentage values (APE >2 %) suggest the assumption that the reaction rate is influenced by adsorbate concentration and the number of free sites for adsorption, is not in agreement with the experimental data and so the First-order model is unsuitable in describing the desorption characteristics

of IPU and SULPH from GF, PP or EP. This is in keeping with the observations made during the desorption experiments, which found that initial concentrations of 10, 50 and 100 mg g<sup>-1</sup>, did not have a significant effect ( $p \leq 0.05$ ) on the percentage off-loaded after a 35 day desorption period.

#### 4.3.4.2 Elovich Model

The graphs in Figure 4.21 represent the Elovich model and show IPU (a) and SULPH (b) desorbed vs. ln of reaction time (days). A linear fit indicates multilayer sorption processes, on heterogeneous surfaces which are mainly driven by bulk and surface diffusion (Sparks, 2003). The Elovich equation parameters were determined using the slope and intercept of the linear plot and are listed in Table 4.10. An increase in parameter  $\alpha$  (mg g<sup>-1</sup> day<sup>-1</sup>) points to an increase in desorption rate.

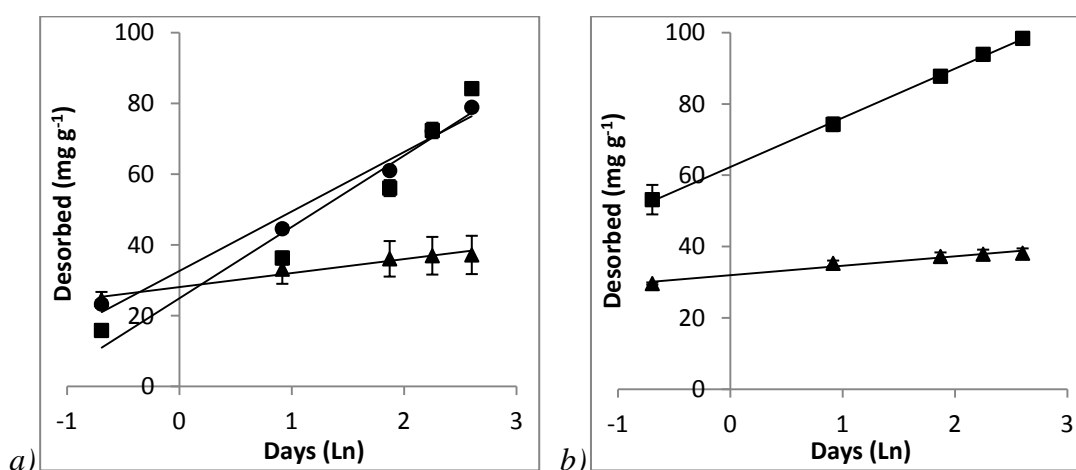


**Figure 4.21** - Elovich desorption model showing IPU (a) and SULPH (b) desorbed from different support materials; Graphite Felt (■), Pumice Pellets (▲) and Expanded Perlite (●), at set time intervals, after an initial loading of 100 mg g<sup>-1</sup> of support material. The error bars represent 95 % confidence intervals.

This model best describes SULPH desorption from GF and PP with the high correlation coefficients of > 0.99 and 0.98 respectively, being supported by low average percentage error values (APE  $\leq 2$  %). This implies that the assumption that sorption processes are multilayer and driven by diffusion (Šćiban and Klašnja, 2002), is in agreement with the experimental data and so the Elovich model is

suitable in describing the desorption behaviour of SULPH from GF and PP. The observed increase in  $\alpha$  value (Table 4.10) suggests SULPH desorbs five times more quickly from PP ( $0.39 \text{ mg g}^{-1} \text{ day}^{-1}$ ), than GF ( $0.07 \text{ mg g}^{-1} \text{ day}^{-1}$ ). The parameter  $a$ , relates to surface coverage and may be useful in providing an indication of the amount (in grams) of adsorbent required for each mg of adsorbate, used in this study. However, in light of the difficulties described during the loading of IPU and SULPH onto the three support materials (Section 4.2.7), in that adsorption was most likely limited to the surface so omitting any of the adsorption sites within the pores of the materials, any conclusions made using this parameter may be questionable.

#### 4.3.4.3 Modified Freundlich Model

Historically, the Freundlich model was used as an empirical model to determine the thermodynamic equilibrium of adsorption in homogeneous adsorbents. However, later modifications to the equation have enabled its use to describe adsorption in porous materials, whose surfaces are usually heterogeneous (Elkhatib et al., 2007, Skopp, 2009). Figure 4.22 illustrates the modified Freundlich model, proposed by Elkhatib et al. (2007), of log IPU (a) and log SULPH (b) desorbed from GF, PP and EP vs. log of the reaction time (days). Freundlich equation parameters were calculated using the slope and intercept of the linear plots and are shown in Table 4.10.

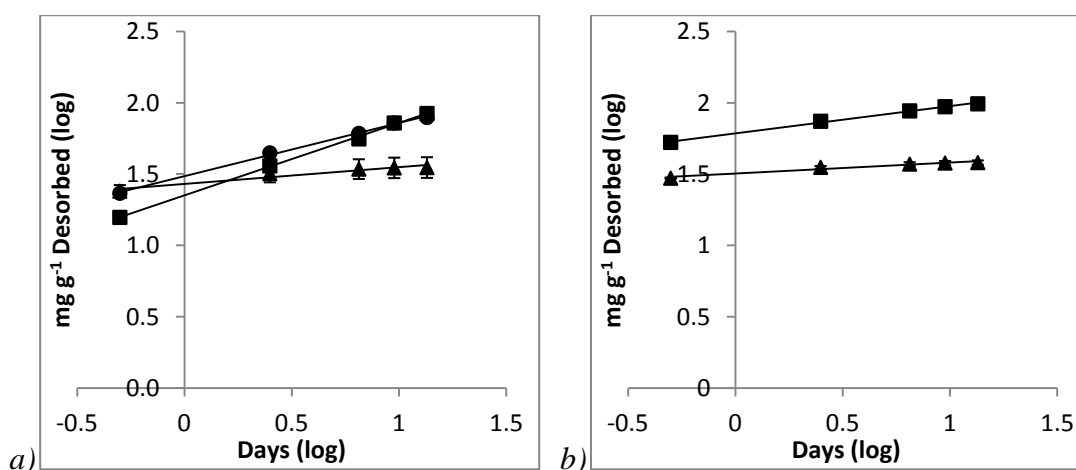


**Figure 4.22** – Modified Freundlich desorption model showing IPU (a) and SULPH (b) desorbed from different support materials; Graphite Felt (■), Pumice Pellets (▲) and Expanded Perlite (●), at set time intervals, after an initial loading of  $100 \text{ mg g}^{-1}$  of support material. The error bars represent 95 % confidence intervals.

Overall, the modified Freundlich model best describes sorption processes for both adsorbates and the three support materials, which is supported by average percentage values of  $\leq 2\%$ . In particular, desorption of IPU from GF and EP and SULPH from GF had, in addition,  $R^2 > 0.99$ . The fit suggests that sorption processes are dominated by diffusion and in particular, considers that adsorption sites, in porous material, will not have equal access to the bulk solution and so diffusion, from the centre of the pores will be slower than that occurring at the surface of the adsorbent (Skopp, 2009). Figure 4.23 shows the five diffusion processes which can impact the rate at which sorption occurs.

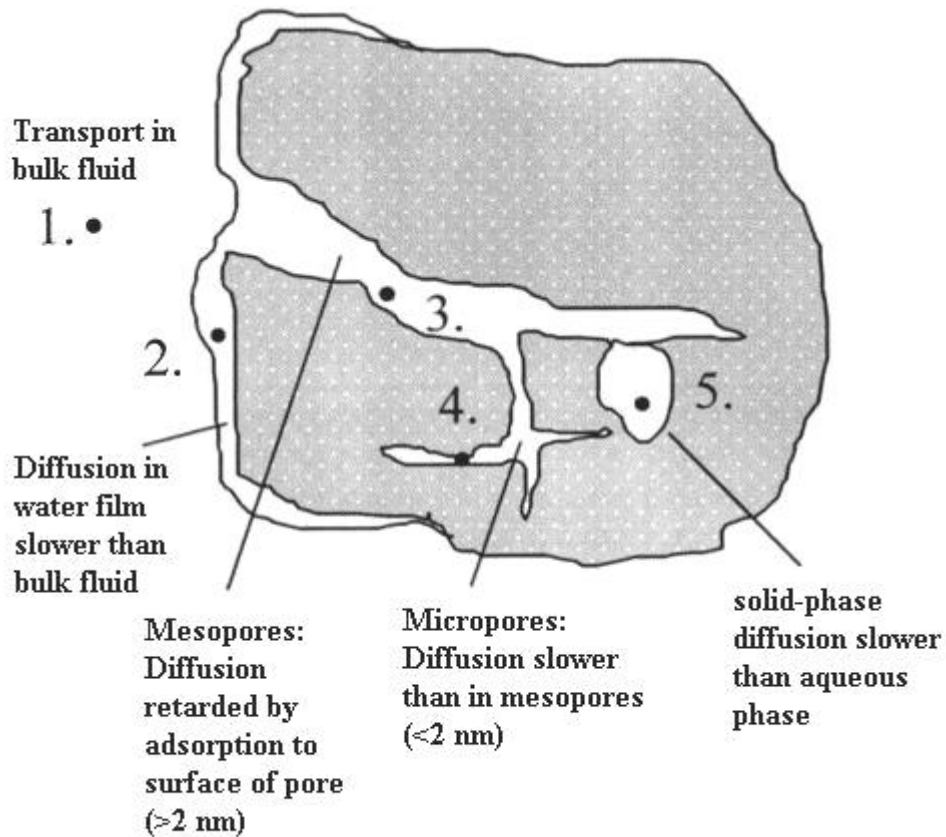


**Figure 4.23** – Schematic picture showing the diffusion process involved during adsorption, adapted from (Pignatello and Xing, 1995).

Steps 3 to 5 are considered to be the cause of slow diffusion in comparison to 1 and 2 which are relatively fast (Björklund et al., 2000). Slow kinetics can be attributed to diffusion limitations. This is true in porous materials because the adsorbate is subjected to diffusive constraints when trying to reach adsorption sites. In this study, the diffusion limitations will be mostly restricted to stages 1 and 2 in Figure 4.23, with pore diffusion unlikely due to the method used to load the adsorbate. However, as mentioned earlier, the limitations encountered during loading of the support materials make any interpretations regarding pore diffusion unlikely. Furthermore, the models were simply used to tease out an understanding of sorption processes involved within the limited time frame of the batch experiments and so they should not be used for predictive purposes because true equilibrium was not reached and in instances where diffusion dominates it can take years to truly reach equilibrium (Pignatello and Xing, 1995). The desorption rate coefficients ( $K_d$ ) were lowest for IPU from GF ( $0.01 \text{ days}^{-1}$ ) followed by both IPU from EP ( $0.02 \text{ days}^{-1}$ ) and SULPH from GF ( $0.02 \text{ days}^{-1}$ ) which proposes GF was able to retain both adsorbates for the longest period of time.

**Table 4.10** – Kinetic Model Parameters.

<b>Kinetic Model Parameters</b>	<b>GF - IPU</b>	<b>GF - SULPH</b>	<b>PP - IPU</b>	<b>PP - SULPH</b>	<b>EP - IPU</b>
<b><i>First Order:</i></b>					
k (mg g <sup>-1</sup> day <sup>-1</sup> )	0.13-0.15	0.26-0.28	0.54-0.75	0.34-0.40	0.19-0.21
Half-life (days)	4.7-5.3	2.5-2.7	0.90-1.3	1.7-2.1	3.2-3.6
R <sup>2</sup>	0.99	0.89-0.91	0.96	0.35-0.67	0.98
APE %	6.2	27	35	69	9.9
<b><i>Elovich:</i></b>					
α (mg g <sup>-1</sup> day <sup>-1</sup> )	0.05	0.07	0.20-0.34	0.39	0.06
a (g mg <sup>-1</sup> ) x10 <sup>3</sup>	0.07-0.08	0.74-1.5	0.79-21	130–3400	0.11-0.13
R <sup>2</sup>	0.93-0.95	>0.99	0.91-0.95	0.97-0.99	0.98
APE %	17	0.56	2.6	1.4	5.7
<b><i>Modified Freundlich:</i></b>					
1/m	0.50–0.52	0.16–0.22	0.10-0.14	0.07-0.09	0.35-0.39
k <sub>d</sub> (days <sup>-1</sup> )	0.01	0.02	0.04	0.09	0.02
R <sup>2</sup>	> 0.99	> 0.99	0.90-0.94	0.94-0.96	> 0.99
APE %	1.8	0.28	3.2	0.48	2.0

The models which best describe desorption of IPU and SULPH were determined according to the goodness of fit criterion of  $R^2 > 0.99$ , which was further tested using average percentage value of  $\leq 2\%$ . Despite the goodness of fit values obtained for the First-order model the high APE values (6.2-69 %) indicate this model does not describe the desorption process. The Elovich model fits the experimental data for SULPH desorption (APE  $\leq 2\%$ ), suggesting multilayer sorption processes may be involved, but does not give a satisfactory explanation of IPU desorption (APE 2.6-17 %). The modified Freundlich model best describes the IPU experimental data (APE

≤ 2%); indicating diffusion is involved in the sorption process. This model also fits SULPH desorption from PP. The experimental data for IPU desorption from PP is not explained by any of the three tested models (APE 2.6-35%).

In terms of this study, of interest is the retention capacity of each of the three support materials. The linear plots of the three kinetic models were used to ascertain the desorption rate coefficients;  $t_{1/2}$ ,  $\alpha$  and  $K_d$ , of IPU and SULPH from GF, PP and EP. Table 4.11 summarises the findings and lists the adsorbent-adsorbate interaction in order of desorption rate for each of the models, from fastest to slowest.

**Table 4.11** – Summary of desorption rates showing the fastest to slowest calculated for each kinetic model.

Model	Desorption rate (fast to slow)	
	IPU	SULPH
First-order	PP > EP >> GF	PP > GF
Elovich	PP > EP >> GF	PP > GF
Modified Freundlich	PP > EP >> GF	PP > GF

Desorption rate coefficients, for all three models, predict the same hierarchy for the studied adsorbent materials in terms of their ability to retain IPU and SULPH. In particular, the coefficients indicate that GF has a higher retention capacity for both IPU ( $K_d = 0.01$ ) and SULPH ( $K_d = 0.02$ ) than PP ( $K_d = 0.04$  and  $0.09$  respectively). Of these two compounds, GF was able to retain IPU for twice as long as SULPH. Interestingly the retention capacity of IPU by EP ( $K_d = 0.02$ ) is matched by that of SULPH by GF ( $K_d = 0.02$ ). From an economical point of view, the rate coefficients would suggest that EP may be a viable alternative to the more expensive adsorbent GF for IPU.

#### 4.4 Conclusion

Returning to the research questions that were raised in the introduction. Question one was, “Would the background concentrations of IPU and SULPH, already present at the study site, contaminate the supports and in so doing compromise the loaded tracer?” The adsorption study, which focused on adsorption of IPU and SULPH, from the aqueous phase, to GF, PP and EP, found there was no risk of contamination by background concentrations of IPU and SULPH ranging from 0.1 to 50 mg L<sup>-1</sup>. These results suggest IPU and SULPH had a greater affinity for the bulk solution than the adsorption sites of the support materials, which is not surprising considering their hydrophilic character.

Question two was: “Could a tracer be loaded onto the support materials and if so how would each support compare?” Three different concentrations 10, 50 and 100 mg g<sup>-1</sup> of IPU and SULPH were loaded, using solvent evaporation methods, onto GF, PP and EP. The results indicated no significant difference between the three different concentrations when loaded onto the same support material. This suggests that either concentration does not have an effect on the adsorption of IPU and SULPH onto GF, PP and EP, or the concentrations used in this study were too low for the support materials to exceed saturation. Furthermore, when comparisons were made between the two different adsorbates there was no significant difference between loading either IPU or SULPH at 100 mg g<sup>-1</sup> onto the same support material. Subsequent comparisons focused on the types of support material and found there was a significant difference between the three materials, with adsorptive capacity being greater for GF > EP >> PP. However, further work would be necessary to determine whether these differences are linked to ease of loading, i.e. greater run-off was observed when loading PP and EP than GF, or surface area, i.e. comparable weights of support material were used in the study which meant they had varying external surface areas with EP having the largest at ~9 cm<sup>2</sup>, GF ~6 cm<sup>2</sup> and PP ~2 cm<sup>2</sup>.

The third question was: “Could a viable concentration of tracer be retained by the support material for an adequate timeframe to allow biofilm development?” The desorption study focused on the support materials ability to retain ~30 % of the loaded <sup>14</sup>C-IPU and <sup>14</sup>C-SULPH for a period of 2 weeks. The study found that none

of the three support materials were able to retain SULPH and so for the purpose of this study would not be suitable supports for this compound biodegradation. The inability of GF, PP and EP to retain SULPH can mostly likely be attributed to its high solubility in water ( $7.5 \text{ g L}^{-1}$ ). Of these three supports, PP was also unable to retain a sufficient quantity of IPU after two weeks. However, GF and EP were able to retain ~30 % of IPU for the period of two weeks. These findings suggest both GF and EP would make suitable supports for *in-situ* microcosms loaded with an isotopic tracer of IPU. Nevertheless, due to the manufacturing production costs associated with activated carbon products, EP may be of considerable benefit in terms of its low economic and environmental costs because these studies suggest it is equally effective at retaining an isotopic tracer as GF.

Although there is a huge advantage to sampling attached biomass instead of groundwater biomass because it has the advantage of higher cell density, there are issues associated with surrogate supports in that they are not truly representative of the aquifer environment and as previously discussed, surface characteristics of such materials play a major role in terms of favourable attachment by microbes.

Therefore, further work should focus on biofilm development on surrogates compared to the substrates used by indigenous microbes in an aquifer to determine whether they are truly representative. In fact, studies mentioned above do suggest that the support material itself can be a deciding factor on biofilm development. Lehman et al. (2004) also found that when dialysis chambers, containing the same parent support material as the aquifer, were suspended in groundwater the biomass recovered was greater than that obtained from original core samples. In addition there were observed differences in microbial communities present. The reason for this has not been established and is still undergoing investigation. However, it does highlight the difficulties involved in studying such a complex environmental system and does throw doubt on the use of surrogate support materials in accurately establishing NA potentials at a contaminated site.

Subsequent to these experiments the EPA (2008) and more recently the Environment Agency (2011) have issued more stringent guidelines on the use of tracers in the environment for scientific purposes. In particular, the guidelines from the EPA (2008) pay particular attention to the use of  $^{13}\text{C}$ -labelled tracers and their detrimental impact to natural abundance isotopic research. If such labelled compounds enter the

natural environment being studied they severely limit the use of natural abundance research which relies on very small shifts in natural  $^{13}\text{C}$   $\delta$  values, i.e. 6-10‰ (Meckenstock et al., 1999). Compound specific isotope analysis is advancing techniques which enable evidence of biodegradation, for NA purposes, to be collected directly from groundwater samples by monitoring natural enrichments of  $^{13}\text{C}$  isotopes caused by biodegradation. Results relating to the desorption study indicated considerable desorption of both IPU and SULPH from GF, PP and EP. This loss of  $^{13}\text{C}$ -compound from these supports could potentially alter the natural relative abundance of  $^{12}\text{C}/^{13}\text{C}$  associated with the analyte of interest and in so doing undermine the opportunity for assessment using compound specific isotope analysis. In light of this and the revised guidance, further development of the alternative support for use in *in-situ* microcosms was abandoned. Although this may limit the use of isotopic tracers, it should not detract from the important role support materials play in providing a means to understanding microbial ecology.

To continue the pursuit of evidence to support natural attenuation at the field study site, the following chapter (Chapter 5) investigates the role of *ex-situ* microcosms in determining the potential for biodegradation of IPU and SULPH. Recent advances in compound specific isotope analysis have enabled the measurement of natural isotopic changes to determine biodegradation of non-volatile compounds. Consequently, Chapter 6 explores its use in providing evidence to support natural attenuation.

# Chapter 5: Ex-situ Microcosm Studies of Sulphanilamide and Isoproturon Natural and Enhanced degradation in the presence of chalk aquifer material

---

## 5.1 Introduction

*Ex-situ* microcosms are an established method for determining the fate of contaminants in the natural environment (Environment Agency, 2000a). They are designed to replicate *in-situ* conditions and can provide important insights of microbial processes occurring at a contaminated site and can reveal potential biodegradation rates (Haack and Bekins, 2000). However, rates established in this way should only be used as an indication as there will always be uncertainties surrounding the scaling up of laboratory results, which focuses on the sampled scale (mm - cm), compared to the actual aquifer environment (m - km) (Chapelle et al., 1996). The aim of this chapter is to explore whether biodegradation processes play a role in removing/reducing the concentrations of SULPH and/or IPU from the groundwater beneath the field study site. Additionally, both aerobic and anaerobic biodegradation processes are investigated; with a view to enhancing the rate of biodegradation should it be taking place. The following sections detail the techniques and methods employed to gather representative environmental samples and to determine the catabolic activity, if any, of the indigenous microbes in metabolising SULPH and/or IPU as a carbon source.

There is strong evidence in the literature to support the aerobic biodegradation of IPU in groundwater environments. Favourable environments have included: limestone (Janniche et al., 2010), chalk (Johnson et al., 2003a, Kristensen et al., 2001) and sandstone aquifers (Larsen and Aamand, 2001). However, other than the work by Larsen and Aamand (2001), who considered, albeit unsuccessfully denitrifying and methanogenic conditions, most of this research has focused on the

impact of IPU concentration on the rate of aerobic biodegradation with little attention being given to anaerobic processes. Figure 5.1.1b shows the biodegradation pathway of IPU, the intermediate products and its eventual conversion to carbon dioxide and water.

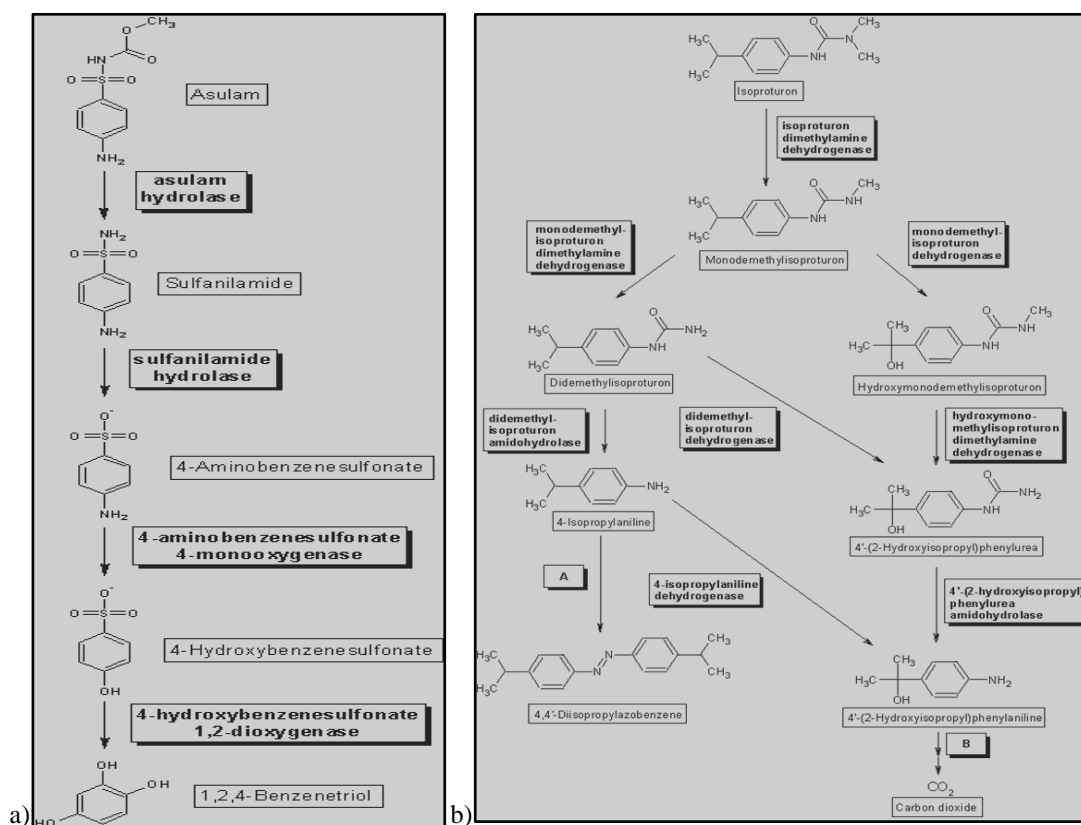


**Figure 5.1.1** – Biodegradation pathways for a) Asulam (Gonzales, 2008) and b) Isoproturon (Chi Leng Lai, 2012)

There are limited accounts of SULPH biodegradation in the literature, particularly with reference to groundwater environments. Early work by Walker (1978), demonstrated that SULPH, along with its parent compound Asulam, could be aerobically biodegraded by soil microbes. Figure 5.1.1a shows the biodegradation pathway of Asulam and its daughter product - SULPH. It is believed the SULPH contamination, at the field study site (Chapter 3) has resulted from the hydrolysis of Asulam (Figure 5.1.1a), which was spilled at the site (Arcadis Geraghty & Miller International Ltd, 2008). Direct input of SULPH is unlikely as no SULPH has been stored at the site. This account of SULPH presence is further substantiated by the findings of Balba et al. (1979) who, during biodegradation studies of topsoil

environments, found Asulam rapidly metabolised to SULPH before disappearing altogether.

In addition to the work on SULPH biodegradation in soil, some studies have focused on its removal, using biodegradation processes, during wastewater treatments (Ingerslev and Halling-Sørensen, 2000). Moreover, other contaminants such as sulfamethoxazole and *p*-toluenesulphonamide, part of the sulphonamide group of compounds and shown to be favourable to SULPH degraders, have been removed during wastewater treatment via aerobic biodegradation (Drillia et al., 2005, van Haperen et al., 2001). As mentioned for IPU, there has been little attention given to the anaerobic biodegradation of SULPH. Interestingly, Kameya et al. (1995), while investigating the role anaerobic degradation played in protecting the environment, found it was ineffective in removing Asulam.

There are many factors influencing biodegradation in the environment, including: the presence of viable microbes or community of microbes, a suitable organic food source (electron donor), and the type of electron acceptor, all of which, can be further influenced by spatial distribution (Haack and Bekins, 2000). Figure 5.1.2 provides a simplistic view of the metabolic pathway used by microbes when consuming contaminants in the natural environment.

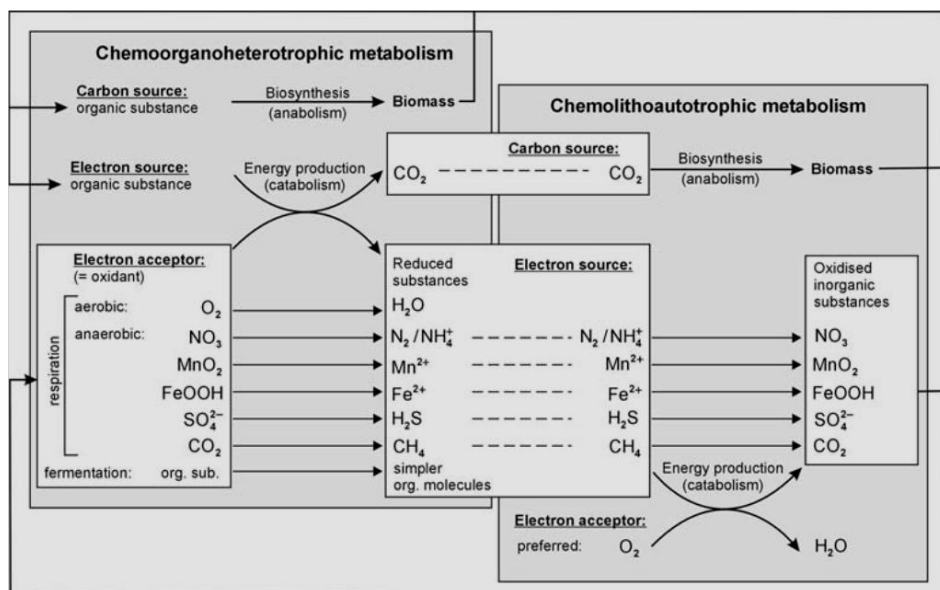


**Figure 5.1.2** - Simplified illustration of the metabolic pathways used by microbes in aquifer environments (Goldscheider et al., 2006).

Spatial disparity can also influence which electron donors and acceptors are available to microbes and hence, can affect the rate of biodegradation. Different redox zones often accompany contaminated groundwater (Wiedemeier et al., 2007c), which will not only determine the microbial physiology within specific areas of an aquifer, but also the type of contaminant available for biodegradation within that zone (Haack and Bekins, 2000). It is likely that multiple species of microbes, which form diverse communities capable of various degradative capabilities, are responsible for the biodegradation of contaminants in aquifers, rather than the result of a single population of microbes (Haack and Bekins, 2000). For example, co-metabolism involving the combined activities of multiple populations, may result in one population producing enzymes, as a result of metabolic activity involving one type of carbon source (e.g. toluene), which are of subsequent use to a different population in metabolising another carbon source (e.g. trichloroethylene) (Fries et al., 1997). Furthermore, microbial populations may need to co-exist. For example, during the methanogenic degradation of fuel contaminants, a second population of microbes is required. This utilises the excess H<sub>2</sub> of methanogenesis as an electron acceptor to ensure that H<sub>2</sub> does not reach toxic levels and subsequently inhibit continued degradation of the fuel contaminants (Ferry and Wolfe, 1976).

To predict the behaviour of indigenous microbes in a contaminant plume, there is a need to encompass all the factors that may influence the degradation process. At plume scale, factors such as changes in redox, nutrients, co-contaminants, can influence degradation rates established in the laboratory (Chapelle et al., 1996). Furthermore, once understood, it may be possible to manipulate the key factors involved in the process, e.g. replenishing the groundwater with electron acceptors to speed up a biodegradation process that has become limited or has stopped altogether. This practice is known as enhanced biodegradation (Environment Agency (EA), 2000).

As discussed earlier, there is evidence in the literature to suggest both IPU and SULPH can undergo aerobic biodegradation in the natural environment. However, contaminated groundwater can quickly turn from an aerobic to anaerobic environment once the indigenous microbial population exhausts the electron acceptors. As shown in Chapter 3, a mixture of synthetic organic compounds has contaminated the groundwater at the field study site for several decades, resulting in

an anaerobic environment beneath the site. Therefore, there is an interest in whether IPU and/or SULPH can be biodegraded anaerobically and whether refreshing the exhausted electron acceptors at the site could speed up or initiate the biodegradation process.

Given that the overview of the site characteristics, described in Chapter 3, points to a reduction in SULPH and IPU concentrations at the field study site, the following questions were posed:

1. Do the results of the *ex-situ* microcosms provide supporting evidence that the observed reduction in IPU and/or SULPH concentration across the site is due to biodegradation processes?
2. Can the extent of IPU and/or SULPH mineralisation be enhanced by increasing the concentration of electron acceptors available to the indigenous microbes?
3. Is there any evidence to show that changes in groundwater chemistry and/or the presence of other contaminants, discussed in Chapter 3, impact on the extent of SULPH and/or IPU mineralisation?

## 5.2 Methods

### 5.2.1 Collection of core samples and groundwater.

There are many problems associated with the study of microbial activity in aquifers, including, the heterogeneity of the environment, difficulties in accessing samples, and the sensitivity of microbial communities to disturbances (Goldscheider et al., 2006). Furthermore, microbes are four times more abundant in aquifer material than the surrounding groundwater (Alfreider et al., 1997). However, as illustrated in Figure 5.2.1, the most fundamental problem associated with representative solid phase sampling, is the varied distribution of microbial communities within the aquifer (Goldscheider et al., 2006). These distributions are the result of, “overlapping spatially heterogeneous distributions of numerous physical, chemical and microbiological (and their interactions) that yield patches of optimal, sub-optimal or constrained, and excluding conditions for microbes” (Brockman and Murray, 1997). Thus, spatial variation has the potential to both over- or underestimate microbial activity within an aquifer, with the possibility for biodegradation rates to be 4 – 10 times longer in the field compared with those obtained in the laboratory due to such scale dependent limitations (Sturman et al., 1995b).

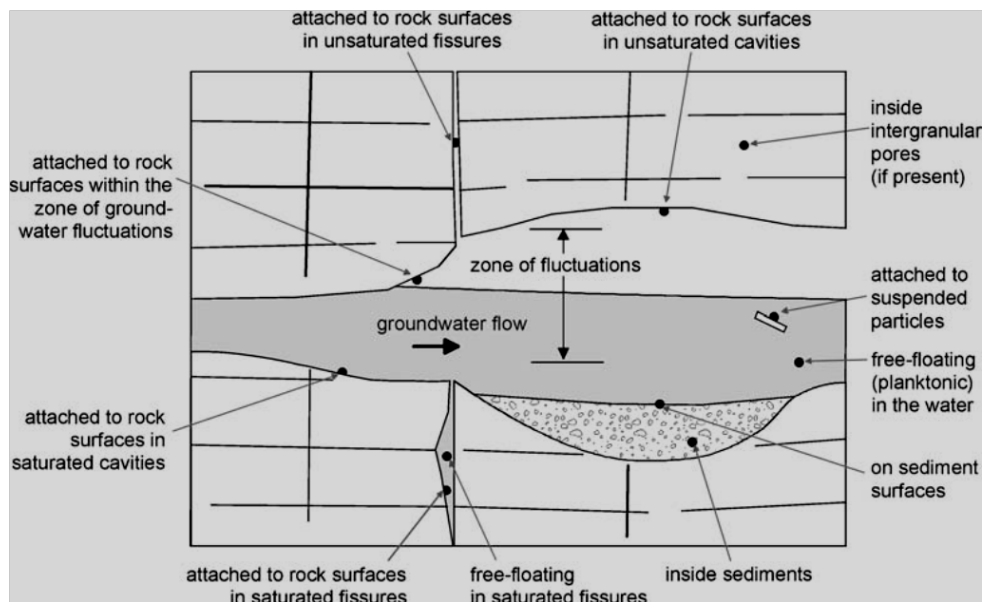


**Figure 5.2.1** - Schematic showing the habitats of microbial communities found in a fractured, karstic aquifer, illustrating the difficulty associated with the heterogeneity of the environment when considering where to obtain a representative sample (Goldscheider et al., 2006).

To address these issues, all core samples were collected from 10 mbs, within the saturated chalk zone. To overcome the sensitivity of microbial communities to disturbances, the solid phase material, used for the microcosm studies, was taken from the centre of the cores, disregarding the outer limits (which encountered the PVC liner) and the ends (which were exposed to surface conditions prior to capping).

In 2008, sampling occurred at the field study site (details in Chapter 3) in and around the area where levels of synthetic organic chemical contamination had been reported (Arcadis Geraghty & Miller International Ltd, 2008) and of particular interest to this study, the compounds SULPH and IPU. During the construction of 11 monitoring wells at the site (Figure 5.2.2), cores were collected, using hollow stem auger techniques (Figure 5.2.3) from the saturated chalk zone, approximately 10 m below ground level, using PVC liners (0.1 m in diameter by 0.50 m in length), similar to that described by Johnson et al. (1998). Of these new wells, the circled wells, shown in Figure 5.2.2, represent the core and groundwater samples used to conduct *ex-situ* microcosm studies in the laboratory.

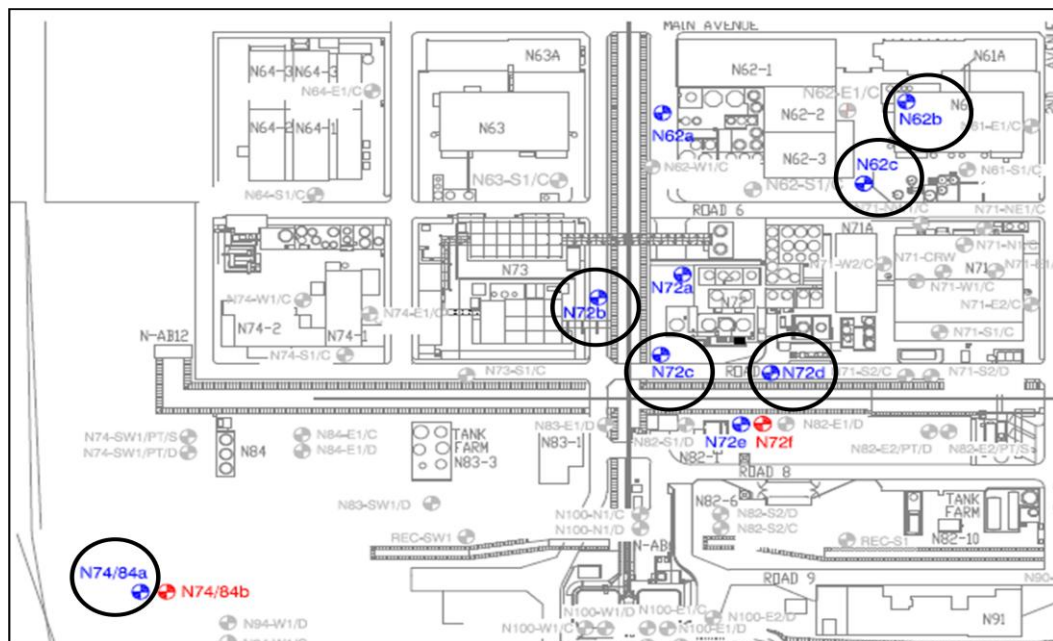


**Figure 5.2.2** – Map of field study site showing the position of the 11 new monitoring wells. The circled wells show where core and groundwater samples were collected for the *ex-situ* microcosm studies.

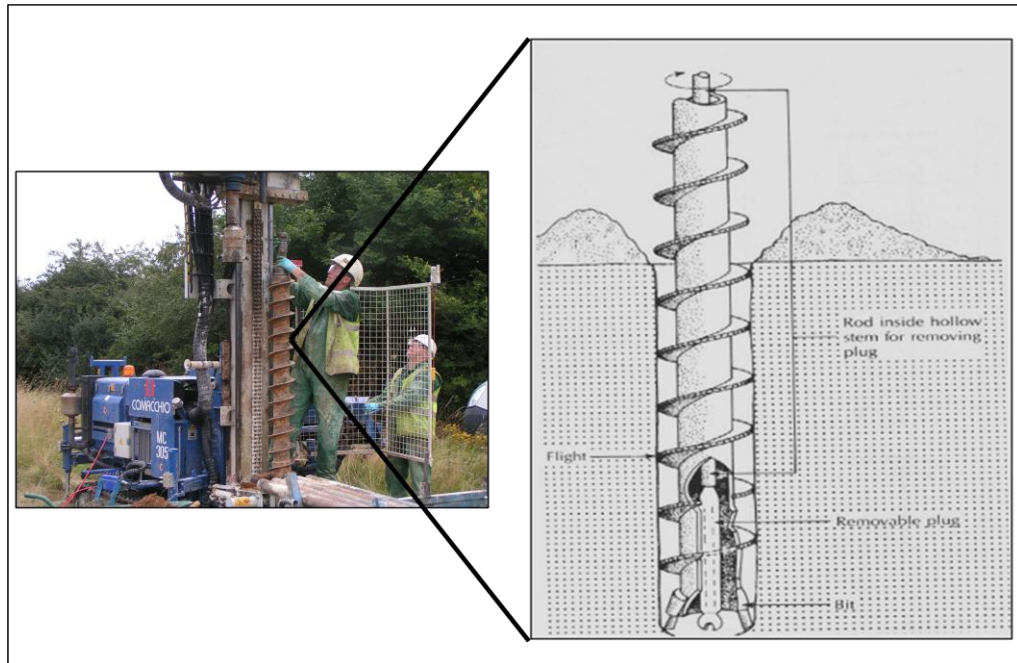


**Figure 5.2.3** - Drilling rig COMACHIO MC305 used to collect core samples and a schematic of a Hollow-Stem Auger apparatus (San Diego State University, n.d.).

Hollow stem auger techniques, used to limit cross-contamination, are favoured when collecting unconsolidated core materials. No drilling fluid is required, the auger flights remain in place during drilling limiting the risks associated with back filling or borehole collapse, and the PVC liner keeps the sample intact and covered, which prevents contamination via exposure to different environmental conditions during sampling (Chapelle, 1993). Figure 5.2.4 provides a description of the core collection method employed in this study.

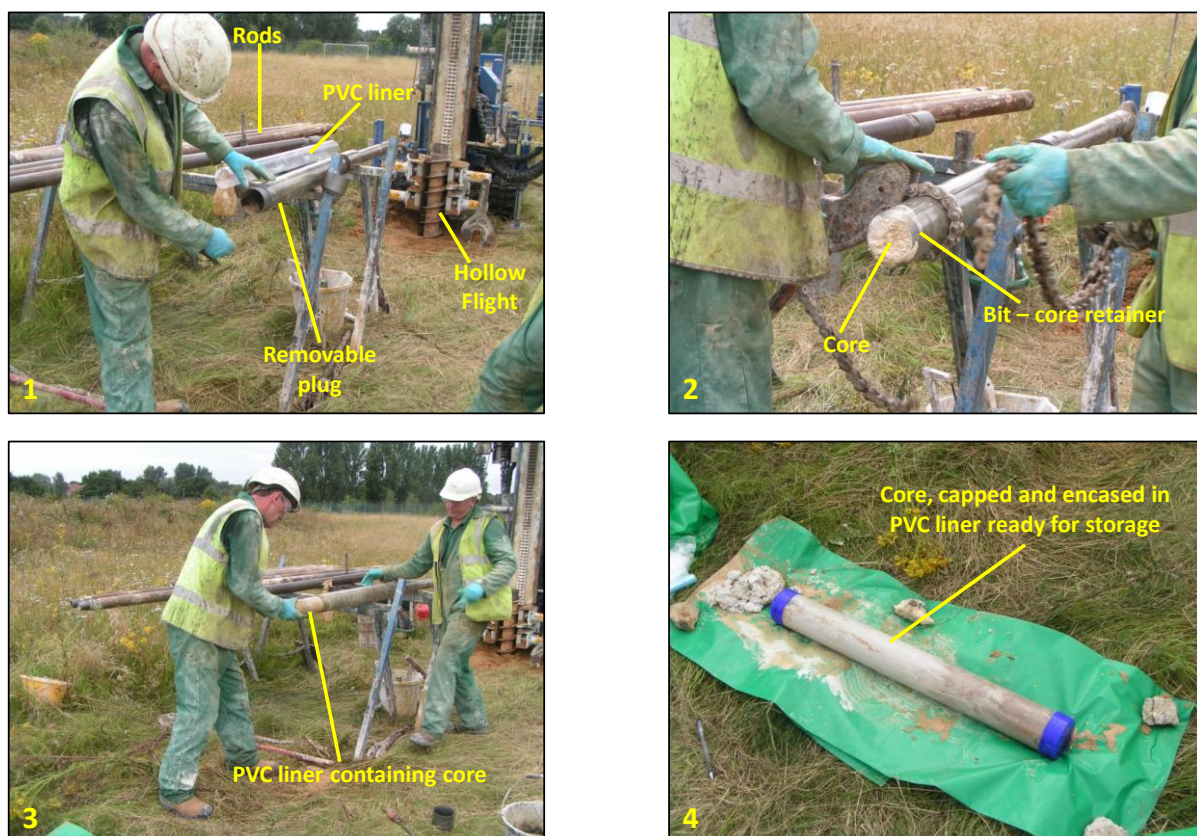


**Figure 5.2.4** - Collection of core sample. 1) The plug was loaded with a PVC liner and inserted into the hollow flight with the aid of rods. 2) At 1 m intervals, the rods were removed and the core recovered from the plug. 3) The bit was unscrewed and the PVC liner, containing the core, removed from the plug. 4) The PVC liner was capped, sealed and the core placed in cold storage.

Following construction, the monitoring wells were allowed to settle prior to groundwater sample collection. After two weeks, the wells were purged and the stagnant water discarded before the collection of 2 L of water in sterile polyethylene bottles (Goldscheider et al., 2006). The bottles were filled, leaving no headspace as this may contaminate the sample with oxygen, then placed in cold storage (4 °C) for 2 – 3 months, until required for *ex-situ* microcosm studies (Section 5.2.3).

### 5.2.2 Chemicals

Radiolabelled analogues of sulphanilamide [ring- $^{14}\text{C}(\text{U})$ ] were obtained from American Radiolabeled Chemicals Inc., USA, and [benzene ring-UL- $^{14}\text{C}$ ] isoproturon from Amersham Co. Ltd., UK. The physical and chemical properties of

which are presented in Table 3.1 of Chapter 3. Analytical grade (99%) acetone and ethanol, and the salts sodium hydroxide (NaOH), sodium sulphate (Na<sub>2</sub>SO<sub>4</sub>) and sodium nitrate (NaNO<sub>3</sub>), were obtained from Fisher Scientific, UK, while the scintillation cocktail, Ultima Gold™ XR, was obtained from Perkin Elmer Life & Analytical Sciences, UK.

### 5.2.3 *Ex-situ* Microcosms

To ensure samples were representative of the *in-situ* microbial activity in the aquifer environment, both solid phase material and groundwater were sampled (Sturman et al., 1995b). The microcosms, in this study (designed to replicate *in-situ* conditions, 10 mbs at the field study site) were anaerobic and saturated with groundwater. Each microcosm (n=3) contained 10 g of solid phase material and 30 ml of groundwater, collected from the same monitoring well. This approach was similar to that described by Johnson et al. (1998), when studying IPU contaminated chalk aquifers in Hampshire, U.K. The purpose of this study was to gain insights of potential metabolic pathways, involving SULPH and IPU as a carbon source, which could be utilised by *in-situ* microbes present in the aquifer underlying the field study site.

The *ex-situ* microcosms were monitored using a flask-based <sup>14</sup>C-respirometer system (Figure 5.2.6), described by Reid et al. (2001), to establish whether the microbial population present at the field study site had the potential to biodegrade <sup>14</sup>C-labelled SULPH and IPU, and whether the biodegradation of these compounds could be enhanced by increasing the concentration of electron acceptors (oxygen, sulphate or nitrate). The *ex-situ* microcosms measured the mineralisation of SULPH and IPU to CO<sub>2</sub>. The CO<sub>2</sub> is a by-product, which results from the complete biodegradation of the compound.

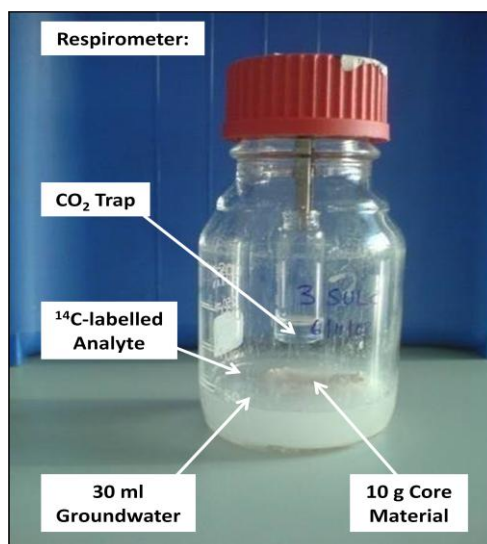


*Figure 5.2.5 - Flask-based <sup>14</sup>C-respirometer system.*

The microcosms (n = 3 per monitoring well) were prepared inside a nitrogen filled glove box, where oxygen levels were kept  $\leq 1.5\%$ , in order to preserve the integrity of the collected anaerobic samples. 10 g of the contaminated solid phase material, collected from the centre of the cores (after discarding the outer and ends of the core material) were placed into autoclaved 250 mL Duran® bottles (Figure 5.2.6). The solid phase material was spiked with either 100  $\mu$ L of <sup>14</sup>C-IPU in ethanol, or <sup>14</sup>C-SULPH in acetone, in accordance with preferred solubilities, giving each resultant microcosm an activity of 2 kBq. Following this, 30 mL aliquots of groundwater, obtained from the same well as the solid phase material, was added to each microcosm.

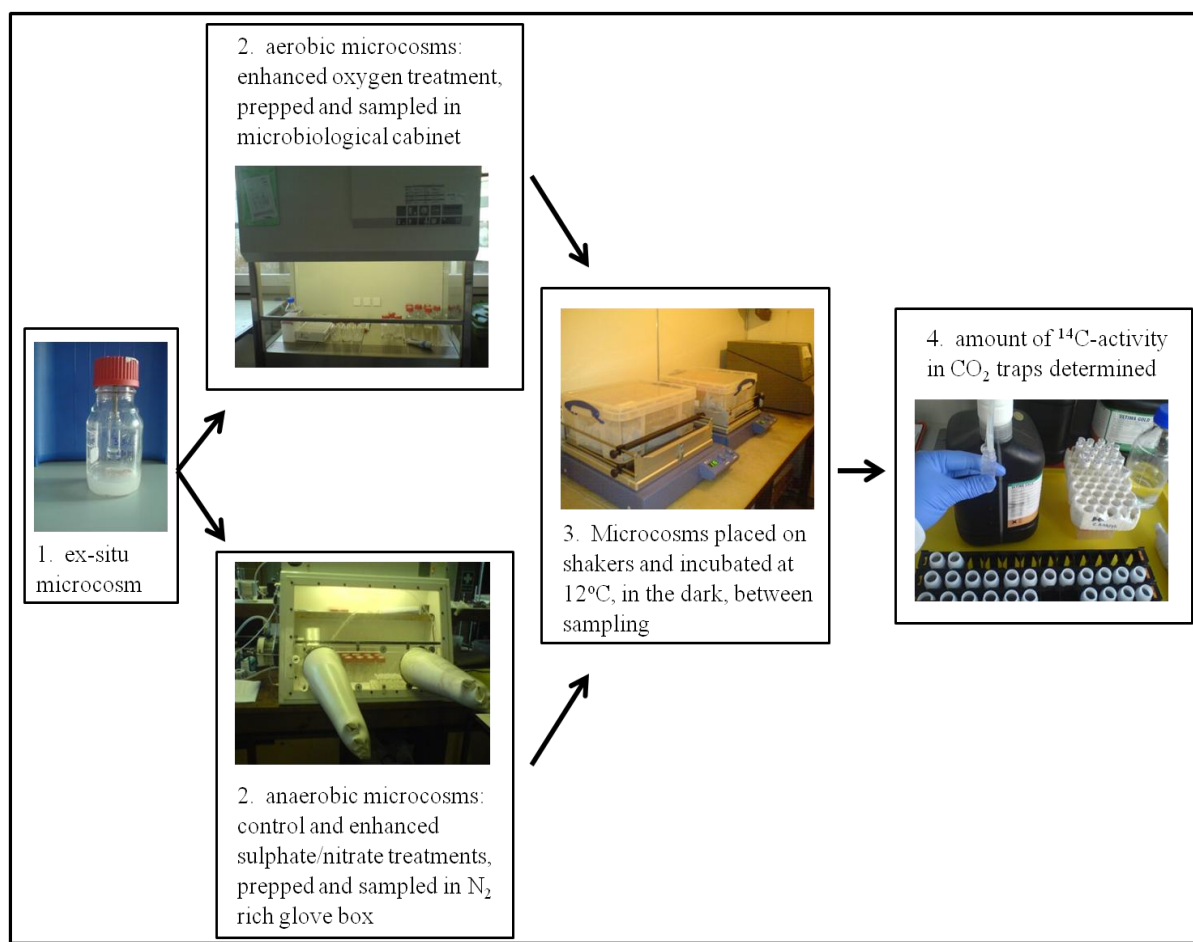


**Figure 5.2.6** – *Ex-situ microcosm experimental approach.*

CO<sub>2</sub> traps (Figure 5.2.6) were prepared by adding 1 mL of NaOH (1 M) to an autoclaved 7 ml glass scintillation vial (*Perkin Elmer Life & Analytical Sciences*). The vials were attached to a stainless steel crocodile clip suspended from the inside of the Duran® bottle lid. The lids were carefully screwed onto the bottles and sealed using parafilm® tape.

Once prepared, the microcosms were placed on a shaker that was kept at 12°C, in the dark, between sampling, reflecting the *in-situ* conditions observed at the field site. At each sampling point, every 3 days, the CO<sub>2</sub> traps were removed and 6 ml of Ultima Gold scintillation fluid added to each vial. Spent traps were then analysed for <sup>14</sup>C –activity using the scintillation counting methods (*Packard Tri-Carb 2900TR Liquid Scintillation Analyser*) (described in Chapter 4). After a period of 4 weeks, sampling reduced from every 3 days to weekly.

Alongside the control microcosms, described above, three enhanced treatments were also studied to establish whether increasing the concentration of electron acceptors (oxygen, nitrogen or sulphur) would affect the mineralisation of SULPH and IPU. Appendix 1 shows the calculations for oxygen additions (1). These represent an assumption based on the amount of atmospheric oxygen the microcosms were exposed to rather than the addition of an oxidising agent. Appendix 2 shows the calculations for nitrate and sulphate additions (2 and 3) and represent the increased regulated concentration additions agreed by the field study site and the Environment Agency. Therefore, three further sets of microcosms were set up with the following amendments made to facilitate the enhanced treatments:

1. Oxygen - microcosms were sampled inside a microbiological cabinet, which prevented contamination from external microbes but facilitated the exposure to approximately 5 mg of atmospheric oxygen.
2. Nitrate – microcosms were spiked with  $\text{NaNO}_3$  to give an additional nitrate concentration of  $548 \text{ mg L}^{-1}$  in the groundwater.
3. Sulphate – microcosms were spiked with  $\text{Na}_2\text{SO}_4$  to give an additional concentration of  $572 \text{ mg L}^{-1}$  in the groundwater.

#### *5.2.4 Statistical Analysis*

An analysis of variance (ANOVA) test was performed using SPSS v.18 to establish whether there were any significant differences ( $p \leq 0.05$ ) among the enhanced treatments for each of the two compounds at each borehole. Any significant differences highlighted in the group were then analysed using appropriate post-hoc tests, depending on whether equal variance was established, to identify which, if any, of the enhanced treatments were significantly different ( $p \leq 0.05$ ).

Additionally, student t-tests and analysis of variance tests were conducted to establish whether there was any significance difference ( $p \leq 0.05$ ) between the mineralisation of SULPH across the study site, in particular, three transects moving downgradient of the source area of contamination.

### 5.3 Results/discussion

#### 5.3.1 IPU Microcosm Study

Figure 5.3.1 shows the accumulation of  $^{14}\text{CO}_2$  resulting from the complete mineralisation of  $^{14}\text{C}$ -IPU. The radiochemical impurity of IPU was  $\leq 1\%$  and hence it is impossible to distinguish between the mineralisation of  $^{14}\text{C}$ -IPU and  $^{14}\text{C}$ -impurities in the stock solution at percentages within this range. Of the six boreholes studied, mineralisation, beyond the scope of impurities (set at  $>1\%$ ), was only observed in N62b. Here IPU concentrations were  $9\ \mu\text{g L}^{-1}$  and  $50\ \mu\text{g L}^{-1}$  in the surrounding area (N61). The concentration of IPU in the remaining tested boreholes was  $\leq 1\ \mu\text{g L}^{-1}$ . The findings (Figure 5.3.1 b, c, d, e and f) suggest, at low concentrations ( $\leq 1\ \mu\text{g L}^{-1}$ ), IPU mineralisation becomes inhibited.

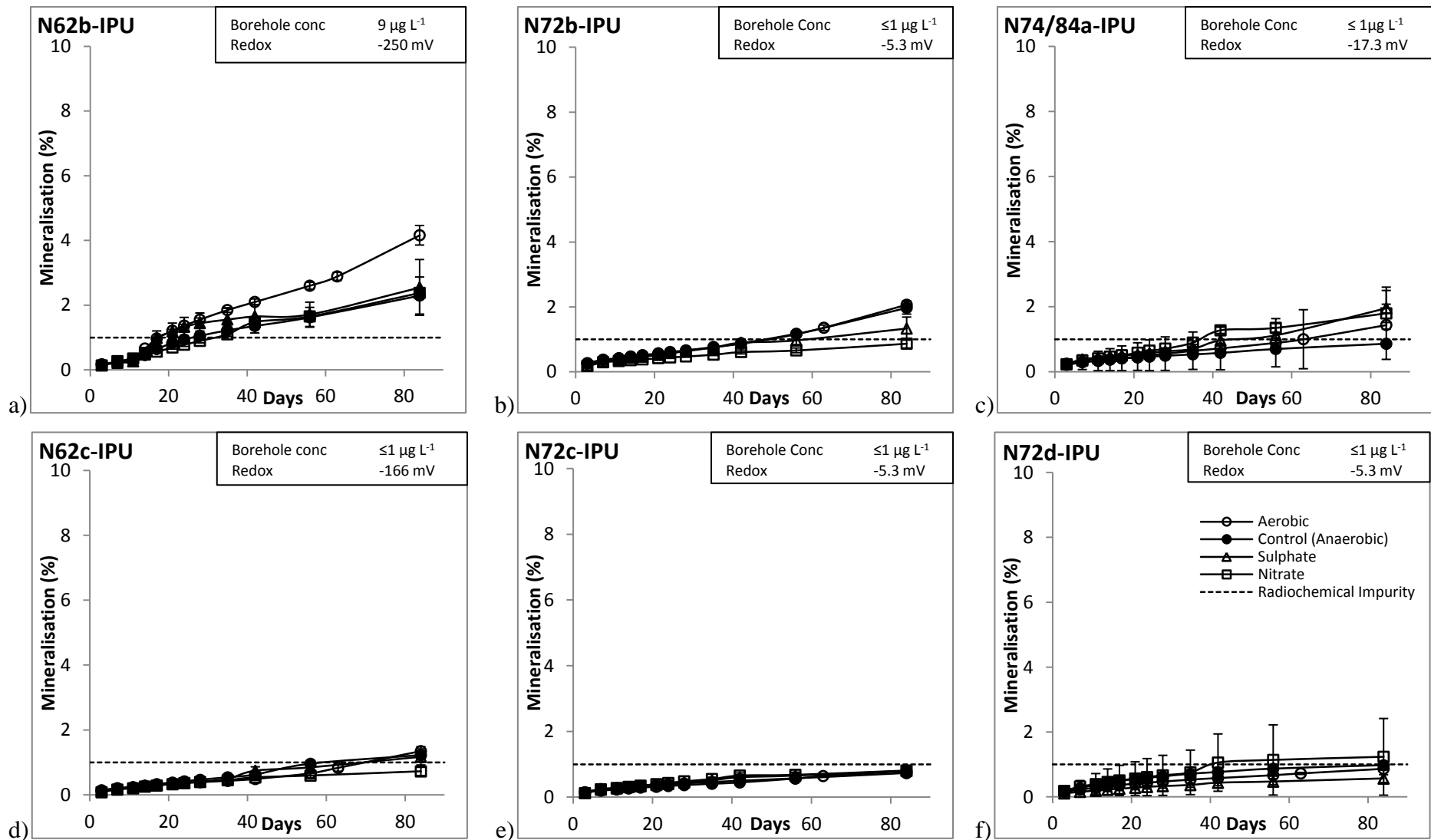


Figure 5.3.1 -The percentage of  $^{14}\text{C}$ -IPU mineralisation vs. time, shown as number of days. Each graph represents the results of ex-situ microcosms prepared from core material and groundwater samples obtained from six newly drilled boreholes at the field study site

After 84 days, the extent of the enhanced aerobic mineralisation was  $4.2 \pm 0.3$  % in the microcosm from borehole N62b (Table 4.3.1). This was significantly higher ( $p \leq 0.05$ ) than the control microcosm ( $2.3 \pm 0.6$  %) and the other enhanced treatments: sulphate-reducing ( $2.6 \pm 0.9$  %) and denitrification ( $2.4 \pm 0.2$  %). Although dissolved oxygen levels at the site are low ( $\leq 2$  mg L<sup>-1</sup>), they are not low enough to limit IPU biodegradation. This is demonstrated by the stoichiometric equations (Appendix 1), which show that at concentrations of 9  $\mu$ g L<sup>-1</sup> (found in borehole N62b), 0.02 mg L<sup>-1</sup> of dissolved oxygen is required for complete aerobic biodegradation to occur. This suggests, despite the anaerobic nature of the contaminated environment (redox -250 mV), there is sufficient dissolved oxygen present in the groundwater to sustain aerobic biodegradation of IPU, albeit at levels below 5 %. These findings support those of Janniche et al. (2010), who found the extent of IPU aerobic biodegradation to be 1.7 – 4.7 %, despite low levels of oxygen (5 %), in a limestone aquifer, 19 mbs.

**Table 5.3.1** - Extent of <sup>14</sup>C-IPU mineralisation in sampled boreholes after 84 days of respirometry assays.

Borehole (10 mbs)	[IPU] ( $\mu$ g L <sup>-1</sup> )	Redox (mV)	Anaerobic (control) (%)	Sulphate-reducing (%)	Denitrifying (%)	Aerobic (%)
N62b	9	-250	2.3 $\pm$ 0.6 <sup>a</sup>	2.6 $\pm$ 0.9 <sup>a,c</sup>	2.4 $\pm$ 0.2 <sup>a,c</sup>	4.2 $\pm$ 0.3 <sup>b</sup>
N62c	$\leq 1$	-166	1.2 $\pm$ 0.1 <sup>a</sup>	1.2 $\pm$ 0.2 <sup>a</sup>	0.7 $\pm$ 0.1 <sup>c</sup>	1.4 $\pm$ 0.1 <sup>b</sup>
N72b	$\leq 1$	-5.3	2.0 $\pm$ 0.2 <sup>a</sup>	1.3 $\pm$ 0.4 <sup>b</sup>	0.9 $\pm$ 0.1 <sup>c</sup>	2.1 $\pm$ 0.1 <sup>a</sup>
N72c	$\leq 1$	-5.3	0.7 $\pm$ 0.1 <sup>a</sup>	0.8 $\pm$ 0.1 <sup>b</sup>	0.8 $\pm$ 0.2 <sup>b</sup>	0.8 $\pm$ 0.1 <sup>a</sup>
N72d	$\leq 1$	-5.3	1.0 $\pm$ 0.1 <sup>a</sup>	0.6 $\pm$ 0.1 <sup>b</sup>	1.2 $\pm$ 1.2 <sup>a,b</sup>	0.9 $\pm$ 0.1 <sup>a</sup>
N74/84a	$\leq 1$	-17.3	0.9 $\pm$ 0.1 <sup>a</sup>	2.0 $\pm$ 0.6 <sup>b</sup>	1.8 $\pm$ 0.3 <sup>b</sup>	1.4 $\pm$ 1.1 <sup>a</sup>

*Superscript lowercase letters represent the significant difference ( $p \leq 0.05$ ) between the four treatments whereas, the colour represents the significant difference ( $p \leq 0.05$ ) from the control with red indicating no difference and green a difference.*

Conversely, while oxygen levels ( $\leq 2$  mg L<sup>-1</sup>) may be sufficient at the field study site to biodegrade IPU, the enhanced microcosm results imply that increasing the level of oxygen two-fold, to 5 mg L<sup>-1</sup>, doubles the extent of IPU mineralisation from

approximately 2 % to 4 % (Table 4.3.1). Therefore, it would be fair to assume that given time, there is enough dissolved oxygen in the groundwater below the site to support the complete removal of IPU. However, should the rate of mineralisation continue at 2.4 % per 84 days (extent observed in the control microcosm (Table 5.3.1)), and assuming no lateral transport of IPU, then the half-life for the removal of 9 µg L<sup>-1</sup> of IPU from the field site, at well N62, would be 9.5 days (Box 5.3.1). Although, the microcosm studies indicate biodegradation of IPU is taking place at the site, the calculated half-life is somewhat generous compared to the degradation half-life values listed in Table 3.1, which suggest a value of 40 days when in the water phase and 149 days when in a water-sediment phase. This variability in half-life highlights the changeable nature of biodegradation, when faced with different environmental factors.

<b>Box 5.3.1: Half-life calculations for IPU</b>	
Assuming removal of IPU can be described using a first-order degradation curve (Starner et al., 1999):	
$C_t = C_0 e^{-kt}$	
Where	<p><math>C_t</math> is the concentration of IPU at time <math>t</math></p> <p><math>C_0</math> is the initial concentration of IPU</p> <p><math>k</math> is the rate constant</p>
A plot of $\ln(C_t/C_0)$ vs. time yields a straight line with slope equal to $k$ . The rate constant can then be used to derive the half life $t_{1/2}$ :	
$t_{1/2} = (\ln 2)/k$	
The IPU rate constant for $k$ was calculated to be 0.0002 (assuming 2.4 % of 9 µg L <sup>-1</sup> was mineralised after 84 days):	
$t_{1/2} = 0.693/0.0002$	
<b>IPU half-life (<math>t_{1/2}</math>) = 9.5 days</b>	

However, further work, involving longer time frames, which consider the long lag phases often reported for IPU ( $\geq 250$  days) (Janniche et al., 2010, Johnson et al., 2001, Kristensen et al., 2001, Larsen and Aamand, 2001), would be prudent to fully understand the extent of biodegradation of IPU at the field study site. Furthermore, the groundwater contains high concentrations of other carbon sources; toluene and

SULPH (as shown in Chapter 3), which may place selection pressures on the indigenous microbial population (Schmidt and Alexander, 1985).

Previous studies that consider groundwater contaminated by IPU have used *ex-situ* microcosm studies to determine the potential of IPU biodegradation by indigenous microbes. In an attempt to understand the processes involved in the biotransformation of IPU in the environment, Johnson et al (1998) studied IPU aerobic biodegradation using high concentration levels ( $100\mu\text{g L}^{-1}$ ), not normally associated with groundwater contamination, that are typically of the order of  $\leq 1\mu\text{g L}^{-1}$  (Centre for Ecology and Hydrology (CEH), 2000). Johnson et al. (2000a) found that after 220 days, the extent of aerobic biodegradation was  $\leq 95\%$  in a chalk aquifer 10 mbs, which reduced to  $\leq 40\%$  at a depth of 19 mbs. Furthermore, they found the potential for IPU aerobic biodegradation also existed in the saturated zone of both sandstone aquifers ( $\leq 70\%$  at 5-7 mbs) and limestone aquifers ( $\leq 80\%$  4-5 mbs) (Johnson et al., 2003a). However, studies involving high concentrations may be open to criticism because they often do not reflect concentrations found in the environment (Environment Agency (EA), 1999, Chapelle et al., 1996, Sturman et al., 1995b, Wiedemeier et al., 2007b). To address this issue, Kristensen et al. (2001) studied IPU at concentrations of  $6\mu\text{g L}^{-1}$  using microcosms containing saturated chalk from 2.6 – 4.4 mbs and found aerobic biodegradation occurred, albeit at a much slower rate, reaching  $\leq 4\%$  after 250 days.

Larsen and Aamand (2001) found no potential for either aerobic or anaerobic degradation of IPU at concentrations of  $25\mu\text{g L}^{-1}$  after 250 days in the saturated zone, 5 - 9 mbs, in a sandy aquifer. More recently, the potential for IPU aerobic degradation at concentrations ranging from  $0.5 - 100\mu\text{g L}^{-1}$  were studied in a deep sandy aquifer at depths reaching 59 mbs (Janniche et al., 2010). Here, contrary to the findings of Larsen and Aamand (2001), Janniche et al (2010) found the extent of IPU aerobic biodegradation was  $\leq 4.7\%$  after 250 days for concentrations  $>20\mu\text{g L}^{-1}$  at 19 mbs.

The literature indicates a discontinuity between the potential for IPU aerobic biodegradation in chalk and sandy aquifers, with the potential being more favourable in chalk environments. The lack or limited extent of IPU biodegradation in sandy aquifers may be linked to the chemistry of the environment and in particular the pH of the groundwater (Johnson et al., 2003a). Studies of IPU biodegradation in soils

have shown there to be a relationship between IPU biodegradation and soil pH, in that, as pH decreases so too does IPU biodegradation (Walker et al., 2001). Generally, sandy aquifers are more acidic than chalk because they have less of a buffer capacity. This could explain why IPU biodegradation appears to be absent/reduced in sandy aquifers (Kristensen et al., 2001).

Previous studies by Johnson et al. (1998) found that biodegradation of  $100 \mu\text{g L}^{-1}$  of IPU in microcosms: containing a mixture of chalk aquifer material and groundwater; from 10 mbs, remained below 1 % after a period of 125 days. These findings were also supported by Kristensen et al. (2001) who studied IPU biodegradation in a chalk aquifer. Both, Johnson et al. (1998) and Kristensen et al. (2001) attribute their findings to: i) a decrease in microbial density at depths below 2 m, and ii) the fractured structure of chalk making sampling difficult as IPU biodegradation may be isolated within the aquifer fissures. Furthermore, Larsen and Aamand (2001) studied IPU biodegradation at much lower concentrations ( $25 \mu\text{g L}^{-1}$ ) in a sandy aquifer. They were interested in the different redox zones of the aquifer and found no biodegradation of IPU in the aerobic zone (3 mbs), denitrifying zone (5 mbs), sulphate-reducing zone (7mbs) and the methanogenic zone (9mbs). Like Johnson et al. (1998), Larsen and Aamand (2001) attribute this to a reduction in microbial density with depth.

Both these findings partly support the observations of this study in that mineralisation remained  $<1 \%$  but only in so far as the boreholes containing less than  $1 \mu\text{g L}^{-1}$  of IPU (N62c, 72b, 72c, 72d and N74/84a). However, where IPU concentrations were higher ( $9 \mu\text{g L}^{-1}$ ) aerobic mineralisation did reach 4.2 % and in the anaerobic conditions (including enhanced sulphate and nitrate treatments),  $2.4 \pm 0.5 \%$  in 84 days from a sampled depth of 10 mbs and so contradicts the findings of Johnson et al. (1998) and Larsen and Aamand (2001). In terms of their findings regarding less microbial density at depths below 2 m, this is unlikely to be the case in our study, which investigated samples from a field site heavily contaminated for decades, and so there is an expectation that a dense consortium of microbial degraders would already be present. By comparison the work of Johnson et al. (1998), Larsen and Aamand (2001) and Kristensen et al. (2001) focused on aquifers below agricultural land where IPU had been previously in use.

In a later study by Johnson et al. (2004), it is inferred that microbial selection pressures are weak at IPU concentrations of  $100 \mu\text{g L}^{-1}$  and hence, would be even more restricted in the natural environment where IPU concentrations are significantly lower. However, this research finds this is not the case. The low concentration of IPU ( $9 \mu\text{g L}^{-1}$ ), coupled with the high levels of an alternative carbon source, SULPH ( $236 \text{mg L}^{-1}$ ), in the borehole, may limit the percentage of IPU mineralisation but does not appear to restrict it all together. What is apparent from previous studies is that IPU biodegradation takes a long time (i.e. typically between 125-267 days) (Janniche et al., 2010, Johnson et al., 1998, Kristensen et al., 2001). This microcosm study only ran for 84 days and so it may be possible that the mineralisation had yet to increase beyond the lag phase. Figure 5.3.1a shows the slow increase in aerobic mineralisation from  $>2\%$  at 40 days to approximately  $5\%$  after 84 days. Ideally, the microcosm study should run for a sufficient time to enable each phase of the growth curve to be established (Figure 5.3.2), and in particular, to identify at what point the activity reaches the stationary phase as this determines the optimum extent of mineralisation.

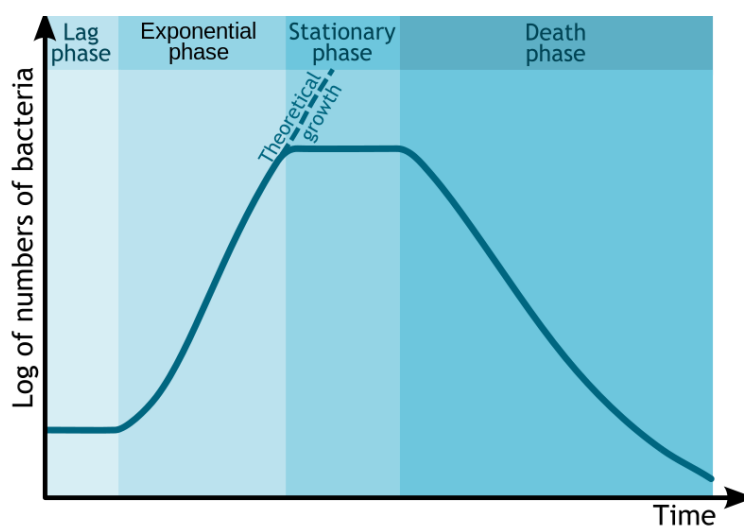


*Figure 5.3.2 - Bacterial growth curve (Wikipedia, 2012)*

Several reasons may account for the minimal and/or no mineralisation of IPU observed. First, the concentration of IPU in the samples was too low to produce a selection pressure. For example, mineralisation may be restricted to  $5\%$  at

concentrations between 1 and 5  $\mu\text{g L}^{-1}$  (Pahm and Alexander, 1993) and at  $< 0.5 \mu\text{g L}^{-1}$  there would be no growth or energy benefit to warrant utilisation by microorganisms (Skipper et al., 1996). Second, that the heterogeneity of a chalk aquifer system imposed a spatial variation on collected samples so that biodegradation potentials were not evenly distributed or missed altogether (Johnson et al., 2000a). Third, that more favourable carbon sources (i.e. SULPH and/or toluene) both of which are present at much higher concentrations at the field study site, as shown in Chapter 3. Fourth, the literature suggests IPU can only be biodegraded aerobically and so low dissolved oxygen levels ( $< 2 \text{ mg L}^{-1}$ ), recorded at the field study site, may be limiting the extent of biodegradation (Larsen and Aamand, 2001). Finally, that biodegradation rates reported for IPU have been  $> 100$  days (Johnson et al., 1998, Janniche et al., 2010, Kristensen et al., 2001) this experiment only ran for 84 days.

An alternative explanation for the low levels ( $< 5 \%$ ) of  $^{14}\text{CO}_2$  evolution observed in this study may be the incomplete mineralisation of IPU. Reports indicate that IPU biodegradation, in chalk aquifers, often results in the production and persistence of the metabolic by-product, containing the phenyl ring (e.g. monodesmethyl-isoproturon) (Johnson et al., 1998, , 2003a, Tuxen, 2002). During this study, there was no analyses of metabolic by-products and hence, the mineralisation observed, albeit at low levels, was only representative of the complete biotransformation of IPU, including the  $^{14}\text{C}$ -labelled phenyl ring. The results here show, for the first time, that the complete mineralisation of IPU has been observed in a contaminated chalk aquifer at concentrations as low as  $9 \mu\text{g L}^{-1}$ .

### 5.3.2 Sulphanilamide Microcosm Studies

Figure 5.3.2 shows the accumulation of  $^{14}\text{CO}_2$  resulting from the complete mineralisation of  $^{14}\text{C}$ -SULPH under anaerobic (control) and enhanced: sulphate, nitrate and oxygen conditions. The maximum extent of SULPH mineralisation, observed in wells N62b and 72b (Figure 5.3.3 a, c), was 40 - 55 %, following an 11 to 14 day lag phase.

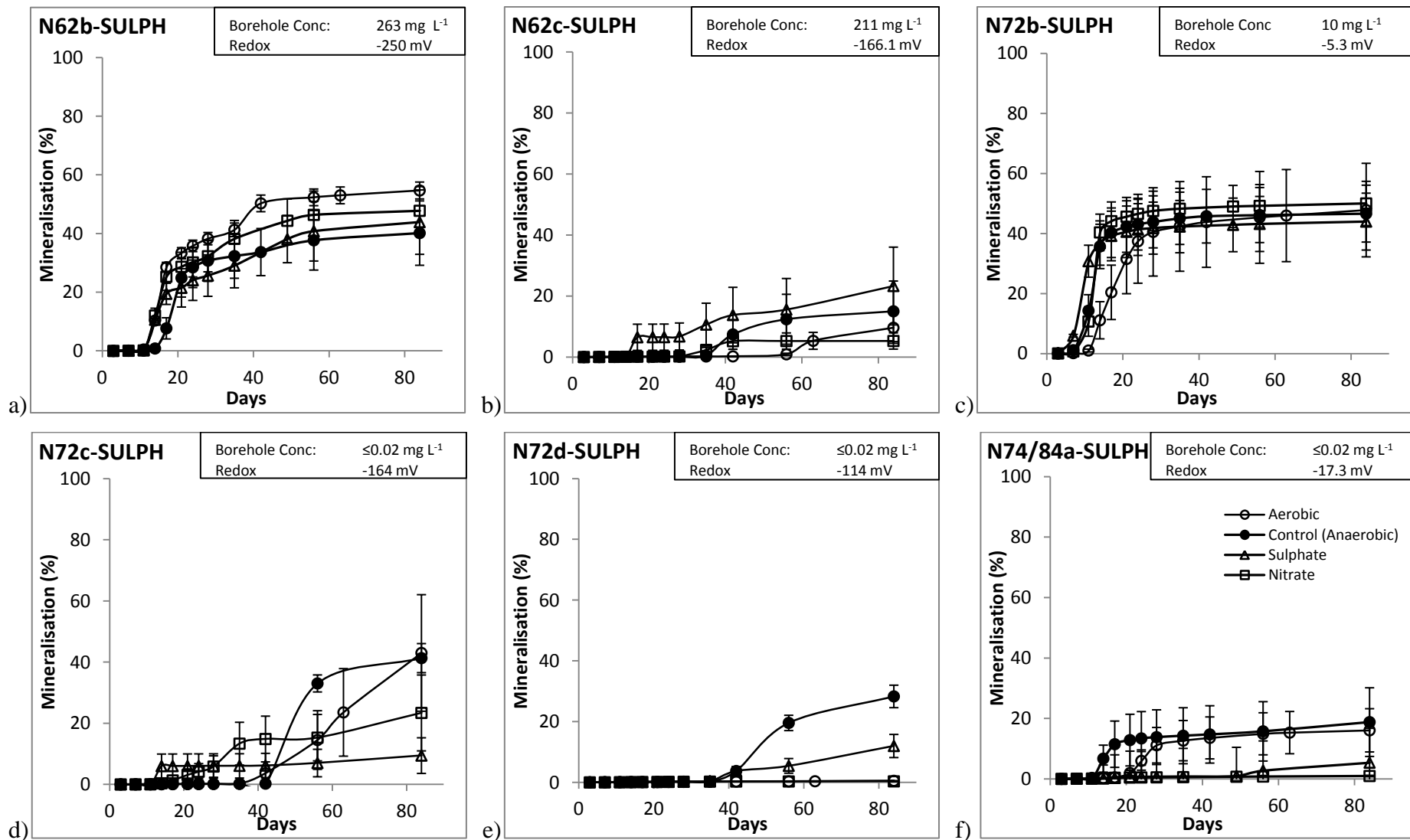


Figure 5.3.3 – The percentage of <sup>14</sup>C-SULPH mineralisation vs. time, shown as number of days. Each graph represents the results of ex-situ microcosms prepared from core material and groundwater samples obtained from six newly drilled boreholes at the field study site.

Table 5.3.2 shows the extent of mineralisation after 84 days, observed for the anaerobic (control) and enhanced treatments, for all six boreholes (Figure 5.2.2) tested during the *ex-situ* microcosm study. At the source zone (N62b), none of the three enhanced treatments, involving the addition of oxygen, sulphate and nitrate as electron acceptors, differed significantly ( $p \leq 0.05$ ) from the control, with average mineralisation ranging from approximately 40 % to 55 %. This suggests oxygen, sulphate and nitrate are not limiting factors in the mineralisation of SULPH in this area of the site. In addition, concentrations of SULPH are particularly high at this location ( $263 \text{ mg L}^{-1}$ ), suggesting that, although part of the sulphonamide group, which have anti-microbial properties, SULPH does not inhibit the growth of the indigenous microbial community. These results are in keeping with other research that has found that  $172 \text{ mg L}^{-1}$  SULPH was aerobically degraded by the soil microbe *Flavobacterium* sp., (Walker, 1978) and, during activated sludge treatments the microbial community tolerated SULPH concentrations up to  $400 \text{ mg L}^{-1}$  (Ingerslev and Halling-Sørensen, 2000).

**Table 5.3.2** - Extent of  $^{14}\text{C}$ -SULPH mineralisation in sampled boreholes after 84 days of respirometry assays.

Borehole (10 mbs)	[SULPH] ( $\text{mg L}^{-1}$ )	Redox (mV)	Anaerobic (control) (%)	Sulphate-reducing (%)	Denitrification (%)	Aerobic (%)
N62b	263	-250	$40 \pm 11^a$	$44 \pm 12^{a,b,c}$	$48 \pm 8.2^{a,c}$	$55 \pm 2.8^{a,b}$
N62c	211	-166	$15 \pm 10^a$	$23 \pm 13^{a,c}$	$5.3 \pm 2.3^{a,d}$	$10 \pm 5.1^{a,b}$
N72b	10	-5	$47 \pm 10^a$	$44 \pm 7.0^a$	$50 \pm 7.4^a$	$48 \pm 16^a$
N72c	$\leq 0.02$	-164	$41 \pm 4.8^a$	$9.4 \pm 5.8^b$	$23 \pm 12^c$	$43 \pm 19^a$
N72d	$\leq 0.02$	-144	$28 \pm 3.7^a$	$12 \pm 3.8^c$	$0.4 \pm 0.1^d$	$0.5 \pm 0.1^b$
N74/84a	$\leq 0.02$	-17	$19 \pm 11^a$	$5.4 \pm 3.3^b$	$1.0 \pm 0.2^c$	$16 \pm 7.2^a$

Superscript lowercase letters represent the significant difference ( $p \leq 0.05$ ) between the four treatments whereas, the colour represents the significant difference ( $p \leq 0.05$ ) from the control with red indicating no difference and green a difference.

The same results observed at N62b were seen at N72b, which is situated South West, approximately 130 m downgradient of the source zone. Even though the concentration of SULPH reduces by one order of magnitude to that at N62b, from 263 to 10 mg L<sup>-1</sup>, the percentage of mineralisation remains unchanged with no significant difference ( $p \leq 0.05$ ) between the enhanced treatments (Table 5.3.2). This implies SULPH concentrations of  $\geq 10$  mg L<sup>-1</sup> may still be a viable electron donor for the indigenous microbes because the lower concentration does not appear to limit the extent of mineralisation (Boethling and Alexander, 1979). Using the microcosm data from N62b, a half-life for SULPH degradation of 21.3 days has been calculated (Box 5.3.2). At present, a half-life value for SULPH is not reported in the literature and so it has not been possible to clarify the half-life presented here.

**Box 5.3.2: Half-life calculations for SULPH**

Assuming removal of SULPH can be described using a first-order degradation curve (Starnier et al., 1999):

$$C_t = C_0 e^{-kt}$$

Where  $C_t$  is the concentration of IPU at time  $t$   
 $C_0$  is the initial concentration of IPU  
 $k$  is the rate constant

A plot of  $\ln(C_t/C_0)$  vs. time yields a straight line with slope equal to  $k$ . The rate constant can then be used to derive the half life  $t_{1/2}$ :

$$t_{1/2} = (\ln 2)/k$$

The IPU rate constant for  $k$  was calculated to be 0.03 (assuming 48% of 263 mg L<sup>-1</sup> was mineralised after 20 days):

$$t_{1/2} = 0.693/0.03$$

$$\text{SULPH half-life } (t_{1/2}) = 21.3 \text{ days}$$

The drop in SULPH concentration at N74/84a ( $\leq 0.02$  mg L<sup>-1</sup>), unlike that observed in borehole N72b (10 mg L<sup>-1</sup>), did have an effect on the extent of mineralisation, with average percentages dropping from approximately 50 % to 20% from that observed in the source area. This indicates that low concentration levels may inhibit SULPH mineralisation with concentrations of SULPH needing to reach a certain threshold before indigenous microbial communities consider biodegradation as being

energy efficient (Boethling and Alexander, 1979). However, this does not explain why at well N72c, although SULPH concentrations dropped to  $\leq 0.02 \text{ mg L}^{-1}$  that the extent of mineralisation observed for the control and oxygen treatment, remains the same as seen in the source zone area (approximately 50 %). Furthermore, threshold concentrations would usually indicate the start or cessation of biodegradation rather than a reduction in the extent. This suggests that a factor, other than a drop in concentration, of four orders of magnitude, is influencing the extent of mineralisation at these two wells (N72c and 74/84a) and in particular the extents observed for the enhanced sulphate and nitrate treatments, which are significantly different ( $p \leq 0.05$ ) from that observed in the control.

One such factor could be a switch in the metabolism of SULPH (Figure 5.2.5) as an electron donor (i.e. as a carbon source) to an electron acceptor (i.e. as a sulphur and/or nitrogen source). Studies by Drillia et al. (2005), considered the biodegradation of sulfamethoxazole (SMX), a member of the sulphonamide group of compounds and found it acted as both a carbon and nitrogen source, during activated sludge treatments. They found SMX was completely biodegraded when it was the only carbon source present in a culture medium and when it was present alongside a second carbon source (acetate), both compounds were fully degraded. However, when SMX, acetate and ammonium (as a nitrogen source) were present only the acetate was degraded and SMX degradation ceased. This suggests that SMX was used as a nitrogen source in the presence of acetate, which is a more easily degraded carbon source than SMX (Drillia et al., 2005).

Furthermore, biodegradation studies of *p*-toluenesulphonamide, again during activated sludge treatment, found that, in a sulphate- and nitrogen-free medium, microbes utilise *p*-toluenesulphonamide as a sulphur and nitrogen source (van Haperen et al., 2001). In addition, van Haperen et al. (2001) found when 95 % of *p*-toluenesulphonamide was biodegraded as a carbon source, 90 % of the available sulphate and 80 % of the available nitrogen remaining in the culture medium was from the breakdown of the *p*-toluenesulphonamide.

This helps to explain why there is a reduction in the extent of mineralisation but not a complete cessation. When SULPH is metabolised as an electron donor its extent of mineralisation is in the region of 50 %, while as an electron acceptor its extent

becomes limited to approximately 20%. In addition, this may explain why adding sulphate and nitrate to the *ex-situ* microcosms further limits the extent of SULPH mineralisation when acting as an electron acceptor as, sulphate and nitrate are more readily available sources of sulphur and/or nitrogen to the indigenous microbial population than SULPH.

The suggestion that SULPH could be metabolised as both an electron donor and acceptor is further supported by the longer lag phases, of approximately 40 days, observed in the *ex-situ* microcosms for the enhanced sulphate and nitrate treatments from wells N62c, 72c, 72d and 74/84a (Figure 5.3.3 d, e and f). Whereby, initially, the more readily available sulphate and/or nitrate were metabolised instead of the SULPH. Once these additional resources became depleted, the microbial community reverted to metabolising SULPH. Moreover, if the microbial community had switched from using sulphate and nitrate instead of SULPH as a sulphur and/or nitrogen source, then there would also have been an adaptation period, during which time changes in metabolic pathways and the production of new enzymes would have been necessary (Drillia et al., 2005).

Finally, reflecting the average temperature of the field site, the temperature of the mineralisation study was 12°C. Temperature can influence the lag phase in mineralisation studies, with lower temperatures causing longer lag phases. In particular, Ingerslev and Halling-Sørensen, (2000) found the lag phase for SULPH increased from 7 to 10 days at 20°C to 34 to 47 days at 6°C. In keeping with these findings, the lag phases observed during this study, apart from the microcosms mentioned above (N62c, 72c, 72d and 74/84a), were between 11 to 14 days. Therefore, as the temperature of the microcosms remained consistent throughout the experiment, it is unlikely that the longer lag phase of 40 days, observed in the above-mentioned microcosms (Figure 5.3.3 d, e and f), was the result of changes in temperature.

#### *5.3.2.1 Relating SULPH mineralisation to the field study site conditions*

By considering the results of the individual *ex-situ* microcosms, examination turned to the three transects linking the sampled wells used in the laboratory to the field site. Questions considered:

- a) The impact, if any, of SULPH mineralisation as the contaminant moved downgradient of the source zone
- b) Whether the natural attenuation process, responsible for the decrease in SULPH concentrations across the site, could be identified (i.e. biodegradation or dispersion)
- c) Whether the hydrochemistry of the groundwater (i.e. redox potentials) influenced the extent of SULPH mineralisation
- d) Whether the presence of co-contaminants at the field study site influenced SULPH mineralisation

Transect (1) moves from the source zone (N62b), 330 m downgradient in a south westerly direction, at a depth of 10 m. This transect lay west of the main toluene works area (N71) and hence, would not be impacted by toluene contamination, which in turn may influence the extent of SULPH mineralisation. Therefore, it is probable that the decrease in SULPH concentrations, recorded across this transect, are the result of biodegradation and/or dilution/dispersion.

Transect (2) moves from the source zone (N62b), 140 m downgradient in a south-south-westerly direction at a depth of 10 m. This transect travels 80 m closer to the toluene works area (N71) and hence, in contrast to transect (1), will be exposed to toluene contamination. This transect will consider whether the presence of another carbon source (i.e. toluene) will affect the extent of SULPH mineralisation.

Transect (3) moves against the gradient of the site in a south easterly direction, linking transects 1 and 2, 140 m from the source zone (N62b). Here, SULPH concentrations reduce by one order of magnitude compared to those at the source zone. This transect considers whether there is an observable transition between the use of SULPH and toluene as a carbon source. Figure 5.3.4 shows the three transects and a summary of the groundwater chemistry at the site.

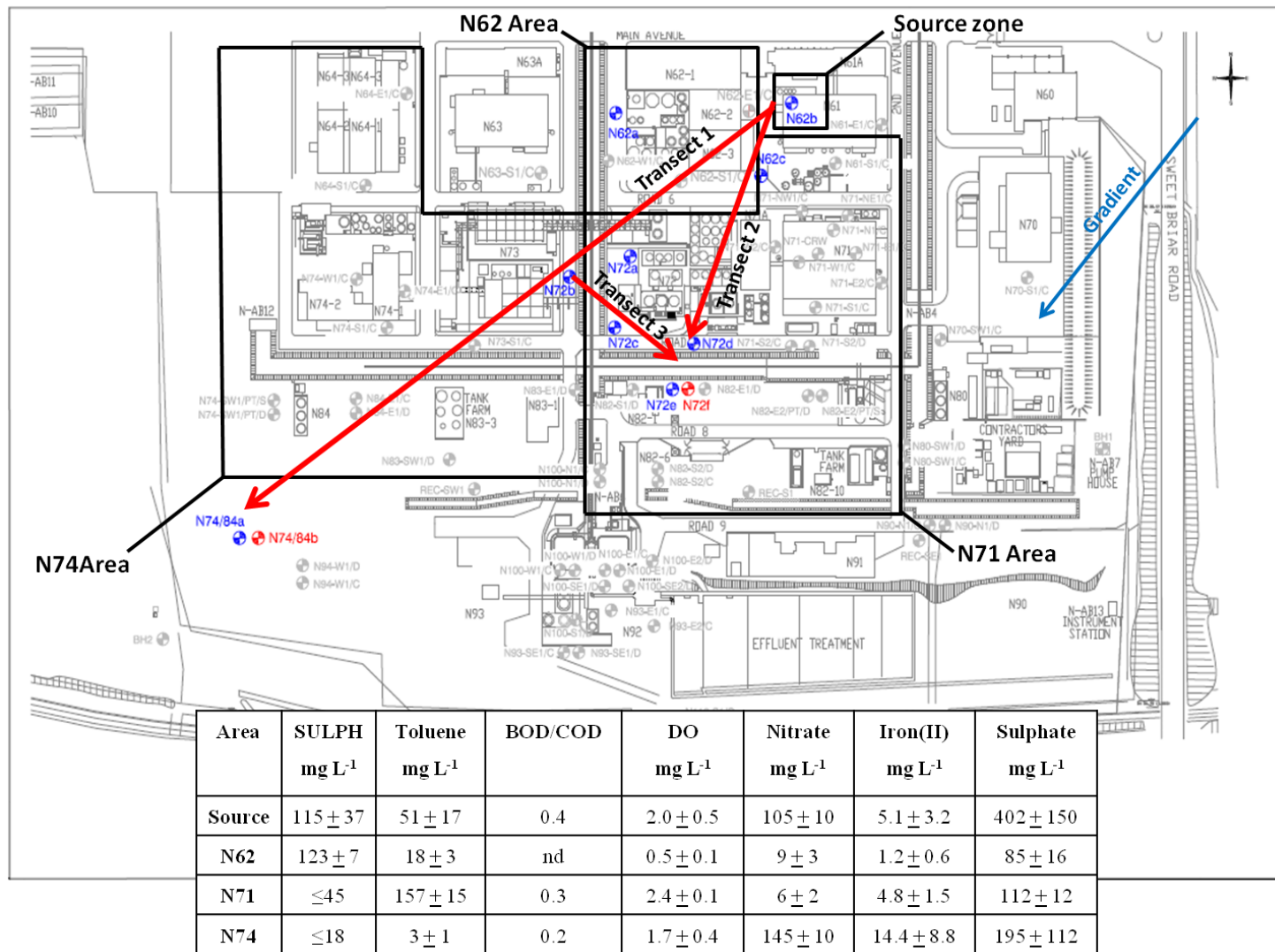
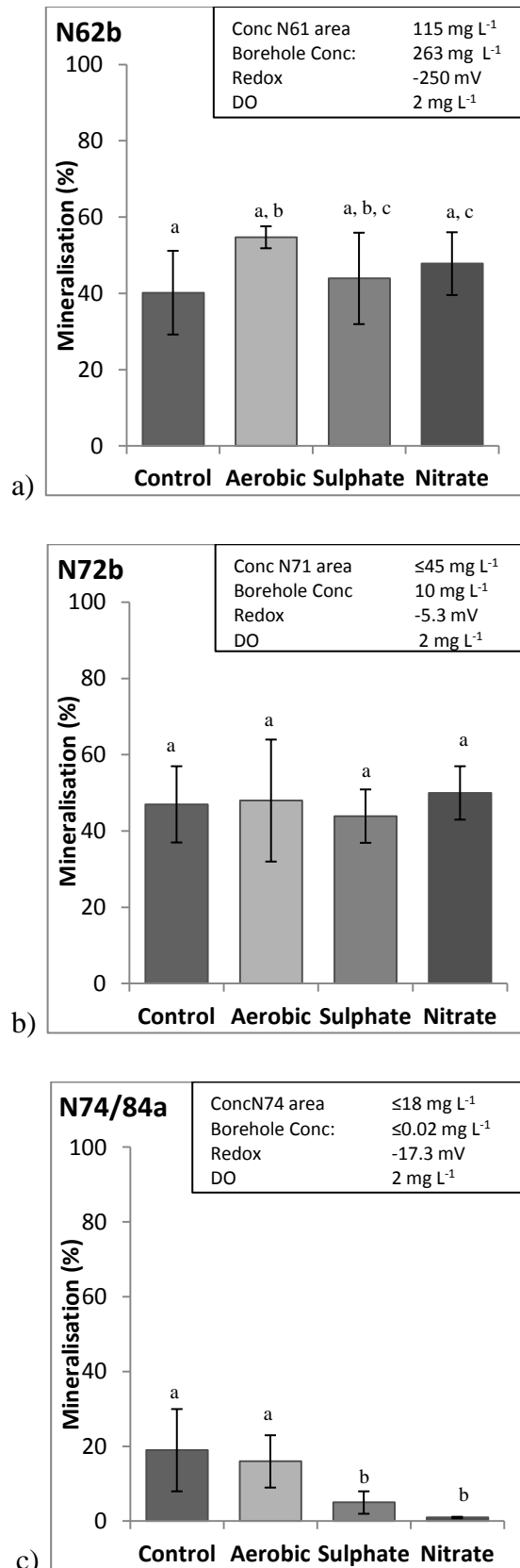


Figure 5.3.4 - Map of field study site showing the positions of the new boreholes and the transects used to explore biodegradation processes occurring across the site.

**Transect (1)** - Moving down gradient from the source zone (N62b), the SULPH concentration reduced from 263 to 10 mg L<sup>-1</sup> at well N72b, located 140 m from the source, to ≤0.02 mg L<sup>-1</sup> at well N74/84a, 330 m from the source. The greatest reduction in SULPH (approximately. 96 %) occurred between the source and N72c, with a further loss of approximately 3.8 % taking place between N72c and N74/84a.

The results presented in Figure 5.3.5 indicates the significant difference ( $p \leq 0.05$ ), if any, between the control microcosms and the enhanced treatments (sulphate-reducing, denitrifying and aerobic) in the same well. There was no significant difference ( $p \leq 0.05$ ) between the extents of mineralisation ( $46 \pm 17$  %) observed in the controls at both N62b and 72b when compared to the enhanced treatments.

The results presented in Table 5.3.3 indicate the significant difference ( $p \leq 0.05$ ), if any, between the extents of mineralisation observed for the same treatments in different wells. Surprisingly, although SULPH concentrations differed by one order of magnitude between N62b (263 mg L<sup>-1</sup>) and N72b (10 mg L<sup>-1</sup>) there was no significant difference ( $p \leq 0.05$ ) when comparing the same enhanced treatments at the two wells.



**Figure 4.3.5 - Transect 1: Extent of SULPH mineralisation after 84 days, with lower case letters representing the significant difference ( $p \leq 0.05$ ) between the control and enhanced treatments.**

**Table 5.3.3** – Student T test results for Transect 1: significant difference between the extent of mineralisation for the same treatments and different wells.

<b>Borehole</b> [SULPH mg L <sup>-1</sup> ]	<b>Anaerobic (Control)</b>	<b>Sulphate-reducing</b>	<b>Denitrification</b>	<b>Aerobic</b>
<b>N62b vs. N72b</b> [263] vs. [10]	+	+ +	+	+
<b>N62b vs. N74/84a</b> [263] vs. [≤0.02]	+ +	+ +	+ + +	+ + +
<b>N72b vs. N74/84a</b> [10] vs. [≤0.02]	+ +	+ + +	+ + +	+ +

(*p*-value ≤0.5 (+), *p*-value ≤0.05 (++) and *p*-value ≤0.005 (+++)) red indicating the same, green sig. different.

Furthermore, as described in Chapter 3, although redox conditions change from an area of methanogenesis at the source zone (N62b) to Fe (III)-reduction at N72b, this does not appear to influence the extent of SULPH mineralisation. Suggesting that both methane and Fe (III) - degraders may have the potential to metabolise SULPH. Moving from methanogenic conditions in the source area to Fe(III)-reducing conditions down gradient, coupled with extensive loss of SULPH, that is to say approximately 96% as stated above between N62c and 72b, is usually indicative of highly efficient natural attenuation processes (Wiedemeier et al., 2007b). Studies have linked an accumulation of sulphate in *ex-situ* microcosms resulting from the biodegradation of *p*-toluenesulphonamide (van Haperen et al., 2001). This could account for the high levels of sulphate ( $402 \pm 150 \text{ mg L}^{-1}$ ) reported in the source zone and be useful in terms of supporting the occurrence of natural attenuation at the field study site (Wiedemeier et al., 2007b).

Interestingly, the predicted percentage of biodegradation for all dissolved contaminants measured at these two wells, obtained using BOD/COD ratio calculations (represented in Chapter 3 and summarised in Figure 4.3.4), was approximately 40 %, which is in keeping with the results obtained in the *ex-situ* microcosms. The BOD/COD ratio predicts the total biodegradation potential of all the organic contaminants present (Robinson and Thorn, 2005, Srinivas, 2008). Since the extent of SULPH biodegradation matches the BOD/COD

prediction, it would be reasonable to assume, that of the available carbon sources in this area of the site, SULPH biodegradation dominates. Therefore, a fair speculation would be that of the 96 % SULPH reduction occurring between N62b and 72b,  $46 \pm 17$  % is most likely the result of complete biodegradation and the remaining loss of  $50 \pm 17$  % may be attributable to another natural attenuation process. For example dispersion, causing SULPH, which is highly soluble ( $7.5 \text{ g L}^{-1}$  in water at  $20 \text{ }^\circ\text{C}$ ), to move from an area of high concentration in the source zone to an area of low concentration down gradient (Wiedemeier et al., 2007a). However, this study focused on the complete degradation of SULPH by measuring the evolved  $^{14}\text{CO}_2$  resulting from the breakdown of the radiolabelled benzene ring. Therefore, the results exclude any daughter products, which may have formed during biodegradation of the parent product, SULPH. Furthermore, the addition of electron acceptors (oxygen, sulphate and nitrate), factors considered to limit biodegradation if depleted (Haack and Bekins, 2000), had no positive influence on the extent of biodegradation during the laboratory trials. Therefore, it is possible that a factor other than the availability of electron acceptors was limiting the extent of SULPH biodegradation to approximately 50 % at the site. One factor could be the lack of available nutrients to sustain higher levels of biodegradation by the indigenous microbial population (Bragg et al., 1994) as studies have found that nitrogen and phosphorus can limit the biodegradation of hydrocarbons in the environment (Das and Chandran, 2011, Cooney et al., 1985, Leahy and Colwell, 1990). In this study, it is unlikely that nitrogen was the limiting factor as the enhanced treatments, which used nitrate, did not increase the extent of biodegradation. Therefore, phosphorus may have been the limiting factor responsible for restricting SULPH biodegradation to approximately 50 % in the source zone area.

Moving further downgradient, a distance of approximately 330 m from the source zone to 74/84a the extent of biodegradation falls from approximately 50 % to 20 % for the control and oxygen treatment, and to 5 % for the sulphate and nitrate enhanced treatments (Figure 4.3.5c). The enhanced treatments appear to separate out into two groups, with a significant difference ( $p \leq 0.05$ ) between the control/oxygen and sulphate/nitrate treatments (Table 4.3.3). In addition, there is now a significant difference ( $p \leq 0.05$ ) between this well and the other two wells along transect (1). There are two distinct changes in the biodegradation at N74/84a (Figure 4.3.5c), which do not occur at wells N62b or 72b. First, the extent of biodegradation is limited to approximately 20 % and second, the lag phase for the sulphate

and nitrate treatments has changed from 11-14 to 40-45 days (Figure 4.3.3). As previously discussed, these changes are unlikely to be the result of a reduction in SULPH concentration, even though it is four orders of magnitude lower than the source zone. Why the extent of biodegradation has reduced but not completely stopped, and increasing the concentration of sulphate and nitrate has hindered biodegradation in this area of the site remains unclear. However, as suggested earlier, it may be indicative of a change in the metabolism of SULPH from electron donor, at wells N62b and 72b, to electron acceptor at N74/84a.

Furthermore, the BOD/COD calculations, from Chapter 3, for this region of the site are approximately 20 %, which is consistent with the results obtained for the control and oxygen treatment but not the sulphate and nitrate treatments (Figure 5.3.5c). These findings support the idea that SULPH may be metabolised as an electron acceptor in N74/84a. Because the SULPH concentrations observed here, despite not limiting mineralisation under the control and aerobic treatments, were too low in N74/84a to sustain SULPH utilisation as an electron acceptor when more readily available substrates were present (e.g. such as the additional sulphate and nitrate, which was added during experimentation) (Drillia et al., 2005). Moreover, the rate limiting step in SULPH mineralisation (i.e. only reaching approximately 20 %) when utilised as an electron acceptor, appears to be the demand for nitrogen by the indigenous microbial population.

Finally, the redox potentials have shifted in this area to Fe (III) reduction (-17 mV) from methanogenesis (-250 mV) in the source zone. However, as observed in well N72b, a switch to Fe (III) reduction does not necessarily control the extent of SULPH mineralisation. Nevertheless, if the SULPH metabolic pathway has changed from an electron donor to an acceptor in this region of the site (Drillia et al., 2005), then further investigation would be necessary to establish what biological reactions require sulphur and/or nitrate in N74/84a to warrant using the sulphur and/or nitrogen components of SULPH.

**Transect (2)** – This transect tentatively follows the expected groundwater flow at the site but any SULPH plume would be expected to follow a more south westerly direction with increasing distance from the source zone (N62b). The SULPH concentration reduces from 263 to 211 mg L<sup>-1</sup> at well N62c, which is approximately 80 m from the source, and to ≤

0.02 mg L<sup>-1</sup> at N72d, approximately 140 m from the source zone. Because of the direction of this transect it is possible that the observed reduction in SULPH concentration may point towards the fringes of the SULPH plume, rather than the result of biological activity. This theory is further supported by well N72b (10 mg L<sup>-1</sup>), situated at a similar distance from the source along transect (1), having a higher concentration than N72d ( $\leq 0.02$  mg L<sup>-1</sup>).

Surprisingly, although wells N62b and c have comparable SULPH concentrations there is a significant difference ( $p < 0.05$ ) in the extent of mineralisation between the two wells for the control, oxygen, sulphate and nitrate treatments, reducing from approximately 50 % to  $\leq 20$  % respectively (Table 5.3.4). This suggests that some factor, other than the concentration of SULPH is limiting the extent of mineralisation in this area (N62c).

**Table 5.3.4** – Student T test results for Transect 2: significant difference between the extent of mineralisation for the same treatments and different wells.

<b>Borehole</b> [SULPH mg L <sup>-1</sup> ]	<b>Anaerobic (control)</b>	<b>Sulphate-reducing</b>	<b>Denitrification</b>	<b>Aerobic</b>
<b>N62b vs. N62c</b> [263] vs. [211]	+ +	+ +	+ + +	+ + +
<b>N62b vs. N72d</b> [263] vs. [ $\leq 0.02$ ]	+	+ +	+ + +	+ + +
<b>N62c vs. N72d</b> [211] vs. [ $\leq 0.02$ ]	+	+	+ +	+ +

( $p$ -value  $\leq 0.5$  (+),  $p$ -value  $\leq 0.05$  (++) and  $p$ -value  $\leq 0.005$  (+++)) red indicating the same, green sig. different.

Furthermore, in well N62c the oxygen, sulphate and nitrate enhanced treatments do not show any significant difference ( $p \leq 0.05$ ) from the control microcosm (Figure 5.3.6b), implying that these electron acceptors are not responsible for limiting the extent of mineralisation to  $\leq 20$  % in well N62c.

Therefore, one factor limiting the extent of mineralisation at well N62c, compared to that at N62b (Figures 5.3.6 a and b) may be the presence of another, more readily available carbon source, such as toluene, which is also present in this area of the site. However, toluene concentrations are higher at N62b ( $51 \pm 17 \text{ mg L}^{-1}$ ) than reported in N62c ( $18 \pm 3 \text{ mg L}^{-1}$ ). Therefore, it is doubtful the reduction in SULPH mineralisation is the result of toluene being an alternative carbon source. Furthermore, in the presence of a more readily available carbon source it is probable that SULPH mineralisation would cease rather than the extent become limited.

Another factor, which may be influencing biological activity, is the change in redox potential from methanogenesis ( $-250 \text{ mV}$ ) at the source zone (N62b) to sulphate reduction ( $-167 \text{ mV}$ ) at N62c (Figure 5.3.6 a and b). This is further supported by the noticeable reduction in sulphate from  $402 \pm 105 \text{ mg L}^{-1}$  at the source zone to  $85 \pm 16 \text{ mg L}^{-1}$  at N62c (Figure 5.3.4), indicating the consumption of sulphate as an electron acceptor within this area. From these findings, it would be reasonable to assume SULPH mineralisation is more favourable under methanogenic than sulphate-reducing conditions, with the extent of mineralisation in N62b being twice that observed in N62c.

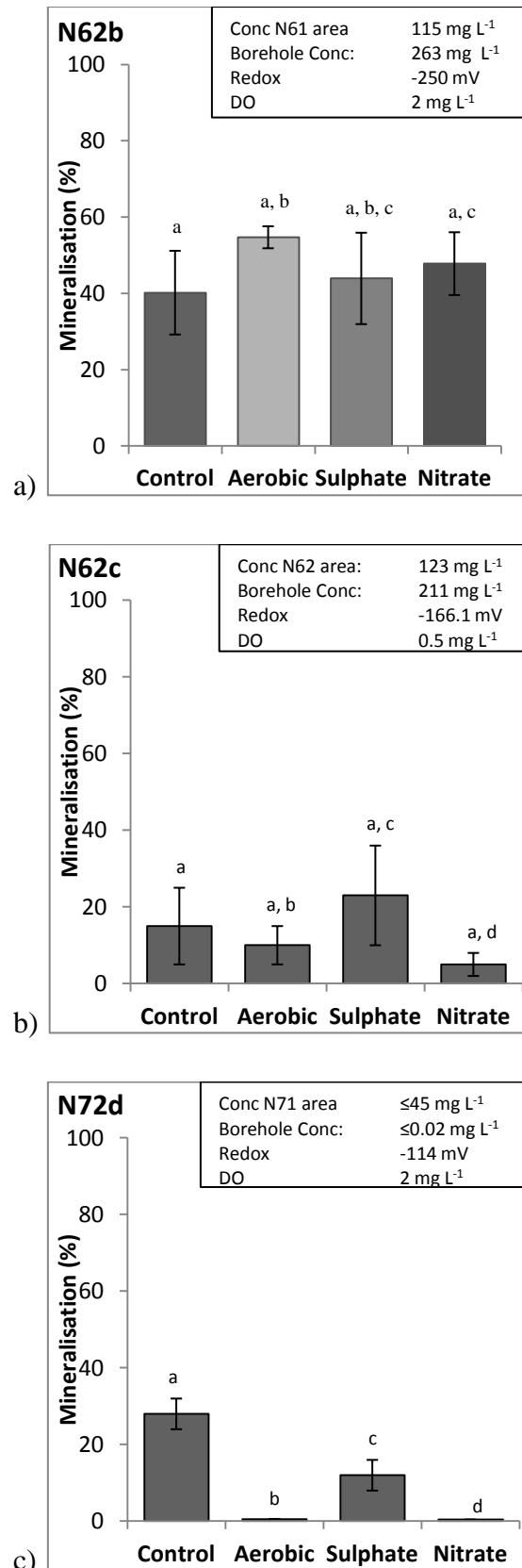


**Figure 5.3.6 - Transect 2: Extent of SULPH mineralisation after 84 days, with lower case letters representing the significant difference ( $p \leq 0.05$ ) between control and enhanced treatments.**

Moreover, nitrate concentrations are reduced from 105 to 9 mg L<sup>-1</sup> between the two wells (Figure 5.3.4). This could be indicative of a forced selection pressure on the indigenous microbes to find a means to replenish the depleted nitrogen. Thus driving a change in SULPH metabolism from an electron donor, at the source zone, to an acceptor at N62c, with the nitrogen component of SULPH used to compensate for the depletion of nitrate in N62c. As previously described for well N74/84a in transect (1), this could also account for the extended lag phase, from 14 to 40 days, observed in the enhanced nitrate treatment (Figure 5.3.3) and, the reduction in the extent of mineralisation between these two wells (Figure 5.3.5). In that, there would be an observable adaptation period indicating a change in metabolic pathway from electron donor to acceptor and, the extent would now be representative of the new pathway.

Moving to the final well in this transect (N72d), the SULPH concentration dropped by four orders of magnitude to  $\leq 0.02$  mg L<sup>-1</sup>. The redox potential (-114 mV) suggested sulphate-reducing conditions do remain, with the measured sulphate and nitrate concentrations in the groundwater comparable with N62c (Figure 5.3.4). However, as expected, toluene concentrations increase sharply from 18 mg L<sup>-1</sup> in N62c to 157 mg L<sup>-1</sup> (Figure 5.3.4), due to the well being in close proximity to the toluene works (area N71). With the SULPH concentration being much lower than the toluene concentration it was expected that toluene would now place a selection pressure on the indigenous microbial population for use as a carbon source. What was apparent was the same phenomenon as seen in transect (1) at well N74/84a. Whereby, adding an additional nitrate source to the *ex-situ* microcosm limited the extent of SULPH mineralisation to <1 % (Table 5.3.2) when concentrations of SULPH were lower ( $\leq 0.02$  mg L<sup>-1</sup>). Furthermore, there is a significant difference ( $p \leq 0.05$ ) between the enhanced nitrate treatment at N72d and that at N62c (Table 5.3.4), where SULPH concentrations were much higher (211 mg L<sup>-1</sup>). Again, suggesting the possibility of SULPH being used as an electron acceptor rather than a donor (Drillia et al., 2005). However, as discussed previously, when SULPH concentrations are lower, more readily available electron acceptors (i.e. nitrogen), when available, will be utilised first.

However, as shown in well N62c, SULPH concentration does not appear to activate a metabolic change from electron donor to acceptor. Therefore, it is more likely

changes in groundwater chemistry are driving the microbial activity, with methanogenic conditions being favourable for SULPH metabolism as a carbon source and sulphate-reducing conditions favouring SULPH metabolism as a nitrogen source.

BOD/COD values were only available for area N71 and not N62, and indicated approximately 30% of the organic contaminants in this area are biodegradable (Chapter 3). This is only true for the control microcosm, with the extent of biodegradation being  $28 \pm 3.7$  % after 84 days. This was not the case for the sulphate ( $12 \pm 3.8$  %), nitrate ( $0.4 \pm 0.1$  %) and oxygen ( $0.5 \pm 0.1$  %) treatments (Table 5.3.2). This suggests that under representative site conditions, as observed in the control, high toluene concentrations ( $100 - 275$  mg L<sup>-1</sup> recorded in area N71 at the site) did not limit SULPH mineralisation as the results observed here (N72d) were similar to those already reported for N74/84a, where toluene concentrations were only  $3 \pm 1$  mg L<sup>-1</sup> (Figure 5.3.2).

What the findings do suggest however, is the impact that groundwater chemistry has on the extent of mineralisation of SULPH, notably, that changes in redox conditions may cause a switch in SULPH metabolism from an electron donor (favourable in both Fe (III)-reducing and methanogenic conditions) to an acceptor (favourable in both Fe (III) and sulphate-reducing conditions). Furthermore, the extent of mineralisation indicates it is more beneficial, in terms of natural attenuation at the field study site, when SULPH is metabolised as an electron donor with percentages reaching as much as 55 % compared to those as an electron acceptor where mineralisation becomes limited to approximately 20 %. These findings propose that when SULPH concentrations are  $\geq 10$  mg L<sup>-1</sup>, then mineralisation, as an electron donor, shows a preference for degradation by Fe (III)-reducing and methanogenic microbial populations. However, the extent of mineralisation becomes limited in the presence of sulphate reducers, which appear to have the ability to out-compete the Fe (III)-reducing and methanogenic microbial populations so that the use of SULPH as an electron acceptor dominates.

**Transect (3)** – aims to investigate changes in both the extent of biodegradation (Figure 5.3.7 b and c) and lag phases (Figure 5.3.3), observed in the microcosms from wells N72c and d, with regard to changes in groundwater chemistry in and around the area of these two wells (Figure 5.3.4). There are two main requirements for biodegradation of groundwater contaminants to be successful; (1) the presence of a microbes with the capacity to degrade the contaminants and, (2) favourable geochemical and hydrological conditions (Haack and Bekins, 2000). The results of the *ex-situ* microcosms, in particular wells N62b (Figure 5.3.5a) and 72b (Figure 5.3.7a), show the presence of viable microbial communities able to degrade SULPH.

Between N72b and c, although the SULPH concentration fell by three orders of magnitude, the extent of mineralisation for the control and oxygen treatment was not significantly different ( $p \leq 0.05$ ) (Table 5.3.5). However, the lag phases did change from 11 to 40 days respectively (Figure 5.3.3c and d). For the sulphate and nitrate treatments, the converse was true, with lag phases remaining the same for both wells but the extent of mineralisation reducing significantly, ( $p \leq 0.05$ ) from 50 % (N72b) to  $<20$  % (N72c). There has also been a change in redox conditions, shifting from Fe(III)-reducing (N72b) to sulphate-reducing (N72c).

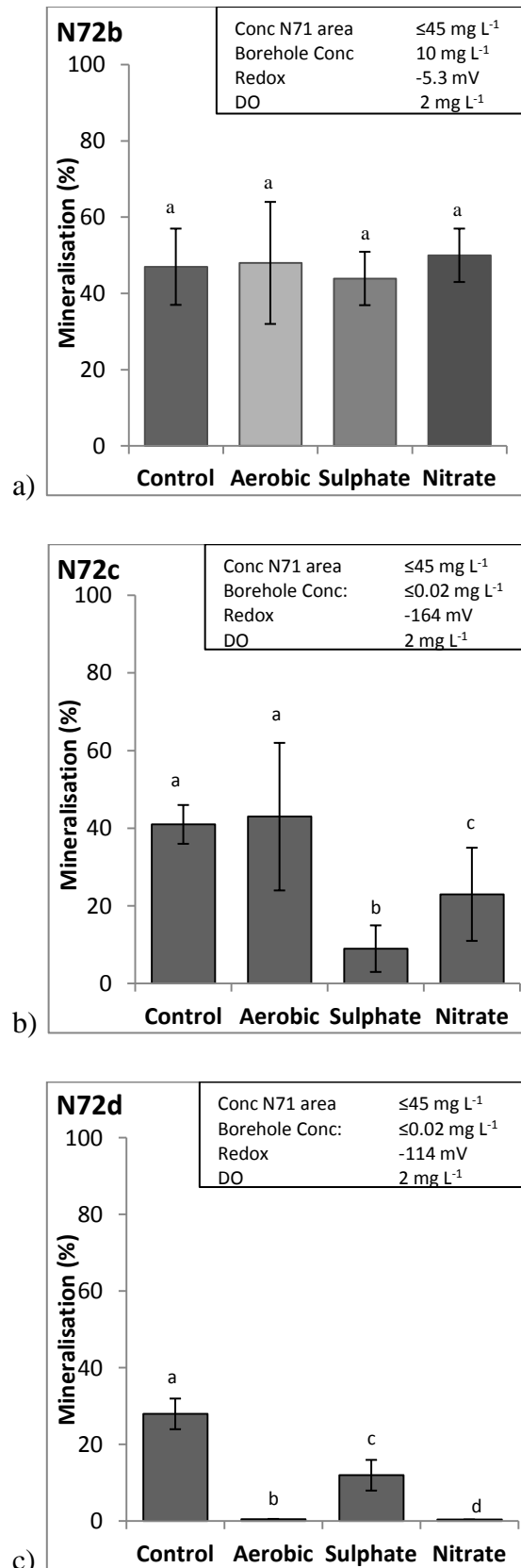


**Figure 5.3.7 - Transect 3: Extent of SULPH mineralisation after 84 days, with lower case letters representing the significant difference ( $p \leq 0.05$ ) between control and enhanced treatments.**

**Table 5.3.5** – Student T test results for Transect 3: significant difference between the extent of mineralisation for the same treatments and different wells.

<b>Borehole</b> [SULPH mg L <sup>-1</sup> ]	<b>Anaerobic</b> <b>(control)</b>	<b>Sulphate-</b> <b>reducing</b>	<b>Denitrification</b>	<b>Aerobic</b>
N72b vs. N72c [10] vs. [≤0.02]	+	+ + +	+ +	+
N72b vs. N72d [10] vs. [≤0.02]	+ +	+ + +	+ + +	+ +
N72c vs. N72d [≤0.02] vs. [≤0.02]	+ +	+	+ +	+ +

(*p*-value ≤0.5 (+), *p*-value ≤0.05 (++) and *p*-value ≤0.005 (+++)) red indicating the same, green sig. different.

At well N72d, the lag phases for the control and enhanced treatments were all approximately 40 days (Figure 5.3.3e). Furthermore, the extent of mineralisation for the control microcosms, observed between wells N72b vs. N72d and N72c vs. N72d, reduced significantly ( $p \leq 0.05$ ) (Table 5.3.5) from approx. 50 to 20% (Fig. 5.3.7). These observations were also seen in well N74/84a discussed in transect (1). The extent of mineralisation appeared to be inhibited to ≤0.5 % for both the oxygen and nitrate treatments at well N72d. The redox conditions remained sulphate reducing as observed in N72c.

The results of Transect (3) suggested a change in SULPH metabolism from that of electron donor to electron acceptor. This is supported by longer lag phases - indicative of an adaption period, and the addition of nitrate, in particular, being detrimental to the extent of SULPH mineralisation. Nitrogen in nitrate form is more readily available to the indigenous microbial population than the nitrogen obtained from the metabolism of SULPH (Drillia et al., 2005, van Haperen et al., 2001).

#### 5.4 Conclusion

Returning to the research questions raised in the introduction, “Do the results of the ex-situ microcosms provide supporting evidence that the observed reduction in IPU and/or SULPH concentration is due to biodegradation processes?” The results infer biodegradation processes are responsible for a 2 % reduction in IPU concentration at the field study site, albeit limited to the microcosms from area N62, where IPU concentrations were  $9 \mu\text{g L}^{-1}$ . However, in the microcosms where concentrations of IPU were less than  $1 \mu\text{g L}^{-1}$  IPU catabolic activity was absent. As far as this study is aware this is the first time IPU mineralisation has been reported for low concentrations ( $9 \mu\text{g L}^{-1}$ ), 10 mbs in a chalk aquifer.

The results of the SULPH *ex-situ* microcosms suggested biodegradation processes were more prevalent across the study site than those observed for IPU. When SULPH concentrations were between 10 and  $263 \text{ mg L}^{-1}$ , the extent of SULPH mineralisation reached 40 to 55 % at the source area (N62b) and 140 m downgradient at N72b. However, once concentrations were less than  $0.02 \text{ mg L}^{-1}$ , then the extent of mineralisation reduced by more than half to 20 %. As far as we are aware, this is the first time SULPH mineralisation has been reported for *ex-situ* microcosms, sampled from 10 mbs in a chalk aquifer.

Question two was, “Can the extent of IPU and/or SULPH mineralisation be enhanced by increasing the concentration of electron acceptors available to the indigenous microbes?”

Adding sulphate and nitrate electron donors to the IPU microcosms did not enhance the extent of mineralisation. The mineralisation in the control microcosm, designed to replicate *in-situ* conditions, was enhanced from 2 to 4 % by increasing the concentration of available oxygen. The findings suggest increasing oxygen levels by a factor of two (from 2 to  $5 \text{ mg L}^{-1}$ ), has the potential to increase the extent of IPU mineralisation by the same factor. However, the solubility of oxygen at  $12^\circ\text{C}$  (groundwater temperature at the field study site) is approx.  $10 \text{ mg L}^{-1}$ . Therefore, the capacity of the groundwater to support increased levels of dissolved oxygen is limited.

Increasing the concentrations of oxygen, sulphate and nitrate available in the SULPH microcosms did not enhance the extent of mineralisation compared to that of the control microcosms. Interestingly, the addition of electron acceptors, in particular sulphate and nitrate, appeared to inhibit the extent of mineralisation, reducing it by

more than a half (from 40 to 20%). Furthermore, the increase in these available electron acceptors also increased the lag phase from 11 to 40 days. A likely explanation for this is that the indigenous microbial community are able to utilise SULPH as both an electron donor and acceptor (albeit to a lesser extent when utilised as an electron acceptor). However, further investigation would be necessary to understand what is driving this switch from SULPH utilisation as an electron donor to an acceptor. The literature does offer some suggestion of factors that may influence changes in SULPH metabolism:

- i) A change in localised redox conditions from iron- to sulphate-reduction can have an impact on the use of sulphate and/or nitrate as electron acceptors (Dalsgaard and Bak, 1994).
- ii) The concentration of SULPH is too low to maintain its use as carbon source.
- iii) The presence of other carbon sources e.g. toluene. Microbial communities can biodegrade mixtures of carbon compounds. The simultaneous biodegradation of two carbon compounds is usually concentration dependent in that, at low concentrations both compounds would be biodegraded at the same time whereas, at high concentrations biodegradation occurs consecutively. This is because compounds at higher concentrations are more favourable in meeting the maintenance and growth requirements of the microbial community (Schmidt and Alexander, 1985).

The third question was, “Is there any evidence to show that changes in groundwater chemistry and/or the presence of other contaminants, discussed in Chapter 3, impact on the extent of IPU and/or SULPH mineralisation?” The concentrations of IPU ( $\leq 9 \mu\text{g L}^{-1}$ ) present at the field study site were 3 to 4 orders of magnitude less than those for SULPH ( $\leq 300,000 \mu\text{g L}^{-1}$ ). As mentioned above, microbial populations usually biodegrade compounds present at higher concentrations first and so it is most likely that the extent of IPU mineralisation was impacted by the presence of other contaminants at the site. In addition, the groundwater chemistry also influenced the extent of IPU mineralisation. In that, the low levels of dissolved oxygen, in the control microcosms, restricted the extent of mineralisation by half.

The results indicate that both changes in groundwater chemistry and the presence of other contaminants, in particular toluene, have an impact of SULPH mineralisation. With respect to groundwater chemistry at the field study site, it would appear SULPH mineralisation favoured either methanogenic and/or Fe(III)-reducing conditions, with the extent of mineralisation reaching as much as 55 %. In contrast, when sulphate-reducing conditions dominated, then the extent reduced by more than half to 20%. It is not entirely clear if the presence of other contaminants (e.g. toluene in this instance) or changes in water chemistry, or both, were effecting a change in the extent of mineralisation because different results were observed for areas containing the same high levels of toluene. What is clear, however, is when sulphate and/or nitrogen were present in high enough concentrations then SULPH appears to be used as an electron donor (50 %). However, when levels of sulphate and/or nitrogen are exhausted then SULPH may be used as an electron acceptor (20 %). Further investigation would be necessary to be sure of these relationships as they most likely involve complex microbial community interactions.

Lastly, of environmental interest, even at low levels, IPU biodegradation can be important in reducing groundwater pollution, especially in fractured aquifers where groundwater residence times often span decades (Kristensen et al., 2001, Janniche et al., 2010). In terms of the remediation of SULPH in the environment, Ingerslev and Halling-Sørensen,(2000) found that microbes exposed to one sulphonamide could later easily degrade other sulphonamides within the same group without the need of an adaption period. This suggests the degradation pathway and subsequent utilization by microbes is similar if not the same for all compounds within the group i.e. the microbes had acquired general properties to degrade several sulphonamides during their first exposure to a member of the group. Therefore, the results of this study may be of interest to the wastewater, farming and veterinary industries.

# Chapter 6: Compound Specific Isotope Analysis – a tool to substantiate sulphanimide biodegradation in a chalk aquifer

---

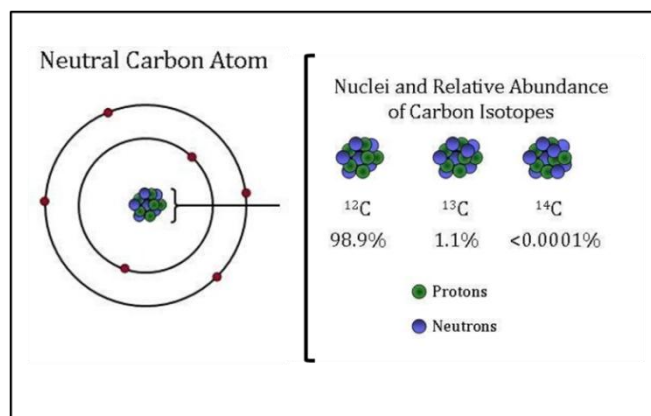
## 6.1 Introduction

The aims and objectives of this chapter were to examine the merits of compound specific isotope analysis in evaluating the existence of SULPH biodegradation at the field site, with a view to substantiating the evidence of natural attenuation presented in Chapters 3 and 4. Of particular interest were:

1. Can SULPH, a non-volatile, hydrophilic compound, be analysed using compound specific isotope analysis?
2. Is there evidence of isotope fractionation to substantiate biodegradation processes at the study site?
3. Should fractionation be evident, can biodegradation be quantified, to support the evidence already obtained via *ex-situ* microcosm studies and the site model results from previous chapters?

### 6.1.1 Stable Isotopes

Isotopes exist because atoms of the same element can have a different number of neutrons (Fig.6.1). The atoms that contain a greater number of neutrons are referred to as heavy isotopes because they contain more mass than those atoms with fewer neutrons, which are called light isotopes.



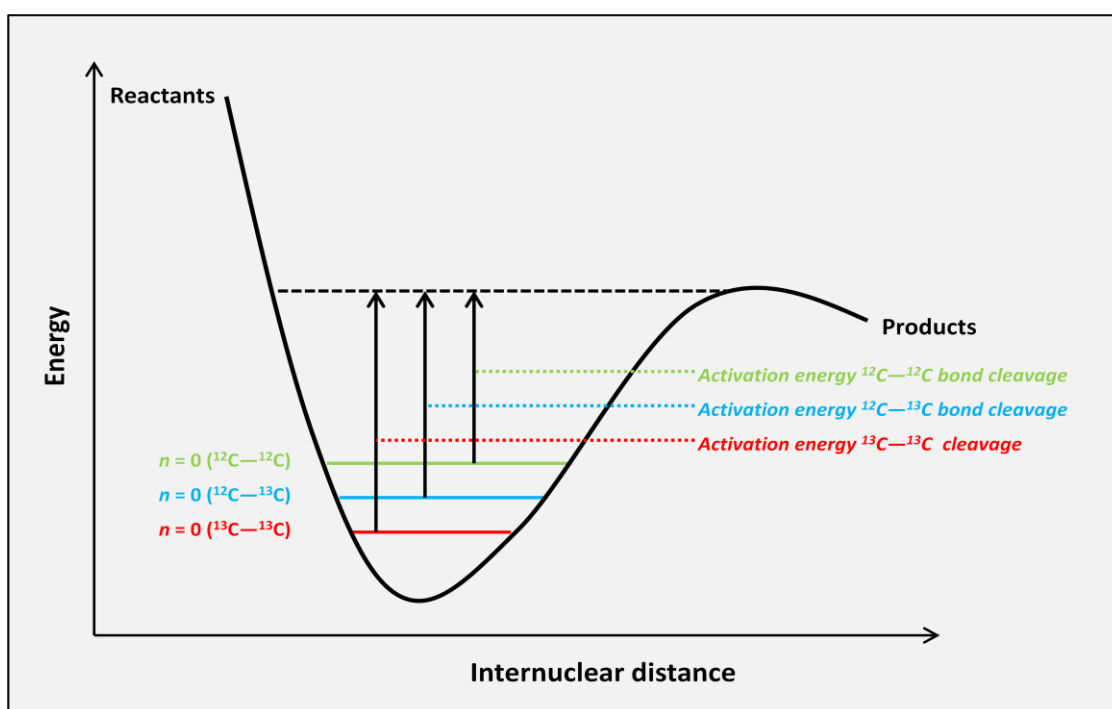
**Figure 6.1** – Stable carbon isotopes. Modified from NOAA Research (N.D.).

Table 6.1 lists the natural abundance of stable isotopes for some of the key elements usually involved in biodegradation processes. The variations of stable isotopes in chemical compounds are often unique, much like a chemical fingerprint, and can be used to obtain different types of information. Some of which include, the identification of a contaminant source, distinguishing between biotic and abiotic reactions in the environment, quantifying the extent of biodegradation and tracing the origin of illegal disposal of organic waste (Aelion and Hohener, 2010, Blessing et al., 2008).

<b>Table 6.1 Natural Abundance of Stable Isotopes H C N O S</b>				
<i>Element</i>	<i>Stable Isotopes and natural abundance (%)</i>			
Hydrogen	$^1\text{H}$ (99.9885)	$^2\text{H}$ (0.0115)		
Carbon	$^{12}\text{C}$ (98.93)	$^{13}\text{C}$ (1.07)		
Nitrogen	$^{14}\text{N}$ (99.636)	$^{15}\text{N}$ (0.364)		
Oxygen	$^{16}\text{O}$ (99.757)	$^{17}\text{O}$ (0.038)	$^{18}\text{O}$ (0.205)	
Sulphur	$^{32}\text{S}$ (94.99)	$^{33}\text{S}$ (0.75)	$^{34}\text{S}$ (4.25)	$^{36}\text{S}$ (0.01)

*Source: modified from Aelion and Hohener (2010).*

During biochemical reactions, such as biodegradation, the transition state theory states reactants must first overcome an “activation energy” barrier, in order to initiate cleavage between its chemical bonds before new products can be formed. During such reactions, kinetic isotope effects occur, whereby bonds formed of atoms with lighter isotopes ( $^{12}\text{C}$ ) are typically broken more easily, because they require less activation energy, than those with heavier isotopes ( $^{13}\text{C}$ ) (Fig. 6.2). This results in a quantitative enrichment of heavier isotopes, in the remaining reactant pool (Bigeleisen and Wolfsberg, 2007).



**Figure 6.2** - The energy a bond possesses in its ground state is referred to as the zero-point energy, (shown as  $n$  on the graph. This represents the starting point for the reactivity differences between isotopologues. Graph modified from Knowles(2005).

Consequently, when organic contaminants are biodegraded in the environment, the ratio of the stable isotopes often changes. The difference in mass between isotopes (brought about by the number of neutrons present in the atom) offers an opportunity to evaluate and quantify biodegradation, using mass spectrometry to measure changes in isotope ratio (United States Environmental Protection Agency, 2008).

### *6.1.2 Compound specific isotope analysis*

Of particular interest to this study, is the use of kinetic isotope effects - also known as isotope fractionation, to ascertain the presence of biodegradation of contaminants in groundwater environments, and in so doing establishing evidence to support the use of natural attenuation as a means of bioremediation. Compound specific isotope analysis, simplifies the identification of biodegradation, by monitoring changes in the natural abundance of isotope ratios in hydrocarbon contaminants, directly in groundwater (Kuder and Philp, 2008, Meckenstock et al., 1999). The success of compound specific isotope analysis relies on the principle that, during biodegradation processes, microbes show a preference to breaking down  $^{12}\text{C}$ - $^{12}\text{C}$  bonds over bonds containing heavier  $^{13}\text{C}$  atoms (Meckenstock et al., 2004). Therefore, should biodegradation be occurring, an enrichment of  $^{13}\text{C}$  isotopes should be observable down gradient of a contaminant plume.

Previously, evidence of biodegradation has had to rely on measuring reductions in contaminant concentrations. This is often extremely difficult because of the need for definitive mass balances, which are often hindered by the limited knowledge of groundwater flow regimes, limitations in the number of available monitoring wells and not enough sample collections (Schmidt et al., 2004). Moreover, once these measurements are obtained they are often ambiguous because they may not consider other processes that may be affecting a reduction in concentration. Crucially, for compound specific isotope analysis, as a tool to monitor natural attenuation, kinetic isotope effects are usually only observed during biodegradation with no observable change in isotope composition evident during dilution, dispersion or volatilisation processes (Schmidt et al., 2004). For example, research relating to toluene biodegradation, that studied the isotopic effects of biotic and abiotic reactions, indicated that chemical oxidation did not alter the isotope composition, whereas biodegradation did (Ahad and Slater, 2008). Additionally, a study of toluene biodegradation by Meckenstock et al. (1999) identified no difference in isotopic signature was caused by adsorption processes. Moreover, studies of BTEX compounds in the field also found that physical interactions between the groundwater and aquifer did not affect the isotopic composition (Richnow et al., 2003).

Therefore, isotope fractionation may offer a more robust approach in the determination of biodegradation because the ratio of light to heavy isotopes remains stable during other natural attenuation processes (Aelion and Hohener, 2010). However, a caveat to using compound specific isotope analysis to establish and quantify biodegradation in contaminated aquifers is the presumption that mainly microbiological processes result in isotope fractionation (Bloom et al., 2000, Sherwood Lollar et al., 1999, Kopinke et al., 2005).

### *6.1.3 Biodegradation and compound specific isotope analysis*

There is mounting evidence in the literature to support the use of compound specific isotope analysis to quantify biodegradation of both volatile and chlorinated hydrocarbons in groundwater environments. The success of which has, for the most part, been driven by the improvement of analytical techniques, which have enabled the coupling of mass spectrometers to gas and liquid chromatographs and, elemental analyzers, making isotope analyses more readily available (Aelion and Hohener, 2010).

Compound specific isotope analysis has identified that isotope fractionation occurs during the reductive dechlorination of chlorinated ethenes to non-toxic products. Bloom et al. (2000) found significant isotope fractionation occurred during microbial dechlorination of chlorinated ethenes, in sediment material under methanogenic conditions. Similarly, Sherwood Lollar et al. (2000) were able to use evidence of isotope fractionation to support the natural attenuation of chlorinated ethenes in contaminated groundwater beneath an air force base. Moreover, compound specific isotope analysis has been used to establish *in-situ* biodegradation of chlorinated hydrocarbons in a complex contaminated groundwater system containing several geological units (Imfeld et al., 2008).

In addition to chlorinated compounds, isotope fractionation has also been used to determine biodegradation of volatile hydrocarbons, mainly petroleum based products (e.g. BTEX compounds), in contaminated groundwater environments. The extent of aerobic biodegradation occurring at the fringes of a hydrocarbon plume (aviation gas), which consequently prevented/checked the plumes migration towards environmental receptors was made apparent using compound specific isotope analysis (Conrad et al., 1999). Evidence of isotope fractionation (combined with

metabolite detection) was used to identify biodegradation of BTEX and PAH compounds in groundwater beneath a contaminated gasworks (Griebler et al., 2003, Richnow et al., 2003). Furthermore, laboratory based studies have shown that, during toluene biodegradation, kinetic isotope effects occurred despite the presence of different environmental conditions (i.e. the use of oxygen, ferric iron, nitrate or sulphate reduction as an electron acceptor) (Meckenstock et al., 1999). Spence et al. (2005) used isotope fractionation evidence to support the biodegradation of benzene, in a chalk aquifer, occurred under denitrifying conditions. Additionally, compound specific isotope analysis has been used as evidence to support natural attenuation of monochlorobenzene at a plume fringe (Kaschl et al., 2005), methyl tertiary butyl ether in groundwater beneath a gasoline spill site (Kolhatkar et al., 2002) and *o*-xylene by direct field application (Peter et al., 2004).

The acceptance of natural attenuation often hinges on the quantification of biodegradation, in order to be sure of contaminant mass removal from an aquifer. This chapter explores the suitability of using compound specific isotope analysis to determine the occurrence of biodegradation of SULPH. As discussed earlier, compound specific isotope analysis is promising to be a successful tool in determining biodegradation of volatile and chlorinated hydrocarbons in groundwater environments.

With the advances in liquid chromatography methods, which can be coupled to isotope ratio mass spectrometers, it was the aspiration of the research to make use of these liquid chromatography methods to assess stable isotope composition of non-volatile hydrophilic compounds, i.e. (SULPH) in environmental samples. Assessment of isotopic fractionation of SULPH has not, to date, been reported in the literature. Furthermore, to substantiate isotopic fractionation for the field site would provide persuasive evidence for in situ biodegradation (should it indeed be observed). For these reasons, the endeavours of the following chapter represent considerable analytical challenges and an important aspect of the thesis.

It is brought to the reader's attention at this point that this chapter succinctly reports the successful outcomes of several months' laboratory work. In the end, the analytical approach adopted was established to be the only tenable option available. This method progressed samples as follows: extraction; clean up; fractionation using

HPLC; re-crystallised and final stable isotope analysis performed by isotope ratio mass spectrometry (following sample combustion). Unfortunately, the efforts to establish a superior analytical method, using the direct interfacing of the liquid chromatography with the isotope ratio mass spectrometer for stable isotope quantification, did not reach fruition. Appendix 5 provides an account of the considerable efforts made in this regard.

## 6.2 Method

The methods employed in this chapter aim to test whether high performance liquid chromatography, coupled with compound specific isotope analysis, may be useful in providing evidence to support the natural attenuation of SULPH in groundwater environments. The method has been adapted from that of Mohammadzadeh et al. (2005), who utilised compound specific isotope analysis to establish the origin of dissolved organic carbon in groundwater. Figure 6.3 below gives an overview of the steps used to isolate SULPH from the mixture of contaminants contained in the groundwater at the field study site, and measure its isotopic signature.

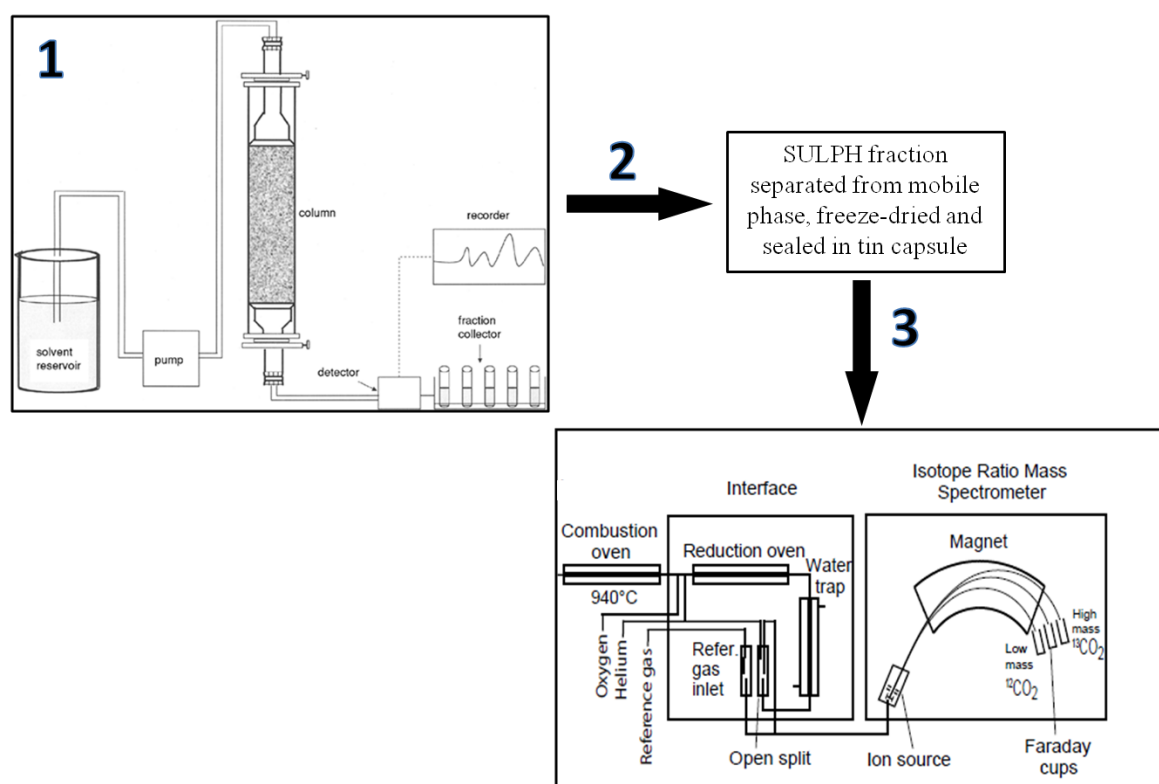


**Figure 6.3** – Schematic of method development: 1) HPLC fractionation, to isolate SULPH; 2) Separation and preparation of SULPH for stable isotope analysis and, 3) Measurement of carbon isotope ratio (Chakravarti et al., 2008, United States Environmental Protection Agency, 2008).

In summary, dry organic material is placed in a tin capsule to provide approximately 100  $\mu\text{g}$  of carbon. The tin capsule is sealed and dropped into an elemental analyser reaction tube containing chromium oxide at 1000°C to 1050°C. The sample is

quantitatively converted into carbon dioxide and water. Water is then removed from the carrier stream by a chemical trap containing drying agent and the carbon dioxide is separated on a packed GC column. The GC effluent then flows into the stable isotope ratio mass spectrometer via an interface and the ratio of the isotopomers of carbon dioxide are determined against carbon dioxide reference materials of known  $^{13}\text{C}/^{12}\text{C}$  ratios versus accepted international standards.

### *6.2.1 Chemicals*

Sulphanilamide was obtained from Bayer Cropscience, UK. Analytical grade (99%), acetone and methanol were obtained from Fisher Scientific, UK. The constituents of the mobile phase: disodium hydrogen phosphate and ortho-phosphoric acid (89 % w/w) were obtained from Sigma Aldrich, UK.

### *6.2.2 Sample selection*

To ensure the samples to be combusted were within the detection limits of the Delta XP, the minimum quantity of carbon required for isotope analysis should be 100  $\mu\text{g}$ . SULPH contains 41.8 % of carbon. Therefore, groundwater samples with concentrations  $> 0.4 \text{ mg ml}^{-1}$  were selected for analysis, which ensured a minimum carbon quantity of 162  $\mu\text{g}$ . The quantity of carbon was deliberately over-estimated to allow for loss of analyte during the preparation stages (Section 6.23 and 6.24). Of the 41 groundwater samples collected from the site, 22 were within the acceptable concentration range.

### *6.2.3 Pre-concentration of SULPH groundwater samples using freeze drying techniques.*

In order to obtain adequate concentrations of SULPH for isotope analysis, the groundwater, collected during the field site sampling stage (described in Chapter 5, Section 5.2.1), was pre-concentrated. The method used a *Hetotrap CT60e* freeze-drying apparatus. This method solidified the contaminants, dissolved in the groundwater samples, by freezing the water fraction, which was then evaporated by sublimation when heated (Castro and Garcia, 2002). The concentration of SULPH, in the groundwater samples varied from 0.5 to 630  $\text{mg L}^{-1}$ . The rationale behind the pre-concentration step was to ensure the samples fell within the detection limits ( $\leq 0.2 \text{ mg ml}^{-1}$ ) of the HPLC fraction collector and the isotope ratio mass spectrometer.

As discussed previously (Chapters 3 and 5), the groundwater beneath the field study site contains a mixture of different contaminants. To remove the unwanted contaminants, the dry portion (yellow/white powder), obtained during the freeze-drying step, was first dissolved in 10 mL of acetone, sonicated for 10 minutes and, finally filtered using 0.22  $\mu\text{m}$  PTFE syringe filters (Millex®). The solubility of SULPH in acetone is  $100 \text{ mg L}^{-1}$  and calculations were made to ensure the quantity of SULPH contained in the dry sample was soluble in the volume of acetone used. The filtration step ensured no solid particulates remained in the sample, which could later damage or block the HPLC column, during the fraction collection stage. Following filtration, the acetone was then evaporated off to leave a dry sample suitable for fraction collection by HPLC.

#### *6.2.4 Collection of SULPH fractions using HPLC fractionation techniques (quantification).*

A High Performance Liquid Chromatography (HPLC) fraction collector was used to collect the SULPH fractions contained within the dry portion of the groundwater samples. The HPLC samples were prepared by dissolving the dried solid phase fractions, from the pre-concentration step, in mobile phase. The mobile phase was made up using  $6.8 \text{ g L}^{-1}$  disodium hydrogen phosphate ( $\text{KH}_2\text{PO}_4$ ) in Milli-Q water ( $18.2 \text{ M}\Omega\cdot\text{cm}$ ) and reduced to pH3 with ortho-phosphoric acid (89 % w/w) ( $\text{H}_3\text{PO}_4$ ). Table 6.2 below shows the settings for the HPLC fraction collector. Optimum peak amplitude and retention times for SULPH were established using pure standards, obtained from Bayer Cropscience UK.

**Table 6.2 - HPLC Fraction Collector Settings.**

<b>HPLC parameters:</b>	
Mobile phase	6.8 g L <sup>-1</sup> disodium hydrogen phosphate reduced to pH3 using ortho-phosphoric acid (89 % w/w)
Injection volume	25 µL
Column	Gemini 5 µ C18 110A 150 x 2.00 mm 5 micron particle size (Phenomenex)
Flow rate	200 µL min <sup>-1</sup>
Oven temperature	20 °C (leave running at room temperature)
Peak detection	25 µL injection of 0.1 mg mL <sup>-1</sup> [SULPH] gave a signal of ~ 7 V and a retention time of 267 seconds

Based on the detection limits of the isotope ratio mass spectrometer (a minimum of 1 nmol of SULPH is required to provide an accurate and precise measurement of isotope ratio) the quantity of SULPH fractions to be collected from the HPLC were calculated accordingly (United States Environmental Protection Agency, 2008).

#### 6.2.5 Isotope analysis of SULPH.

The isotope analysis of carbon involves the measurement of the relative abundance of the two stable isotopes of carbon (<sup>13</sup>C and <sup>12</sup>C). To maintain inter-laboratory comparability and accuracy the ratios are expressed relative to an international standard, typically Vienna-PeeDee Belemnite (V-PDB), for carbon. These measured values are reported using *delta* notation ( $\delta^{13}\text{C}$ ) and are defined in Box 6.1. Delta values are very precise and small ( $\delta^{13}\text{C}$  are usually <0.05) and so for convenience are multiplied by 1000 and expressed by ‰ (*per mil*) (Verkouteren and Klinedinst, 2004, United States Environmental Protection Agency, 2008).

Box 6.1 Stable Isotope Nomenclature	
$\delta^{13}\text{C} (\text{‰}) =$	$\left[ \frac{(^{13}\text{C}/^{12}\text{C})_{\text{sample}} - (^{13}\text{C}/^{12}\text{C})_{\text{standard}}}{(^{13}\text{C}/^{12}\text{C})_{\text{standard}}} \right] \times 1000$

Once the SULPH fractions were collected from the HPLC, the freeze-dried methods described in section 6.2.3 were used to isolate the SULPH from the mobile phase. This involved a two-step process in that firstly the excess water, of the mobile phase, was removed to leave a dry portion, which contained both SULPH and remnants of the mobile phase (i.e. disodium hydrogen phosphate and ortho-phosphoric acid). Secondly, 1.5 mL of acetone was added to the dry portion to separate SULPH from the dried mobile phase because only SULPH is soluble in acetone. The supernatant containing the dissolved SULPH fraction was then removed and the acetone evaporated off. Step two was repeated to ensure all the SULPH fraction was recovered.

The volume of acetone, which contained the SULPH fractions, was evaporated to approximately 500  $\mu\text{L}$  before being transferred to a tin capsule (*Elemental Microanalysis, 13.5 x 8 mm, weight 82 mg, volume 679  $\mu\text{L}$* ). Once loaded into the capsule the remaining acetone was evaporated. The dried capsules were then crimped into 6-8 mm cylinders, ensuring the openings were folded over at least twice.

Using modifications of stable isotope mass spectrometry methods already established in the literature, the capsules were loaded onto an auto-sampler and introduced to the combustion furnace. Here the samples were combusted and oxidised to  $\text{CO}_2$ . The resulting  $\text{CO}_2$  was carried into the isotope mass spectrometer (*Delta XP, Conflow interface II, Thermo Finnigan, Bremen, Germany*), using helium as a carrier gas. The mass spectrometer measures the  $^{12}\text{C}/^{13}\text{C}$  ratio of the  $\text{CO}_2$  resulting from the combustion of the sample (Kelly et al., 1997, United States Environmental Protection Agency, 2008, Sherwood Lollar et al., 2000).

The linearity and precision of the mass spectrometer was checked by measuring the peak amplitudes and  $\delta^{13}\text{C}$  values of SULPH standards over a range of concentrations, from 0.2 to 0.8 mg.

### 6.3 Results/discussion

#### 6.3.1 Linearity, uncertainty and detection limit of isotope mass spectrometer.

A linearity test ascertains whether a measured output signal (in this case peak amplitude) increases in direct proportion with an input signal (i.e. amount of analyte). The data, represented in Figure 6.4, was obtained by measuring the different peak sizes for increasing amounts of a standard working material of SULPH.

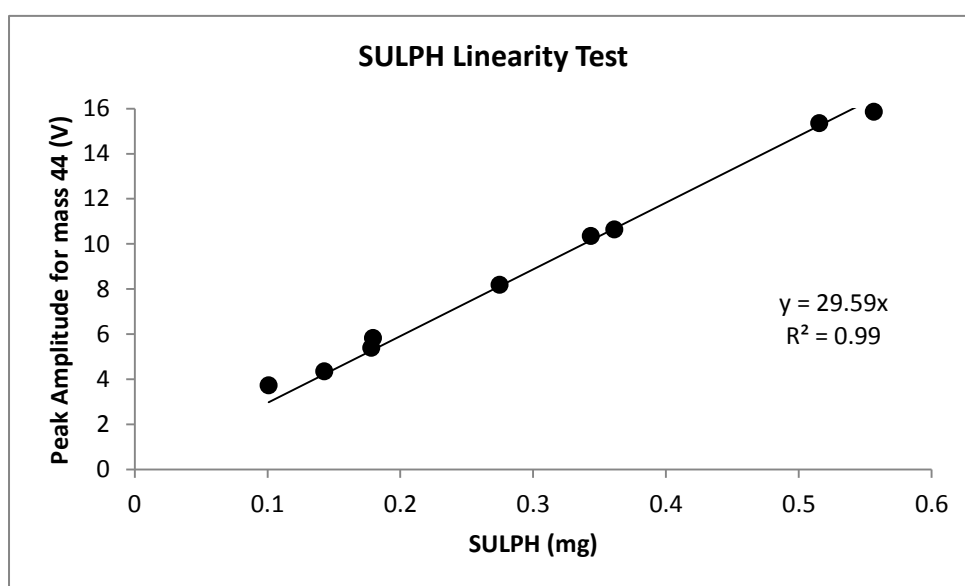
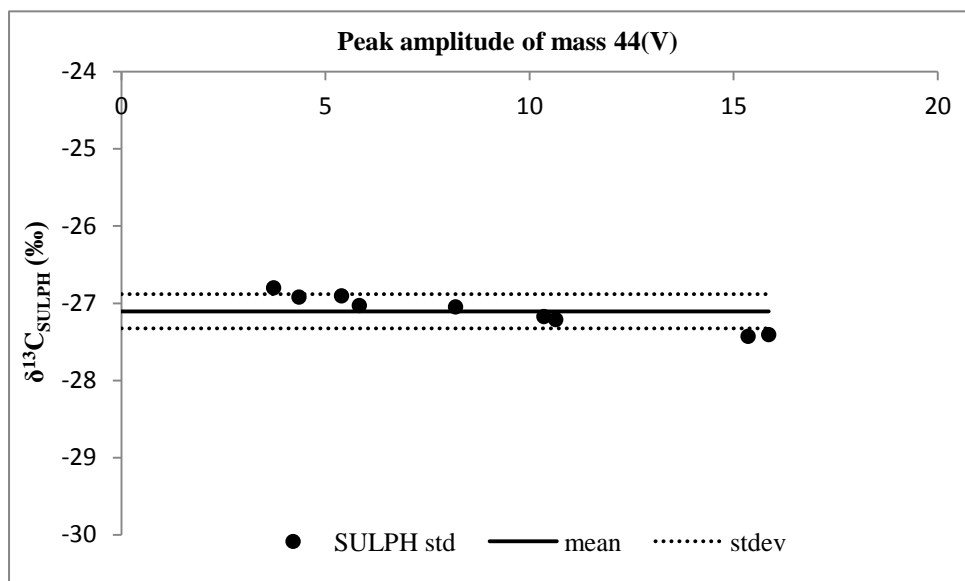


Figure 6.4 – Linearity test: mass of SULPH (mg) vs. peak amplitude of mass 44 (V).

The linear regression of the curve on Figure 4.6 provided an  $R^2$  value of 0.99, suggesting good linearity between signal strength and increasing amount of analyte. The supplier of the isotope ratio mass spectrometer (*Thermo Finnigan, Bremen, Germany*) recommend the peak amplitude should be  $\geq 3$  V. Thus, the linear equation (Fig. 6.4) was used to ascertain a minimum detection limit (MDL) for SULPH of 0.1 mg.

Moreover, the uncertainty of the isotope ratio mass spectrometer was investigated by plotting the peak amplitude against the  $\delta^{13}\text{C}$  values obtained for the SULPH standards. The results of which are represented in Figure 6.5.



**Figure 6.5** – Plot of peak amplitude of mass 44(V) vs.  $\delta^{13}C_{SULPH}$  (‰).

Ideally, all the delta values should be the same because the standards were made from the same stock material. However, plotting the mean (solid black line) and standard deviation (hatched lines) suggests that at low signal values (< 5 V) the isotope ratio mass spectrometer may report more enriched  $\delta^{13}C$  values and at high signal values (>10 V) more depleted  $\delta^{13}C$  values (Fig. 6.5). This phenomenon has also been observed by Sherwood Lollar et al. (2007), who suggest, in their research, that this is typical of hydrocarbon contaminants and so care should be taken to include both reproducibility of duplicate samples and analytical uncertainty before drawing conclusions from the  $\delta^{13}C$  values measured.

This phenomenon was addressed, in that during the HPLC fraction collection of SULPH, sufficient quantities were collected to ensure a final signal strength of approximately 6 V. Therefore, the linear equation (Fig. 6.4) was used to ascertain a minimum quantity of SULPH (0.2 mg), which was then used as a guide during the sample preparation stage. If the linear equation was used alone to establish a MDL for SULPH then, as discussed earlier, it would have been assumed that 0.1 mg of SULPH was sufficient to determine an isotopic signature for SULPH. However, as shown by Figure 6.5, SULPH measured at these quantities would have produced a more enriched  $\delta^{13}C$  value, which in turn could have resulted in an over-estimation of biodegradation occurring at the field study site (Sherwood Lollar et al., 2007, United States Environmental Protection Agency, 2008).

### 6.3.2 Compound specific isotope analysis

The results presented in Table 6.3 show the individual results obtained for the isotope analysis of the SULPH contained within the groundwater samples at the site.

**Table 6.3 – Results of isotope analysis for each well sampled at the site**

<b>Monitoring Well</b>	<b>Date</b>	<b>Depth (m)</b>	<b>Sample</b>	<b><math>\delta^{13}\text{C}/^{12}\text{C}</math></b> (mean value with 95% confidence interval)
BH1	2009	18	n=1	-26.10
BH1	2011	18	n=3	-26.01 $\pm$ 0.25
BH2	2009	-	n=1	-25.41
BH2	2009	-	n=1	-29.64
N61-SW1/C	2009	12.5	n=1	-25.93
N61-SW1/C	2011	12.5	n=3	-25.91 $\pm$ 0.14
N61-S1/C	2009	12	n=1	-25.93
N61-N1/C	2009	12.5	n=1	-22.83
N62-S1/C	2010	10	n=3	-27.40 $\pm$ 0.05
N62-S1/C	2011	10	n=3	-26.37 $\pm$ 0.22
N62-W1/C	2009	14	n=3	-27.20 $\pm$ 0.02
N62-W1/C	2011	14	n=3	-27.30 $\pm$ 0.03
N62-E1/C	2009	11	n=3	-26.56 $\pm$ 0.11
N62-E1/C	2010	11	n=3	-26.73 $\pm$ 0.08
N62-E1/C	2011	11	n=3	-26.98 $\pm$ 0.03
N71-CRW	2010	18	n=6	-26.32 $\pm$ 0.01
N71-W2/C	2010	18	n=3	-26.73 $\pm$ 0.19
N71-NW1/C	2009	18	n=1	-26.24
Sentinel E1/C	2011	10.5	n=1	-18.2

The results (Table 6.3) suggest there is no change in the isotopic composition of SULPH in and around the source area (N61, 62 and 70). However, the isotopic composition increases considerably at the offsite well sentinel E1/C (-18.2 ‰), suggesting biodegradation has occurred after the SULPH moved downgradient from the source area (N62-E1/C), where isotopic compositions were  $-26.98 \pm 0.03$  ‰.

The isotopic signature, which represents the original source for SULPH, i.e. prior to any fractionation, was measured using standard material obtained from the field study site. Replicates ( $n = 23$ ) of SULPH (0.4 mg) were analysed using the isotope mass spectrometer and an average  $\delta^{13}\text{C}$  value calculated, with 95 % confidence intervals, of  $-27.04 \pm 0.4$  ‰.

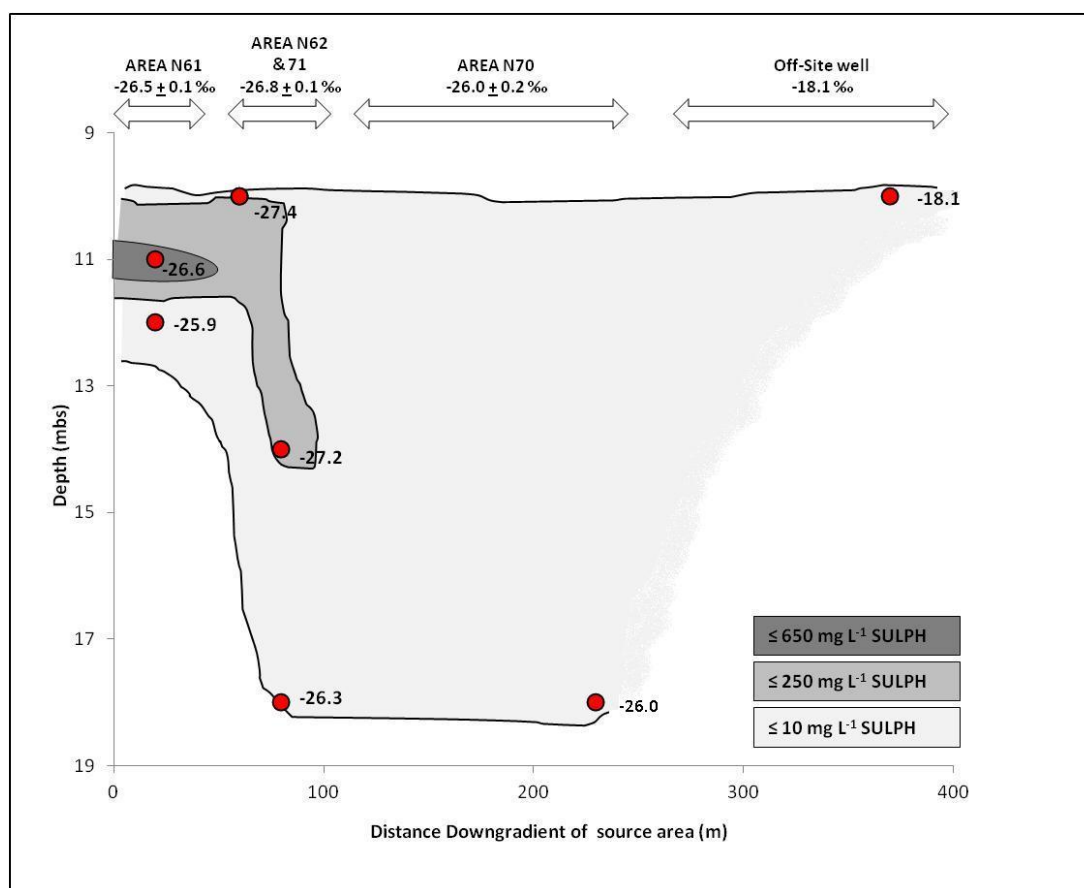


**Figure 6.6** – Concentrations and carbon isotope ratios of SULPH downgradient of source zone. All values are in ‰ relative to the V-PDB standard. The filled circles represent depths sampled for both concentration and  $\delta^{13}\text{C}$ .

In order to visualise the stable isotope data it was represented on a 2D-cross-section of the field site (Figure 6.6). This figure represents the results of the compound specific isotope analysis for SULPH to be presented alongside the data relating to SULPH concentrations (see Chapter 3). SULPH concentrations between the source zone ( $650 \text{ mg L}^{-1}$ ) and the monitoring well situated approximately 250 m downgradient ( $250 \text{ mg L}^{-1}$ ) decrease; *however*, there was no observable change in the isotopic composition in this region of the site. An explanation as to why the concentration has decreased but there is no evidence of biodegradation supported by isotopic enrichment is discussed in Section 6.3.4. In contrast, SULPH concentrations, along the same pathway, had reduced from  $650$  to  $10 \text{ mg L}^{-1}$  by the time they had reached the off-site well, situated approximately 400 m downgradient from the source zone. Furthermore, comensurate with this decrease in SULPH concentration was an enrichment in  $\delta^{13}\text{C}$ ; with values increasing from  $-26.6$  to  $-18.1\%$ . The change in isotope composition of SULPH, downgradient supports the occurrence of biodegradation at the site.

### 6.3.3 *Quantifying biodegradation at the field site*

Box 6.1 shows the equations used to determine the extent of biodegradation occurring at the field site. Using the isotopic ratios ( $-26.6$ ) measured for the source area (N61), where concentrations were approximately  $650 \text{ mg L}^{-1}$ , and the isotopic ratio for the off-site well ( $-18.1$ ), where concentrations reduced to  $10 \text{ mg L}^{-1}$  (represented in Figure 6.6), the percentage of biodegradation proposed from the isotopic analysis is  $56 \%$ . However, the decrease in concentration from  $650$  to  $10 \text{ mg L}^{-1}$  is a reduction of approximately  $98 \%$ . Therefore, should the isotopic ratios be correct they suggest of this  $98 \%$  reduction in concentration,  $56 \%$  was due to biodegradation processes, leaving the remaining  $42 \%$  due to other natural attenuation processes, such as dilution or dispersion (United States Environmental Protection Agency, 2008).

**Box 6.1** – Quantifying the extent of biodegradation at the field site.

**Quantification of the degree of biodegradation for the zone between the source and a monitoring point:**

**Step 1:**

$$\alpha = R_a/R_b$$

Fractionation factor ( $\alpha$ ):  
R is the stable isotope ratio ( $^{13}\text{C}/^{12}\text{C}$ ) of the compound and the subscripts *a* and *b* represent the compound in the source zone, versus a down gradient monitoring point.

**Step 2:**

$$f = \left[ R_b / R_a \right]^{1 / (\alpha_{ab} - 1)}$$

Fraction remaining (*f*):  
 $R_b$  is the isotope ratio for downgradient monitoring well and  $R_a$  the isotope ratio for source or up gradient monitoring point.

**Step 3:**

$$B = (1-f) * 100$$

The amount of biodegradation as a percentage of material originally present (B)

Step 1: ( $\alpha = 1.47$ )Step 2: ( $f = 0.44$ )Step 3: (B = 56 %)

*Source: (United States Environmental Protection Agency, 2008)*

**6.3.4 - Disadvantages of compound specific isotope analysis**

As shown in Figure 6.7, one factor that could hinder the identification of an isotopic fractionation is the recharging and/or mixing effects of fresh contaminant. In calculating isotopic fractionation, an assumption is made that the source of contamination, undergoing biodegradation, represents a closed system in that there is no additional mixing of fresh contaminant during the biodegradation event. This would mean that small observable isotopic fractionations may be diluted and/or undetectable as a result of the addition of un-degraded contaminant. Therefore, the

lack of an observable isotopic shift does not necessarily mean biodegradation is absent if there has been a fresh delivery of contaminant during the previous biodegradation event (Wilkes et al., 2008).

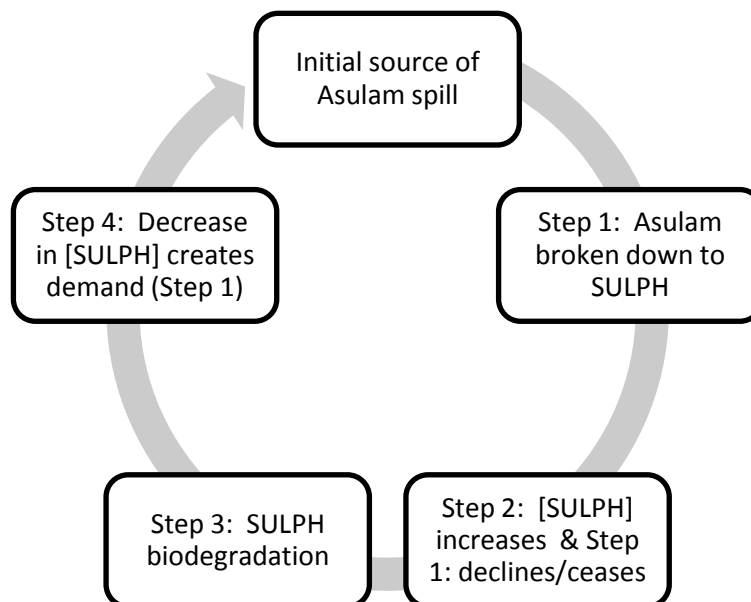


*Figure 6.7 – Suggested drivers in biodegradation of SULPH at the field site.*

Another problem can be that groundwater flow is rarely homogeneous, and in this study in particular, is unlikely because chalk aquifers generally contain fractures and fissures. This introduces contaminants at the monitoring point that may have undergone different residence times within different areas of the aquifer. Thus, groundwater usually contains a mixture of contaminant molecules that have travelled at various velocities between the source and sampling point. This can make identifying the pathway of a plume very difficult. It is highly likely that different sections of the plume may take separate pathways, becoming exposed to different geochemical conditions and microbial populations and so be more or less susceptible to biodegradation. Should these groundwater flow paths then converge at a monitoring well then any isotopic fractionation could become diluted or undetectable. Consequently, this may cause an underestimation in the calculation of biodegradation rates (Kopinke et al., 2005, Abe and Hunkeler, 2006). Compounding this problem further is the abstraction wells at the site, situated to the south, and downgradient of the plume. It is likely during abstraction that groundwater from up gradient is drawn down gradient causing a subsequent mixing of contaminants.

Different biodegradation processes will usually have a different isotopic fractionation and in some cases no fractionation is detected even though biodegradation is occurring e.g. aerobic biodegradation is usually better discernable from hydrogen isotope measurements than carbon (Schmidt et al., 2004). For example, a previous chapter (Chapter 3) suggests SULPH may be utilised as both a carbon source and as a source of sulphur. This may have an impact on the isotopic fractionation.

#### 6.4 Conclusion

Returning to the objectives raised in the introduction, the first objective was “can SULPH, a non-volatile, hydrophilic compound, be analysed using compound specific isotope analysis”. The results confirm that compound specific isotope analysis can be used to determine the isotopic composition of SULPH contained in contaminated groundwater samples from a chalk aquifer. Having isolated the SULPH fraction, with high performance liquid chromatography fractionation techniques, it was possible to combust the dried fraction and analyse the carbon isotope ratio.

The second objective was “is there evidence of isotope fractionation to substantiate biodegradation processes at the study site”. A carbon isotope enrichment of -8 ‰ was observed when comparing isotope ratios of SULPH found in the monitoring wells at the source area to the ratios measured in an off-site well. The non-destructive natural attenuation processes (dilution, dispersion, adsorption and volatilisation) do not cause significant enrichments in carbon isotopes. Therefore, the results observed here provide unequivocal evidence that *in-situ* biodegradation of SULPH is occurring at the contaminated site.

The third objective was “should fractionation be evident, can biodegradation be quantified, to support the evidence already obtained via *ex-situ* microcosm studies and the site model results from previous chapters”. The difference in carbon isotope enrichment values observed between the source area and an offsite well can be used to quantify the SULPH biodegradation that has already occurred at the site. The values observed suggest 56 % of the SULPH has been biodegraded between the source area and the offsite well. However, there is a 98 % reduction in SULPH concentration between the two wells, which suggests natural attenuation processes, other than biodegradation, are occurring between these two wells. These results highlight the danger in making assumptions regarding the presence of biodegradation at a contaminated site from concentration data alone. Therefore, isotope fractionation offers a more robust approach in the determination of biodegradation because the ratio of light to heavy isotopes remains stable during other natural attenuation processes.

Compound specific isotope analysis, simplifies the identification of biodegradation, by monitoring changes in the natural abundance of isotope ratios in hydrocarbon contaminants, directly in groundwater. Furthermore, it can identify biodegradation

directly from groundwater samples, which removes the need for time-consuming microcosm studies when determining the occurrence of biodegradation. Moreover, the results from this chapter suggest 56 % of SULPH is biodegraded and these findings along with those of Chapter 3, which predicted a 50 % biodegradation potential for all the contaminants present in the groundwater (via BOD/COD calculations), and Chapter 5, which estimated 55 % SULPH mineralisation, provide strong evidence to support the argument for the occurrence of natural attenuation.

# Chapter 7: Summary and Conclusion

---

This thesis has explored novel aspects of natural attenuation. Originality in this research is evident with regards to: i) chemical class investigated (namely, immobile agrochemicals), ii) herbicide occurrence in high concentrations owing to their point-source origin, and iii) aquifer type (a fractured chalk aquifer).

## *7.1 Summary of research and how it was achieved*

This research investigated the natural attenuation of isoproturon and sulphanilamide in the chalk aquifer below a chemical works. Evaluation of natural attenuation, as a means to assist in the remediation of the contaminated groundwater, was explored from a number of perspectives. In this regard the research made use of the lines of evidence (as required by regulators) to evaluate the existence (and vigour) of natural attenuation processes within the aquifer; to establish if these processes might be enhanced, and; to advance the practical techniques with which to make these evaluations.

Having access to this contaminated site facilitated a unique opportunity to study natural attenuation of novel synthetic organic compounds situated below a chemical production plant within a fractured chalk aquifer. Towards these ends representative field samples, of aquifer material and groundwater, were collected during the installation of eleven new monitoring wells at the site. The samples were used to construct *ex-situ* microcosms to investigate the presence/absence of biodegradation spatially across the site and to establish if biodegradation could be enhanced by altering the redox conditions. Separate groundwater samples were collected, during the scheduled monitoring programmes of the site owners, and were examined using carbon-isotope analysis to establish evidence of biodegradation using new analytical techniques that were developed as a significant component of this research.

## 7.2 *The main findings*

In chapter 3, the historical monitoring data, pertaining to the contaminated site, was investigated and trends in the data were evaluated to establish whether there was evidence to support the occurrence of natural attenuation at the site. Analysis of the site concentration data identified the presence of a SULPH plume, which had spread 300 m, downgradient from the source with concentrations being observed to reduce by two orders of magnitude along the plume pathway. It was possible to calculate a biodegradation potential from the biological and chemical oxygen demands recorded at the site. According to these data, the groundwater had the potential to assimilate 50 % of the contaminants present. However, these values could not identify specific contaminants and only estimated the potential for *all* the contaminants present. Furthermore, mass balance calculations involving the increased levels of sulphate measured in the groundwater predicted 90 % of the original chemical spill may have been degraded already. Redox conditions at the site were analysed spatially; anaerobic conditions were established with most of the site being Fe(III) reducing, *however*, in areas where SULPH mixed with toluene there was a change in redox conditions to sulphate reduction.

To summarise, the results suggested natural attenuation was occurring at the site. However, the results were only an indication and to satisfy regulatory requirements, further, more robust, data were required. With this in mind, the next chapter advanced the research and investigated the microbiological activity, present at the site, in order to substantiate the findings indicated by the historical data.

Chapter 5 investigated the potential for SULPH and IPU biodegradation using *ex-situ* microcosms, which replicated the groundwater conditions at the site. While the evidence from Chapter 3, regarding biodegradation potential for the site, was vague in so much as it was not specific to individual contaminants the *ex-situ* microcosm approach provided direct evidence of biodegradation for specific compounds of interest. It was the intention of this chapter to establish if SULPH and/or IPU biodegradation could explain the reduction in concentration observed in Chapter 3. Additional *ex-situ* microcosms were also examined to explore whether SULPH and IPU biodegradation could be enhanced by increasing the available electron acceptors (nitrate and sulphate). Results indicated IPU biodegradation to be minimal at the site (max. 2 % when concentrations were  $9 \mu\text{g L}^{-1}$ ) and in most cases was completely

absent. In stark contrast SULPH biodegradation was widespread across the site, reaching 55 % when concentrations were  $>10 \text{ mg L}^{-1}$ . However, at low concentrations ( $\geq 0.02 \text{ mg L}^{-1}$ ) biodegradation fell to 20 %. The results of Chapter 4 corroborate with those of Chapter 3 in so much as they substantiate that biodegradation (of SULPH) is occurring at the site. Furthermore, the microcosm results and those of Chapter 3 are comparable in magnitude (both suggesting the potential for biodegradation to be around 50 %). By extension, this suggests that SULPH may be the major contaminant undergoing degradation at the site.

Where redox conditions were altered (to be aerobic, sulphate reducing or nitrate reducing) neither IPU nor SULPH biodegradation could be enhanced. These results suggest that opportunities to facilitate enhanced remediation would be limited. Interestingly, the addition of sulphate and nitrate inhibited the extent of SULPH biodegradation (to a maximum of 20%). A likely explanation for this being that the indigenous microorganisms were able to utilise SULPH as both an electron donor and acceptor and that changes in redox conditions and/or the presence of a more favourable carbon source (e.g. toluene) could drive this change.

Of novel interest, in terms of the remediation of SULPH, is that microbes acclimatised to one sulphonamide may later easily degrade other sulphonamides within the same group. Therefore, the results of this study may be of interest to the wastewater, farming and veterinary industries. The finding of IPU biodegradation at low concentrations ( $9 \mu\text{g L}^{-1}$ ), 10 mbs, in a chalk aquifer is novel and even though the rate of biodegradation was established to be low it may be important in aquifers exhibiting long residence times.

The results from the investigations in Chapters 3 and 5 make a reasonable case for the occurrence of natural attenuation processes at the site. Most pertinent, from a regulatory perspective, is the evidence that destructive biodegradation processes were clearly identified. However, as discussed previously (Chapter 5), *ex-situ* microcosms can be open to scrutiny because they do not give a true representation of *in-situ* aquifer conditions. To address this criticism, the development of *in-situ* microcosms were explored to test whether the findings of the *ex-situ* results could be replicated in the field. Thus, validating the evidence of biodegradation obtained from the laboratory-based studies.

Chapter 4 explored the development of *in-situ* microcosms and in particular the use of alternative support materials. The purpose of the chapter was to develop the concept of biofilm passive samplers and to explore whether an isotopic tracer could be loaded onto a support material to form an *in-situ* microcosm, which could then be used as a passive sampler at the site.

The development of an *in-situ* microcosm was abandoned at the initial stages of experimentation because the support materials (GF, PP and EP) were only able to retain 30 % of an IPU and/or SULPH isotopic tracer for a period of 2 weeks. This low level of compound retention was deemed insufficient for field deployment. Furthermore, loss of 70% of the loaded tracer into the aquifer would undermine the isotopic integrity across the site; this in turn would undermine future efforts to evidence natural attenuation as demonstrated in Chapter 6. This issue was recognised and addressed by environmental regulating authorities, during the course of this research. In response, the regulating authorities have issued stringent guidelines on the use of tracers in the environment for scientific purposes, with particular attention being given to isotopic tracers and their detrimental impact to natural abundance isotopic research.

Alongside the announcements from the regulators were advances in compound specific isotope analysis, which were making it possible to analyse the biodegradation of non-volatile organic compounds, directly from groundwater samples by monitoring natural enrichments of  $^{13}\text{C}$  isotopes. These developments culminated in the redirection of the research and the new science developed and reported in Chapter 6.

To support the evidence of natural attenuation presented in Chapters 3 and 5, Chapter 6 explored the merits of compound specific isotope analysis in evaluating SULPH biodegradation at the field site. Enrichment of SULPH  $^{13}\text{C}$  isotopes was evident at the site, with  $\delta^{13}\text{C}$  values increasing from -26 to -18 ‰. This result provides unequivocal evidence that SULPH biodegradation is occurring at the site.

Furthermore, the data quantified the percentage of SULPH biodegradation taking place to date as 56 %. Significantly, this value is in agreement with the findings of Chapters 3 and 5 that indicated the total site biodegradation to date to be 50 % and SULPH biodegradation to be 55 %. These three separate lines of evidence, together, provide robust evidence to support the occurrence of natural attenuation at the site.

Compound specific isotope analysis simplifies the assessment of natural attenuation in aquifers by enabling the quantification of biodegradation processes directly from groundwater samples. This is a significant line of evidence required by regulators. This technique has been used successfully to identify the biodegradation of volatile organic compounds in groundwater, by using gas chromatography isotope ratio mass spectrometry methods. However, the coupling of liquid chromatography to isotope ratio mass spectrometers has made this an exciting development for the investigation of non-volatile organic biodegradation in groundwater environments. The results of this chapter are novel in that compound specific isotope techniques have been used to identify natural attenuation processes with respect to a non-volatile organic contaminant (SULPH). The establishment of SULPH natural attenuation in a fractured chalk aquifer has not been reported previously.

### *7.3 Future research/further work*

Like any research, while advance may provide answers to some questions and provide new insights they also prompt new questions to be asked and further investigations to be undertaken. Concerning the research presented herein, the following areas of further work have emerged:

- The application of sulphur isotope fractionation analysis to explore areas of the site where SULPH appears to be used as an electron acceptor (i.e. for its sulphur component) and to investigate if this phenomenon promotes a co-metabolism of SULPH and toluene (wherein they are coupled as electron acceptors and donors).
- The isolation and identification of SULPH degraders
- To establish applications of these degraders in sewage and veterinary industries in order to mitigate problems associated with the sulphonamide group of compounds in the environment.
- To further investigate the impediment to IPU biodegradation at the site.

### *7.4 Contribution and significance of research to field of natural attenuation*

For the successful application of natural attenuation, a reliable assessment of the mechanisms responsible for the removal of contaminants in an aquifer is essential.

This thesis presents evidence to support the natural attenuation of IPU and SULPH in a chalk aquifer.

Based on the historical data and *ex-situ* microcosms IPU biodegradation was occurring at the site albeit at very low levels (2 %). The high concentrations of other contaminants at the site (up to 650 mg L<sup>-1</sup>), compared to the low IPU concentrations (9 µg L<sup>-1</sup>) may have prevented higher levels of biodegradation. However, even these low levels of IPU may be important in aquifers exhibiting long residence times.

Based on the compound specific isotope analysis, 56 % of the SULPH has been biodegraded at the contaminated field site. This result corresponds with the information gleaned from the historical data and the predictions of the *ex-situ* microcosms. Of novel interest is the identification of SULPH degradation in a chalk aquifer and the quantification of biodegradation of a non-volatile organic contaminant (SULPH) using compound specific isotope analysis.

This research makes a valuable contribution to the field of natural attenuation in that it demonstrates the potential for SULPH natural attenuation in a chalk aquifer.

Furthermore, this potential can be demonstrated via lines of evidence recognised by environment regulating authorities (Environment Agency, 1999, United States Environment Protection Agency, 1999):

- 1. An observed reduction in contaminant concentration along the flowpath downgradient from the contaminant source.** Chapter 3 identifies a reduction in SULPH concentration, by two-orders of magnitude, downgradient of the source area
- 2. A documented loss of contaminant mass at the field scale using chemical and geochemical analytical data.** The site data presented in Chapter 3 shows the presence of SULPH, a by-product of Asulam degradation, catalogues changes in electron acceptor concentrations, in particular sulphate. Additionally, compound specific isotope analysis of SULPH (Chapter 6), present in the groundwater, identified the presence of biodegradation and was able to predict the rate of decay.
- 3. Microbiological laboratory data (e.g. microcosm studies) that supports the occurrence of biodegradation and ascertains**

**biodegradation rates.** *Ex-situ* microcosm studies presented in Chapter 5 supported the occurrence of biodegradation, the results of which were able to establish half-life degradation rates for IPU and SULPH.

Collectively these lines of evidence support the potential role that natural attenuation may play in remediating synthetic organic compounds within a chalk aquifer.

More widely, this research supports the work of others in proving the potential for biodegradation, of mobile organic compounds in aquifers. In particular, the biodegradation of IPU in a fractured chalk aquifer (Johnson et al., 2000a, Johnson et al., 2003a) and a limestone aquifer (Janniche et al., 2010). There were no reports in the literature to support the biodegradation of SULPH in aquifers; however, this research may offer insights to support current developments in the wastewater industry, which are investigating the biodegradation potential of sulphonamide compounds, of which SULPH forms part of the group (Drillia et al., 2005, Ingerslev and Halling-Sørensen, 2000, van Haperen et al., 2001).

Additionally, Chapter 6 supports the use of compound specific isotope analysis to verify the occurrence of natural attenuation in aquifers (Griebler et al., 2003, Kaschl et al., 2005, Meckenstock et al., 2004, Richnow et al., 2003, Sherwood Lollar et al., 2000) and, in particular, advances in the technology that now enable the analyse of non-volatile compounds via high performance liquid chromatography (Aelion and Hohener, 2010).

# References

---

- ABE, Y. & HUNKELER, D. (2006) Does the Rayleigh Equation Apply to Evaluate Field Isotope Data in Contaminant Hydrogeology? *Environmental Science & Technology*, 40, 1588-1596.
- ACTON, D. W. & BARKER, J. F. (1992) In situ biodegradation potential of aromatic hydrocarbons in anaerobic groundwaters. *Journal of Contaminant Hydrology*, 9, 325-352.
- ADHOUM, N. & MONSER, L. (2004) Removal of phthalate on modified activated carbon: application to the treatment of industrial wastewater. *Separation and Purification Technology*, 38, 233-239.
- AELION, C. M. & HOHENER, P. (2010) Fundamentals of Environmental Isotopes and Their Use in Biodegradation. IN AELION, C. M., HOHENER, P., HUNKELER, D. & ARAVENA, R. (Eds.) *Environmental Isotopes in Bioremediation and Biodegradation* United States of America, CRC Press.
- AHAD, J. M. E. & SLATER, G. F. (2008) Carbon isotope effects associated with Fenton-like degradation of toluene: Potential for differentiation of abiotic and biotic degradation. *Science of The Total Environment*, 401, 194-198.
- AIR FORCE CENTRE FOR ENVIRONMENTAL EXCELLENCE (AFCEE) (1995) Technical protocol for implementing intrinsic remediation with long-term monitoring for natural attenuation of fuel contamination dissolved in groundwater. Texas, AFCEE.
- ALBRECHTSEN, H.-J. R., SMITH, P. M., NIELSEN, P. & CHRISTENSEN, T. H. (1996a) Significance of biomass support particles in laboratory studies on microbial degradation of organic chemicals in aquifers. *Water Research*, 30, 2977-2984.
- ALBRECHTSEN, H. J., SMITH, P. M., NIELSEN, P. & CHRISTENSEN, T. H. (1996b) Significance of biomass support particles in laboratory studies on microbial degradation of organic chemicals in aquifers. *Water Research*, 30, 2977-2984.
- ALFREIDER, A., KRÖSSBACHER, M. & PSENNER, R. (1997) Groundwater samples do not reflect bacterial densities and activity in subsurface systems. *Water Research*, 31, 832-840.
- ALLEN, D. J. (1995) Permeability and fractures in the English Chalk: a review of hydrogeological literature. British Geological Commissioned report: Hydrogeology Series Technical Report WD/95/43.
- ANDER, E. L., SHAND, P. & WOOD, S. (2006) Baseline Report Series: 21. The Chalk and Crag of north Norfolk and the Waveney Catchment. British Geological Survey Commissioned Report No. CR/06/043N.
- ANDERSON, R. T. & LOVLEY, D. R. (2000) Anaerobic Bioremediation of Benzene under Sulfate-Reducing Conditions in a Petroleum-Contaminated Aquifer. *Environmental Science & Technology*, 34, 2261-2266.
- ARCADIS GERAGHTY & MILLER INTERNATIONAL LTD (2008) Site-Wide Groundwater Monitoring Report– November 2007. Newmarket.
- ASHMAN, M. R. & PURI, G. (2002) *Essential soil science: a clear and concise introduction to soil science*, Oxford, Blackwell Science.
- BABIKER, A. G. T. & DUNCAN, H. J. (1977) Influence of soil depth on asulam adsorption and degradation. *Soil Biology and Biochemistry*, 9, 197-201.

- BALBA, M. T., KHAN, M. R. & EVANS, W. C. (1979) The microbial degradation of a sulphanilamide-based herbicide (Asulam). *Biochemical Society Transactions: 508th Meeting*. Nottingham.
- BAYER, P., HEUER, E., KARL, U. & FINKEL, M. (2005) Economical and ecological comparison of granular activated carbon (GAC) adsorber refill strategies. *Water Research*, 39, 1719-1728.
- BEDIENT, P. B. & RIFAI, H. S. (1992) Ground water contaminant modeling for bioremediation: A review. *Journal of Hazardous Materials*, 32, 225-243.
- BEKINS, B. A., RITTMANN, B. E. & MACDONALD, J. A. (2001) Natural Attenuation Strategy for Groundwater Cleanup Focuses on Demonstrating Cause and Effect. [Online], Available from: URL<<http://toxics.usgs.gov/pubs/eos-v82-n5-2001-natural/>>, [Accessed 02 May 2011].
- BELLER, H. R. (2000) Metabolic indicators for detecting in situ anaerobic alkylbenzene degradation. *Biodegradation*, 11, 125-139.
- BESIEN, T. J., WILLIAMS, R. J. & JOHNSON, A. C. (2000) The transport and behaviour of isoproturon in unsaturated chalk cores. *Journal of Contaminant Hydrology*, 43, 91-110.
- BIGELEISEN, J. & WOLFSBERG, M. (2007) Theoretical and Experimental Aspects of Isotope Effects in Chemical Kinetics. *Advances in Chemical Physics*. John Wiley & Sons, Inc.
- BIGGERSTAFF, J. P., LE PUIL, M., WEIDOW, B. L., LEBLANC-GRIDLEY, J., JENNINGS, E., BUSCH-HARRIS, J., SUBLETTE, K. L., WHITE, D. C. & ALBERTE, R. S. (2007) A novel and in situ technique for the quantitative detection of MTBE and benzene degrading bacteria in contaminated matrices. *Journal of Microbiological Methods*, 68, 437-441.
- BJÖRKLUND, E., NILSSON, T., BØWADT, S., PILORZ, K., MATHIASSEN, L. & HAWTHORNE, S. B. (2000) Introducing selective supercritical fluid extraction as a new tool for determining sorption/desorption behavior and bioavailability of persistent organic pollutants in sediment. *Journal of Biochemical and Biophysical Methods*, 43, 295-311.
- BLESSING, M., JOCHMANN, M. & SCHMIDT, T. (2008) Pitfalls in compound-specific isotope analysis of environmental samples. *Analytical and Bioanalytical Chemistry*, 390, 591-603.
- BLOOM, Y., ARAVENA, R., HUNKELER, D., EDWARDS, E. & FRAPE, S. K. (2000) Carbon Isotope Fractionation during Microbial Dechlorination of Trichloroethene, cis-1,2-Dichloroethene, and Vinyl Chloride:  $\delta^{13}C$  Implications for Assessment of Natural Attenuation. *Environmental Science & Technology*, 34, 2768-2772.
- BOETHLING, R. S. & ALEXANDER, M. (1979) Effect of Concentration of Organic Chemicals on Their biodegradation by Natural Microbial Communities. *Applied and Environmental Microbiology*, 37, 1211-1216.
- BOSCHKER, H. T. S. & MIDDELBURG, J. J. (2002) Stable isotopes and biomarkers in microbial ecology. *FEMS Microbiology Ecology*, 40, 85-95.
- BOSCHKER, H. T. S., MOERDIJK-POORTVLIET, T. C. W., VAN BREUGEL, P., HOUTEKAMER, M. & MIDDELBURG, J. J. (2008) A versatile method for stable carbon isotope analysis of carbohydrates by high-performance liquid chromatography/isotope ratio mass spectrometry. *Rapid Communications in Mass Spectrometry*, 22, 3902-3908.

- BOSCHKER, H. T. S., NOLD, S. C., WELLSBURY, P., BOS, D., DE GRAAF, W., PEL, R., PARKES, R. J. & CAPPENBERG, T. E. (1998) Direct linking of microbial populations to specific biogeochemical processes by <sup>13</sup>C-labelling of biomarkers. *Nature*, 392, 801-805.
- BOUWER, E. J. & MCCARTY, P. L. (1982) Removal of trace chlorinated organic compounds by activated carbon and fixed-film bacteria. *Environmental Science & Technology*, 16, 836-843.
- BOUWER, E. J. & MCCARTY, P. L. (1984) Modeling of Trace Organics Biotransformation in the Subsurface. *Ground Water*, 22, 433-440.
- BRADLEY, P. M., CHAPPELLE, F. H. & WILSON, J. T. (1998) Field and laboratory evidence for intrinsic biodegradation of vinyl chloride contamination in a Fe(III) -reducing aquifer. *Journal of Contaminant Hydrology*, 31, 111-127.
- BRAECKEVELT, M., ROKADIA, H., IMFELD, G. L., STELZER, N., PASCHKE, H., KUSCHK, P., KÄSTNER, M., RICHNOW, H.-H. & WEBER, S. (2007a) Assessment of in situ biodegradation of monochlorobenzene in contaminated groundwater treated in a constructed wetland. *Environmental Pollution*, 148, 428-437.
- BRAECKEVELT, M., ROKADIA, H., IMFELD, G. L., STELZER, N., PASCHKE, H., KUSCHK, P., KÄSTNER, M., RICHNOW, H. H. & WEBER, S. (2007b) Assessment of in situ biodegradation of monochlorobenzene in contaminated groundwater treated in a constructed wetland. *Environmental Pollution*, 148, 428-437.
- BRAGG, J. R., PRINCE, R. C., HARNER, E. J. & ATLAS, R. M. (1994) Effectiveness of bioremediation for the Exxon Valdez oil spill. *Nature*, 368, 413-418.
- BROCKMAN, F. J. & MURRAY, C. J. (1997) Subsurface microbiological heterogeneity: current knowledge, descriptive approaches and applications. *FEMS Microbiology Reviews*, 20, 231-247.
- BURKE, J. J. & MOENCH, M. H. (2000) *Groundwater and society: Resources, Tensions and Opportunities - themes in groundwater management for the twenty-first century.*, New York, United nations publication.
- BUSH-HARRIS, J. L., SUBLETTE, K. L., JENNINGS, E., ROBERTS, K., WHITE, D. C., PEACOCK, A., DAVIS, G., HOLMES, W. E., KOLHATKAR, R. & YANG, X. (2006) *Assessment of In Situ Biodegradation Potential of Benzene Using Stable Isotope Probing (SIP)*. [Online], Available from URL: <[http://www.epa.gov/oem/docs/oil/fss/fss06/sublette\\_1.pdf](http://www.epa.gov/oem/docs/oil/fss/fss06/sublette_1.pdf)> [Accessed 11 Dec 2006].
- CABAÑERO, A. I., RECIO, J. L. & RUPÉREZ, M. (2006) Liquid Chromatography Coupled to Isotope Ratio Mass Spectrometry: A New Perspective on Honey Adulteration Detection. *Journal of Agricultural and Food Chemistry*, 54, 9719-9727.
- CAIMI, R. J. & BRENNAN, J. T. (1993) High-precision liquid chromatography-combustion isotope ratio mass spectrometry. *Analytical Chemistry*, 65, 3497-3500.
- CASTRO, M. & GARCIA, J. (2002) Chapter 2 Analytical freeze-drying. *Techniques and Instrumentation in Analytical Chemistry*. Elsevier.
- CENTRE FOR ECOLOGY AND HYDROLOGY (CEH) (2000) The Biodegradation of pesticides in the unsaturated and saturated zones of major UK aquifers. Wallingford, Department for Environment Food and Rural Affairs.

- CHAKRAVARTI, B., MALLIK, B. & CHAKRAVARTI, D. N. (2008) Column Chromatography. *Current Protocols Essential Laboratory Techniques*. John Wiley & Sons, Inc.
- CHANG, Y.-J., LONG, P. E., GEYER, R., PEACOCK, A. D., RESCH, C. T., SUBLETTE, K., PFIFFNER, S., SMITHGALL, A., ANDERSON, R. T., VRIONIS, H. A., STEPHEN, J. R., DAYVAULT, R., ORTIZ-BERNAD, I., LOVLEY, D. R. & WHITE, D. C. (2005) Microbial Incorporation of <sup>13</sup>C-Labeled Acetate at the Field Scale: Detection of Microbes Responsible for Reduction of U(VI). *Environmental Science & Technology*, 39, 9039-9048.
- CHAPELLE, F. H. (1993) *Ground-water Microbiology and Geochemistry*, New York, John Wiley & Sons.
- CHAPELLE, F. H. (1999) Bioremediation of petroleum hydrocarbon-contaminated ground water: The perspectives of history and hydrology. *Ground Water*, 37, 11.
- CHAPELLE, F. H., BRADLEY, P. M., LOVLEY, D. R. & VROBLESKY, D. A. (1996) Measuring Rates of Biodegradation in a Contaminated Aquifer Using Field and Laboratory Methods. *Ground Water*, 34, 691-698.
- CHAUHAN, A. & OGRAM, A. (2005) Evaluation of support matrices for immobilization of anaerobic consortia for efficient carbon cycling in waste regeneration. *Biochemical and Biophysical Research Communications*, 327, 884-893.
- CHI LENG LAI (2012) Isoproturon Graphic Pathway Map. [Online], Available from URL: <[http://umbbd.ethz.ch/ipt/ipt\\_image\\_map.html](http://umbbd.ethz.ch/ipt/ipt_image_map.html)>, [Accessed 15 Jul 2012].
- CHRISTENSEN, T. H., BJERG, P. L., BANWART, S. A., JAKOBSEN, R., HERON, G. & ALBRECHTSEN, H.-J. R. (2000) Characterization of redox conditions in groundwater contaminant plumes. *Journal of Contaminant Hydrology*, 45, 165-241.
- CLARET, C. (1998) A Method Based on Artificial Substrates to Monitor Hyporheic Biofilm Development. *International Review of Hydrobiology*, 83, 135-143.
- CONRAD, M. E., TEMPLETON, A. S., DALEY, P. F. & ALVAREZ-COHEN, L. (1999) Isotopic evidence for biological controls on migration of petroleum hydrocarbons. *Organic Geochemistry*, 30, 843-859.
- COONEY, J. J., SILVER, S. A. & BECK, E. A. (1985) Factors influencing hydrocarbon degradation in three freshwater lakes. *Microbial Ecology*, 11, 127-137.
- COSTERTON, J. W., LEWANDOWSKI, Z., CALDWELL, D. E., KORBER, D. R. & LAPPIN-SCOTT, H. M. (1995) Microbial Biofilms. *Annual Review of Microbiology*, 49, 711-745.
- CUNNINGHAM, J. A., RAHME, H., HOPKINS, G. D., LEBRON, C. & REINHARD, M. (2001) Enhanced In Situ Bioremediation of BTEX-Contaminated Groundwater by Combined Injection of Nitrate and Sulfate. *Environmental Science & Technology*, 35, 1663-1670.
- DALSGAARD, T. & BAK, F. (1994) Nitrate Reduction in a Sulfate-Reducing Bacterium, *Desulfovibrio desulfuricans*, Isolated from Rice Paddy Soil: Sulfide Inhibition, Kinetics, and Regulation. *Applied and Environmental Microbiology*, 60, 291-297.
- DANIELOPOL, D. L., GRIEBLER, C., GUNATILAKA, A. & NOTENBOOM, J. (2003) Present state and future prospects for groundwater ecosystems. *Environmental Conservation*, 30, 104-130.

- DAS, N. & CHANDRAN, P. (2011) Microbial Degradation of Petroleum Hydrocarbon Contaminants: An Overview. *Biotechnology Research International*, 13.
- DEEB, R. A., SCOW, K. M. & ALVAREZ-COHEN, L. (2000) Aerobic MTBE biodegradation: an examination of past studies, current challenges and future research directions. *Biodegradation*, 11, 171-186.
- DI LORENZO, A., VARCAMONTI, M., PARASCANDOLA, P., VIGNOLA, R., BERNARDI, A., SACCEDDU, P., SISTO, R. & DE ALTERIIS, E. (2005) Characterization and performance of a toluene-degrading biofilm developed on pumice stones. *Microbial Cell Factories*, 4, 1-7.
- DOĞAN, M., ALKAN, M. & ONGANER, Y. (2000) Adsorption of Methylene Blue from Aqueous Solution onto Perlite. *Water, Air, & Soil Pollution*, 120, 229-248.
- DRILLIA, P., DOKIANAKIS, S. N., FOUNTOULAKIS, M. S., KORNAROS, M., STAMATELATOU, K. & LYBERATOS, G. (2005) On the occasional biodegradation of pharmaceuticals in the activated sludge process: The example of the antibiotic sulfamethoxazole. *Journal of Hazardous Materials*, 122, 259-265.
- ELKHATIB, E. A., MAHDY, A. M., SALEH, M. E. & BARAKAT, N. H. (2007) Kinetics of copper desorption from soils as affected by different organic ligands. *International Journal of Environmental Science and Technology*, 4, 331-338.
- EMITIAZI, G., SHAKARAMI, H., NAHVI, I. & MIRDAMADIAM, S. H. (2005) Utilization of petroleum hydrocarbons by *Pseudomonas* sp. and transformed *Escherichia coli*. *African Journal of Biotechnology*, 4, 172-176.
- ENVIRONMENT AGENCY (1999) Natural Attenuation of Petroleum Hydrocarbons and Chlorinated Solvents in Groundwater, R&D Technical Report P305. Bristol, Environment Agency.
- ENVIRONMENT AGENCY (2000a) Guidance on the Assessment and Monitoring of Natural Attenuation of Contaminants in Groundwater. Wiltshire, Environment Agency R&D Dissemination Centre.
- ENVIRONMENT AGENCY (2000b) Guidance on the Assessment and Monitoring of Natural Attenuation of Contaminants in Groundwater R&D Publication 95. Environment Agency.
- ENVIRONMENT AGENCY (2009) Groundwater Quality Reports. [Online], Available from URL: <<http://www.environment-agency.gov.uk/cy/ymchwil/llyfrgell/data/107996.aspx>>, [Accessed 02 Oct 2012].
- ENVIRONMENT AGENCY (2012) Underground, under threat - Groundwater Protection: Policy and Practice. Part 3 - Tools. IN (EA), E. A. (Ed. [Online], Available from URL: <<http://publications.environment-agency.gov.uk/PDF/GEHO1006BLMU-E-E.pdf>>, [Accessed 28 JUL 2012].
- ENVIRONMENT AGENCY (EA) (1999) R&D Technical Report P305: Natural Attenuation of Petroleum Hydrocarbons. Wiltshire, Environment Agency R&D Dissemination Centre
- ENVIRONMENT AGENCY (EA) (2000) Guidance on the Assessment and Monitoring of Natural Attenuation of Contaminants in Groundwater. Wiltshire, Environment Agency R&D Dissemination Centre.

- ENVIRONMENT AGENCY (EA) (2011) Additional guidance for: Groundwater tracer tests and substances used as part of specified remediation schemes. Horizontal Guidance H1 – Annex J 2. Guidance on the discharge of small quantities of substances for scientific purposes. Bristol, Environment Agency.
- ENVIRONMENT AGENCY (EA) (2012a) Aquifers. [Online], Available from URL: <<http://www.environment-agency.gov.uk/homeandleisure/117020.aspx>>, [Accessed 01 Aug 2012].
- ENVIRONMENT AGENCY (EA) (2012b) Groundwater Norwich, Norfolk. [Online], Available from URL: <<http://maps.environment-agency.gov.uk/wiyby/wiybyController?topic=groundwater&x=623930.0&y=307640.0&scale=5&layerGroups=4&location=Norwich,%20Norfolk&textonly=off&ep=map&lang=e#x=622779&y=330976&lg=2.&scale=4>>, [Accessed 01 Aug 2012].
- ENVIRONMENT AGENCY (EA) (2012c) Underground, under threat - Groundwater Protection: Policy and Practice. Part 3 - Tools. IN (EA), E. A. (Ed. [Online], Available from URL: <<http://publications.environment-agency.gov.uk/PDF/GEHO1006BLMU-E-E.pdf>>, [Accessed 28 JUL 2012].
- ENVIRONMENT PROTECTION AGENCY (EPA) (2008) A guide for assessing biodegradation and source identification of organic groundwater contaminants using compound specific isotope analysis (CSIA). [Online], Available from URL: <<http://www.epa.gov/nrmrl/pubs/600r08148/600r08148.pdf>>, [Accessed 03 Jun 2009].
- EUROPEAN COMMUNITY (2000) Directive 2000/60/EC of October 23 2000 of the European Parliament and of the Council establishing a framework for community action in the field of water policy. [Online], Available <<http://www.doeni.gov.uk/wfd.pdf>>, [Accessed 02 May 2011].
- FARHADIAN, M., VACHELARD, C., DUCHEZ, D. & LARROCHE, C. (2007) Insitu bioremediation of monoaromatic pollutants in groundwater: a review. *Bioresource Technology*, Article in Press.
- FARHADIAN, M., VACHELARD, C., DUCHEZ, D. & LARROCHE, C. (2008) Insitu bioremediation of monoaromatic pollutants in groundwater: a review. *Bioresource Technology*, 99, 5296-5308.
- FERRY, J. G. & WOLFE, R. S. (1976) Anaerobic degradation of benzoate to methane by a microbial consortium. *Archives of Microbiology*, 107, 33-40.
- FERYAL, A. (2005) Sorption of phenol and 4-chlorophenol onto pumice treated with cationic surfactant. *Journal of Environmental Management*, 74, 239-244.
- FISCHER, A., THEUERKORN, K., STELZER, N., GEHRE, M., THULLNER, M. & RICHNOW, H. H. (2007) Applicability of Stable Isotope Fractionation Analysis for the Characterization of Benzene Biodegradation in a BTEX-contaminated Aquifer. *Environmental Science & Technology*, 41, 3689-3696.
- FRANCI, M., ANDREONI, N. & FUSI, P. (1981) Identification and determination of asulam and related degradation products in soil. *Bulletin of Environmental Contamination and Toxicology*, 26, 102-107.
- FRIES, M. R., FORNEY, L. J. & TIEDJE, J. M. (1997) Phenol- and toluene-degrading microbial populations from an aquifer in which successful trichloroethene cometabolism occurred. *Applied and Environmental Microbiology*, 63, 1523-30.

- GAMARRA, N., VILLENA, G. & GUTIÉRREZ-CORREA, M. (2010) Cellulase production by *Aspergillus niger* in biofilm, solid-state, and submerged fermentations. *Applied Microbiology and Biotechnology*, 87, 545-551.
- GEYER, R., PEACOCK, A. D., MILTNER, A., RICHNOW, H. H., WHITE, D. C., SUBLETTE, K. L. & KÄSTNER, M. (2005a) In Situ Assessment of Biodegradation Potential Using Biotraps Amended with <sup>13</sup>C-Labeled Benzene or Toluene. *Environmental Science & Technology*, 39, 4983-4989.
- GEYER, R., PEACOCK, A. D., MILTNER, A., RICHNOW, H. H., WHITE, D. C., SUBLETTE, K. L. & KÄSTNER, M. (2005b) In Situ Assessment of Biodegradation Potential Using Biotraps Amended with <sup>13</sup>C-Labeled Benzene or Toluene. *Environmental Science & Technology*, 39, 4983-4989.
- GINSBURG, M. A. & KARAMANEV, D. (2007) Experimental study of the immobilization of *Acidithiobacillus ferrooxidans* on carbon based supports. *Biochemical Engineering Journal*, 36, 294-300.
- GODIN, J.-P., FAY, L.-B. & HOPFGARTNER, G. (2007) Liquid chromatography combined with mass spectrometry for <sup>13</sup>C isotopic analysis in life science research. *Mass Spectrometry Reviews*, 26, 751-774.
- GODIN, J.-P., HAU, J., FAY, L.-B. & HOPFGARTNER, G. (2005) Isotope ratio monitoring of small molecules and macromolecules by liquid chromatography coupled to isotope ratio mass spectrometry. *Rapid Communications in Mass Spectrometry*, 19, 2689-2698.
- GOLDSCHIEDER, N., HUNKELER, D. & ROSSI, P. (2006) Review: Microbial biocenoses in pristine aquifers and an assessment of investigative methods. *Hydrogeology Journal*, 14, 926-941.
- GONZALES, T. (2008) Asulam Graphical Pathway Map [Online], Available from URL: <[http://umbbd.msi.umn.edu/asu/asu\\_image\\_map.html](http://umbbd.msi.umn.edu/asu/asu_image_map.html)>, [Accessed 31 Mar 2010].
- GOOGLE MAPS (2012) Norfolk. [Online], Available from URL:<[http://maps.google.co.uk/maps?aq=f&rlz=1T4GGLJ\\_enGB240GB249&q=norfolk&gs\\_upl=01010132341111111110&aqi=g5s3&um=1&ie=UTF-8&hl=en&sa=N&tab=w1](http://maps.google.co.uk/maps?aq=f&rlz=1T4GGLJ_enGB240GB249&q=norfolk&gs_upl=01010132341111111110&aqi=g5s3&um=1&ie=UTF-8&hl=en&sa=N&tab=w1)>, [Accessed 30 JUL 2012].
- GRIEBLER, C., MINDL, B., SIEZAK, D. & GREIGER-KAISER, M. (2002) Distribution patterns of attached and suspended bacteria in pristine and contaminated shallow aquifers studied with an in situ sediment exposure microcosm. *Aquatic Microbial Ecology*, 28, 117-129.
- GRIEBLER, C., SAFINOWSKI, M., VIETH, A., RICHNOW, H. H. & MECKENSTOCK, R. U. (2003) Combined Application of Stable Carbon Isotope Analysis and Specific Metabolites Determination for Assessing In Situ Degradation of Aromatic Hydrocarbons in a Tar Oil-Contaminated Aquifer. *Environmental Science & Technology*, 38, 617-631.
- GUPTA, V. K. & SUHAS (2009) Application of low-cost adsorbents for dye removal - A review. *Journal of Environmental Management*, 90, 2313-2342.
- GUZZETTA, A. (2010) Calculating the Appropriate Flow Rates for Columns of Differing Diameters or "Maintaining Linear Velocity". [Online], Available from URL: <<http://www.ionsource.com/Card/linvelocity/linvol.htm>>, [Accessed 28 Apr 2010].
- HAACK, S. K. & BEKINS, B. A. (2000) Microbial populations in contaminant plumes. *Hydrogeology Journal*, 8, 63-76.

- HALL, S. H., LUTTRELL, S. P. & CRONIN, W. E. (1991) A Method for Estimating Effective Porosity and Ground-Water Velocity. *Ground Water*, 29, 171-174.
- HAMDAOUI, O. & NAFFRECHOUX, E. (2007) Modeling of adsorption isotherms of phenol and chlorophenols onto granular activated carbon: Part I. Two-parameter models and equations allowing determination of thermodynamic parameters. *Journal of Hazardous Materials*, 147, 381-394.
- HARVEY, R. W., SMITH, R. L. & GEORGE, L. (1984) Effect of Organic Contamination upon Microbial Distributions and Heterotrophic Uptake in a Cape Cod, Mass., Aquifer. *Applied and Environmental Microbiology*, 1197-1202.
- HE, J. M., NG, K. C., YAP, C. & SAHA, B. B. (2009) Effect of Pressure on the Adsorption Rate for Gasoline Vapor on Pitch-Based Activated Carbon. *Journal of Chemical & Engineering Data*, 54, 1504-1509.
- HIRSCH, P. & RADES-ROHKOHL, E. (1988) Some special problems in the determination of viable counts of groundwater microorganisms. *Microbial Ecology*, 16, 99-113.
- HOLDEN, P. A., HUNT, J. R. & FIRESTONE, M. K. (1997) Toluene diffusion and reaction in unsaturated *Pseudomonas putida* biofilms. *Biotechnology and Bioengineering*, 56, 656-670.
- HOLLIGER, C., GASPARD, S., GLOD, G., HEIJMAN, C., SCHUMACHER, W., SCHWARZENBACH, R. P. & VAZQUEZ, F. (1997) Contaminated environments in the subsurface and bioremediation: organic contaminants. *FEMS Microbiology Reviews*, 20, 517-523.
- HOLT-WILSON, T. (2010) Norfolk's Earth Heritage - valuing our geodiversity. [Online], Available from URL: <<http://www.geo-east.org.uk/pages/norfolk.htm>>, [Accessed 16 APR 2012].
- IMFELD, G. L., NIJENHUIS, I., NIKOLAUSZ, M., ZEIGER, S., PASCHKE, H., DRANGMEISTER, J. R., GROSSMANN, J., RICHNOW, H. H. & WEBER, S. (2008) Assessment of in situ degradation of chlorinated ethenes and bacterial community structure in a complex contaminated groundwater system. *Water Research*, 42, 871-882.
- INGERSLEV, F. & HALLING-SØRENSEN, B. (2000) Biodegradability properties of sulfonamides in activated sludge. *Environmental Toxicology and Chemistry*, 19, 2467-2473.
- INGERSLEV, F., TORÄNG, L. & NYHOLM, N. (2000) Importance of the test volume on the lag phase in biodegradation studies. *Environmental Toxicology and Chemistry*, 19, 2443-2447.
- JANNICHE, G. S., LINDBERG, E., MOUVET, C. & ALBRECHTSEN, H. J. (2010) Mineralization of isoproturon, mecoprop and acetochlor in a deep unsaturated limestone and sandy aquifer. *Chemosphere*, 81, 823-831.
- JOHNSON, A., LLEWELLYN, N., SMITH, J., VAN DER GAST, C., LILLEY, A., SINGER, A. & THOMPSON, I. (2004) The role of microbial community composition and groundwater chemistry in determining isoproturon degradation potential in UK aquifers. *FEMS Microbiology Ecology*, 49, 71-82.
- JOHNSON, A. C., BESIEN, T. J., BHARDWAJ, C. L., DIXON, A., GOODDY, D. C., HARIA, A. H. & WHITE, C. (2001) Penetration of herbicides to groundwater in an unconfined chalk aquifer following normal soil applications. *Journal of Contaminant Hydrology*, 53, 101-117.

- JOHNSON, A. C., HUGHES, C. D., WILLIAMS, R. J. & JOHN CHILTON, P. (1998) Potential for aerobic isoproturon biodegradation and sorption in the unsaturated and saturated zones of a chalk aquifer. *Journal of Contaminant Hydrology*, 30, 281-297.
- JOHNSON, A. C., WHITE, C. & LAL BHARDWAJ, C. (2000a) Potential for isoproturon, atrazine and mecoprop to be degraded within a chalk aquifer system. *Journal of Contaminant Hydrology*, 44, 1-18.
- JOHNSON, A. C., WHITE, C. & LAL BHARDWAJ, C. (2000b) Potential for isoproturon, atrazine and mecoprop to be degraded within a chalk aquifer system. *Journal of Contaminant Hydrology*, 44, 1-18.
- JOHNSON, A. C., WHITE, C., LAL BHARDWAJ, C. & DIXON, A. (2003a) The ability of indigenous micro-organisms to degrade isoproturon, atrazine and mecoprop within aerobic UK aquifer systems. *Pest Management Science*, 59, 1291-1302.
- JOHNSON, A. C., WHITE, C., LAL BHARDWAJ, C. & DIXON, A. (2003b) The ability of indigenous micro-organisms to degrade isoproturon, atrazine and mecoprop within aerobic UK aquifer systems. *Pest Management Science*, 59, 1291-1302.
- JOSEPH, C. & RODIER, C. (1994) Renovation of domestic wastewater by unsaturated filtration in a bed of expanded perlite. *Environmental Technology*, 7, 157-165.
- KAMEYA, T., MURAYAMA, T., URANO, K. & KITANO, M. (1995) Biodegradation ranks of priority organic compounds under anaerobic conditions. *Science of The Total Environment*, 170, 43-51.
- KAMPBELL, D. H., WIEDEMEIER, T. H. & HANSEN, J. E. (1996) Intrinsic bioremediation of fuel contamination in ground water at a field site. *Journal of Hazardous Materials*, 49, 197-204.
- KAO, C. M. & PROSSER, J. (1999) Intrinsic bioremediation of trichloroethylene and chlorobenzene: field and laboratory studies. *Journal of Hazardous Materials*, 69, 67-79.
- KAO, C. M. & PROSSER, J. (2001) Evaluation of natural attenuation rate at a gasoline spill site. *Journal of Hazardous Materials*, 82, 275-289.
- KAO, C. M. & WANG, C. C. (2000) Control of BTEX Migration by Intrinsic Bioremediation at a Gasoline Spill Site. *Water Research*, 34, 3413-3423.
- KASCHL, A., VOGT, C., UHLIG, S., NIJENHUIS, I., WEISS, H., KÄSTNER, M. & RICHNOW, H. H. (2005) Isotopic fractionation indicates anaerobic monochlorobenzene biodegradation. *Environmental Toxicology and Chemistry*, 24, 1315-1324.
- KÄSTNER, M., FISCHER, A., NIJENHUIS, I., GEYER, R., STELZER, N., BOMBACH, P., TEBBE, C. C. & RICHNOW, H. H. (2006) Assessment of Microbial In Situ Activity in Contaminated Aquifers. *Engineering in Life Sciences*, 6, 234-251.
- KELLY, S., PARKER, I., SHARMAN, M., DENNIS, J. & GOODALL, I. (1997) Assessing the authenticity of single seed vegetable oils using fatty acid stable carbon isotope ratios ( $^{13}\text{C}/^{12}\text{C}$ ). *Food Chemistry*, 59, 181-186.
- KNOWLES, R. (2005) Kinetic Isotope Effects in Organic Chemistry. [Online], Available from URL: <http://www.princeton.edu/chemistry/macmillan/group-meetings/RRK-KIE.pdf>, [Accessed 28 August 2012].

- KOCADAGISTAN, B., KOCADAGISTAN, E., TOPCU, N. & DEMIRCIOĞLU, N. (2005) Wastewater treatment with combined upflow anaerobic fixed-bed and suspended aerobic reactor equipped with a membrane unit. *Process Biochemistry*, 40, 177-182.
- KOLHATKAR, R., KUDER, T., PHILP, P., ALLEN, J. & WILSON, J. T. (2002) Use of Compound-Specific Stable Carbon Isotope Analyses To Demonstrate Anaerobic Biodegradation of MTBE in Groundwater at a Gasoline Release Site. *Environmental Science & Technology*, 36, 5139-5146.
- KOPINKE, F.-D., GEORGI, A., VOSKAMP, M. & RICHNOW, H. H. (2005) Carbon Isotope Fractionation of Organic Contaminants Due to Retardation on Humic Substances: Implications for Natural Attenuation Studies in Aquifers. *Environmental Science & Technology*, 39, 6052-6062.
- KRISTENSEN, G. B., SØRENSEN, S. R. & AAMAND, J. (2001) Mineralization of 2,4-D, mecoprop, isoproturon and terbuthylazine in a chalk aquifer. *Pest Management Science*, 57, 531-536.
- KRUMMEN, M., HILKERT, A. W., JUCHELKA, D., DUHR, A., SCHLÜTER, H.-J. & PESCH, R. (2004) A new concept for isotope ratio monitoring liquid chromatography/mass spectrometry. *Rapid Communications in Mass Spectrometry*, 18, 2260-2266.
- KUDER, T. & PHILP, P. (2008) Modern geochemical and molecular tools for monitoring in-situ biodegradation of MTBE and TBA. *Reviews in Environmental Science and Biotechnology*, 7, 79-91.
- KUMAR, D. (2008) *Definitional Glossary Of Agricultural Terms Volume 1*, New Delhi, I.K. International Publishing Ltd.
- LANDMEYER, J. E., CHAPELLE, F. H., HERLONG, H. H. & BRADLEY, P. M. (2001) Methyl *tert*-Butyl Ether Biodegradation by Indigenous Aquifer Microorganisms under Natural and Artificial Oxidic Conditions. *Environmental Science & Technology*, 35, 118-1126.
- LANDMEYER, J. E., VROBLESKY, D. A. & CHAPELLE, F. H. (1996) Stable Carbon Isotope Evidence of Biodegradation Zonation in a Shallow Jet-Fuel Contaminated Aquifer. *Environmental Science & Technology*, 30, 1120-1128.
- LARSEN, L. & AAMAND, J. (2001) Degradation of herbicides in two sandy aquifers under different redox conditions. *Chemosphere*, 44, 231-236.
- LEAHY, J. G. & COLWELL, R. R. (1990) Microbial degradation of Hydrocarbons in the Environment. *Microbiological Reviews*, 54, 305-315.
- LEGLIZE, P., SAADA, A., BERTHELIN, J. & LEYVAL, C. (2006) Evaluation of matrices for the sorption and biodegradation of phenanthrene. *Water Research*, 40, 2397-2404.
- LEHMAN, R. M., COLWELL, F. S. & BALA, G. A. (2001) Attached and Unattached Microbial Communities in a Simulated Basalt Aquifer under Fracture- and Porous-Flow Conditions. *Applied and Environmental Microbiology*, 67, 2799-2809.
- LIU, S., JIANG, B., HUANG, G. & LI, X. (2006) Laboratory column study for remediation of MTBE-contaminated groundwater using a biological two-layer permeable barrier. *Water Research*, 40, 3401-3408.
- LYEW, D., GUIOT, S. R., MONOT, F. D. R. & FAYOLLE-GUICHARD, F. (2007) Comparison of different support materials for their capacity to immobilize *Mycobacterium austroafricanum* IFP 2012 and to adsorb MtBE. *Enzyme and Microbial Technology*, 40, 1524-1530.

- MARSH, H. & RODRIGUEZ-REINOSO, F. (2006) Applicability of Activated Carbon. *Activated carbon*. Oxford, Elsevier.
- MARTUS, P. & PÜTTMANN, W. (2003) Formation of alkylated aromatic acids in groundwater by anaerobic degradation of alkylbenzenes. *The Science of the Total Environment*, 307, 19-33.
- MCCULLAGH, J. S. O., JUCHELKA, D. & HEDGES, R. E. M. (2006) Analysis of amino acid  $^{13}\text{C}$  abundance from human and faunal bone collagen using liquid chromatography/isotope ratio mass spectrometry. *Rapid Communications in Mass Spectrometry*, 20, 2761-2768.
- MCGUIRE, T. M., NEWELL, C. J., LOONEY, B. B., VANGELAS, K. M. & SINK, C. H. (2004) Historical Analysis of Monitored Natural Attenuation: A Survey of 191 Chlorinated Solvent Sites and 45 Solvent Plumes. *Remediation Journal*, 15, 99-112.
- MCKELVIE, J. R., HIRSCHORN, S. K., LACRAMPE-COULOUME, G., LINDSTROM, J., BRADDOCK, J., FINNERAN, K., TREGO, D. & SHERWOOD LOLLAR, B. (2007a) Evaluation of TCE and MTBE in situ Biodegradation: Integrating Stable Isotope, Metabolic Intermediate, and Microbial lines of Evidence. *Ground Water Monitoring & Remediation*, 27, 63-73.
- MCKELVIE, J. R., MACKAY, D. M., DE SIEYES, N. R., LACRAMPE-COULOUME, G. & SHERWOOD LOLLAR, B. (2007b) Quantifying MTBE biodegradation in the Vandenberg Air Force Base ethanol release study using stable carbon isotopes. *Journal of Contaminant Hydrology*, 94, 157-165.
- MECKENSTOCK, R. U., MORASCH, B., GRIEBLER, C. & RICHNOW, H. H. (2004) Stable isotope fractionation analysis as a tool to monitor biodegradation in contaminated aquifers. *Journal of Contaminant Hydrology*, 75, 215-255.
- MECKENSTOCK, R. U., MORASCH, B., WARTHMAN, R., SCHINK, B., ANNWEILER, E., MICHAELIS, W. & RICHNOW, H. H. (1999)  $^{13}\text{C}/^{12}\text{C}$  isotope fractionation of aromatic hydrocarbons during microbial degradation. *Environmental Microbiology*, 1, 409-414.
- MIDWOOD, A. J. & MCGAW, B. A. (1999) Recent developments in the analysis of light isotopes by continuous flow isotope ratio mass spectrometry. *Analytical Communications*, 36, 291-294.
- MOHAMMADZADEH, H., CLARK, I., MARSCHNER, M. & ST-JEAN, G. (2005) Compound Specific Isotopic Analysis (CSIA) of landfill leachate DOC components. *Chemical Geology*, 218, 3-13.
- MORGENROTH, E. & MILFERSTEDT, K. (2009) Biofilm engineering: linking biofilm development at different length and time scales. *Reviews in Environmental Science and Biotechnology*, 8, 203-208.
- MUCCIO, Z. & JACKSON, G. P. (2009) Isotope ratio mass spectrometry. *Analyst*, 134, 213-222.
- NATIONAL WATER RESEARCH INSTITUTE (2004) Evaluation of MTBE Remediation Options. USA, Center for Groundwater Restoration and Protection National Water research Institute
- NOAA RESEARCH (N.D.) Fingerprints of Emissions and the Carbon Cycle: Stable and Radiocarbon Isotopes of Carbon Dioxide. [Online], Available from: URL < <http://www.esrl.noaa.gov/gmd/outreach/isotopes/chemistry.html> > [Accessed 02 Dec 2012].

- NOBLE, M. (2004) Biomaterials Tutorial. [Online], Available from URL: <<http://www.uweb.engr.washington.edu/research/tutorials/biofilm.html>>, [Accessed 17 Oct 2011].
- NORWICH CITY COUNCIL (2010) Planning Application 09/01443/H Bayer Cropscience Ltd [Online], Available from URL: <<http://www.norwich.gov.uk/CommitteeMeetings/Planning%20applications/Document%20Library/118/Repplanning51bayercropscienceltdsweetbriarrd20101014.pdf>>, [Accessed 30 JUL 2012].
- O'TOOLE, G., KAPLAN, H. B. & KOLTER, R. (2000) Biofilm Formation as Microbial Development. *Annual Review of Microbiology*, 54, 49-79.
- ORGANISATION FOR ECONOMIC CO-OPERATION AND DEVELOPMENT (OECD) (2000) OECD Guideline for Testing of Chemicals: Adsorption – Desorption Using a Batch Equilibrium Method. [Online], Available from URL: <[http://www.epa.gov/scipoly/sap/meetings/2008/october/106\\_adsorption\\_desorption\\_using.pdf](http://www.epa.gov/scipoly/sap/meetings/2008/october/106_adsorption_desorption_using.pdf)>, [Accessed 17 Oct 2008].
- PAHM, M. A. & ALEXANDER, M. (1993) Selecting inocula for the biodegradation of organic compounds at low concentrations. *Microbial Ecology*, 25, 275-286.
- PALOMO, M. (2008) Stabilization of enzymatically polymerized 2,4 dichlorophenol in model subsurface geomaterials. Masters Thesis. *Department of Civil Engineering*. Manhattan, Kansas, Kansas State University.
- PAZARLIOĞLU, N. K. & TELEFONCU, A. (2005) Biodegradation of phenol by *Pseudomonas putida* immobilized on activated pumice particles. *Process Biochemistry*, 40, 1807-1814.
- PEACOCK, A. D., CHANG, Y. J., ISTOK, J. D., KRUMHOLZ, L., GEYER, R., KINSALL, B., WATSON, D., SUBLETTE, K. L. & WHITE, D. C. (2004) Utilization of Microbial Biofilms as Monitors of Bioremediation. *Microbial Ecology*, 47, 284-292.
- PÉREZ, S., EICHHORN, P. & AGA, D. S. (2005) Evaluating the biodegradability of sulfamethazine, sulfamethoxazole, sulfathiazole, and trimethoprim at different stages of sewage treatment. *Environmental Toxicology and Chemistry*, 24, 1361-1367.
- PETER, A., STEINBACH, A., LIEDL, R., PTAK, T., MICHAELIS, W. & TEUTSCH, G. (2004) Assessing microbial degradation of o-xylene at field-scale from the reduction in mass flow rate combined with compound-specific isotope analyses. *Journal of Contaminant Hydrology*, 71, 127-154.
- PIGNATELLO, J. J. & XING, B. (1995) Mechanisms of Slow Sorption of Organic Chemicals to Natural Particles. *Environmental Science & Technology*, 30, 1-11.
- REID, B. J., MACLEOD, C. J. A., LEE, P. H., MORRISS, A. W. J., STOKES, J. D. & SEMPLE, K. T. (2001) A simple <sup>14</sup>C-respirometric method for assessing microbial catabolic potential and contaminant bioavailability. *FEMS Microbiology Letters*, 196, 141-146.
- RICE, D. W., DOOHER, B. P., CULLEN, S. J., EVERETT, L. G., KASTENBERG, W. E., GROSE, R. D. & MARINO, M. A. (1995a) Recommendations to Improve the Cleanup Process for California's Leaking Underground Fuel Tanks (LUFTs). Submitted to the California State Water Resources Control Board Underground Storage tank program and the senate Bill 1764 Leaking Underground Fuel Tank Advisory Committee.

- RICE, D. W., GROSE, R. D., MICHAELSEN, J. C., DOOHER, B. P., MACQUEEN, D. H., CULLEN, S. J., KASTENBERG, W. E., EVERETT, L. G. & MARINO, M. A. (1995b) California Leaking Underground Fuel Tank (LUFT) Historical Case Analyses. IN AGENCY, E. P. (Ed., U. S. Department of Energy.
- RICHNOW, H. H., ANNWEILER, E., MICHAELIS, W. & MECKENSTOCK, R. U. (2003) Microbial in situ degradation of aromatic hydrocarbons in a contaminated aquifer monitored by carbon isotope fractionation. *Journal of Contaminant Hydrology*, 65, 101-120.
- ROBINSON, L. & THORN, I. (2005) *Toxicology and ecotoxicology in chemical safety assessment*, Blackwell Pub.
- ROSE, J. (2009) Early and Middle Pleistocene landscapes of eastern England. *Proceedings of the Geologists' Association*, 120, 3-33.
- ROSE, S. & LONG, A. (1988) Monitoring Dissolved Oxygen in Ground Water: Some Basic Considerations. *Ground Water Monitoring & Remediation*, 8, 93-97.
- RÜGNER, H., FINKEL, M., KASCHL, A. & BITTENS, M. (2006) Application of monitored natural attenuation in contaminated land management - A review and recommended approach for Europe. *Environmental Science & Policy*, 9, 568-576.
- SAEID, A. (2004) Kinetic models of sorption: a theoretical analysis. *Journal of Colloid and Interface Science*, 276, 47-52.
- SALZMAN, J., HERMAN, J. S. & CULVER, D. C. (2001) Groundwater Ecosystems and the Service of Water Purification, Stanford Environmental Law Journal 479-495 (2001). [Online], Available from: URL <[http://scholarship.law.duke.edu/faculty\\_scholarship/696](http://scholarship.law.duke.edu/faculty_scholarship/696)>, [Accessed 02 May 2012].
- SAN DIEGO STATE UNIVERSITY (n.d.) Hollow-Stem Auger Drilling - For Sediment Sampling and Well Installation. [Online], Available from URL: <<http://www.geology.sdsu.edu/classes/geol552/hollowstem.htm>>, [Accessed 08 Jul 2008].
- SCHIRMER, M. & BUTLER, B. J. (2004) Transport behaviour and natural attenuation of organic contaminants at spill sites. *Toxicology*, 205, 173-179.
- SCHIRMER, M., BUTLER, B. J., BARKER, J. F., CHURCH, C. D. & SCHIRMER, K. (1999) Evaluation of Biodegradation and Dispersion as Natural Attenuation Processes of MTBE and Benzene at the Borden Field Site. *Physics and Chemistry of the Earth, Part B: Hydrology, Oceans and Atmosphere*, 24, 557-560.
- SCHMIDT, S. K. & ALEXANDER, M. (1985) Effects of dissolved organic carbon and second substrates on the biodegradation of organic compounds at low concentrations. *Applied and Environmental Microbiology*, 49, 822-827.
- SCHMIDT, T., ZWANK, L., ELSNER, M., BERG, M., MECKENSTOCK, R. & HADERLEIN, S. (2004) Compound-specific stable isotope analysis of organic contaminants in natural environments: a critical review of the state of the art, prospects, and future challenges. *Analytical and Bioanalytical Chemistry*, 378, 283-300.
- ŠĆIBAN, M. B. & KLAŠNJA, M. T. (2002) The kinetics of Chromium(VI) adsorption from water on some natural materials. *Acta Periodica Technologica*, 33, 101-107.

- SCOTTISH ENVIRONMENT PROTECTION AGENCY (SEPA) (2004) Final Report WFD28 - Development of a groundwater vulnerability screening methodology for the Water Framework Directive. Edinburgh, Scotland and Northern Ireland Forum for Environmental Research
- SEAR, D. A., NEWSON, M., OLD, J. C. & HILL, C. (2006) Geomorphological appraisal of the River Wensum Special Area of Conservation. English Nature Commissioned Report No. 685.
- ŞEN, S. & DEMIRER, G. N. (2003) Anaerobic treatment of real textile wastewater with a fluidized bed reactor. *Water Research*, 37, 1868-1878.
- SHAH, N. W., THORNTON, S. F., BOTTRELL, S. H. & SPENCE, M. J. (2009) Biodegradation potential of MTBE in a fractured chalk aquifer under aerobic conditions in long-term uncontaminated and contaminated aquifer microcosms. *Journal of Contaminant Hydrology*, 103, 119-133.
- SHERWOOD LOLLAR, B., HIRSCHORN, S. K., CHARTRAND, M. M. G. & LACRAMPE-COULOUME, G. (2007) An Approach for Assessing Total Instrumental Uncertainty in Compound-Specific Carbon Isotope Analysis: Implications for Environmental Remediation Studies. *Analytical Chemistry*, 79, 3469-3475.
- SHERWOOD LOLLAR, B., SLATER, G. F., AHAD, J., SLEEP, B., SPIVACK, J., BRENNAN, M. & MACKENZIE, P. (1999) Contrasting carbon isotope fractionation during biodegradation of trichloroethylene and toluene: Implications for intrinsic bioremediation. *Organic Geochemistry*, 30, 813-820.
- SHERWOOD LOLLAR, B., SLATER, G. F., SLEEP, B., WITT, M., KLECKA, G. M., HARKNESS, M. & SPIVACK, J. (2000) Stable Carbon Isotope Evidence for Intrinsic Bioremediation of Tetrachloroethene and Trichloroethene at Area 6, Dover Air Force Base. *Environmental Science & Technology*, 35, 261-269.
- SHERWOOD LOLLAR, B., SLATER, G. F., SLEEP, B., WITT, M., KLECKA, G. M., HARKNESS, M. & SPIVACK, J. (2001) Stable Carbon Isotope Evidence for Intrinsic Bioremediation of Tetrachloroethene and Trichloroethene at Area 6, Dover Air Force Base. *Environmental Science & Technology*, 35, 261-269.
- SHROVE, G. S., OLSEN, R. H. & VOGEL, T. M. (1991) Development of pure culture biofilms of *P. putida* on solid supports. *Biotechnology and Bioengineering*, 37, 512-518.
- SINKE, A. & LE HECHO, I. (1999) Monitored Natural Attenuation: review of existing guidelines and protocols. TNO Institute of Environmental Sciences Energy Research and Process Innovation.
- SKIPPER, H. D., WOLLUM, A. G., II, TURCO, R. F. & WOLF, D. C. (1996) Microbiological Aspects of Environmental Fate Studies of Pesticides. *Weed Technology*, 10, 174-190.
- SKOPP, J. (2009) Derivation of the Freundlich Adsorption Isotherm from Kinetics. *Journal of Chemical Education*, 86, 1341-1343.
- SMETS, B. F. & PRITCHARD, P. H. (2003) Elucidating the microbial component of natural attenuation. *Current Opinion in Biotechnology*, 14, 283-288.
- SPARKS, D. L. (2003) *Environmental Soil Chemistry (2<sup>nd</sup> Ed.)*, London, Academic Press. 147-152.
- SPENCE, M. J., BOTTRELL, S. H., THORNTON, S. F., RICHNOW, H. H. & SPENCE, K. H. (2005) Hydrochemical and isotopic effects associated with

- petroleum fuel biodegradation pathways in a chalk aquifer. *Journal of Contaminant Hydrology*, 79, 67-88.
- SRINIVAS, T. (2008) *Environmental Biotechnology*, New Age International (P) Ltd., Publishers.
- ST-JEAN, G. (2003) Automated quantitative and isotopic (<sup>13</sup>C) analysis of dissolved inorganic carbon and dissolved organic carbon in continuous-flow using a total organic carbon analyser. *Rapid Communications in Mass Spectrometry*, 17, 419-428.
- STARNER, K., KUIVILA, K. M., JENNINGS, J. & MOON, G. E. (1999) Degradation Rates of Six Pesticides in Water from the Sacramento River, California. [Online] Available from URL: <http://ca.water.usgs.gov/archive/reports/wrir994018/CA-0216.pdf>, [Accessed 10 Jan 2013].
- STELZER, N., BÜNING, C., PFEIFER, F., DOHRMANN, A. B., TEBBE, C. C., NIJENHUIS, I., KÄSTNER, M. & RICHNOW, H. H. (2006a) In situ microcosms to evaluate natural attenuation potentials in contaminated aquifers. *Organic Geochemistry*, 37, 1394-1410.
- STELZER, N., BÜNING, C., PFEIFER, F., DOHRMANN, A. B., TEBBE, C. C., NIJENHUIS, I., KÄSTNER, M. & RICHNOW, H. H. (2006b) In situ microcosms to evaluate natural attenuation potentials in contaminated aquifers. *Organic Geochemistry*, 37, 1394-1410.
- STOCKING, A. J., DEEB, R. A., FLORES, A. E., STRINGFELLOW, W., TALLEY, J., BROWNELL, R. & KAVANAUGH, M. C. (2000) Bioremediation of MTBE: a review from a practical perspective. *Biodegradation*, 11, 187-201.
- STURMAN, P. J., STEWART, P. S., CUNNINGHAM, A. B., BOUWER, E. J. & WOLFRAM, J. H. (1995a) Engineering scale-up of in situ bioremediation processes: a review. *Journal of Contaminant Hydrology*, 19, 171 - 203.
- STURMAN, P. J., STEWART, P. S., CUNNINGHAM, A. B., BOUWER, E. J. & WOLFRAM, J. H. (1995b) Engineering scale-up of in situ bioremediation processes: a review. *Journal of Contaminant Hydrology*, 19, 171-203.
- SUBLETTE, K., PEACOCK, A., WHITE, D., DAVIS, G., OGLES, D., COOK, D., KOLHATKAR, R., BECKMANN, D. & YANG, X. (2006) Monitoring Subsurface Microbial Ecology in a Sulfate-Amended, Gasoline-Contaminated Aquifer. *Ground Water Monitoring & Remediation*, 26, 70-78.
- TEAS, C., KALLIGEROS, S., ZANIKOS, F., STOURNAS, S., LOIS, E. & ANASTOPOULOS, G. (2001) Investigation of the effectiveness of absorbent materials in oil spills clean up. *Desalination*, 140, 259-264.
- TEFFERA, Y., KUSMIERZ, J. J. & ABRAMSON, F. P. (1996) Continuous-Flow Isotope Ratio Mass Spectrometry Using the Chemical Reaction Interface with Either Gas or Liquid Chromatographic Introduction. *Analytical Chemistry*, 68, 1888-1894.
- THRASHER, J., MORGAN, P. & BUSS, S. R. (2004) Attenuation of mecoprop in the subsurface. IN ENVIRONMENT AGENCY SCIENCE GROUP: AIR, L. W. (Ed. Bristol, Environment Agency.
- TNO INSTITUTE OF ENVIRONMENTAL SCIENCES ENERGY RESEARCH AND PROCESS INNOVATION (NICOLE REPORT) (1999) Monitored Natural Attenuation: review of existing guidelines and protocols (TNO-MEP-R99/313)

[Online], Available from URL:

<<http://www.nicole.org/news/downloads/Rapport%2099-313%20compleet+kaft.pdf>>, [Accessed 25 Oct 2007].

TOMOHITO, A. (1999) In situ detection of changes in soil bacterial and fungal activities by measuring <sup>13</sup>C incorporation into soil phospholipid fatty acids from <sup>13</sup>C acetate. *Soil Biology and Biochemistry*, 31, 1015-1020.

TUXEN, N. (2002) In situ bioremediation of groundwater contaminated by herbicides from point sources. PhD Thesis. *Environment and Resources*. Denmark, DTU Technical University.

TUXEN, N., EJLSKOV, P., ALBRECHTSEN, H., REITZEL, L. A., PEDERSEN, J. K. & BJERG, P. L. (2003) Application of Natural Attenuation to Ground Water Contaminated by Phenoxy Acid Herbicides at an Old Landfill in Sjoelund, Denmark. *Ground Water Monitoring & Remediation*, 23, 48-58.

UNITED STATES ENVIRONMENTAL PROTECTION AGENCY (1999) Use of Monitored Natural Attenuation at Superfund, RCRA Corrective Action, and Underground Storage Tank Sites. Washington, Environment Protection Agency.

UNITED STATES ENVIRONMENTAL PROTECTION AGENCY (2002) Title XIV of the Public Health Service Act Safety of Public Water Systems (Safe Drinking Water Act). [Online], Available from URL: <<http://epw.senate.gov/sdwa.pdf>>, [Accessed 17 Oct 2011].

UNITED STATES ENVIRONMENTAL PROTECTION AGENCY (2008) A guide for Assessing Biodegradation and Source Identification of Organic Ground Water Contaminants using Compound Specific Isotope Analysis (CSIA). Washington D.C., Office of Research and Development (8101R).

UNITED STATES ENVIRONMENTAL PROTECTION AGENCY (EPA) (1999) OSWER directive (9200.4-17P) - Use of monitored natural attenuation at superfund, RCRA corrective action, and underground storage tank sites. Washington D.C., Office of Solid Waste and Emergency Response

UNITED STATES ENVIRONMENTAL PROTECTION AGENCY (EPA) (2002) Title XIV of the Public Health Service Act Safety of Public Water Systems (Safe Drinking Water Act). [Online], Available from URL: <<http://epw.senate.gov/sdwa.pdf>>, [Accessed 17 Oct 2011].

UNITED STATES ENVIRONMENTAL PROTECTION AGENCY (EPA) (2008) A guide for Assessing Biodegradation and Source Identification of Organic Ground Water Contaminants using Compound Specific Isotope Analysis (CSIA). Washington D.C., Office of Research and Development (8101R).

VAN HAPEREN, A. M., VAN VELDE, J. W. & VAN GINKEL, C. G. (2001) Biodegradation of p-toluenesulphonamide by a *Pseudomonas* sp. *FEMS Microbiology Letters*, 204, 299-304.

VERKOUTEREN, R. M. & KLINEDINST, D. B. (2004) Standard Reference Materials® Value Assignment and Uncertainty Estimation of Selected Light Stable Isotope Reference Materials: RMs 8543-8545, RMs 8562-8564, and RM 566. Washington, USA, U.S. Department of Commerce.

VILAR, E. O., CAVALCANTI, E. B., CARVALHO, H. R. & SOUSA, F. B. (2003) Cr (VI) electromechanical reduction using RVG 4000 graphite felt as the electrode. [electronic print] [Online], Available from URL: <[http://www.scielo.br/scielo.php?script=sci\\_arttext&pid=S0104-66322003000300009](http://www.scielo.br/scielo.php?script=sci_arttext&pid=S0104-66322003000300009)>, [Accessed 17 Oct 2011].

- WALKER, A., JURADO-EXPOSITO, M., BENDING, G. D. & SMITH, V. J. R. (2001) Spatial variability in the degradation rate of isoproturon in soil. *Environmental Pollution*, 111, 407-415.
- WALKER, N. (1978) A Soil *Flavobacterium sp.* that Degrades Sulphanilamide and Asulam. *Journal of Applied Microbiology*, 45, 125-129.
- WALTER, N. (1974) Adsorption Processes. *Pure and Applied Chemistry*, 37, 375-392.
- WIEDEMEIER, T. H., RIFAI, H. S., NEWELL, C. J. & WILSON, J. T. (2007a) Abiotic Processes of Natural Attenuation. *Natural Attenuation of Fuels and Chlorinated Solvents in the Subsurface*. John Wiley & Sons, Inc.
- WIEDEMEIER, T. H., RIFAI, H. S., NEWELL, C. J. & WILSON, J. T. (2007b) Evaluating Natural Attenuation. *Natural Attenuation of Fuels and Chlorinated Solvents in the Subsurface*. John Wiley & Sons, Inc.
- WIEDEMEIER, T. H., RIFAI, H. S., NEWELL, C. J. & WILSON, J. T. (2007c) Intrinsic Bioremediation of Petroleum Hydrocarbons. *Natural Attenuation of Fuels and Chlorinated Solvents in the Subsurface*. John Wiley & Sons, Inc.
- WIEDEMEIER, T. H., RIFAI, H. S., NEWELL, C. J. & WILSON, J. T. (2007d) Overview of Natural Attenuation. *Natural Attenuation of Fuels and Chlorinated Solvents in the Subsurface*. New York, John Wiley & Sons, INC.
- WIEDEMEIER, T. H., RIFAI, H. S., NEWELL, C. J. & WILSON, J. T. (1999) *Natural attenuation of Fuels and Chlorinated Solvents in the Subsurface.*, USA, John Wiley & Sons Inc.
- WIEDEMEIER, T. H., WILSON, J. T., KAMPBELL, D. H., MILLER, R. N. & HANSEN, J. E. (1995) Technical Protocol for Implementing Intrinsic Remediation with Long-term Monitoring for Natural Attenuation of Fuel Contamination Dissolved in Groundwater. Air Force Center for Environmental Excellence, Technology Transfer Division, Brooks Air Force Base, San Antonio, Texas.
- WIKIPEDIA (2012) Bacterial Growth. [Online], Available from URL: <[http://en.wikipedia.org/wiki/Bacterial\\_growth](http://en.wikipedia.org/wiki/Bacterial_growth)>, [Accessed 10 Jul 2012].
- WILKES, H., VIETH, A. & ELIAS, R. (2008) Constraints on the quantitative assessment of in-reservoir biodegradation using compound-specific stable carbon isotopes. *Organic Geochemistry*, 39, 1215-1221.
- WILSON, J. T., ADAIR, C., KAISER, P. M. & KOLHATKAR, R. (2005) Anaerobic Biodegradation of MTBE at a Gasoline Spill Site. *Ground Water Monitoring & Remediation*, 25, 103-115.
- WILSON, R. D., THORNTON, S. F. & MACKAY, D. M. (2004) Challenges in monitoring the natural attenuation of spatially variable plumes. *Biodegradation*, 15, 359-369.
- WILSON, S. B. & BROWN, R. A. (1989) In Situ Bioreclamation: A Cost-Effective Technology to Remediate Subsurface Organic Contamination. *Ground Water Monitoring & Remediation*, 9, 173-179.

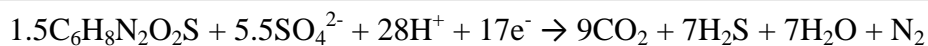
# Appendices

---

## APPENDIX 1

### Mass calculations

Sulphanilamide sulphate reduction:



For 1.5 mole of sulphanilamide to undergo sulphate reduction 5.5 mole of sulphate are required. A ratio of 1:3.67.

The concentration of sulphanilamide in the borehole N62b (source zone) is 263 mg L<sup>-1</sup>. Therefore the number of mole:

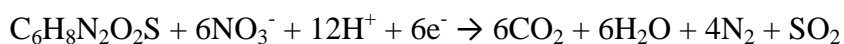
No. of moles of sulphanilamide =	mass (g) / molar mass (g mol <sup>-1</sup> )
	0.26 / 172.20
	0.0015 mol

Mass (g) of sulphate =	no. of moles x molar mass (g mol <sup>-1</sup> )
	(0.0015 x 3.67 mol) x 96.06
	0.529 g
	529 mg L <sup>-1</sup> of groundwater

The concentration of sulphate added during laboratory trials was 572 mg L<sup>-1</sup>. This, in addition to the sulphate already present (169 mg L<sup>-1</sup>), equates to a total of 741 mg L<sup>-1</sup>. Therefore, this was at a level so as to ensure sulphate, as an electron acceptor, would not be a limiting factor in terms of the mineralisation of <sup>14</sup>C-sulphanilamide.

The average concentration of sulphate across the contaminated site is 169 ± 34 mg L<sup>-1</sup>. This is below the sulphate concentration required for sulphate reduction and so would impose a limiting factor on the amount/rate of mineralisation of sulphanilamide currently contaminating the field study site.

Mineralisation of sulphanilamide via denitrification:



This shows that 6 mole of nitrate is required to mineralise 1 mole of sulphanilamide.  
A ratio of 1:6.

Mass (g) of nitrate =	no. of moles x molar mass (g mol <sup>-1</sup> )
	(0.0015 x 6 mol) x 62.00
	0.558 g
	558 mg L <sup>-1</sup> of groundwater

The average concentration of nitrate across the site is 33 ± 8 mg L<sup>-1</sup>. During laboratory trials 548 mg L<sup>-1</sup> was added to the microcosms. This, in addition to the nitrate already present equates to 581 mg L<sup>-1</sup>. Therefore, this was at a level so as to ensure nitrate, as an electron acceptor, would not be a limiting factor in terms of the mineralisation of <sup>14</sup>C-sulphanilamide.

Aerobic mineralisation of sulphanilamide:



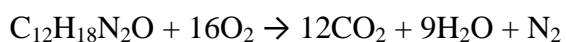
This shows that 8 mole of oxygen is required to mineralise 1 mole of sulphanilamide.  
The groundwater at the contaminated site is depleted of oxygen and redox potential measurements of < 2 volts across the site point to reducing conditions.

Mass (g) of oxygen =	no. of moles x molar mass (g mol <sup>-1</sup> )
	(0.0015 x 8 mol) x 32.00
	0.384 g
	384 mg L <sup>-1</sup> of groundwater

The microcosm flasks in the aerobic trials were exposed to air during each sampling phase, which contained 220 mL of head space. Using Avogadro's Law that '1 mole of any gas at STP takes up a volume of 22.4 L' calculations were made to ascertain a total mass of 25.2 mg of oxygen ( 0.3 mg x 84 sampling days) available to the

microcosm during the experiment. This is below that required for aerobic respiration calculated above. In addition, the calculation assumes 100 % oxygen. Whereas, in reality this would only have been ~20%, leaving the actual oxygen mass closer to 5 mg.

Aerobic mineralisation of isoproturon (N62b 9  $\mu\text{g L}^{-1}$ )



This shows that 16 mole of oxygen is required to mineralise 1 mole of isoproturon. The groundwater at the contaminated site is depleted of oxygen and redox potential measurements of < 2 volts across the site point to reducing conditions.

No. of moles of isoproturon =	mass (g) / molar mass ( $\text{g mol}^{-1}$ )
	0.000009 / 206.29
	0.00000004 mol

Mass (g) of oxygen =	no. of moles x molar mass ( $\text{g mol}^{-1}$ )
	(0.00000004 x 16 mol) x 32.00
	0.00002 g
	0.02 $\text{mg L}^{-1}$ of groundwater

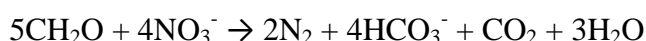
Although site redox measurements show an highly anaerobic environment there is still enough dissolved oxygen at the site (2  $\text{mg L}^{-1}$ ) to enable the aerobic mineralisation of 9  $\mu\text{g L}^{-1}$  of the isoproturon located in borehole N62b.

## APPENDIX 2

Calculation of nitrate and sulphate concentrations for the enhanced biodegradation studies:

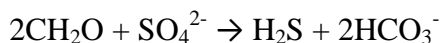
Simple biodegradation of glucose (Ashman and Puri, 2002):

### *Denitrification*



Therefore, require 4/5 or 8/10 (i.e. 5CH<sub>2</sub>O + 4NO<sub>3</sub><sup>-</sup>) moles of NO<sub>3</sub><sup>-</sup> for every mole of glucose

### *Sulphate reduction*



Therefore, require 1/2 or 5/10 (i.e. 2CH<sub>2</sub>O + 1SO<sub>4</sub><sup>2-</sup>) moles of SO<sub>4</sub><sup>2-</sup> for every mole of glucose

Thus, to work out how many more moles of NO<sub>3</sub><sup>-</sup> are required than SO<sub>4</sub><sup>2-</sup>:

$$= (8/10) / (5/10)$$

$$= (8/10) \times (10/5)$$

$$= 8/5$$

$$= 1.6 \text{ x more moles of NO}_3^- \text{ than SO}_4^{2-} \text{ for every mole of glucose}$$

Using these calculations as a guide, in addition to the environment agencies approval to allow the addition of 400 mg L<sup>-1</sup> of nitrate to the groundwater at the site, the concentration of nitrate and sulphate for the enhanced ex-situ microcosms were calculated as follows:

Molar Masses (g mol<sup>-1</sup>):

<b>Na<sub>2</sub>SO<sub>4</sub></b> (23 x 2) + (32 x 1) + (16 x 4) = 142	<b>SO<sub>4</sub></b> (32 x 1) + (16 x 4) = 96
<b>NaNO<sub>3</sub></b> (23 x 1) + (14 x 1) + (16 x 3) = 85	<b>NO<sub>3</sub></b> (14 x 1) + (16 x 3) = 62

**NO<sub>3</sub> concentration required:**

Environment Agency licensed addition is 400 mg L (0.4 g L)

Thus,  $\text{mass (g L}^{-1}\text{) / molar mass (g mol}^{-1}\text{)}$

$$= 0.4 / 62$$

$$= 6.45 \times 10^{-3} \text{ mol L}^{-1} \text{ of NO}_3$$

Therefore, concentration required when made using NaNO<sub>3</sub>

$$\text{NO}_3 \text{ (mol L}^{-1}\text{) x molar mass of NaNO}_3 \text{ (g mol}^{-1}\text{)}$$

$$= (6.45 \times 10^{-3}) \times 85$$

$$= 0.548 \text{ g L}^{-1}$$

**SO<sub>4</sub> concentration required:**

From the calculations above, the amount of SO<sub>4</sub> required is 1.6 times less than that calculated for NO<sub>3</sub>, which was  $6.45 \times 10^{-3} \text{ mol L}^{-1}$ .

$$= (6.45 \times 10^{-3}) / 1.6$$

$$= 4.03 \times 10^{-3} \text{ mol L}^{-1} \text{ of SO}_4$$

Therefore, concentration required when made using Na<sub>2</sub>SO<sub>4</sub>

$$\text{SO}_4 \text{ (mol L}^{-1}\text{) x molar mass of Na}_2\text{SO}_4 \text{ (g mol}^{-1}\text{)}$$

$$= 0.572 \text{ g L}^{-1}$$

### APPENDIX 3

#### *Packard Tri-Carb® 2900TR Liquid Scintillation Analyser's Detection Limit*

The LSA's detection limit was ~0.3 Becquerels. Therefore, the minimum amount of  $^{14}\text{C}$ -activity required per 100 ml sample was calculated using the following equations:

$$A = N\lambda \quad [1]$$

Where: A = total activity

N = total number of atoms

$\lambda$  = decay constant

Equation [1] was rearranged to calculate the minimum value for N:

$$N = A/\lambda \quad [2]$$

The number of  $^{14}\text{C}$  atoms in each labelled molecule was 6 (forming the benzene ring). Therefore,  $N/6$  gave the minimum number of compound molecules,  $N$  in equation [3].

$N$  was converted to a minimum concentration value for each compound using:

$$n = N/N_A \quad [3]$$

$$m = n * MW \quad [4]$$

Where: n = number of moles

$N$  = number of molecules

$N_A$  = Avogadro's constant

m = mass of substance

MW = molecular weight of substance

### Calculation

100 ml samples were prepared with an activity of 3300 Bq, so the minimum activity in each 100  $\mu$ l sub-sample was 3.3 Bq, which was within the detection limit of the LSA (0.3 Bq).

Using equation [2], the minimum number of atoms in each sample was calculated:

$$N = \frac{3300}{\frac{0.693}{(5730 \times 365 \times 24 \times 60 \times 60)}}$$

$$N = 8.605 \times 10^{14} \text{ atoms}$$

The number of  $^{14}\text{C}$  atoms in each labelled molecule was 6. Therefore, the minimum number of molecules required ( $N$  in equation [3]):

$$N = \frac{8.605 \times 10^{14}}{6}$$

$$N = 1.434 \times 10^{14} \text{ molecules}$$

The number of moles needed in 100 ml was calculated using equation [3]:

$$n = \frac{1.434 \times 10^{14}}{6.022 \times 10^{23}}$$

$$n = 2.381 \times 10^{-10} \text{ mol/100 ml}$$

$$= 2.381 \times 10^{-9} \text{ mol L}^{-1}$$

The minimum concentration of  $^{14}\text{C}$  labelled compounds were calculated using equation [4]:

E.g. Isoproturon

$$m = 206.3 \text{ g mol}^{-1} \times 2.381 \times 10^{-9} \text{ mol L}^{-1}$$

$$m = 4.912 \times 10^{-7} \text{ g L}^{-1}$$

The minimum concentration of  $^{14}\text{C}$  labelled compounds used, to allow for the detection limit of the LSA were 0.4 (Sulphanilamide) and 0.5  $\mu\text{g L}^{-1}$  (Isoproturon).

## APPENDIX 4

### *Quench Curve*

The type of solvent mixed with the scintillation cocktail can cause chemical or colour quenching, affecting the transfer of energy, and reduce the counting efficiency of the LSA. An external standard (t-SIE) quench curve of Efficiency (%) vs. t-SIE (Fig.1) was produced following the method described by Thompson (2001), to determine the quenching corrections needed for the solvent, Acetone. No quench curve was necessary for the solvent, Milli-Q as the volumes used were within the capacity of the cocktail (Perkin Elmer, 2003).

Replicate (n=3) standards of known  $^{14}\text{C}$ -activity were prepared in Ultima Gold™ XR and the Efficiency (%) calculated:-

$$(\text{CPM} \times 100) / \text{DPM} = \text{Efficiency}(\%) \quad [1]$$

Where: CPM = counts per minute

DPM = disintegrations per minute

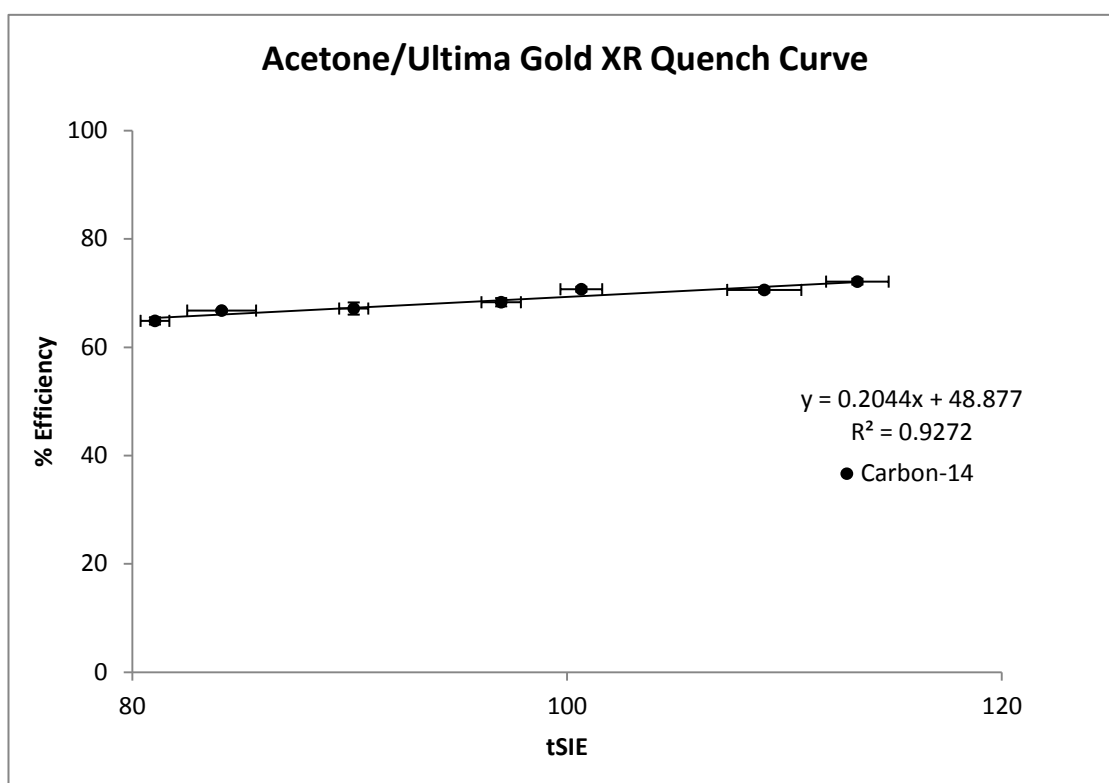
The LSA's Efficiency (%) of known standards, at 95% certainty, was 95.59 +/- 0.04%.

A quench set (Table 1) of varying mixtures of Acetone and Ultima Gold™ XR was created and a quench curve of Efficiency (%) vs. t-SIE plotted (Fig. 1).

**Table 1 – Quench Set.**

Sample	Acetone (ml)	Ultima Gold™ XR (ml)
1	9.0	11.0
2	9.5	10.5
3	10.0	10.0
4	10.5	9.5
5	11.0	9.0
6	11.5	8.5
7	12.0	8.0

**Figure 1: Quench Curve of Efficiency (%) vs. t-SIE.**



The t-SIE and CPM values were recorded by the LSA and the CPM, along with the DPM of the known standards, were used, with equation [1], to determine the Efficiency (%) values for the graph.

The gradient and intercept obtained from the quench curve were used to correct the DPM values obtained for the  $^{14}\text{C}$ -activity measured in subsequent unknown samples prepared in the same matrix.

Firstly by calculating the % Efficiency of the count:-

$$\% \text{ Efficiency} = \text{gradient} \times \text{tSIE} + \text{intercept} \quad [2]$$

Using the result from equation [2], along with the CPM recorded by the LSA, the quench corrected DPM values were obtained:-

$$\text{DPM} = \text{CPM}/(\text{Efficiency}(\text{expressed as a decimal})) \quad [3]$$

## APPENDIX 5

### **LC/IRMS method development for compound specific isotope analysis of non-volatile organic compounds, specifically: Asulam and sulphanilamide.**

#### *Introduction to LC/IRMS techniques*

Isotope ratio mass spectrometry (IRMS) is used widely in a diverse range of scientific principles, including: agriculture, environmental science, marine and clinical studies (Midwood and McGaw, 1999). It is used primarily to study the small variation in the natural abundance of the light bio-elements hydrogen ( $^2\text{H}/^1\text{H}$ ), carbon ( $^{13}\text{C}/^{12}\text{C}$ ), nitrogen ( $^{15}\text{N}/^{14}\text{N}$ ), oxygen ( $^{18}\text{O}/^{16}\text{O}$ ) and sulphur ( $^{34}\text{S}/^{32}\text{S}$ ). An isotope ratio mass spectrometer is a specially configured mass spectrometry (MS) system designed for the precise measurement of these small differences in isotopic abundance. Knowledge of these differences allows a fundamental understanding of geochemical and bio-geochemical cycling of the elements, reaction kinetics, the role of specific chemicals in nutrition, the authenticity of food ingredients and so on. Of particular interest to this study, is the variation in carbon ( $^{13}\text{C}/^{12}\text{C}$ ) isotope abundance, which is brought about by preferential biodegradation of  $^{12}\text{C}$ - $^{12}\text{C}$  bonds over  $^{13}\text{C}$ - $^{12}\text{C}$  (or  $^{13}\text{C}$ - $^{13}\text{C}$ ) bonds.

An isotope ratio mass spectrometer (Fig. 1) consists of five main sections: a sample introduction system, an electron ionization source, a magnetic analyser, Faraday detectors, and a data acquisition system (Muccio and Jackson, 2009). The two most common ways to introduce a sample into the IRMS are via an elemental analyser (EA) and gas chromatography (GC). More recently, liquid chromatography (LC) methods have also been developed to facilitate the introduction of samples to IRMS. Figure 1 shows how each of these sample delivery systems can be coupled to an IRMS (Muccio and Jackson, 2009) .

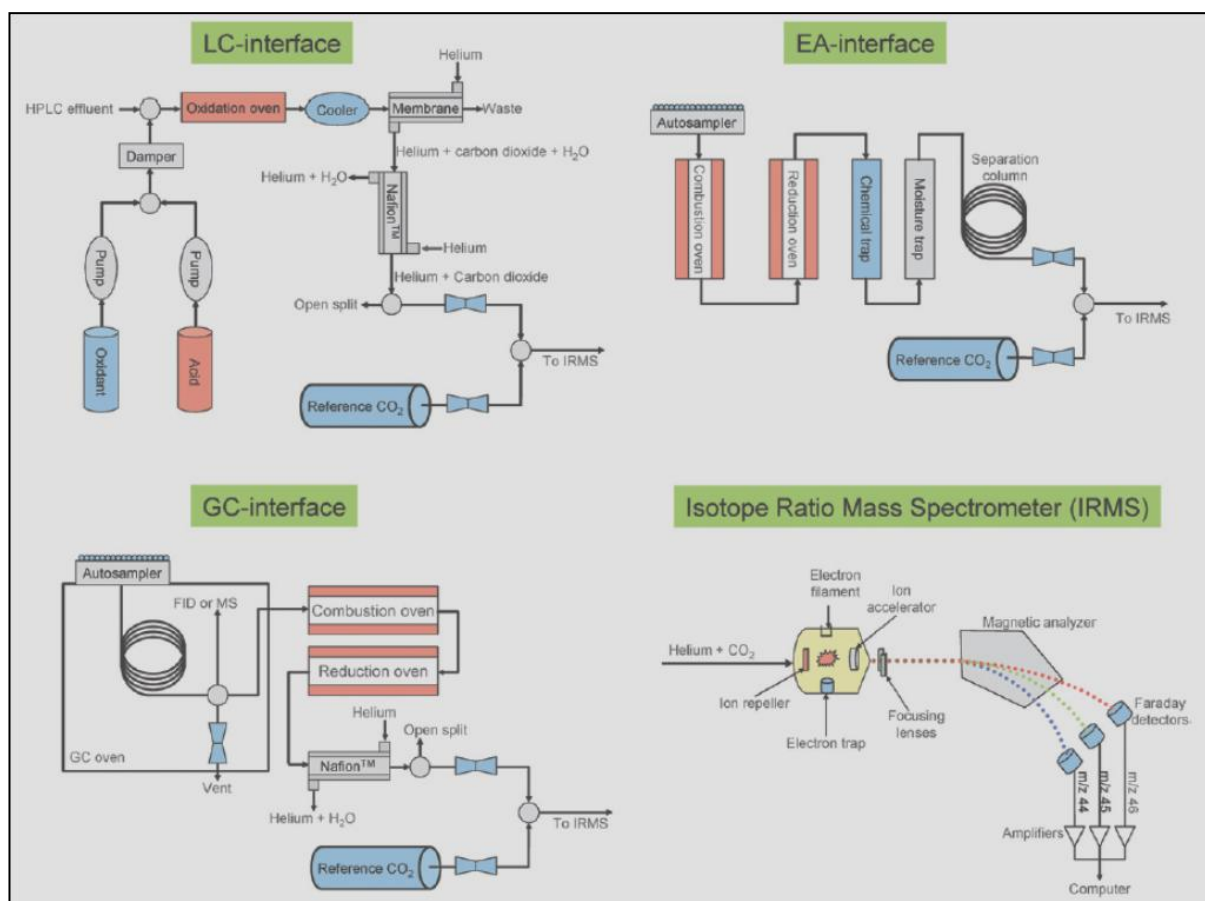


**Figure 1** – Schematics to show the three most common sample introduction interfaces for carbon isotope measurements, as CO<sub>2</sub> and an isotope ratio mass spectrometer. LC: liquid chromatography, EA: elemental analyser, GC: gas chromatography (Muccio and Jackson, 2009).

In its most traditional form carbon dioxide is derived from the action of acid on carbonate minerals or by the combustion of organic material. The CO<sub>2</sub> is introduced into the IRMS system from a suitable air-tight container and the mass distribution of the sample gas is then compared to a calibrated reference CO<sub>2</sub> gas of known isotopic ratio thus facilitating the determination of <sup>13</sup>C-abundance in the test material. Since the 1970s the IRMS analyser has been directly interfaced through various combustion and pyrolysis preparation devices, in particular GC-combustion and EAs, permitting the rapid on-line measurement of compound-specific and overall isotope ratios respectively (Midwood and McGaw, 1999). These preparation systems are characterised by the use of helium, as an inert carrier gas, which transports the sample to the IRMS system.

However, the main disadvantage of gas chromatography isotope ratio mass spectrometry (GC/IRMS) is that analytes must be volatile and thermally stable for a gas phase technique to be effective. Therefore, there are many compounds of interest, in the afore-mentioned research areas, that are excluded from on-line IRMS analysis because they are not sufficiently volatile. In some instances, this may be overcome by derivatisation to form more volatile compounds, which permit GC/IRMS analysis, but is accompanied by problems such as isotopic dilution because the derivatising agent adds extraneous carbon to the analyte, which must be accounted for to obtain true isotope ratios (Caimi and Brenna, 1993). In addition, water soluble inorganic ions such as ammonium and nitrate; require time-consuming extraction techniques and drying prior to analysis by elemental analyser-IRMS. To enable the separation and convenient introduction of non-volatile organic analytes the preferred technique would be high performance liquid chromatography (HPLC).

The two most common interfaces for liquid chromatography isotope ratio mass spectrometry (LC/IRMS) are moving wire and wet-chemical oxidation interfaces. Of these, the wet-chemical oxidation interface shows more promise and has resulted in the development of a commercial instrument (Thermo Finnigan™ LC IsoLink). It works by converting the organic compounds present in the HPLC eluent into CO<sub>2</sub> gas directly in the mobile phase. On account of this, the mobile phase needs to be clear of other organic or oxidizable compounds that could interfere with the results. This may restrict the potential use of LC, as a sample introduction system, because many HPLC separations require organic solvents. The eluent from the HPLC is mixed with an oxidising agent and a catalyst and passed through an oxidation reactor, where the organic compounds are converted into CO<sub>2</sub>. A membrane exchanger then separates out the CO<sub>2</sub> gas, from the liquid phase, whereby it is carried via a stream of helium through a Nafion™ dryer before entering the IRMS (Muccio and Jackson, 2009).

The coupling of an HPLC system with an IRMS was first reported by Caimi and Brenna in 1993 (1993). They used a moving wire to transport the HPLC eluent stream containing non-volatile analytes through an oven, to remove the mobile phase, and then a 900°C combustion furnace to convert the analyte to CO<sub>2</sub>. This approach was similar to those used in the initial interfacing of HPLC and organic

mass spectrometers. Although effective, the presence of a moving stainless steel wire, whose surface is continually cycled through oxidised and reduced forms and temperature gradients, meant that it had a finite lifetime. Furthermore, a limiting factor is the quantity of sample collected on the wire (Caimi and Brenna, 1993). A schematic of the moving wire approach is shown in Figure 2.

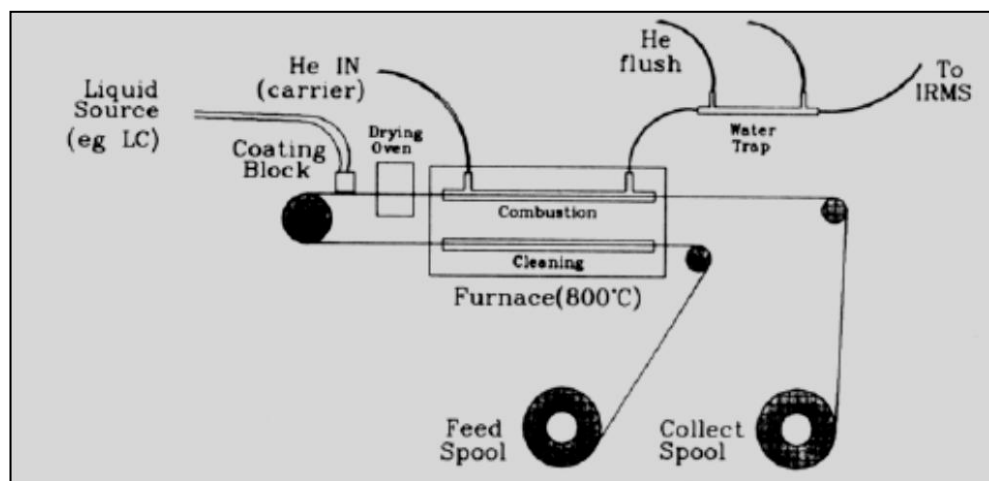


*Figure 2 – Liquid chromatography- combustion interface for IRMS (Caimi and Brenna, 1993)*

Caimi and Brenna (1993) describe how the interface works (Fig.2): firstly, a stainless steel wire passes from the feed spool through a cleaner furnace before collecting the sample at the coating block. Next, the wire passes through a drying oven, where the solvent is evaporated before moving into the combustion furnace. In the combustion furnace, the carbon and hydrogen in the organic sample are oxidised to form  $\text{CO}_2$  and  $\text{H}_2\text{O}$  and the water is removed at the water trap. Lastly, the carbon dioxide passes to the IRMS for isotope analysis.

An alternative approach was reported by Teffera et al. in 1996 (1996). Whose system uses a diffusion based solvent removal interface in conjunction with a heated nebuliser to produce a beam of non-volatile analyte particles in a stream of dry helium. The particles were then converted to  $\text{CO}_2$  using a chemical reaction interface (CRI). The CRI contains a cavity into which the particle beam is introduced. A microwave induced helium plasma, in conjunction with a stream of oxygen, causes the combustion of non-volatile organic material to  $\text{CO}_2$  and water. The helium gas then passes through a nafion dryer (where the water is removed)

before being introduced to the IRMS where the mass distribution and  $^{13}\text{C}$ -abundance of analyte is determined. The major drawback in this system is that it is not possible to measure the isotopic abundance of the stable isotopes ( $^{15}\text{N}/^{14}\text{N}$ ). This is because, oxygen gas, present in the CRI helium stream, interferes with the production of  $^{15}\text{N}^{16}\text{O}$  and  $^{14}\text{N}^{16}\text{O}^+$ , making it impossible to use the system to measure the  $^{15}\text{N}/^{14}\text{N}$  ratio of non-volatile inorganic and organic species (such as  $\text{NH}_4^+$ ,  $\text{NO}_3^-$  and chlorophyll), which are suited to liquid chromatographic introduction.

One of the major challenges of coupling a HPLC to an IRMS is the necessity to remove the liquid phase before the sample can be combusted and transferred into the IRMS. Therefore, early developments of LC/IRMS techniques have focused on the removal of the liquid phase prior to the chemical reaction which produces a gas for analysis (Krummen et al., 2004). Caimi and Brenna (1993) developed an interface whereby the liquid analyte was deposited onto a moving wire and dried prior to combustion. Teffera et al. (1996) system sprayed the liquid analyte onto a heated nebulizer which desolvated the sample which was subsequently combusted. In contrast, the Finnigan<sup>TM</sup> LC IsoLink does not remove the liquid phase prior to combustion. The liquid phase is oxidised while still in the mobile phase and the  $\text{CO}_2$  separated after for isotope analysis. This technique has been proven to be quantitative and is not compromised by isotopic fractionation processes, during the production of  $\text{CO}_2$  (Krummen et al., 2004).

Wet oxidation methods, to analyse dissolved carbon in natural waters were developed by St-Jean (2003). These involved a two step process; (i) removing the dissolved inorganic carbon by acidifying (with phosphoric acid) the water sample and removing the resultant  $\text{CO}_2$  and, (ii) adding persulphate to the remaining liquid sample and heating (at  $100^\circ\text{C}$  the persulphate oxidises the dissolved organic carbon to  $\text{CO}_2$ ). Subsequently, the  $\text{CO}_2$  is purged from the sample, trapped and dried before isotope analysis. A schematic of the equipment used during wet oxidation methods is shown in Figure 3.

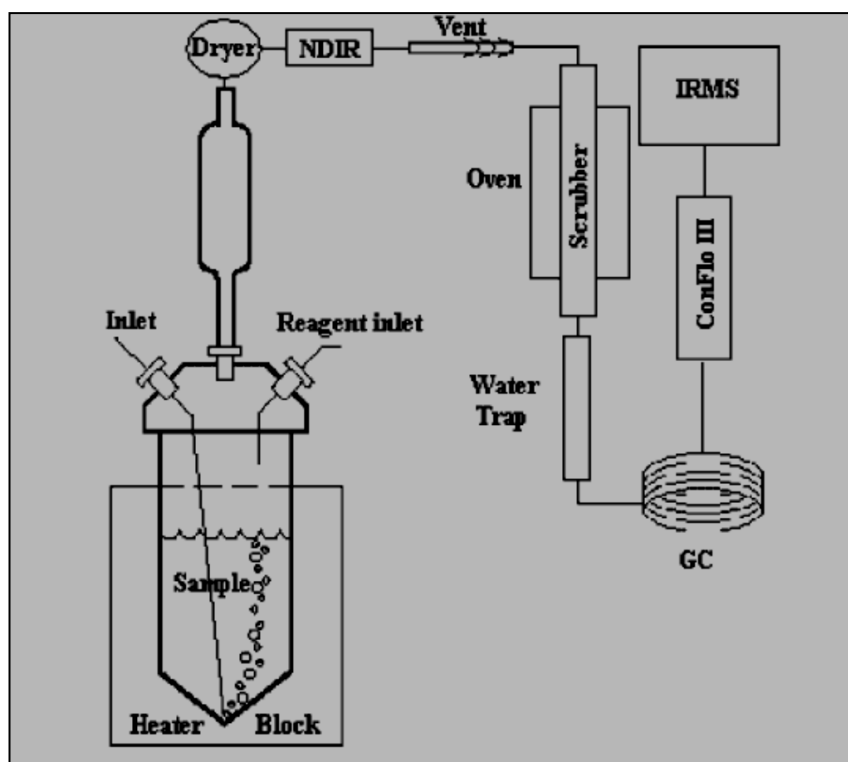
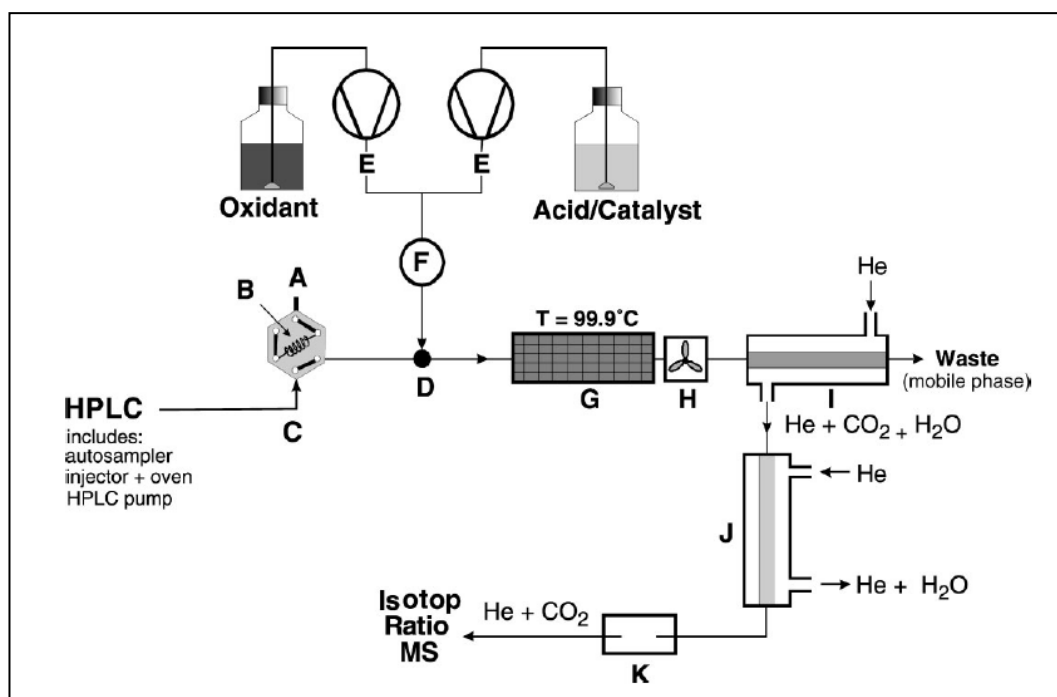


Figure 3 – Total organic carbon analyser and attached IRMS interface (St-Jean, 2003).

In addition to the wet oxidation methods, St-Jean (2003) also illustrates how HPLC techniques can be utilised to separate specific dissolved organic compounds, for compound specific isotope analysis. Whereby a liquid chromatography fraction collector captures and concentrates purified dissolved organic compounds in individual vials, which can then be analysed via IRMS, using the wet oxidation methods described above, to transform the sample from a liquid to a gas phase.

Krummen et al. (2004) utilised the wet oxidation techniques, described by St-Jean (2003), in developing the first direct coupling of a HPLC to an IRMS. Figure 4 shows a schematic.



**Figure 4** – Schematic of Finnigan™ LC IsoLink. A: Needle port; B: sample loop; C: 6-port valve; D: T-piece; E: two-head-pump; F: pulse damper; G: oxidation reactor; H: cooler; I: CO<sub>2</sub> separation unit; J: gas dryer; K: open spilt.

Samples are injected in the needle port (A) into the sample loop (B) or various sizes at the 6-port valve (C) after the HPLC column. At the T-piece (D) a mixture of reagents are added to the mobile phase separately by two-head pumps (E). The pulse damper (F) prevents pulsations caused by the addition of reagents affecting the background signal. The reagents, mobile phase and sample enter the oxidation reactor (G) where all the organic compounds are converted to CO<sub>2</sub>. After oxidation the mobile phase is cooled (H) and the CO<sub>2</sub> is separated from the liquid phase (I) the CO<sub>2</sub> is then dried (J) before entering the isotope mass spectrometer (K) (Krummen et al., 2004).

There are two main issues associated with the coupling of LC to magnetic sector instruments (1) an efficient step for solvent removal and (2) analyte transformation into CO<sub>2</sub> gas without any isotopic effect. Due to these issues, the interface coupling LC with IRMS was only commercialised by Thermo in 2004 (Godin et al., 2007). Therefore, this study focuses on whether LC/IRMS methods are suitable to determine the isotopic abundance of Asulam and sulphanimide dissolved in groundwater.

### *Method Development*

Collaborative work was carried out with Thermo at their research and development centre in Bremen, Germany, prior to the installation of an LC Isolink at the Stable Isotope Laboratory, University of East Anglia. Initial studies focused on establishing a suitable method to enable isotope analysis of the non-volatile organic compounds sulphanilamide and Asulam analysis. This involved developing a mobile phase and suitable reagents to enable the oxidation of the carbon fraction of both sulphanilamide and Asulam. Table 1 presents an outline of the method developed.

**Table 1 – Thermo Finnigan™ LC IsoLink method to determine the <sup>13</sup>C-abundance of sulphanilamide and Asulam.**

<b>Column</b>	250 x 3.0 mm stainless, packed, particle size: 5 µm HyPurity Aquastar (# 22505-253030)
<b>Column Temperature</b>	ambient
<b>Mobile Phase (Isocratic)</b>	0.05 M KH <sub>2</sub> PO <sub>4</sub> , pH 3  Dissolve 6.8 g disodium hydrogen phosphate L.C. in 1 litre of water (HPLC grade) and using a pH meter, adjust to pH 3.0 by the addition of ortho-phosphoric acid (89% w/w)
<b>Flow rate</b>	0.5 mL/min
<b>Injection Volume</b>	10µl
<b>LC IsoLink conditions</b>	Persulphate concentration of 96 g/ 800 mL and flow rate of 50 µL/min  o-Phosphoric acid (89% w/w) concentration of 80 mL/ 800mL and flow rate of 50 µL/min
<b>Approximate Retention Times</b>	Sulphanilamide 500 seconds  Asulam 2000 seconds

Following installation of the LC Isolink, analysis of the standard benzoic acid was investigated, using water as the mobile phase and direct injection mode, to replicate the results obtained by the Thermo engineers during installation. The reason for this was to become familiar with the workings of the LC Isolink and establish running conditions and appropriate start up/shut down routines. Table 2 represents the results obtained for the benzoic acid analysis, which proved to be consistent with those obtained by the engineer during installation.

**Table 2 – Results of Benzoic Acid LC/IRMS analysis.**

<b>Method/conditions</b>	<b>Benzoic acid [ng]</b>	<b>Peak (Vs)</b>	<b><math>\delta^{13}\text{C}</math> [‰]</b>
1. Mobile phase (H <sub>2</sub> O) 500 µl/min Reagents (as per recipe in Table 1) 50 µl direct injection with 10 µl directed to Isolink	200	118.70	-27.99
		117.26	-27.93
		116.84	-27.99
	<b>Mean</b>	<b>118.00</b>	<b>-27.97</b>
2. As method 1 but oxidant reagent concentration reduced from 12.5 to 9 % v/w	200	120.36	-28.20
		120.70	-28.37
		119.78	-28.44
	<b>Mean</b>	<b>120.00</b>	<b>-28.34</b>
3. As method 1 but benzoic acid injected reduced from 200 to 100 ng	100	60.54	-28.63
		58.28	-28.70
		58.57	-28.64
	<b>Mean</b>	<b>59.13</b>	<b>-28.65</b>

The repeatability of the benzoic acid gave an average  $\delta^{13}\text{C}$  [‰] for benzoic acid as -28.32 ‰ with a standard deviation of 0.3 ‰. The standard deviation for repeatability is consistent with published results for LC/IRMS techniques of non-volatile organic compounds (Boschker et al., 2008, Cabañero et al., 2006, Godin et al., 2005, Krummen et al., 2004, McCullagh et al., 2006).

*Method development: Sulphanilamide and Asulam*

The sulphanilamide and Asulam LC Isolink method and retention times had been established during collaboration with the research and development centre at Thermo. Therefore, using the method outlined previously in Table 1, the mobile phase and reagents were prepared and linearity tests were investigated to ascertain the detection limits for sulphanilamide and Asulam analysis. Figure 5 shows a typical LC Isolink chromatogram obtained for sulphanilamide.

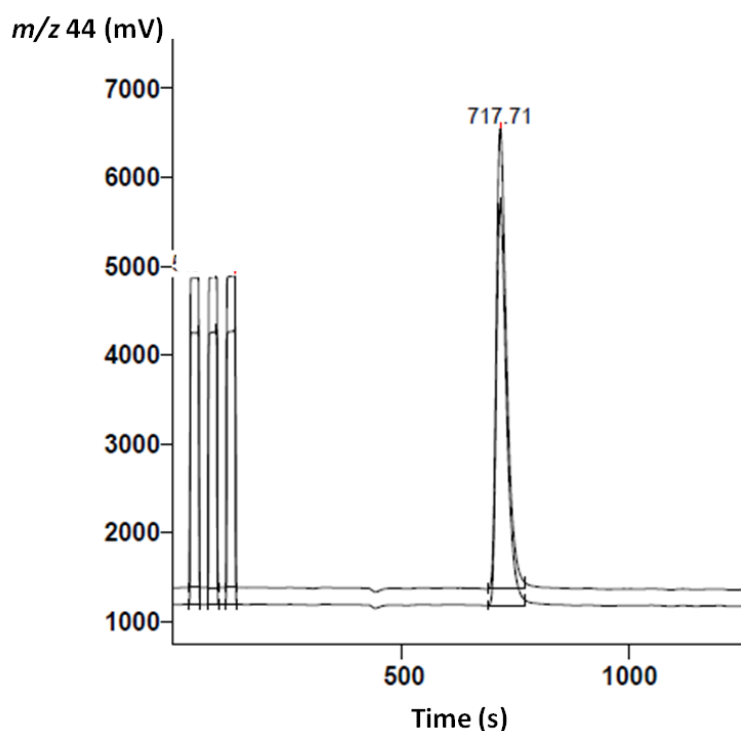


**Figure 5** – LC Isolink chromatogram of sulphanilamide, 2500 ng, 10 $\mu$ l injection, m/z 44. Column: HyPurity Aquastar (250 x 4.6 mm), 25°C. Conditions: HPLC flow 500  $\mu$ l/min (6.8 g L<sup>-1</sup> Disodium hydrogen phosphate (KH<sub>2</sub>PO<sub>4</sub>)) at pH3; reagent flow 50 $\mu$ l/min.

Of initial concern was the retention times for sulphanilamide and Asulam were much longer than those reported during the method development stage (sulphanilamide: 500s, Asulam: 2000s), results of which are shown in Table 1. The retention times observed for sulphanilamide were 717 – 749s and Asulam 3074 -3212s. The most likely explanation was that a HyPurity Aquastar (250 x 4.6 mm) column had been

fitted on the LC Isolink, which was a different size to the column used during the method development stages (250 x 3.0 mm shown in Table 1).

This would mean, including the three reference peaks at the start of each run, the method would take approx 4000s to run (which is just over an hour per sample).

This was considered too long and so attention was given to ways in which the retention time could be decreased.

There are different ways to reduce the time an analyte spends on a column, which include, changing the column temperature, the flow rate of the mobile phase or replacing the column (Guzzetta, 2010). Firstly, calculations were made to ensure the flow rate was suitable for the HyPurity Aquastar (250 x 4.6 mm) column, currently installed on the LC Isolink. The standard flow rate for 4.6 mm column is 1ml/min (Guzzetta, 2010). However, the maximum flow rate of the LC Isolink cannot exceed 0.7 ml/min. Despite investigations, which involved increasing the flow rate from 0.5 to 0.7 ml/min, there was no change to the RT for sulphanilamide or Asulam. Moreover, nor did exploring an increase in column temperature, from ambient room temperature to 95°C, in intervals of 10°C, reduce the RT.

The next step involved replacing the 4.6 mm column with one that could accommodate the flow rate imposed by the LC Isolink. A Gemini 5µ C18 110A 150 x 2.00min 5 micron particle size (Phenomenex serial no; 313897-1), was installed and the RT investigated. The ideal flow rate of 0.2 ml/min was calculated as follows (Guzzetta, 2010):

$$\left(\frac{2.0}{4.6}\right)^2 \times 1 = 0.2 \text{ ml/min}$$

The installation of the new column reduced the RT considerably (sulphanilamide: 200-300 s, Asulam: 550-650s).

Having established suitable HPLC column conditions for sulphanilamide and Asulam, attention was given to the ideal  $m/z$  44 signal required for the LC Isolink. Previous studies, involving IRMS analysis, along with guidelines provided with the LC Isolink, have concluded that the signal should range between  $\geq 3$  V. Therefore,

different concentrations of sulphanilamide and Asulam were analysed to determine the maximum concentration suitable for injection. It is worth noting here, that should the concentration of carbon be too high then there is a risk of damaging the Faraday detectors (Fig. 1). The results demonstrated that following a 25µl injection, 2500 ng of sulphanilamide gave a signal of 7V and 12500 ng Asulam gave a signal of 5V. The revised method, from that shown in Table 1, is shown in Table 3.

**Table 3 – LC Isolink method developed for <sup>13</sup>C-abundance analysis of sulphanilamide and Asulam.**

<b>Column</b>	A Gemini 5µ C18 110A 150 x 2.00min 5 micron particle size (Phenomenex serial no; 313897-1)
<b>Column Temperature</b>	ambient
<b>Mobile Phase (Isocratic)</b>	Dissolve 6.8 g disodium hydrogen phosphate in 1 litre of water (HPLC grade) and using a pH meter, adjust to pH 3.0 by the addition of ortho-phosphoric acid (89% w/w)
<b>Flow rate</b>	0.2 mL/min
<b>Injection Volume</b>	25µl
<b>LC IsoLink conditions</b>	Oxidant: Persulphate concentration of 60 g/ 500 mL and flow rate of 25 µL/min  Acid/catalyst: o-Phosphoric acid (89%w/w) concentration of 50 mL/ 500mL and flow rate of 35 µL/min
<b>Approximate Retention Times</b>	Sulphanilamide 305 seconds  Asulam 720 seconds

### *Precision, linearity and sensitivity of LC Isolink*

Having established a suitable method (Table 3), the performance of the LC Isolink was investigated to determine the precision, linearity and sensitivity of the LC Isolink in analysing the  $^{13}\text{C}$ -abundance of sulphanilamide and Asulam.

Sulphanilamide standards were prepared in mobile phase (6.8 g L<sup>-1</sup> disodium hydrogen phosphate at pH 3) at concentrations ranging from 0.05 to 0.15 mg ml<sup>-1</sup>. Table 3 shows the  $\delta^{13}\text{C}$  [‰] values obtained for sulphanilamide.

**Table 3** -  $\delta^{13}\text{C}$  [‰] values of sulphanilamide by LC Isolink.

Amount		$\delta^{13}\text{C}$ [‰]	Std. Dev. [‰]	n
Sulphanilamide [ng]	Carbon [ng]			
1250	500	-28.26	0.08	3
1875	750	-28.26	0.05	3
2500	1000	-28.25	0.05	3
3125	1250	-28.23	0.01	3
3750	1500	-28.27	0.02	3
<b>Mean</b>		<b>-28.25</b>	<b>0.04</b>	

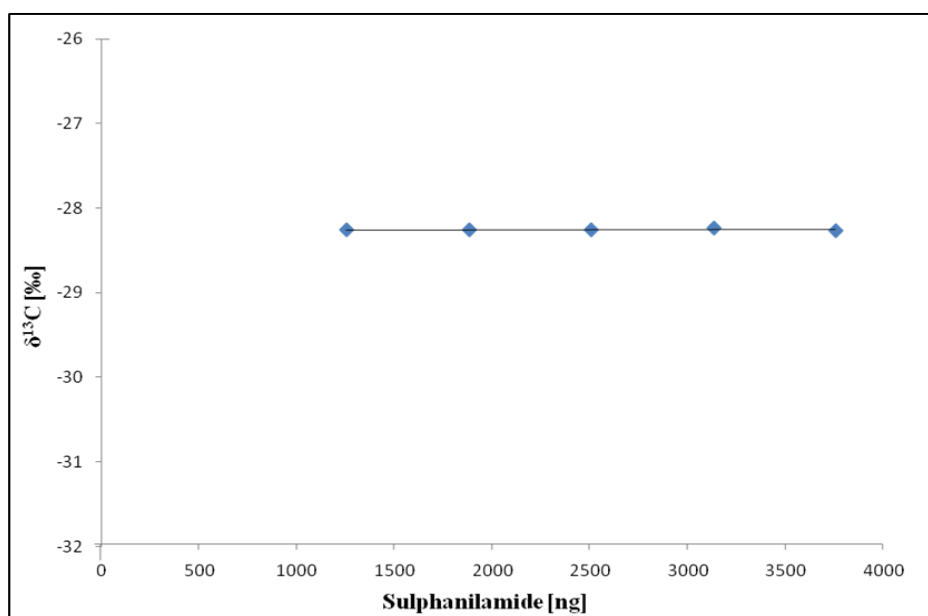
The precision of the LC Isolink was analysed in its ability to reproduce  $\delta^{13}\text{C}$  [‰] values for the same sulphanilamide stock made up into different concentrations. The mean  $\delta^{13}\text{C}$  value was -28.25 ‰, with a standard deviation of 0.04 ‰. These results demonstrate an excellent reproducibility for sulphanilamide, when compared to reported literature values of 0.2 ‰ (Cabañero et al., 2006, Krummen et al., 2004, McCullagh et al., 2006), for other non-volatile organic compounds.

Table 4 shows the  $\delta^{13}\text{C}$  [‰] values obtained for Asulam. The mean  $\delta^{13}\text{C}$  value was -30.42 ‰, with a standard deviation of 0.3 ‰. The results obtained for Asulam were not as impressive as those for sulphanilamide (0.04 ‰). This said, the reproducibility for Asulam is still reasonably good and is comparable to values reported in the literature (Godin et al., 2005).

**Table 4** -  $\delta^{13}\text{C}$  [‰] values of Asulam by LC Isolink.

Amount		$\delta^{13}\text{C}$ [‰]	Std. Dev. [‰]	n
Asulam [ $\mu\text{g}$ ]	Carbon [ $\mu\text{g}$ ]			
10	3.2	-30.40	0.5	3
11.25	3.6	-30.74	0.6	3
12.50	4	-30.13	0.1	3
13.75	4.4	-30.05	0.3	3
15	4.8	-30.80	1.0	3
<b>Mean</b>		<b>-30.42</b>	<b>0.3</b>	

The linearity range for sulphanilamide is presented in Figure 6 and for Asulam, Figure 7.



**Figure 6** -  $\delta^{13}\text{C}$  [‰] vs. sulphanilamide [ng] (sample size) analysis using LC Isolink to establish the range over which the analysis is linear.

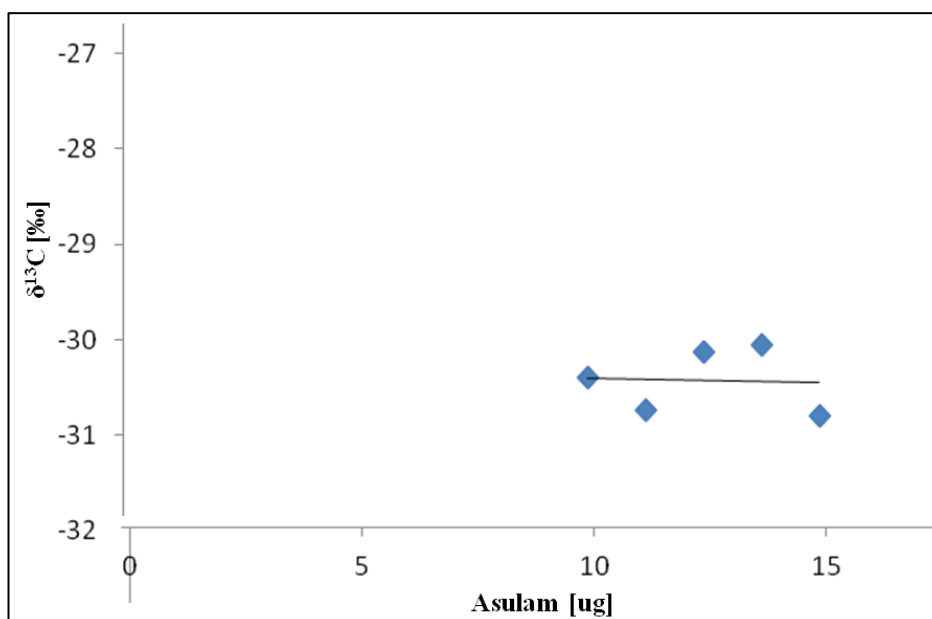


**Figure 7** -  $\delta^{13}\text{C}$  [‰] vs. Asulam [ $\mu\text{g}$ ] (sample size) analysis using LC Isolink to establish the range over which the analysis is linear.

The data presented for sulphanilamide (Fig.6) shows there is excellent linear behaviour between the concentration ranges investigated (1250 – 3750 ng). This provides evidence that within these concentration ranges there is no shift in  $\delta^{13}\text{C}$  values to more positive or negative values. The data presented for Asulam (Fig. 7), however, shows poor linear behaviour between the concentration ranges investigated (10 – 15  $\mu\text{g}$ ). During analysis, Asulam presented itself as a broad peak on the chromatogram, which sometimes separated out into two peaks. Unlike, sulphanilamide, a higher concentration of Asulam was required in order to determine Asulam, which in turn, may have presented the problems associated with peak development and  $\delta^{13}\text{C}$  values.

Figures 8 and 9 show plots of correlation between signal area and the injected amount of sulphanilamide and Asulam, respectively. The response of the signal in relation to the amount of sulphanilamide is linear (Fig. 8), with an  $R^2$  value of 0.99, which demonstrates that the correlation is suitable for quantification purposes.

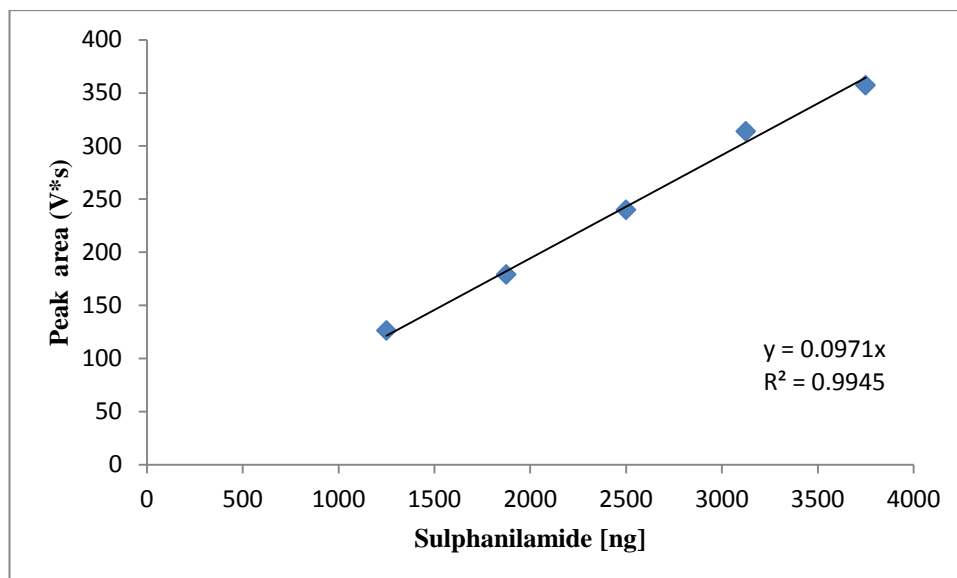


**Figure 8** – Peak area of  $m/z$  44 ( $^{12}C^{16}O_2$ ) in [V\*s] vs. amount injected [ng]; the linear correlation proves that the peak areas can be used for quantification up to 3750 ng.

There is a poor correlation between the signal area and the amount of Asulam injected (Fig.9). The low  $R^2$  value (0.75), recorded for the linear relationship means it would not be suitable for Asulam quantification purposes.

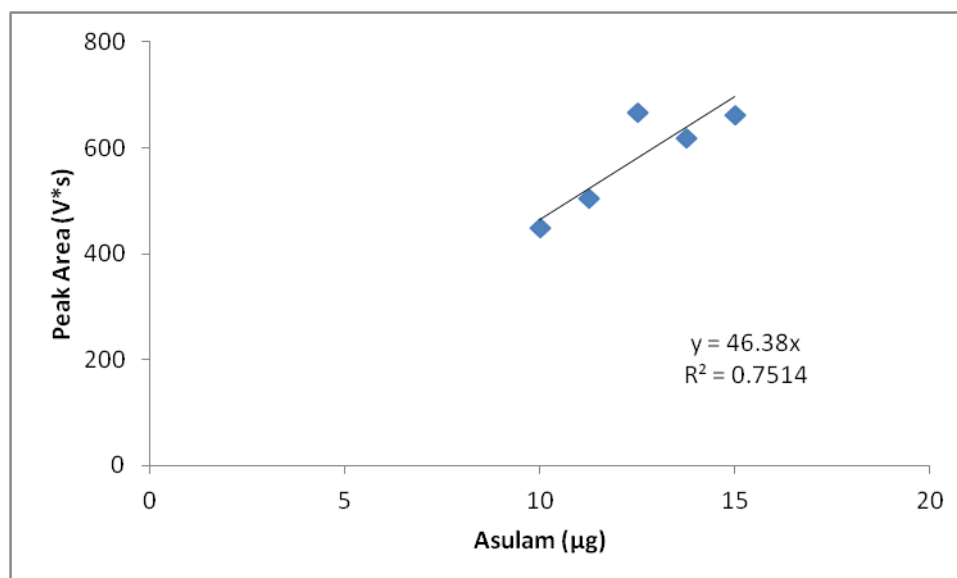


**Figure 9** – Peak area of  $m/z$  44 ( $^{12}C^{16}O_2$ ) in [V\*s] vs. amount injected [µg]; the poor linear correlation proves that the peak areas are not suitable for quantification.

*LC/IRMS analysis of field samples*

From the linearity test a detection limits for Sulphanilamide was established as 0.1 mg ml<sup>-1</sup>. Although Asulam was also present in the groundwater, the main point of interest was a shift in <sup>13</sup>C-abundance of sulphanilamide, brought about by biodegradation processes, occurring *in-situ* at the field site. Therefore, the 1L groundwater samples, obtained from monitoring wells at the site, which contained sufficient quantities of sulphanilamide were identified. Table 5 lists the suitable samples.

**Table 5 – Contaminated groundwater samples containing sufficient quantities of sulphanilamide (i.e. ≥ 0.1 mg).**

Borehole	Depth (m)	Sulphanilamide (mg)	Asulam (mg)
BH1 (12.09)	-	0.142	-
BH1 (05.10)	-	2.37	-
BH2 (12.09)	-	0.2	-
N61-S1/C	12	0.48	0.64
N61-SW1C (new well N62c)	12.5	0.4	0.4
N61-N1/C (new well N62b)	12.5	1.36	-
N62-E1/C (12.09)	11	8.3	-
N62-E1/C (05.10)	11	236.0	0.4
N62-S1/C (12.09)	10.5	3.38	-
N62-S1/C (05.10)	10.5	159.25	-
N62-W1/C (12.09)	14	13.620	-
N62-W1/C (05.10)	14	261.1	4.15
N71 CRW (12.09)	15	0.316	-
N71 CRW (05.10)	15	7.696	0.48
N71-W1/C	9	0.039	-
N71-W2/C (12.09)	10	0.456	-
N71-W2/C (05.10)	10	7.04	-
N71-N1/C	11	0.039	-
N71-NE1/C	9.5	0.27	-
N71-NW1/C	10	1.21	2.12
N74-SW1/PT/S	7	0.175	-
N100-E1/C	6	0.06	-
Sentinel W1/C	13	0.03	-
Sentinel S1/C	12	0.165	-
Sentinel E1/C	6.5	0.055	-
Sentinel SE1/C	12	0.067	-

### Results of field sample N61-N1/C

According to site records, the sample contained  $1.36 \text{ mg L}^{-1}$  of sulphanilamide (Table 5). The sample was freeze dried to a powder and prepared in mobile phase  $0.1 \text{ mg ml}^{-1}$  (2500ng sample in a  $25\mu\text{l}$  injection), following the method described in Chapter 6. Filtered, using  $2\mu\text{m}$  filters, to remove particulates from the field sample and sonicated, to degas before analysis. The LC Isolink method, presented in Table 3, was used to analyse the field sample. Table 6 presents the results.

**Table 6 – LC/IRMS analysis of groundwater sample N61-N1/C**

Field sample N61-N1/C				
Sample	RT (s)	Peak Area (Vs)	$m/z$ 44 (mV)	$\delta^{13}\text{C}$ [‰]
1	294	80.81	1253	-28.277
2	293	80.01	1225	-28.099
3	293	78.42	1201	-27.96
4	293	77.66	1189	-27.95
5	293	77.19	1187	-27.90
			<b>Mean</b>	<b>-28.04</b>
			<b>Std. Dev.</b>	<b>0.15</b>

The  $\delta^{13}\text{C}$  value obtained for the sulphanilamide dissolved in the groundwater at monitoring well N61-N1/C was  $-28.04 \text{ ‰}$  with a standard deviation of  $0.15 \text{ ‰}$ . The reproducibility ( $n = 5$ ) of the field sample is good and within values reported in the literature for other non-volatile organic compounds analysed using LC/IRMS methods. The peak area of approximately 80 Vs, according to the results in Figure 8, indicates the amount of sulphanilamide in the sample was approximately 750 ng. However, the concentration recorded at the site was  $1.36 \text{ mg L}^{-1}$ , which was prepared prior to injection to give an amount of 2500 ng. Therefore, this finding suggests

about 70 % of the sulphanilamide recorded in the original sample has been lost during the preparation stage.

### Results of field sample N62-E1/C

According to site records, the sample contained 8.3 mg L<sup>-1</sup> of sulphanilamide (Table 5). The sample was freeze dried to a powder and prepared in 10 ml of mobile phase (therefore would give 8300 ng of sulphanilamide and 3320 ng of carbon) following the method described in Chapter 6. The LC Isolink method, presented in Table 3, was used to analyse the field sample. However, due to the high concentration of the sample a 10 µl injection was used instead of a 25 µl injection so as to prevent the column from becoming overloaded. Table 7 presents the results.

**Table 7 - LC/IRMS analysis of groundwater sample N62-E1/C**

Field sample N62-E1/C				
Sample	RT (s)	Peak Area (Vs)	<i>m/z</i> 44 (mV)	δ <sup>13</sup> C [‰]
1	291	304.86	4977	-27.88
2	292	327.78	5268	-27.96
3	290	302.72	5080	-28.06
4	290	298.20	5058	-27.90
5	290	308.21	5158	-27.96
			<b>Mean</b>	<b>-27.95</b>
			<b>Std. Dev.</b>	<b>0.07</b>

The δ<sup>13</sup>C value obtained for the sulphanilamide dissolved in the groundwater at monitoring well N62-E1/C was -27.95 ‰ with a standard deviation of 0.07 ‰. The reproducibility (n = 5) of the field sample is good and within values reported in the literature for other non-volatile organic compounds analysed using LC/IRMS methods. The peak area of approximately 310 Vs, according to the results in Figure 8, indicates the amount of sulphanilamide in the sample was approximately 3200 ng. However, the concentration recorded at the site was 8.3 mg L<sup>-1</sup>, which was prepared

prior to injection to give an amount of 8300 ng. Therefore, as seen in the results for N61-N1/C, this finding suggests about 60 % of the sulphanilamide recorded in the original sample has been lost during the preparation stage.

In terms of evidence to support *in-situ* biodegradation of sulphanilamide, which would be indicated by an enrichment in the  $\delta^{13}\text{C}$  values of the monitoring wells situated downgradient, the results thus far do not point to biodegradation. The  $\delta^{13}\text{C}$  value of the sulphanilamide, presented in Table 3, which represents the source value, was  $-28.25 \pm 0.04 \text{ ‰}$ , and the  $\delta^{13}\text{C}$  values for the field samples N61-N1/C ( $-28.04 \pm 0.15 \text{ ‰}$ ) and N62- E1/C ( $-27.95 \pm 0.07$ ) show little variation. However, these two field samples are situated in and around the source area of the original contaminant spill and so; it is not surprising that they closely match those representing the source.

Further work will focus attention on the  $^{13}\text{C}$ -abundance of the sulphanilamide recorded in the monitoring wells situated downgradient of the source area to establish any evidence to support the presence of biodegradation.

#### *Un-resolvable technical problems and a forced change of approach*

During the LC Isolink method development stage time consuming technical problems forced a change in approach to the compound specific isotope analysis of sulphanilamide. At the point of installation, the IRMS interface was set up to enable a switched between either LC or GC delivery techniques. Although it was considered advantageous to enable the IRMS to analyse both volatile and non-volatile organic samples, in reality it generated problems with the LC interface. Between interface changeovers, the LC needed to be flushed with water before being switched to GC mode and then the LC lines needed to be reconditioned prior to analysis of liquid samples. The stopping and starting, of the LC produced problems with blockages and leaks in the system, brought about by air bubbles, particulates, or the corrosive action of the harsh reagents used. In ideal circumstances, whilst the system was in GC mode, the LC should have run continuously in the background, which would have kept the lines functioning. However, problems associated with the computer software, which managed the overall system operation, meant the LC and reagent pumps frequently went off-line whilst in GC mode (unbeknownst to the

GC users). Unfortunately, this resulted in the LC often requiring a “mini service” each time it was switched from GC mode, which subsequently restricted the optimum use of the time allocated on the LC Isolink for analysing samples.

Attempts to remedy the problems resulted in three engineer visits to fix the computer software, replace the CO<sub>2</sub> separation unit and repair blocked lines. Although the assistance from Thermo was helpful, the period between booking an engineer and the problem being resolved often took a couple of months, during which time the LC was out of action. In an attempt to speed up this process, efforts were made to fix the problems by utilizing “in house” staff and via email communication with Thermo, prior to an engineer be called. Sometimes the in house efforts to fix the problem worked and where they did not, an engineer was called. Nevertheless, both approaches led to valuable time being lost.

Eventually, time was becoming an issue in terms of obtaining sufficient data to support the biodegradation of sulphanilamide dissolved in groundwater. Therefore, a change in approach was put into practice, which involved completing the HPLC and IRMS analysis separately. This method required an additional sample preparation step to dry the sample (transferring the sulphanilamide from its liquid to solid phase) before isotope analysis. Furthermore, the detection limits of the new approach were not as sensitive, with analysis being restricted to the µg range, whereas the LC Isolink operated in the ng range. Albeit, a more laborious and less sensitive method, it was successful in obtaining results to support the biodegradation of sulphanilamide dissolved in groundwater, which are presented, along with specific details of the method, in chapter 6. However, the restriction in detection limit of the new approach meant many of the collected groundwater samples were not analysed because the sulphanilamide concentration was outside the range of detection.

### *Conclusion*

The purpose of this work was to establish a method capable of analysing carbon isotope ratios of non-volatile organic compounds, in particular sulphanilamide and Asulam (parent compound of sulphanilamide), dissolved in contaminated groundwater. Once a suitable method was set up, the work would then turn to identifying measurable changes in the carbon isotope ratios to establish the

occurrence of sulphanilamide biodegradation. Overall, the work was attempted to compliment earlier chapters (3 and 4), in developing a simplified and robust method to provide evidence of sulphanilamide natural attenuation.

Of significance to this appendix is the development of a method that made use of instrumentation, which directly coupled HPLC and IRMS techniques (*Thermo Finnigan™ LC IsoLink*), to determine the natural abundance of carbon isotopes found in a non-volatile compound (sulphanilamide), dissolved in groundwater. This method was successful in quantifying the amount of carbon, contained in standard sulphanilamide material (41 %) between 0.5 and 1.5 µg, which is supported by a linear correlation and an  $R^2$  value of 0.99. This identifies the LC Isolink as being more sensitive than the Delta XP, used in the approach employed in chapter 6, which although shares a good linear correlation ( $R^2$  0.99), has a detection limit of 100 µg. The calculated  $^{13}\text{C}$ - abundance of sulphanilamide was  $-28.25 \pm 0.04$  ‰, the precision of which is comparable to those reported in the literature for other non-volatile organic compounds (Boschker et al., 2008, Godin et al., 2005, Krummen et al., 2004).

In addition, the method was successful in determining the  $^{13}\text{C}$ -abundance of sulphanilamide dissolved in contaminated groundwater samples at concentrations of  $0.1 \text{ mg ml}^{-1}$  and  $8.3 \text{ mg ml}^{-1}$  with average  $\delta^{13}\text{C}$  values of  $-28.04 \pm 0.15$  ‰ and  $-27.95 \pm 0.07$  ‰, respectively. Although, it is too early to understand at this stage, the relevance of these values in determining the occurrence of sulphanilamide biodegradation in the groundwater, the results, as with the standard material analysed, indicate the method is precise and shows good reproducibility, evident in the low standard deviations obtained (i.e.  $< 0.2$  ‰).

The findings of the method development stage indicate that LC/IRMS techniques would be a suitable method to determine the natural abundance of carbon isotopes found in a non-volatile compound (sulphanilamide), dissolved in groundwater. Moreover, despite the fact that a forced change was made in the methods employed for isotope analysis, the HPLC method developed for the LC Isolink was transferrable and so was utilised in the new approach described in chapter 6.